UNIVERSITY OF CANTERBURY

Department of Mechanical Engineering

Christchurch New Zealand

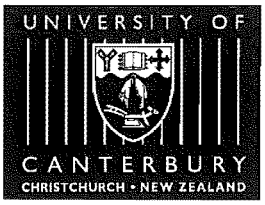

Duct Absorber Design

by

Matthew J Pettersson

Master of Engineering
Thesis

February 2002

Duct Absorber Design

by

Matthew J Pettersson

A thesis submitted in
partial fulfillment of the requirements for
the Degree of Master of Engineering

in the

Department of Mechanical Engineering
University of Canterbury
Christchurch, New Zealand

February 2002

Acknowledgements

I would like to thank my supervisors, Dr John Pearse and Prof Cliff Stevenson of the Department of Mechanical Engineering, University of Canterbury, and Mr. Michael Latimer of D.G. Latimer and Associates Ltd. The results of their guidance, support, and encouragement are embodied in this thesis.

I also wish to thank Mr. Paul Wells, Mr. Bruce Sparks and Mr. Graeme Harris of the of Department of Mechanical Engineering, University of Canterbury, for their expert assistance in the design and construction of the test facility used in this project.

ABSTRACT

The in-duct attenuation performance, or insertion loss, of a range of absorbers was measured, and guidelines for the design and application of absorbers in air ducts were developed from the measured data. A test facility that met the requirements of ISO 7235 was designed and constructed. Insertion loss measurements were made using the test facility to investigate the effects of absorbent material and absorbent thickness, facing type, airflow conditions, and fixing method.

It was found that absorbent flow resistance was the most influential factor in determining the insertion loss of an absorber. The insertion loss of wall absorbers was significantly modified by changes in absorber thickness, which was attributed to the consequential change in flow resistance. Similarly, the insertion loss performance of bar absorbers with significantly varying thickness, and therefore varying flow resistance, was greater than that of bar absorbers with approximately constant thickness.

The insertion loss of wall absorbers was very sensitive to impedance conditions at the boundary between the rear surface of the absorber and the duct wall. Insertion loss performance was improved by applying thin facings to the exposed surface of wall absorbers. Airflow velocity did not affect insertion loss over airflow velocities typical of building services ducts.

Table of Contents

Chapter 1 Literature Survey

Chapter 2 Test Facility Design

Chapter 3 Test Facility Verification

Chapter 4 Absorber Testing

Chapter 5 Project Findings

Appendices

Conventions

The measured data are in one third octave bands, and hence are referred to as frequency bands. To avoid needless repetition much of the discussion refers to frequencies and frequency ranges instead of frequency bands and frequency band ranges.

The insertion loss test facility is located in the Department of Mechanical Engineering, University of Canterbury. It is referred to in uppercase as 'Test Facility'.

This thesis is presented in chapters. A table of contents, list of figures, and list of tables contained within each chapter are presented at the beginning of each chapter. A bibliography and list of references is provided at the end of each chapter.

Project Objectives

The objectives of the project described in this thesis were to measure the in-duct attenuation performance of a range of absorbers, and to develop guidelines for the design and application of in-duct absorbers from analysis of the measurements.

Project Outline

The in-duct absorber design project is presented herein as five chapters: Literature Survey, Test Facility Design, Test Facility Verification, Absorber Testing, and Project Findings. The results of a survey of literature relevant to sound attenuation in air ducts, and a summary of commercially available absorbers for air ducts are provided in the literature survey. The design of the insertion loss test facility is described in the second chapter, and the process by which the performance of the test facility was verified is described in the third. An analysis of the data from the testing program is presented in chapter four, and the results of this analysis are summarized in the concluding chapter.

1

LITERATURE SURVEY

Summary

A survey of local commercially available porous acoustic absorbers for air ducts together with a survey of research relevant to in-duct absorbers was performed to provide a background for the work in this thesis. Porous absorbers consist of a network of interlocking air filled pores that convert incident sound energy to heat. The most commonly used porous absorbing materials are fibreglass, wool, polyester and organic polymer based foams. Facings may be applied to absorbers to modify the attenuation of the absorbing material. Perforations in an absorber facing may be used to further modify the attenuation of the absorber.

Porous absorbers are either non-isotropic, where the absorption of an acoustic wave propagating through the absorber is dependent on direction; or isotropic, where absorption is independent of direction. In locally reacting absorbers propagation of acoustic waves in one or more directions is prevented. Fibrous absorbers are typically non-isotropic, and the majority of foam absorbers are isotropic.

The structure or 'frame' of a porous absorber may be either rigid or elastic. Elastic frames move in response to viscous forces created by an incident sound wave, causing acoustic energy to be absorbed within the fame in addition to the energy absorbed within the pores. Absorption does not occur through this mechanism in rigid framed absorbers.

Porous absorbers are used in ducts in a number of configurations, the most common being a section of ducting lined on one or more sides. Other configurations used are a

centrally located 'pod', one or multiple 'splitters' mounted horizontally or vertically across the duct, or an array of bars mounted with their principle axes parallel to that of the duct. Absorbers that partially obstruct airflow through a duct typically provide a greater attenuation than an equal length of lined duct because they have a greater exposed surface area and greater absorber volume per unit length. Obstruction of the airflow path may generate noise and increase the fan power requirement. Therefore commercially available pods, splitters or bars are shaped to reduce airflow resistance in order to minimise both static pressure drop and self-generated noise.

Table of Contents

1.1 Requirements

Acoustic absorbers for use in air ducts are required to attenuate noise in a duct to the level required. The noise field in a duct is usually generated by air handling plant, and is typically of low frequency. In-duct absorbers must also have a competitive cost to performance ratio.

1.2 Porous Absorbers for Air Ducts

1.2.1 Description

Porous absorbers consist of a network of interlocking air filled pores that increase the viscous forces on the fibre or cell membranes as sound waves propagate through the material, converting sound energy to heat. At high frequencies the gradient velocity, and therefore viscous force inside the material becomes greater, increasing absorption.

Porous absorbers are typically manufactured from fibreglass, wool, polyester, or organic polymer based foams. These materials may be locally reacting, where acoustic propagation through the absorber in the direction of the duct axis is prevented; or bulk reacting, where acoustic waves can propagate in the absorbent parallel to the duct axis. Absorbers can be non-isotropic either through material properties or because of rigid support within the absorber such as webs perpendicular to the duct wall. Fibre based materials such as fibreglass are usually non-isotropic; whereas foam based absorbers are usually isotropic.

Thin facings are applied to absorbers to modify the attenuation characteristic of the absorbing material, often to increase low frequency absorption. The most common facings used with in-duct absorbers are reinforced aluminium foil, fibreglass tissue, spun bonded polyester, and perforated aluminium foil. Rigid framed absorbing materials with a thin facing tend to have a single broad attenuation peak at medium to high frequencies, whereas elastic framed absorbers tend to have two attenuation peaks at low and at medium to high frequency.

Thin facings can be perforated to create additional insertion loss through a Helmholtz resonance mechanism. At low frequencies, insertion loss increases as perforation size increases, and the reverse occurs at high frequencies. A perforated facing can therefore be used to 'tune' an absorber to achieve peak attenuation within a desired narrow frequency band, however attenuation over other frequency bands may be reduced.

Porous absorbers are often used as the absorbing material in duct silencers. Duct silencers are distinct from lined ducts because they can have absorber material that is surrounded by the airstream. Silencer modules are available in a number of configurations, the most common being a centrally located 'pod' (shown in Figure 1), one or more 'splitters' mounted horizontally or vertically across the duct (shown in Figure 2), or an array of bars mounted with their principle axes parallel to that of the duct.

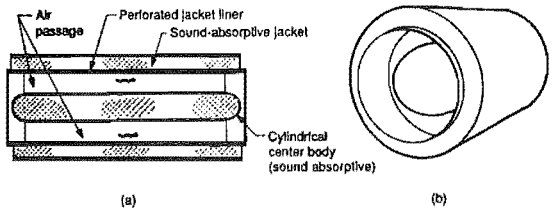

Figure 1: Cylindrical duct silencer in (a) longitudinal section and (b) profile.

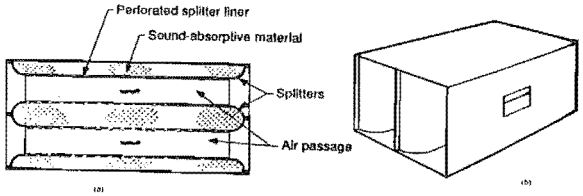

Figure 2: Splitter silencer in (a) longitudinal section and (b) profile.

Splitter silencers provide a greater attenuation than an equivalent length of lined duct because they have a greater exposed area and greater absorber volume per unit length. The greater volume of absorber means that the cross-section of a silencer tends to be smaller than that of the duct in which it is installed, causing resistance to airflow through the silencer. This frequently results in an energy penalty associated with the use of silencer modules. The increased fan power requirement may also increase the fan noise.

Because silencers produce vortices in the airstream they may act as a source of noise within the duct. In commercially available silencers the pods, splitters or bars are shaped to reduce airflow resistance in order to minimise both static pressure drop and self generated noise.

1.3 Theoretical Performance

1.3.1 Material Properties and Geometry

Flow Resistance

The steady flow resistance of a porous layer is the ratio of static pressure drop across the layer and the mean velocity of flow through the layer. This definition assumes that the mean velocity is sufficiently low for the pressure drop to be proportional to velocity. Flow resistance is determined by the equivalent width between fibres or pores in a material, and the number of these per unit area. Flow resistivity is quoted in mks rayls per meter, (or Ns/m^4). Porous materials commonly used for duct attenuation usually have a flow resistivity of 10,000 to 40,000 mks rayls/m.

Kurze and Ver (1972) [1] investigated sound attenuation in ducts with non-isotropic linings. The axial propagation constant was obtained using a transcendental equation that included special cases for a locally reacting lining, and for infinite axial flow resistance. An approximate solution of this equation indicated that optimal attenuation of the fundamental mode would be achieved by a non-isotropic lining with an axial flow resistance that increased with increasing frequency.Bokor [2] found that the attenuation provided by a non-isotropic absorber at low frequency was primarily determined by material properties of the absorber. Thus it was concluded that for non-isotropic absorbers there is a flow resistance in the direction of the duct axis that provides maximum attenuation at low frequencies.

Cummings [3] (1976) compared the results of a theoretical formulation with experimental data for a duct with uniform mean flow lined on two opposite sides with an isotropic porous absorber covered by a perforated facing. The objective of the work was to produce 'design charts' for fibrous absorbent liners for air ducts. Theoretical predictions were found to be in fair agreement with the experimental data.

The effect of varying flow resistance of the absorbent lining on attenuation were investigated. Absorbers of different flow resistance had attenuation peaks at different frequencies, and thus an optimum flow resistance could only be found for a narrow frequency band.

Mass Density

The mass density of an absorber material is the mass per unit volume of the material frame. In elastic absorbers, a portion of the absorption produced by the material can occur via oscillations in the frame. Mass density affects the amount of absorption produced by this mechanism. Mass density does not affect absorption in rigid framed absorbers.

In general, frame borne absorption occurs at low frequency. According to Ingard, there is a transition frequency at which the viscous interaction force on the frame and the inertial force per unit volume are equal. Above this frequency viscous forces are too weak to drive significant oscillations in the frame, thus significant frame borne absorption cannot occur. The transition frequency is calculated from:

$$f = \frac{r}{2\pi M}$$

Where r is the flow resistivity of the material and M the mass density. The range over which frame borne absorption can occur, in terms of the frequency parameter L/λ is therefore:

$$\frac{L}{\lambda} = \frac{r}{2\pi\left(\frac{M}{\rho}\right)}$$

Where L is the thickness of the material, λ is the wavelength, and ρ is the density of the air in the pores of the material.

Structure Factor

Air forced through a porous material is randomly accelerated, causing momentum transfer between air and the frame of the absorber, and a corresponding reaction force on the air. In a model where the motion of air is described in terms of average forward velocity, this interaction between the air and structure can be accounted for in terms of an increase in the inertial mass density of the air. This increase is expressed by a 'structure factor' term. The increase in inertial force on a unit volume of an absorber (frame and air) is partially dependent on viscous interactions, and thus on

frequency. Therefore, structure factor is the sum of a constant and a frequency dependent variable. Kurze and Ver [1] found that the bandwidth over which high attenuation occurred was maximized when the structure factor was near unity.

Thin Facings

Cummings [3] investigated the effect of the orifice size of a thin facing applied to a porous absorber in a duct with mean airflow. Figure 3 shows attenuation per unit length as a function of orifice radius at discrete frequencies. The spacing between orifices remained constant, thus the fraction of open area, or porosity, was proportional to orifice size. For facings with a porosity of less than 40%, it was found that low frequency attenuation was inversely proportional to orifice size, and that high frequency attenuation was proportional to orifice size. This result indicates that the frequency band over which maximum attenuation occurs can be controlled by altering the facing porosity, provided that the porosity does not exceed 40%.

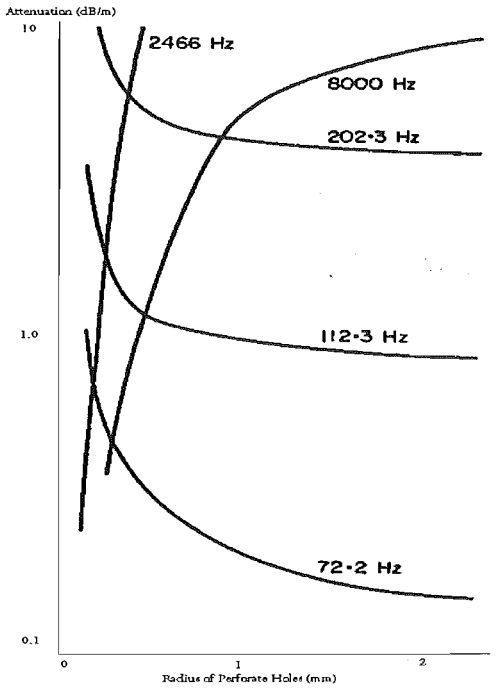

Figure 3: Attenuation per unit length of a porous absorber with perforated facing as a function of perforate orifice radius, [3].

1.3.2 Mode of Propagation

In the work of by Cummings [3], it was found that in most cases the (0, 0) mode was the least attenuated mode; the (1, 0) mode attenuation is always greater than the (0,1) mode, but tends towards it at higher frequencies. The explanation provided for this result is that in the (0,1) mode of propagation in a duct lined on two sides waves are reflected between the unlined walls of the duct, while waves propagate in the same manner as the (0,0) mode between the lined walls (if propagation in the duct is represented by a ray model). As the frequency of the wave increases above cut-on, the ray path per length of duct decreases, and thus the propagation of the (1,0) mode tends toward that of the (0,0) mode. This means that all (m, 0) modes will be more attenuated than the (0, 0) modes, and thus cannot be the least attenuated mode; this is also true of all (m, n) modes, $m > 0$. Any (0, n) mode may be the least attenuated mode.

1.3.3 Airflow

The phase velocity of a plane wave propagating along a duct with mean flow is always increased in the downstream direction by the mean velocity of the airflow through the duct, and decreased by approximately the same amount in the upstream direction. An increase in the phase velocity of a plane wave passing through a duct section with an absorber reduces the amount of time that the wave is resident in the section, thus reducing the amount of time available for absorption.

Plane waves are refracted by the velocity profile that is created across the duct cross-section by friction between moving air and the duct walls. This effect is frequency dependent; higher frequency waves tend to be refracted toward the centre of the duct and lower frequency waves toward the walls. In general, velocity profile diffraction improves the insertion loss of an absorber in the upstream direction and degrades it in the downstream direction.

Pridmore-Brown (1958) [4] performed a mathematical study of a plane acoustic wave propagating in the direction of a fluid flowing through a duct with two opposite lined walls, considering cases where the shear layer had a constant pressure gradient, and when the shear layer was turbulent. Within the shear layer only the lowest mode of propagation was considered. It was found that the acoustic pressure gradient across the duct tended to refract acoustic energy toward the walls, thus increasing

attenuation. This effect was greater at higher frequencies. Where the wavelength was long compared to the shear layer thickness, and at higher flow speeds, attenuation was reduced because of convection of the plane wave increasing its phase speed and thus reducing the amount of energy expended in the absorber per unit length.

Mariano (1971) [5] simulated the effect of boundary layer thickness on attenuation in lined ducts. This work was intended for application to attenuation in lined aircraft engine exhausts, however the general results are relevant to absorption in ducts. It was found that boundary layer refraction shifts the frequency at which peak attenuation occurs. For propagation in the direction of flow, Mariano [5] found that the effects of the boundary layer and of convection on attenuation first noted by Pridmore-Brown [4] were relatively weak. Where propagation was against the direction of flow, both effects were a strong function of Mach number.

When the theoretical results were compared to the experimental data of other authors, Mariano [5] found that the addition of the effects of the boundary layer to the theoretical results improved agreement where propagation was against the direction of the flow. For propagation in the direction of the flow the inclusion of boundary layer effects worsened agreement between experiment and theory. Mariano [5] assumed that the boundary layer did not significantly affect the acoustic impedance of the duct lining, and that each mode of propagation had the same root mean square averaged amplitude, but noted that neither assumption is necessarily correct.

1.4 Practical Performance

Tack and Lambert (1965) [6] compared solutions for the linearised equations for acoustic wave propagation in airflow with attenuation measurements in a duct having two opposite walls lined with a porous fibreglass blanket. The solutions were based on both uniform and power law flow profiles. It was found that attenuation in the upstream direction was greater than that in the downstream direction. It was suggested that this difference was caused by refraction of acoustic plane waves by the boundary layer.

Bokor (1969) [2] measured the characteristic impedance ratio and complex propagation constant of a porous absorber that was both homogenous and isotropic

using a test facility designed to simulate a duct with mean airflow. Bokor [2] compared the data obtained with solutions of Scott's equation [7] for propagation in a lined duct, and thus showed that Scott's equation [7] reliably predicts experimental results for the frequencies and dimensions considered.

Wassileff [8] (1987) performed experimental work to verify the model of Scott [7] for isotropic linings, and the model of Kurze and Ver [1] for non-isotropic linings. A rectangular cross-section duct lined on a single side was used for the experimental work. Lining the duct on one side only restricted propagation to even modes. The duct liners used were 'FH' and 'E' polyurethane foams (isotropic absorbers) manufactured by Vitafoam NZ Ltd, and 'Insulation Blanket', 'Siliner' and 'Hushduct' (non-isotropic absorbers) manufactured by Tasman Insulation. The findings of Wassileff [8] were that Scott's equation [7] correctly predicted the attenuation of non-isotropic polyurethane foam absorbers, and that the model of Kurze and Ver [1] correctly predicted the attenuation of the isotropic fibreglass absorbers over the frequency range investigated.

Cummings and Astley [9] (1987) developed a general finite element formulation for analysis of a duct with uniform mean flow lined with an isotropic porous absorber. The finite element formulation was shown to produce correct results by comparison with the results of analytical expression developed by Cummings [3]. Numerical results for the axial attenuation rate, transverse pressure profile and phase speed were generated for a duct lined on all four sides; with and without mean airflow. These results were found to be in good agreement with experimental data. Design charts for ducts lined on all sides were produced, with duct size and aspect ratio, liner type and flow velocity as the varied parameters.

One of the design charts presented is shown in Figure 4; trends evident from the figure are that the attenuation peak increases as the duct width is reduced (the constant space factor means that liner thickness is proportional to duct width), and greater peaks are achieved at higher frequency (higher frequency waves carry less energy). The sharp peaks in Figure 4 represent changes in the least attenuated mode of propagation.

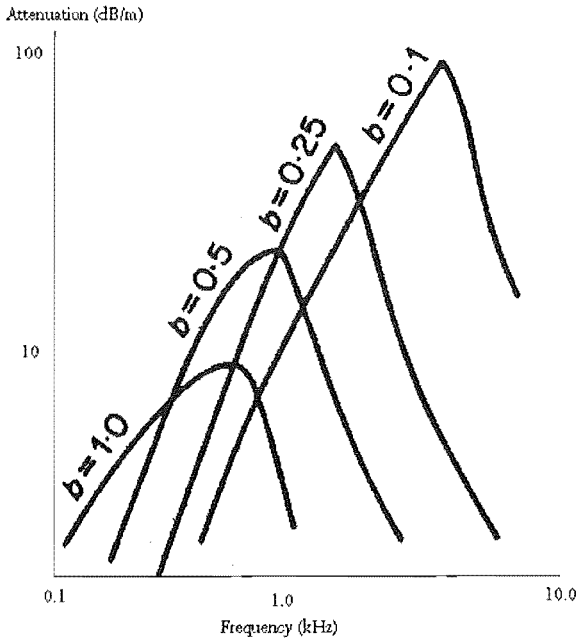

Figure 4: A design chart presented by Cummings and Astley [9] for a porous absorber in a duct with mean flow. Space factor = 75%, Static Flow Resistance = 10 000 SI rayl/m, b = duct width.

The most relevant results of the work performed by Cummings and Astley [9] are that it is more effective to distribute a liner over all four sides of a duct rather than lining only two, and that even at Mach 0.053, the effects of mean flow caused a 50% difference between attenuation of waves travelling with and against the direction of flow.

Cummings and Astley (1996) [10] also developed a finite element formulation for bar silencers inside a rigid walled duct with uniform mean flow. Comparison was made between the attenuation performance of the bar silencers investigated and those of the 'equivalent' splitter silencer and lined duct. Equivalent bar silencers, splitters and lined ducts were given the same absorbent volume, and similar pressure drop characteristics.

The insertion loss of the bar silencers was measured using a test facility that met the requirements of ISO 7235 [11]. The authors found that bar silencers were more effective than equivalent splitters and lined ducts at lower frequency, and that lined ducts had greater insertion loss over mid-range frequencies than equivalent bar or

splitter silencers. It was also found that airflow did not affect silencer performance at low frequencies.

1.5 Survey of Commercial Absorbers

A survey of absorbers available in New Zealand and overseas markets for use in air ducts was carried out to select a range of porous materials and facings for the testing program. All of the products identified are used to line duct walls, with the exception of Soundpac, a bar absorber that is suspended in the centre of the duct. The information collected in the survey is presented in below.

Product	Manufacturer	Description	Performance
Basotech	BASF	Open-celled melamine resin foam	Not available
Soundpac	Lamatherm	Triangular cross section bar silencer made from open-celled melamine resin foam	Not available
Deci-Foam ALR	I.N.C	Polyether foam laminated to aluminium foil facing	25 mm: NRC = 0.61
Deci-Foam F	I.N.C	Polyether foam laminated to vinyl film facing	50 mm: NRC = 1.0 25 mm: NRC = 0.78 12 mm: NRC = 0.51
Autex Acoustic Blanket (AAB)	Autex	Thermally bonded polyester foam	Not available
Autex Rigid Duct Insulation (ARD)	Autex	Thermally bonded polyester foam laminated with 10% free area perforated foil	Not available
Acoustop Absorber-Liner	D.G Latimer & Associates	Polyether Foam	NRC = 0.55
Ductliner	INZCO	Semi-rigid glass wool bonded with thermosetting resin.	25mm: NRC = 0.67 50mm: NRC = 0.94
Siliner	INZCO	Ductliner faced with random felted fibreglass mat	25mm: NRC = 0.67 50mm: NRC = 0.94
Ductwrap	INZCO	Flexible glass wool blanket bonded with thermosetting resin	Not available
Hushduct	INZCO	Rigid glass wool board bonded with thermoset resin, and faced with Flamestop 524, a glass reinforced foil laminate	No air Gap: NRC = 0.71 400mm Air gap: NRC = 0.68, but gives 0.58 at 125 Hz
Ductliner Perforated Sisalation	INZCO	Rigid glass wool board bonded with thermoset resin, faced with perforated Flamestop 530 foil laminate, 10% open area	25mm: NRC = 0.54 50mm: NRC = 0.70
Acoustic Estafoam	INZCO	Open celled urethane foam	Absorption peak of 0.94 at 1000 Hz, 0.1 at 125 Hz
Supertel Glasswool	CSR Bradford	Random felted glass wool board bonded with thermosetting resin	50mm: NRC = 1.0 50mm PFF: NRC = 1.0 75mm: NRC = 1.1
Ultratel Glasswool	CSR Bradford	Random felted glass wool board bonded with thermosetting resin	Not available
Flexitel	CSR Bradford	Flexible glasswool board or blanket bonded with thermosetting resin	25mm: NRC = 0.70 25mm PFF: NRC = 0.8 50mm: NRC = 0.90 50mm PFF: NRC = 1.0

Ductel Glasswool	CSR Bradford	Glasswool board bonded with thermosetting resin	25mm PFF: NRC = 0.88 25mm BMF: NRC = 0.88 50mm PFF: NRC = 1.07
Quietel Glasswool	CSR Bradford	Glasswool board bonded with thermosetting resin	Not available
Exacto Board Glasswool	CSR Bradford	Glasswool board bonded with thermosetting resin	Not available
Blackseal MSB Glasswool	CSR Bradford	Random felted, resin bonded glasswool mat, with black surface treatment on one face	25mm Sprayed Facing: NRC = 0.58
Attenuliner Glasswool	CSR Bradford	Flexible glasswool board bonded with thermosetting resin, one side faced with glass tissue	25mm Tissue Facing: NRC = 0.72 25mm Tissue Facing: NRC = 0.99
Linacoustic Gasswool	CSR Bradford	Random felted, resin bonded, glasswool board faced with glass tissue	25mm Tissue Facing: NRC = 0.72
Fibertex-R4 Ductliner	CSR Bradford	Batts or blanket. Mixture of molten natural rock and blast furnace waste material bonded with thermosetting resin	25mm: NRC = 0.72 50mm: NRC = 1.02 25mm CF/BMF: NRC = 0.82 50mm CF/BMF: NRC = 1.15 25mm PFF: NRC = 0.76 50mm PFF: NRC = 1.02 25mm: NRC = 0.78
Fibertex-R4 Ductliner	CSR Bradford	Batts or blanket. Mixture of molten natural rock and blast furnace waste material bonded with thermosetting resin	50mm: NRC = 1.09 25mm CF/BMF: NRC = 0.79 50mm CF/BMF: NRC = 1.11 25mm PFF: NRC = 0.85 50mm PFF: NRC = 1.02

1.6 Bibliography

Ingard, K. U. (1994) 'Notes on Sound Absorption Technology', Noise Control Foundation, Arlington Branch, Poughkeepsie NY, USA.

1.7 References

1. Kurze U.J., Ver I.L. (1972), "Sound attenuation in ducts lined with non-isotropic material", Journal of Sound and Vibration **24**(2), 177-187.
2. Bokor, A. (1969), "Attenuation of sound in lined ducts", Journal of Sound and Vibration **10**(3), 390-430.
3. Cummings A. (1976) "Sound attenuation in ducts lined on two opposite walls with porous material, with some application to splitters", Journal of Sound and Vibration **49**(1), 9-35.
4. Pridmore-Brown, D.C. (1958), "Sound propagation in a fluid flowing through an attenuating duct", Journal of Fluid Mechanics **4**, 393-406.
5. Mariano, S. (1971), "Effect of shear layers on attenuation in acoustically lined rectangular ducts", Journal of Sound and Vibration **19**(3), 261-275.
6. Tack D., Lambert F. (1965), "Influence of shear flow on sound attenuation in a lined duct", Journal of the Acoustical Society of America 38, 655-666.
7. Scott, R.A (1946), "The absorption of sound in a homogenous porous medium", Proceedings of the Physical Society **58**, 165-183.
8. Wassilef C. (1987), "Experimental verification of the duct attenuating model with bulk reacting linings", Journal of Sound and Vibration **114**(2), 239-251.
9. Astley R.J., Cummings A. (1987), "A finite element scheme for attenuation in ducts lined with porous material: comparison with experiment", Journal of Sound and Vibration **116**(2), 239-263.
10. Astley R.J., Cummings A. (1996), "Finite element computation of attenuation in bar-silencers and comparison with measured data", Journal of Sound and Vibration **196**(3), 351-369.

11. International Standard ISO 7235 1991 'Acoustics - measurement procedures for ducted silencers - insertion loss, flow noise and total pressure loss'.

2

TEST FACILITY DESIGN

Summary

A test facility for measuring the attenuation performance of acoustic absorbers in air ducts was designed and constructed. The test facility was required to:

1. Meet the requirements of an internationally recognised technical standard.
2. Accurately replicate the acoustic and airflow conditions of a typical air duct.

It was determined from a survey of relevant literature that an insertion loss test facility best met these requirements. Insertion loss test facilities can include sections of sheetmetal ducting, and thus accurately replicate the acoustic and airflow conditions of a typical air duct.

The test facility design was based on the requirements and recommendations of ISO 7235 – 'Acoustics – measurement procedures for ducted silencers – insertion loss, flow noise and total pressure loss'. All the requirements of ISO 7235 were not met, however the test facility design was deemed sufficient for the technical requirements of the project.

Table of Contents

2.1 Introduction

Test facilities described in the literature relevant to attenuation measurements in air moving ducts use the impedance tube method, as described by Delany & Bazely [1], Wassilief [2], and Bokor [3], or the insertion loss method, as described by, Cummings [4], and Cummings & Astley [5]& [6].

In the impedance tube, a standing wave is excited in a duct with a reflective termination and at least one wall lined with the test material. The root mean square (rms) pressure maxima, $P_{rms}^{\max}$, and minima, $P_{rms}^{\min}$, of the standing wave are measured by traversing a microphone along the longitudinal axis of the duct. The absorption coefficient α of the absorber is then calculated from:

$$\alpha = 1 - \left[\frac{SWR - 1}{SWR + 1}\right]^2$$

where:

$$SWR = \frac{P_{rms}^{\max}}{P_{rms}^{\min}}$$

In the insertion loss method a sound field is created in a duct connected to a duct containing the test absorber. The sound pressure is measured at the entrance and exit of the test duct, then a duct without absorbing material (called the substitution duct) replaces the test duct and the measurement is repeated. In the work reported here, the insertion loss of the absorber is calculated from:

$$IL(f) = [SPL_1(f) - SPL_2(f)] - [SPL_{1S}(f) - SPL_{2S}(f)]$$

Where IL is insertion loss, SPL is sound pressure level in (dB re 1μPa), and f is frequency in Hz. The subscripts 1 and 2 indicate the SPL at the entrance and exit respectively, and the subscript s indicates the presence of the substitution test duct.

The impedance tube method has the advantage that the test duct does not require a perfectly absorbing termination, as is the case in the insertion loss test method. Because perfectly absorbing (anechoic) terminations are very difficult to create,

insertion loss test facilities typically have axial standing waves in the test duct that reduce the accuracy of the attenuation measurements. The test duct of an impedance tube test facility requires a perfectly reflecting termination, which is much easier to achieve.

Despite the greater design and construction difficulties, the insertion loss method was selected for use in this project. This selection was made because the termination of an insertion loss test facility can be open, which allows mean airflow through the test duct. The termination of an impedance tube test facility must be reflective, and therefore closed. The test duct of an insertion loss test facility is therefore more representative of a typical lined duct.

Wassilieff [2] used the apparatus shown in Figure 1 to measure the axial propagation constant of various modes of propagation in a lined duct. The test duct was lined on one side, with the wall opposite the lined side being reflective. This made the duct equivalent to one of twice the width with two lined sides. Because the first odd mode of propagation in a standing wave has a single velocity maximum along the centre, lining the tube on one side prevents that mode from propagating.

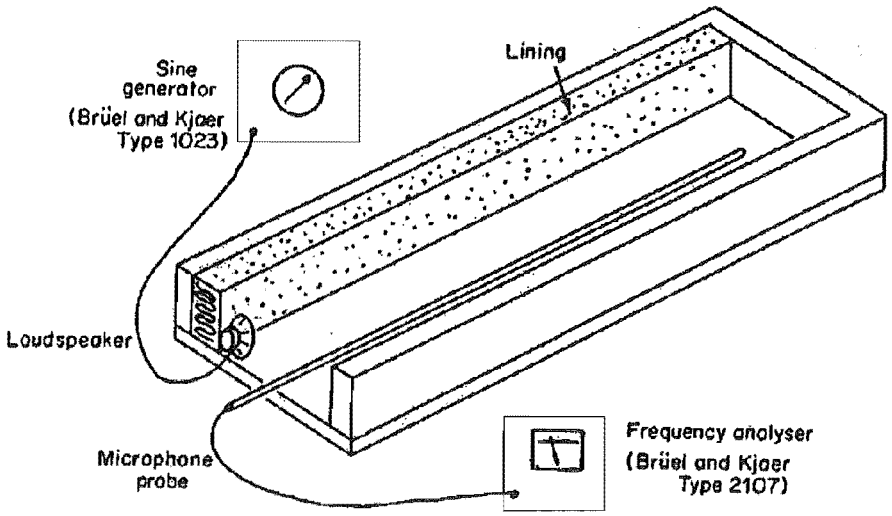

Figure 1: Arrangement of the standing wave test facility used by Wassilieff.

The test facility used by Wassileiff [2] allowed a maximum equivalent gap of 500 mm between the two absorbing sides (250 mm between the lined side and the reflective

wall), and a fixed gap of 95 mm between the two unlined sides (the top and bottom of the tube). The separation of 95mm was designed to correspond to the wavelength of the cut-off frequency of the first mode of propagation.

Bokor [3] used a 1000 mm impedance tube of variable rectangular cross section to measure the attenuation properties of a fibreglass blanket. The top and bottom walls were constructed of 18 mm thick transparent acrylic and had a constant separation of 100 mm. The sidewalls were constructed from 42.5 mm thick acrylic sheet, and could be slid between the top and bottom walls, allowing the cross section of the tube to be varied to a maximum separation of 400 mm. The sidewalls were lined with the test absorber.

Cummings [4] used an insertion loss test facility to measure the attenuation produced by lining as duct on two opposite sides with polyurethane foam. The test section was constructed from standard galvanised steel sheet in order to ensure that its attenuation behaviour was similar to that of a typical duct. The test facility used by Cummings [4] is shown in Figure 2. Four loudspeakers were mounted in a plane at an end the facility, allowing specific modes of propagation to be excited by differentiating the phase of each of the sources.

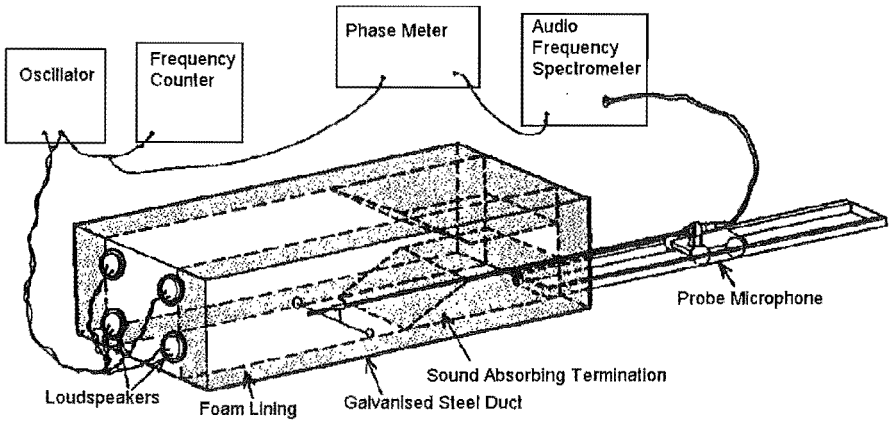

Figure 2: The axial traverse test facility used by Cummings [4].

Astley and Cummings [5] used insertion loss test facilities (referred to as Duct 1 and Duct 2 by the authors) to assess the effectiveness of lining a duct on all four sides. The

arrangement of the test facilities used by Astley and Cummings [5] is shown in Figure 3.

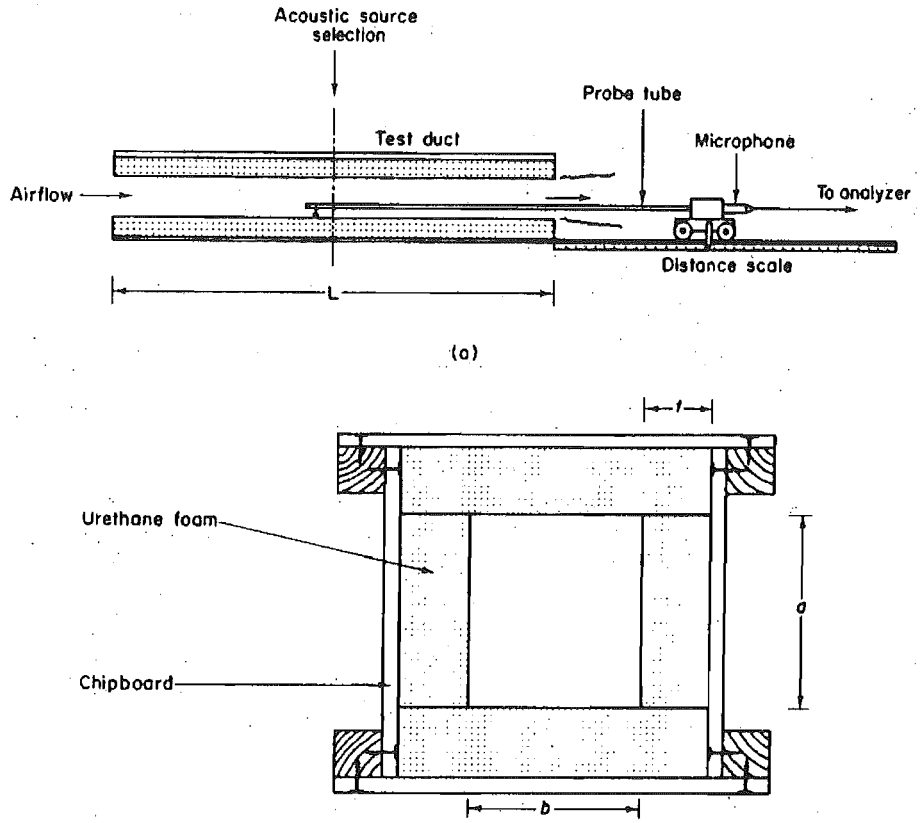

Figure 3: The arrangement of axial traverse test facilities used by Astley and Cummings [5].

Duct 1 was constructed from chipboard, and had a rectangular airway of 151 mm x 101 mm cross-section and 3000 mm length. The duct was lined with 49.5 mm thick urethane foam. Four 'tweeter' loudspeakers mounted in the centre of the duct provided a pure tone acoustic signal. The use of four loudspeakers allowed specific modes of propagation to be excited. Mounting the loudspeakers in the centre of the duct allowed the attenuation of acoustic waves propagating with and against the direction of mean flow to be measured. Airflow was provided by placing the duct in a wind tunnel. Duct 2 had a rectangular airway of 50 mm x 38 mm and 1000 mm length. This duct was constructed from chipboard and lined with urethane foam. A single loudspeaker was used to preferentially excite the first mode of propagation. Three axial fans mounted in series provided mean flow.

Axial and transverse sound pressure measurement traverses were performed in the airways of both ducts using a probe microphone. The probe microphone had a

smooth pointed tip and a sensing hole in the sidewall was used to minimise flow separation when placed in the airstream. Because of reflection of acoustic waves at the open ends of the duct, measurement points were restricted to the central region of the duct where the reflected waves were well attenuated.

In more recent work, Astley and Cummings [6] used an insertion loss test facility that was based on therequirements and recommendations of ISO 7235 [7] to experimentally determine the attenuation characteristics of bar silencers. The general arrangement of the test facility is shown in Figure 4. The duct walls were constructed from 24 mm plywood with an outer cladding of lead, giving a surface density of 32 kg/m^2. Maximum airflow of 17 m^3/s was provided by an axial fan. Noise from the fan was attenuated by two rows of staggered absorbing baffles on the outlet. An anechoic termination was used to attenuate plane wave reflections at the outlet of the test facility, and to prevent noise entering the test facility from the outlet end.

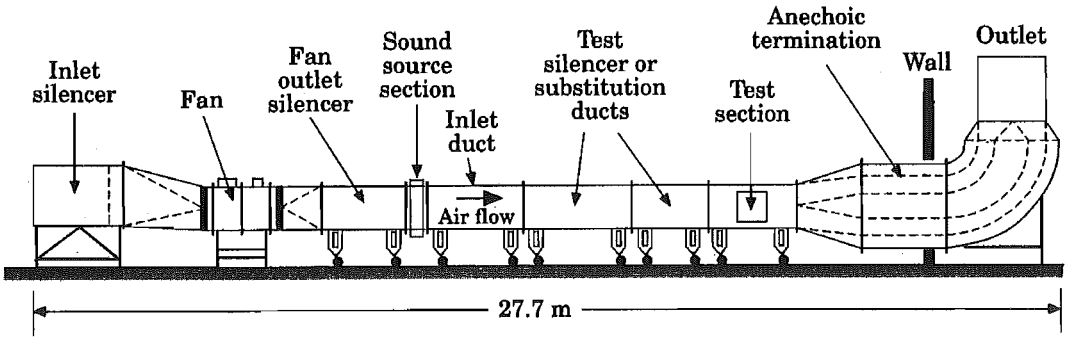

Figure 4: The test facility used by Astley and Cummings [6].

A broadband random noise acoustic field was excited by four 600 W bass speakers mounted in the duct walls powered by random noise generator and a 1.6 kW power amplifier. Measurements of the sound pressure level in the test section were made using a Bruel & Kjear (B&K) type 4133 microphone fitted with a B & K type UA0436 turbulence screen and a two channel FFT analyser. The microphone was traversed on a rail fitted diagonally across the test section by an electrically driven lead screw, and the sound pressure level measured at three separate positions. The logarithmically averaged sound pressure level over these three points was used to determine the insertion loss of the bar silencers.

2.2 Requirements

The requirements for the test facility to be used for the experimental work were:

1. The test facility had to comply with a recognised technical standard to validate data collected from it.
2. The test facility was required to accurately replicate a typical absorber in an air duct.

To satisfy requirement 1, the test facility was designed to meet the requirements of the ISO 7235 [7]. This standard specified that test facility for the measurement of the insertion loss of an in-duct absorber must consist of the following items:

1. A fan to provide airflow.
2. A device for varying the flow rate.
3. A device for measuring the flow rate.
4. Sound source equipment.
5. Sound measurement equipment.
6. Ducts on the source side and receiving side of the test duct.
7. Transitions to connect ducts of different cross-section.
8. A substitution test duct.
9. An anechoic termination on the receiving side of the test duct.

2.3 Description

The test facility was designed and constructed accordance with the requirements of the ISO standard 7235 [7], stated above. The general arrangement of the test facility is shown in Figure 5.

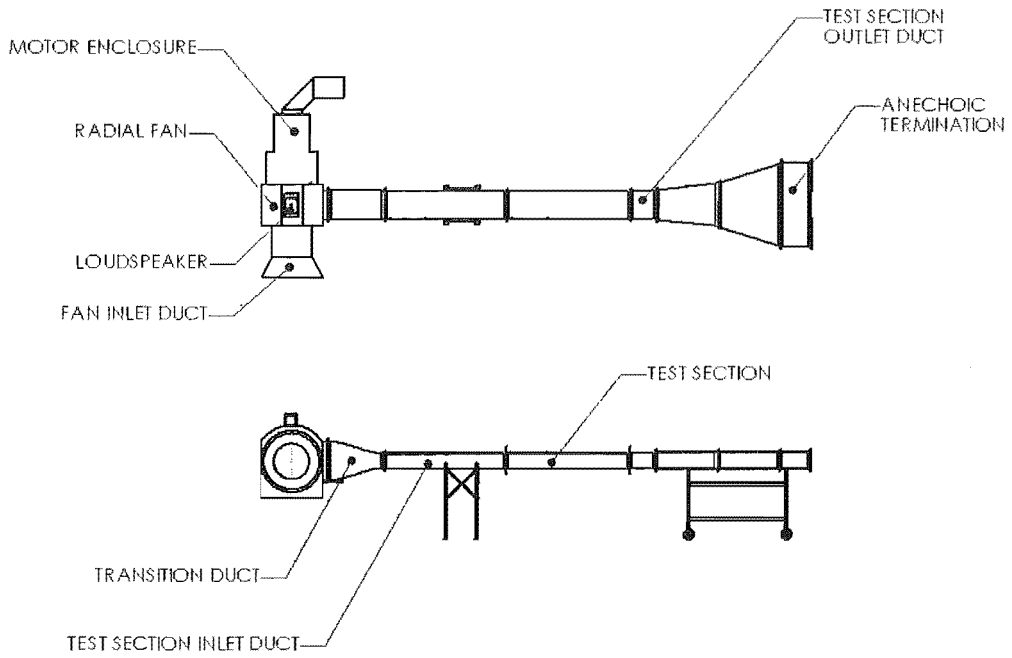

Figure 5: Principal elements of the test facility

2.3.1 The Length Constraint

The maximum length available in the room that housed the test facility was 7.7 m, less than the length needed to meet the requirements of ISO 7235 [7]. To comply with this constraint the length of the transition duct was made shorter than that called for by ISO 7235 [7], and the outlet test duct was incorporated into the anechoic termination. These measures produced a reduction in length sufficient for the entire test facility to be contained within the room with the exception of the anechoic termination.

2.3.2 Fan

An already available eight blade centrifugal flow radial fan manufactured by Taylor's Ltd of Christchurch, New Zealand, was used to provide airflow through the test facility.

2.3.3 Device for Varying the Flowrate

The flow rate was varied by changing the fan speed with a three-phase motor controller.

2.3.4 *Device for Measuring the Flowrate*

Two arrays of four Pitot rakes, one of which is shown in Figure 7, were used to measure the dynamic pressure distribution across the inlet and outlet of the Test Section Duct. Pitot tubes mounted flush with the walls were used to measure static pressure in the Inlet Duct and Outlet Duct.

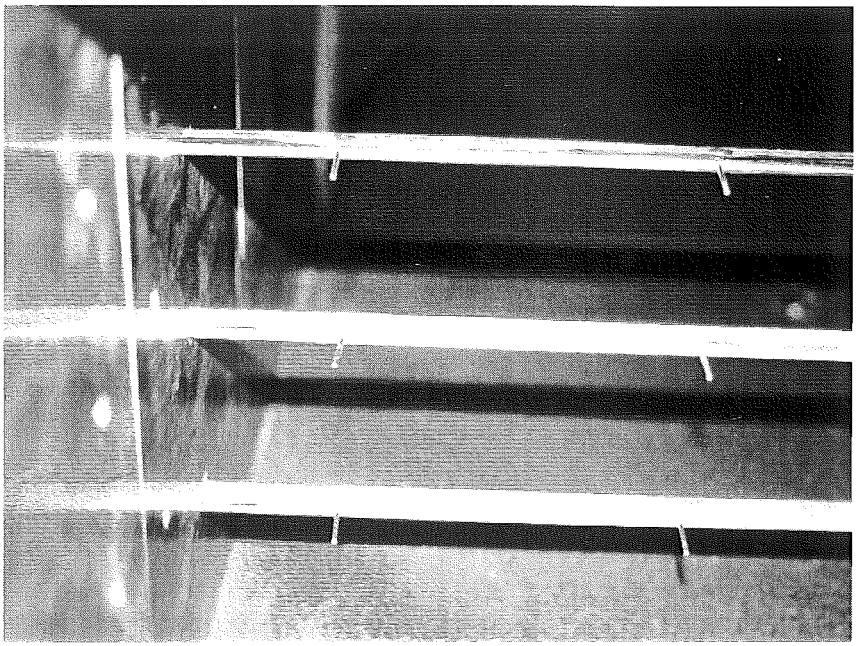

Figure 6: Pitot rake array.

2.3.5 *Sound Source Equipment*

Noise was generated inside the test facility by a loudspeaker mounted over the inspection port on top of the fan casing (as shown in Appendix 1, Drawing ASSY). A Sony type F210 power amplifier powered the loudspeaker, and a Neutrik Minirator type MR1 audio generator provided a pink noise signal.

To make the sound field similar to that in a typical air duct, the sound source equipment was designed to excite many modes of propagation.

2.3.6 *Sound Measurement Equipment*

The sound measurement equipment consisted of two B&K type 4189 condenser microphones with B&K type UA0386 nose cones connected via type JZ0102 dual channel adaptor to a B&K 2260 sound analyser. The microphone assemblies were mounted in the ducts with 'shotgun' microphone holders, shown in Figure 7;

designed to minimize airflow noise. Four different mounting locations, shown in Figure 8, were used for the microphones so that the nodes of transverse standing waves were avoided.

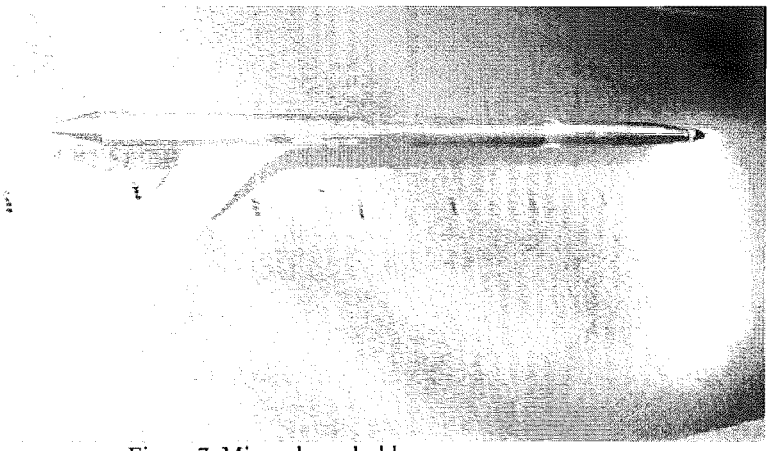

Figure 7: Microphone holders

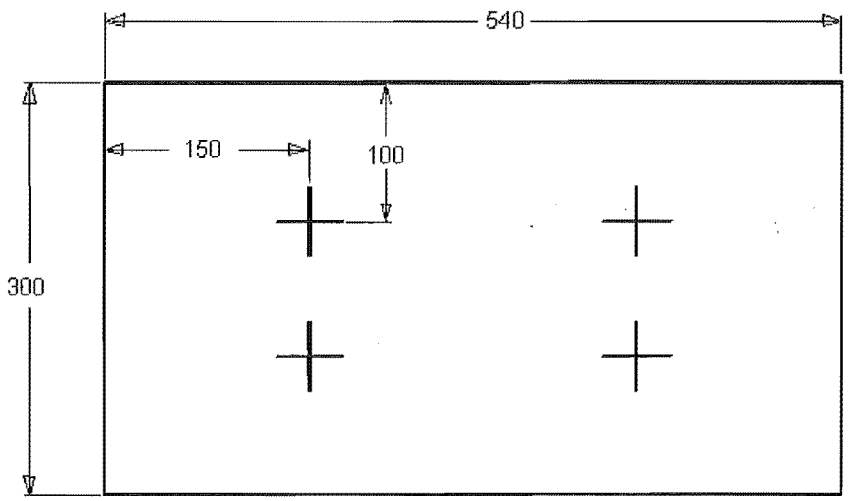

Figure 8: Sound pressure measurement positions.

2.3.7 Transition Duct

Because the cross-section of the fan outlet was larger than the cross section of the inlet side test duct, a contracting transition duct (Appendix 1, Drawing 1) was required. ISO 7235 [7] standard requires that all the maximum angles enclosing the sides of a transition be 15°, and that the minimum length be given by:

$$\frac{l_{\min}}{l_{\max}} = \frac{A_s}{A_l} - 1$$

Where A_l represents the larger area and A_s the smaller. This requirement could not be met because of the constraint on the length of the test facility. The intention of the requirements for transitions in ISO 7235 [7] is to reduce the turbulence caused by a change in duct cross-section to an acceptable level. Therefore, the transition duct was designed with a sinusoidal profile to minimise any turbulence, and to provide a uniform flow. The flow at the entry to the test section would probably be superior to that of a straight transition duct.

The transition duct was manufactured from 12 mm MDF board and 5 mm plywood. The use of sheet metal for the transition duct was avoided because air leaving the fan was directed onto the top wall of the duct, meaning that an unacceptable level of noise may have been generated if the walls had been as flexible and as resonant as sheet metal.

2.3.8 Ducts

The requirements for ducts in ISO 7235 [7] are that each duct be at least as long as half the wavelength of the lowest centre frequency of interest, and not less than four times the maximum duct cross-dimension. In addition, the ducts were required to be straight for a minimum of five times the equivalent diameter of the duct to ensure that the profile of the flow passing through the test section was fully developed. To satisfy the requirement that the test facility replicate the conditions of a commercial silencer installation as closely as possible the test ducts were constructed from 18 gauge steel sheet by Johnson Engineering Ltd of Christchurch using standard industry fabrication techniques.

A duct of 540 mm width, 300 mm height and 2400 mm length (the 'Test Section Inlet Duct' shown in Appendix 1, Drawing 2) was used to allow a stable airflow profile to develop before the entry of the Test Duct. A duct of 540 mm width, 300 mm height and 2400 mm length (the 'Test Section Outlet Duct' shown in Appendix 1, drawing 5) was placed between the exit of the Test Duct and entry of the Anechoic Termination. The purpose of the Test Section Outlet Duct was to contain instrumentation.

Flanges were attached to each end of the test ducts to so that they could be bolted to the other test facility elements. Countersunk rivets were used to fasten the flanges to the duct, with the countersunk hole on the inside of the duct to minimise flow noise due to the rivets interacting with the airstream. The Test Section Inlet Duct was designed with a removable lid to allow access to the microphone and Pitot rake mounted inside it. It was not necessary to have a lid on the outlet test duct because it was only 500 mm long, allowing access from the open ends.

In order to reduce the length of the test facility and thus comply with the space constraint, the anechoic termination was incorporated into the outlet test duct. The test ducts used in the test facility were therefore fully compliant with the requirements stated in section 2.2 'Requirements', including those of ISO 7235 [7].

2.3.9 Test Section Duct

The 'Test Section Duct' is shown in Figure 9, and in Appendix 1, drawing 5. Three Test Section Ducts were constructed to allow absorbers of 25 mm, 50 mm 75 mm to be tested with a constant airflow cross-section. Johnson Engineering Ltd constructed the ducts for the test silencer ducts using standard industry fabrication techniques and materials, thus meeting requirement 2 of section 2.2 'Requirements'.

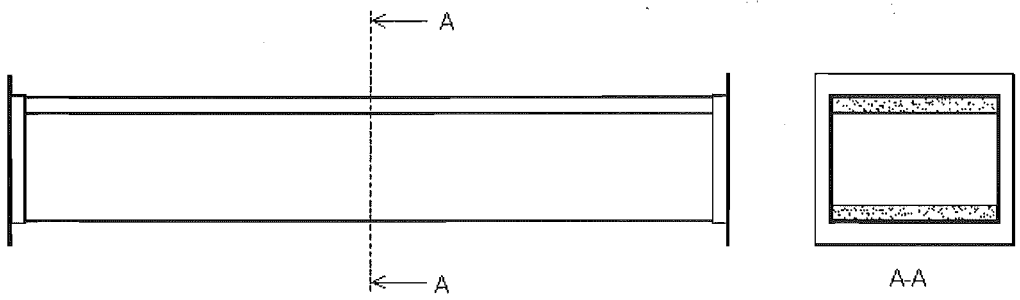

Figure 9: Configuration of wall absorbers in the Test Section Duct.

2.3.10 Anechoic Termination

An anechoic termination (shown in Appendix 1, Drawing 6) was attached to the Outlet Test Duct to attenuate plane wave reflections at the outlet of the test facility, and thus prevent standing waves in the Test Section Inlet Duct, Test Section Duct and Test Section Outlet Duct. ISO 7235 [7] imposed a maximum permissible Pressure wave Refection Coefficient (PRC) on the anechoic termination. The PRC is found from:

$$PRC = \frac{10^{\Delta L/20} - 1}{10^{\Delta L/20} + 1}$$

Where ΔL is the difference between the maximum and minimum sound pressure level along the longitudinal axis of the Test Duct. The PRC of the anechoic termination is compared to the P.R.C requirement of ISO 7235 in Table 1.

Table 1: Maximum permissible and actual pressure wave reflection coefficients

1/3 Octave Band Centre Frequency (Hz)	Maximum PRC (ISO 7235)	PRC of the Anechoic Termination
50	0.4	0.15
63	0.35	0.15
80	0.3	0.07
100	0.25	0.07
> 125	0.15	0.075

The design of the anechoic termination was based on a design suggested in Annex D of the ISO 7235 [7] standard. The duct through the centre of the anechoic termination had a constant cross section of 540 mm x 300 mm. Polyester absorber was placed on both sides of the anechoic termination with a thickness varying from 0 mm to 600 mm to provide broadband absorption.

2.3.11 Fan Inlet Duct

The inlet duct of the fan was lined with 50 mm polyether polyurethane foam to attenuate noise entering the fan, and thus the other test elements, and to attenuate noise leaving the fan via the inlet duct. It was necessary to attenuate the noise leaving the fan inlet duct because it would have increased the level of the sound field in the room, thus contributing to break-in noise in the test ducts and test silencer.

2.3.12 Fan Motor Noise Enclosure

A noise enclosure was required to attenuate the noise produced by the three-phase switching gear of the fan motor. A photograph of the noise enclosure is shown in Figure 10, and drawings of the noise enclosure are shown in Appendix 1, drawing 9. The enclosure was extended to cover the entire motor and shaft assembly, and thus avoid the problem of sealing the enclosure around the shaft.

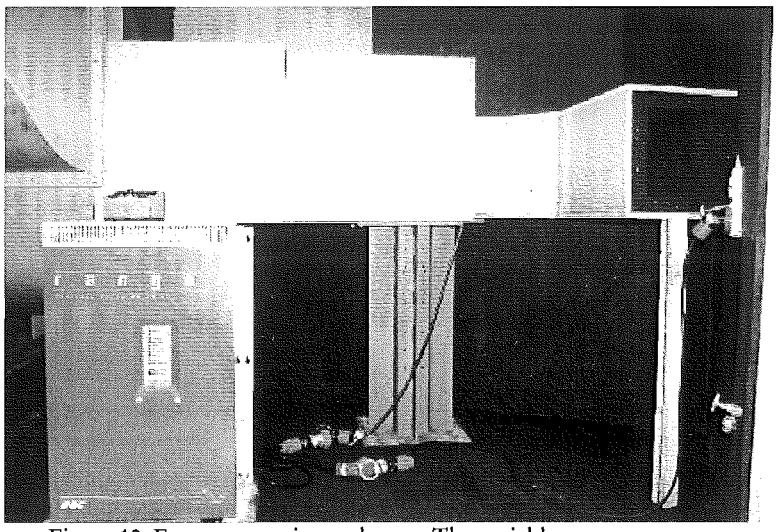

Figure 10: Fan motor noise enclosure. The variable frequency speed controller is shown in the foreground.

The noise enclosure was constructed from 18 mm MDF board, a material with adequate stiffness and density. The interior of the noise enclosure was lined with 50 mm thick Acoustop acoustic foam. The arrangement of acoustic lining in the noise enclosure is shown in Appendix 1, drawings 9A and 9B in.

The motor was cooled by forced convection along fins arranged around the outside of the windings, parallel to its main axis. Convection was driven by a fan attached to the shaft of the motor that drew air through a short annular duct and over the cooling fins. To ensure that the airflow over the cooling fins was not altered the inlet and outlet sides of the duct were separated with a partition around the outer wall of the duct (shown in Appendix 1, Drawing 9-3). A duct with two 45° corners and 50 mm Acoustop foam lining (shown in Appendix 1, Drawing 9-7) was extended from the inlet side of the noise enclosure to attenuate noise radiating for the inlet of the annular duct. Two outlet ducts were used to ensure that there were no areas of stagnation in the flow through the enclosure, which could cause an accumulation of heat.

2.3.13 Room

The room containing the test facility was acoustically treated to reduce the level of the noise field surrounding the test facility. The walls of the room that contained the test facility were lined with 50 mm Acoustop acoustic foam glued to 50 mm battens,

creating a 50 mm cavity behind the absorber material, to attenuate the noise field external to the test ducts and test silencer. The ceiling was covered with 50 mm polyester board held in place by battens. These acoustic treatments are shown in Figure 11 and Figure 12. The floor of the room was covered with cut-pile carpet on heavy duty underlay.

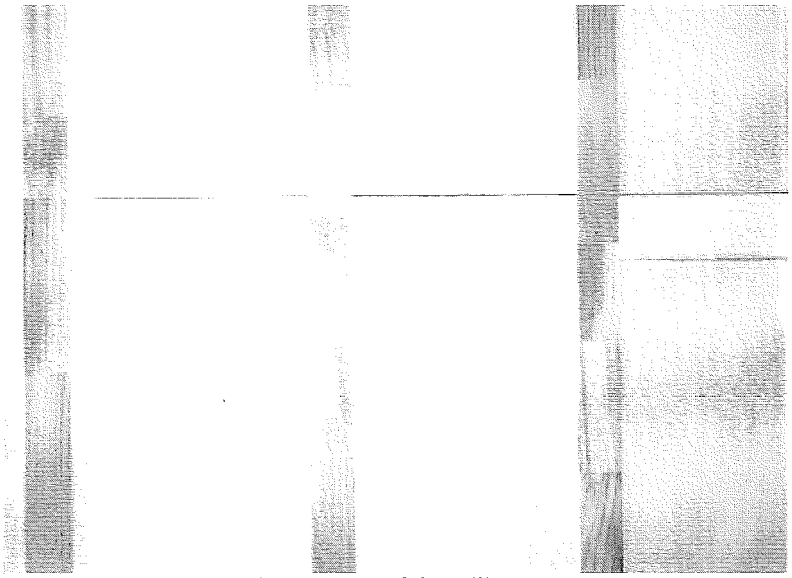

Figure 11: Acoustic treatment of the ceiling.

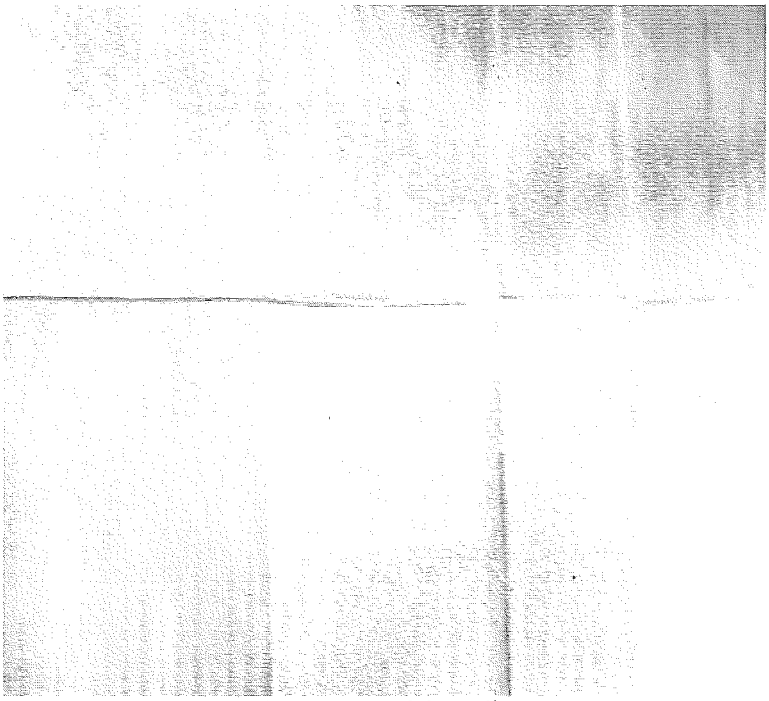

Figure 12: Acoustic treatment of the walls.

2.4 Bibliography

Cummings, A., "Building Services Noise – Acoustics of Air-Moving Ducts", Department of Mechanical Engineering, The University of Canterbury, Christchurch New Zealand.

2.5 References

1. Delany, M.E., Bazely, E.N. 1970, *Applied Acoustics* **3**, 105-117, Acoustical properties of fibrous absorbent materials.
2. C. Wassilieff 1987 *Journal of Sound and Vibration* **114**, 239-251, Experimental verification of duct attenuation models with bulk reacting linings.
3. A. Bokor 1969 *Journal of Sound and Vibration* **10**, 390-403 Attenuation of sound in lined ducts.
4. A. Cummings 1976 *Journal of Sound and Vibration* **49**, 9-35 Sound attenuation in ducts lined on two opposite walls with porous material, with some applications to splitters.
5. A. Cummings and R.J. Astley 1987 *Journal of Sound and Vibration* **116(2)**, 239-263 A finite element scheme for attenuation in ducts lined with porous material: comparison with experiment.
6. A. Cummings and R.J. Astley 1996 *Journal of Sound and Vibration* **196**, 351-369 Finite element attenuation in bar silencers and comparison with measured data.
7. International Standard ISO 7235 1991 'Acoustics – measurement procedures for ducted silencers – insertion loss, flow noise and total pressure loss'

3

TEST FACILITY VERIFICATION

Summary

The performance of the test facility was verified to ensure that data produced by the test program would be meaningful and repeatable. In the verification process the performance of each element of the test facility was evaluated in terms of the requirements of the ISO 7235.

From the literature survey it was known that the noise field inside the test duct, and the profile of the airflow through the test duct influences the insertion loss of in-duct absorbers. Therefore, these parameters were also investigated to assist with the interpretation of measured data from the test program. It was verified that:

1. Sound entering the test duct via indirect direct paths was at least 10 dB lower that the sound entering via the fan outlet.
2. The anechoic termination limited the pressure reflection coefficient in the duct below the maximum specified in ISO 7235.
3. The self-generated noise of microphone holders in airflow did not significantly affect the signal from the microphones.
4. The airflow instrumentation accurately measured differences in dynamic pressure over the cross-section of the inlet and outlet ducts, and the static pressure inside the ducts.

A requirement of the project, that the Test Ducts and Substitution Test Duct must have similar acoustic properties to those of a typical sheetmetal duct, was also verified. There was significant variation in Sound Pressure Level (SPL) over the cross-section of the Test Ducts. Therefore, it was decided that the SPL should be measured

at four positions within the reference planes and an average of the measurements be used in the insertion loss calculations.

Contents

3.1 Introduction

The performance of the test facility was verified to ensure that data produced by the test program would be meaningful and repeatable. In the verification process the performance of each element of the test facility was evaluated in terms of the requirements of the ISO 7235 [1].

From the literature survey it was known that the noise field inside the test duct, and the profile of the airflow through the test duct influences the insertion loss of in-duct absorbers. Therefore, these parameters were also investigated to assist with the interpretation of measured data from the test program.

3.2 Discussion

3.2.1 Break-in Noise

A requirement of ISO 7235 [1] is that the Sound Pressure Level (SPL) of noise entering the Test Section Inlet Duct, Test Section Outlet Duct and Test Section Ducts via paths other than the fan outlet is at least 10 dB lower than the SPL of noise entering these ducts via the fan outlet.

A transmission barrier (30 mm MDF) was inserted between the transition and inlet ducts. The barrier attenuated the direct propagation path from the loudspeaker, through the fan enclosure, to the test duct. The Sound Source Equipment was used to generate a sound field of 80 dB inside the fan casing. The SPL of the sound field in the fan casing and at the reference microphone positions is shown in Figure 1. Because the direct path between the fan casing and the reference microphone positions was blocked, the SPL by the microphones was due to:

1. Propagation through the inlet silencer and break-in through the duct walls.
2. Propagation through the inlet silencer and entry through the exit of the anechoic termination.

Figure 1 shows the difference between the SPL of the field in the fan casing and the field in the ducts. The minimum difference is 13 dB, therefore the test facility meets the requirement of the ISO 7235 [1].

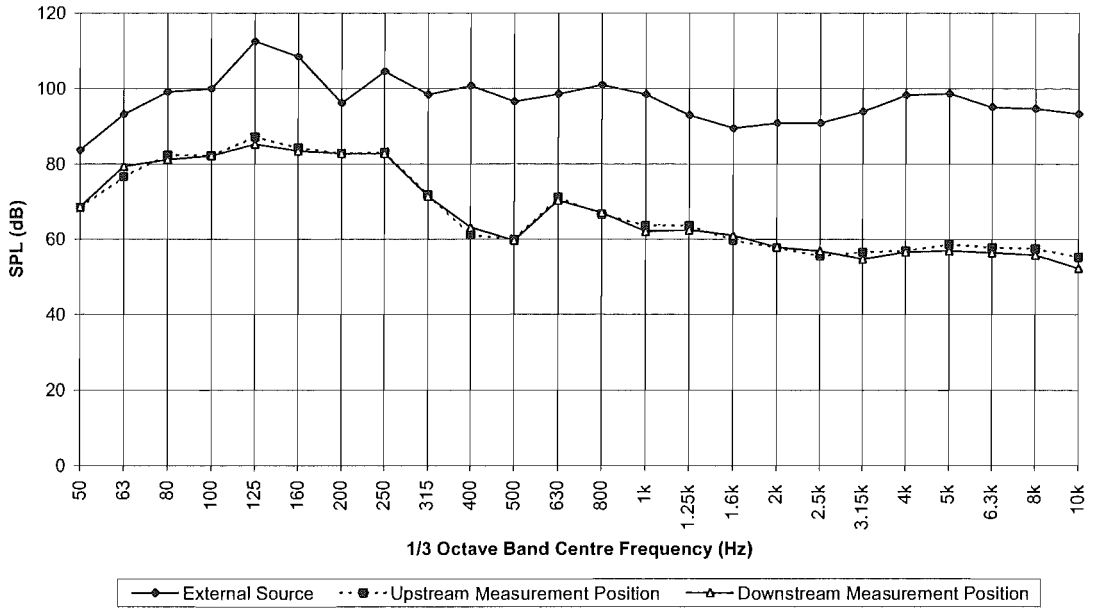

Figure 1: difference between the SPL of the field in the fan casing and the field in the ducts.

3.2.2 Anechoic Termination

ISO 7235 requires that the anechoic termination limit the pressure reflection coefficient in the Test Ducts below a specified maximum. The design of the anechoic termination is described in detail in Chapter 2 'Test Facility Design'. The pressure reflection coefficient is a measure of the difference between the maximum and minimum SPL occurring in the test duct as a result of the standing wave formed by reflection of plane waves at the exit of the duct. The pressure reflection coefficient r_a is found from:

$$r_a = \frac{10^{\Delta L/20} - 1}{10^{\Delta L/20} + 1}$$

Where ΔL is the difference between the maximum and minimum SPL along the longitudinal axis of the Test Duct.

The pressure reflection coefficient along the Substitution Test Duct was measured in the following manner: The sound source equipment was used to create a pink noise sound field in the test duct. A microphone was mounted on a trolley at a position

near, but not at, the centre of the duct cross-section. The microphone was traversed along the test duct to locate the maximum and minium SPL's. These measurements were made at one-third-octave-octave centre frequencies between 50 Hz and the plane wave cut off frequency (the maximum frequency at which plane waves propagate) of the test duct. The data from the microphone traverse is presented in Appendix 2.

The method used was not the method recommended in ISO 7235 because the test signal was broadband pink noise rather than a series of octave band filtered signals. The broadband test signal may have caused the minimum sound pressure level in the standing wave pattern to be overestimated due to axial smearing of the standing wave pattern.

The maximum permissible reflection coefficients and those of the test facility at each one-third-octave band centre frequency are shown in Table 1. The results shown in Table 1 verify that the anechoic termination met the requirements of ISO 7235.

⅓ Octave Band Centre Frequency (Hz)	Maximum PRC (ISO 7235)	Test Facility PRC
50	0.4	0.15
63	0.35	0.15
80	0.3	0.07
100	0.25	0.07
> 125	0.15	0.075

Table 1: Maximum permissible and actual pressure wave reflection coefficients

3.2.3 Acoustic Instrumentation

The acoustic instrumentation is described in detail in Chapter 2 'Test Facility Design'. It was necessary to verify that the self-generated noise of microphone holders in airflow would not significantly affect the signal to noise ratio of data from the microphones.

The microphone holders with microphones were mounted in turn in the centre of the duct at the upstream position, and SPL measurements were made without

airflow, and at airflow velocities of 4 m/s, 8 m/s, 15 m/s and 21 m/s. The substitution test duct was in place during this procedure. It was found that the SPL measured by the microphones was independent of flow velocity. Results of this test are shown in Figure 2, and the measured data is presented in Appendix 4. The maximum deviation from the mean was within 95% confidence bounds at all third octave band centre frequencies. Therefore, it was verified that the self-generated noise of the microphone holders did not significantly influence the SPL measurements.

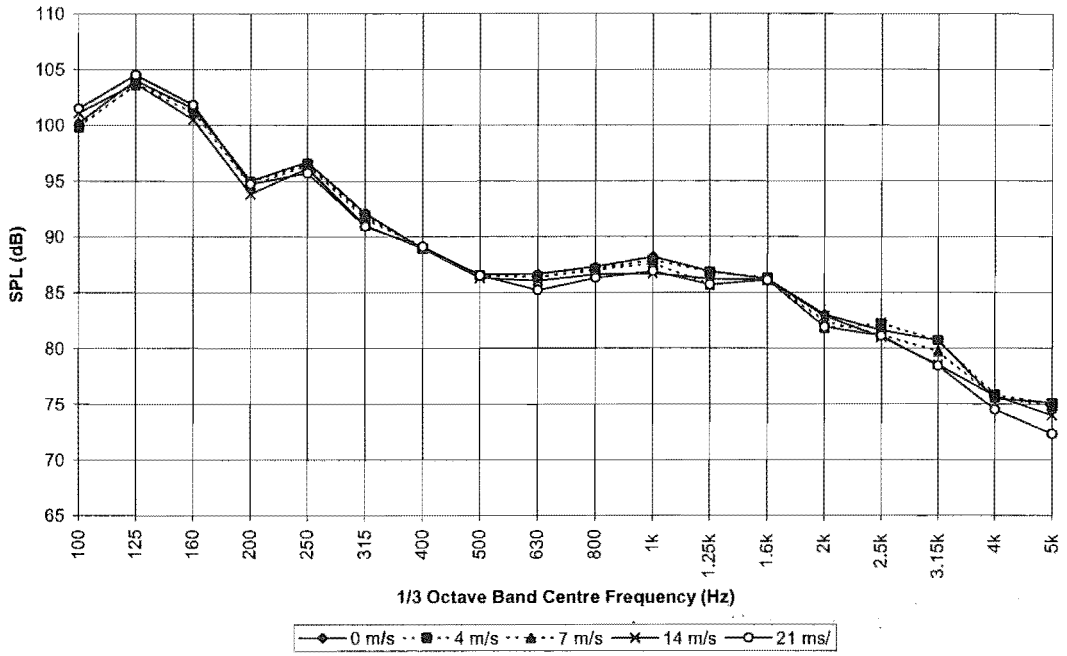

Figure 2: Results of the measurement of the flow induced noise of the microphone holders.

3.2.4 Airflow Instrumentation

The airflow instrumentation was required to accurately measure dynamic pressure over the cross-section of the Test Section Inlet Duct and Test Section Outlet Duct, and the static pressure inside these ducts. The airflow instrumentation consisted of eight Pitot tube rakes containing five Pitot tubes arranged in two arrays of four rakes for measurement of dynamic pressure, and four single static pressure tubes. The instrumentation is described in more detail in Chapter 2 'Test Facility Design'.

The accuracy of the dynamic pressure Pitot tubes was verified by placing each Pitot tube in the airstream of the Low Noise Wind Tunnel in the Department of

Mechanical Engineering, and comparing the output with that of a Pitot tube of known performance. The difference between the test and reference tube was measured at airflow velocities of 0 m/s, 4 m/s, 8 m/s, 14 m/s and 21 m/s. None of the Pitot tubes deviated from the reference tube by more than 1% of the input pressure, and were therefore deemed to be sufficiently accurate.

The accuracy of the static pressure Pitot tubes was verified by placing each of the Pitot tubes near a reference static tube in the wall of the Aeronautical Wind Tunnel in the Department of Mechanical Engineering. Calibration curves were produced for each tube, allowing compensation for differences between tubes. The calibration curves for the static Pitot tubes are shown in Appendix 5.

The output of both the static and dynamic Pitot tubes was converted to a voltage signal by a pressure transducer. The voltage signal was sampled by an analog to digital card in a personal computer. The relationship between the pressure input and voltage output of the transducer was known to be linear:

$$P = mV + c$$

Where P is pressure, V is voltage, and m and c are constants. An input of zero pressure produced an output of 0 volts, therefore the constant c was set equal to 0. The constant m was determined by connecting the pressure transducer and a water manometer in parallel, and varying the pressure in the system with a syringe; the constant was calculated by dividing the pressure shown on the manometer by the voltage output of the transducer. As the transfer function of the transducer was only approximately linear, this operation was performed at a number of different pressures and a line fitted to the data by linear regression.

3.2.5 Internal Noise Field Uniformity

The uniformity of the sound field inside the substitution test duct was investigated. Variation in the sound field had to be quantified to ensure that measurements of insertion loss were not affected by microphone position.

A pink noise field was created inside the test duct using the sound source equipment. SPL was measured at four points in a transverse plane at each reference microphone position, as shown in Figure 3.

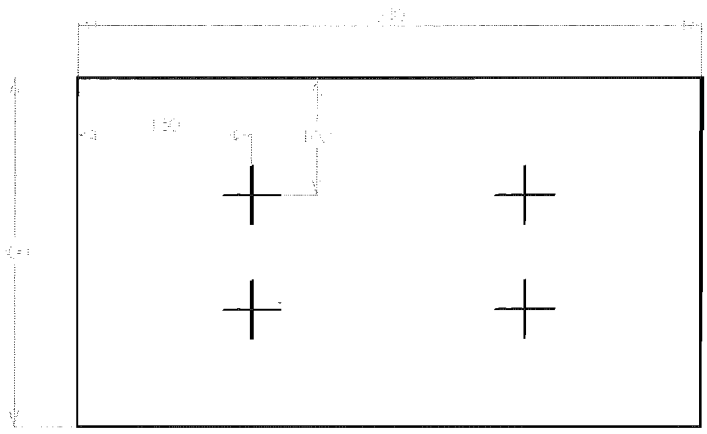

Figure 3: Measurement positions used in noise field uniformity assessment.

The SPL varied significantly between measurement positions (greater than 0.5 dB) within some one-third-octave bands. The variation in SPL over the duct cross-section is presented in Appendix 3. The variation in SPL between measurement positions became significant above the fundamental modal cut-off frequency of the ducts (443 hz), thus the variation was attributed to transverse standing modes.

Because the variation over the duct cross-section was small (less that 2 dB), it was decided that the arithmetic average of four positions within the plane of each reference position provided sufficiently accurate estimate of the SPL at the reference points.

3.2.6 Internal Airflow

From the literature survey it was known that the velocity profile of the airflow through a duct influences the propagation of sound waves; therefore the shape of the velocity profile of the airflow through the substitution test duct was investigated. The dynamic pressure distribution over the transverse sections of the inlet and outlet ducts and internal static pressure was measured at flow velocities between 1.0 and 20.0 m/s with the airflow instrumentation.

The velocity distribution over the transverse section of a duct with mean airflow is affected by friction between the airflow and the walls of the duct. In general, the velocity distribution, or 'velocity profile', has a power law shape, which will increase in definition as the velocity of the flow increases. This effect was observed in the measurements

made. Line plots displaying the velocity profile across each Pitot rake within the ducts are contained in Appendix 6. The velocity profile at 11 m/s is shown in Figure 4(b): Airflow velocity profile at 11.0 m/s at the Pitot rake 120mm from the bottom of the duct.

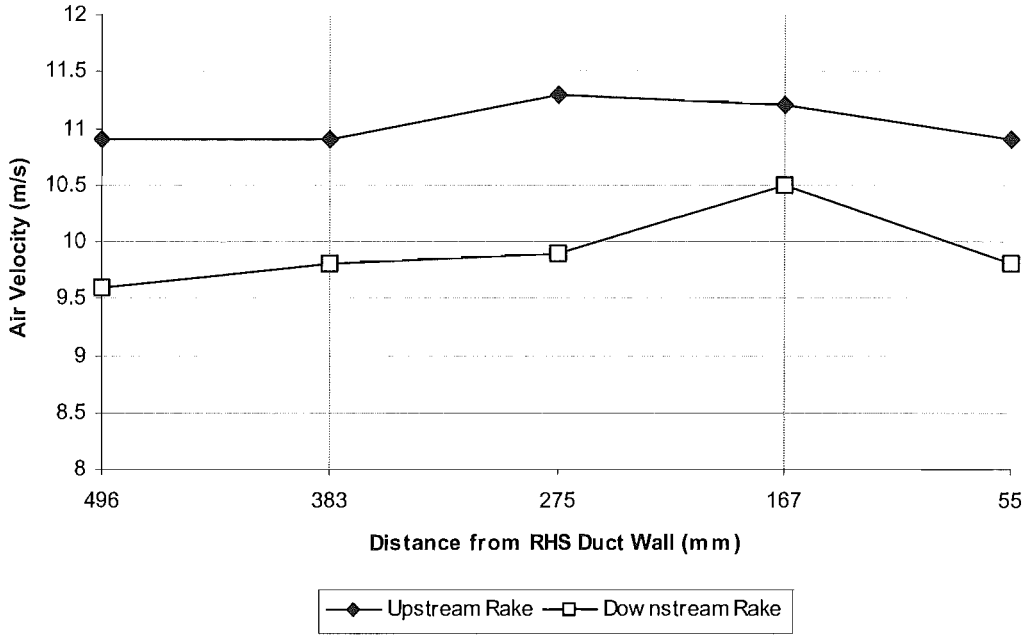

Figure 4(c): Airflow velocity profile at 11.0 m/s at the Pitot rake 180mm from the bottom of the duct.

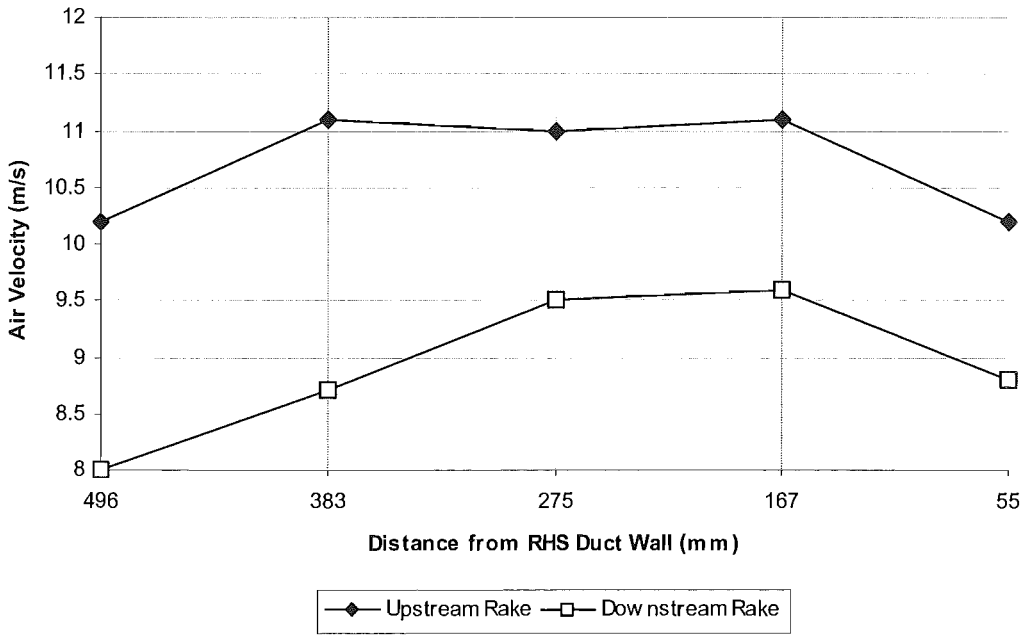

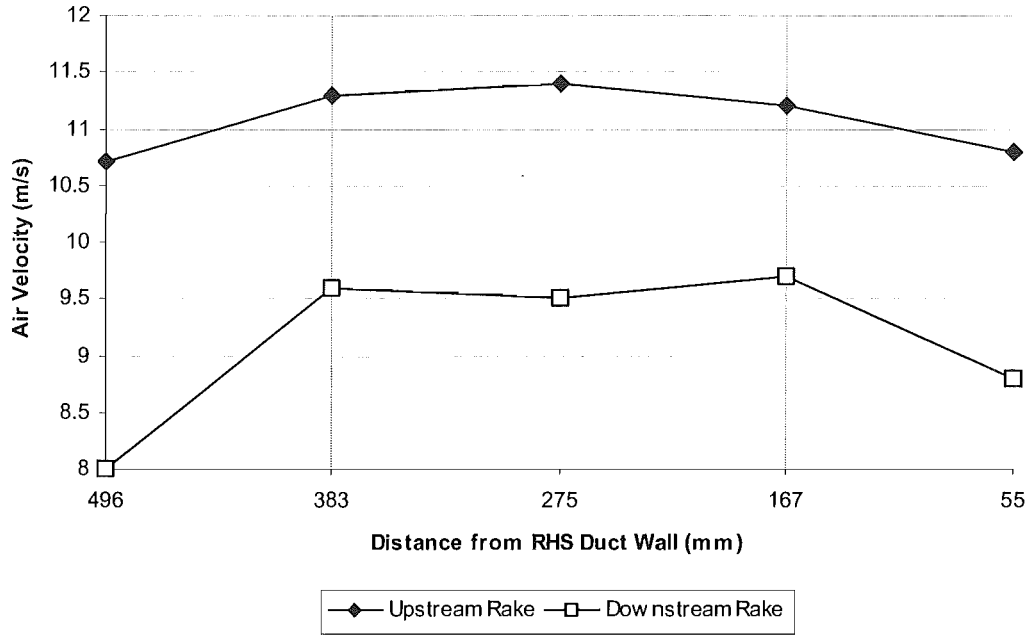

Figure 4(a): Airflow velocity profile at 11.0 m/s at the Pitot rake 60mm from the bottom of the duct.

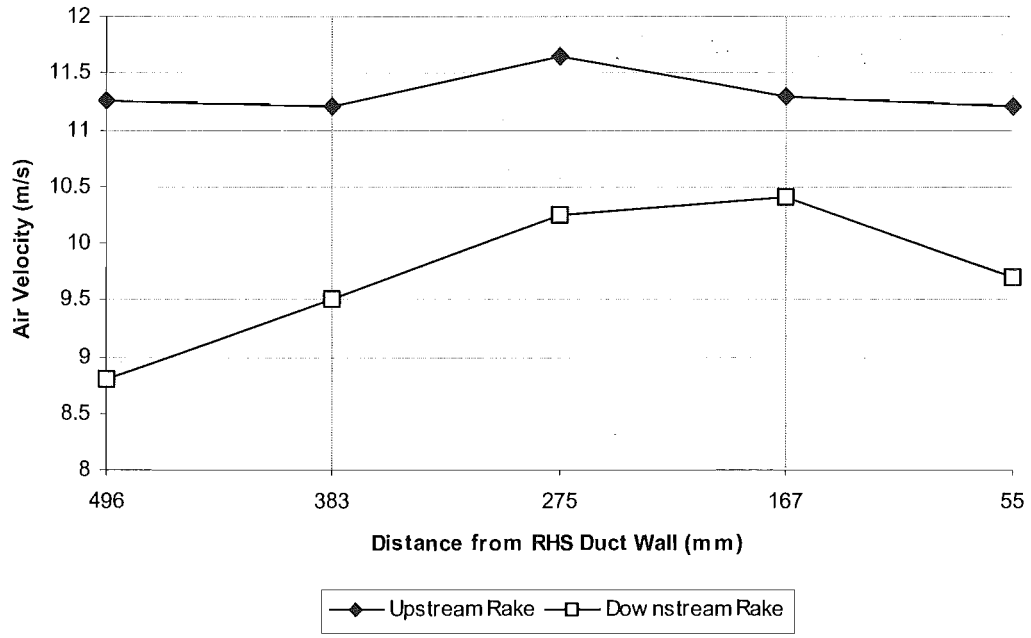

Figure 4(b): Airflow velocity profile at 11.0 m/s at the Pitot rake 120mm from the bottom of the duct.

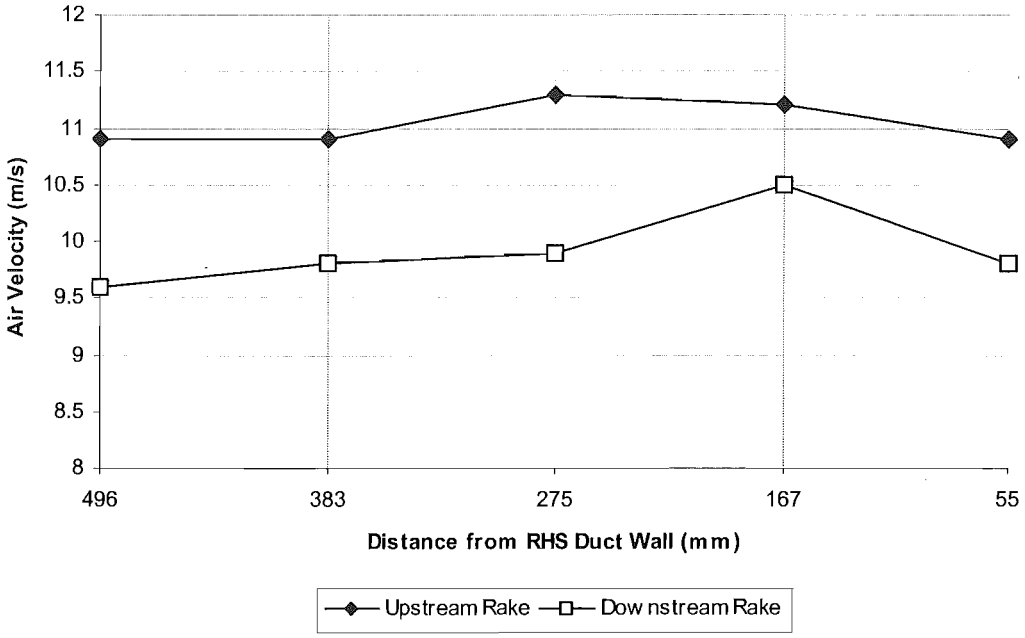

Figure 4(c): Airflow velocity profile at 11.0 m/s at the Pitot rake 180mm from the bottom of the duct.

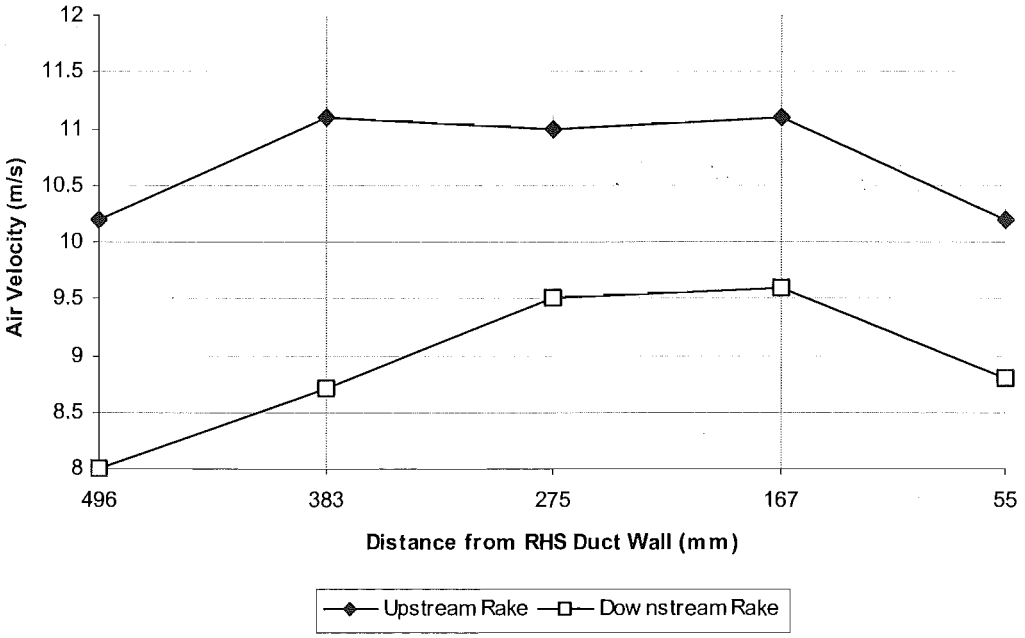

Figure 4(d): Airflow velocity profile at 11.0 m/s at the Pitot rake 240mm from the bottom of the duct.

3.2.7 Duct Wall Vibration

A sheetmetal duct can absorb sound by sound transmission (break out), and by damping when vibrating, usually at its fundamental frequency. It was necessary to verify that the insertion loss of the duct was primarily determined by sound breaking out through the walls, and by internal damping. If insertion loss were not related to noise break out, the duct would be behaving differently to a normal air duct. Such abnormal behaviour would indicate a different mechanism of sound attenuation, for example a poor seal between two flanges allowing sound to escape the duct.

The insertion loss of the substitution test duct is shown in Figure 5. It can be seen that the insertion loss is greatest at low frequency, which is consistent with the behaviour of a typical rectangular sheet metal duct.

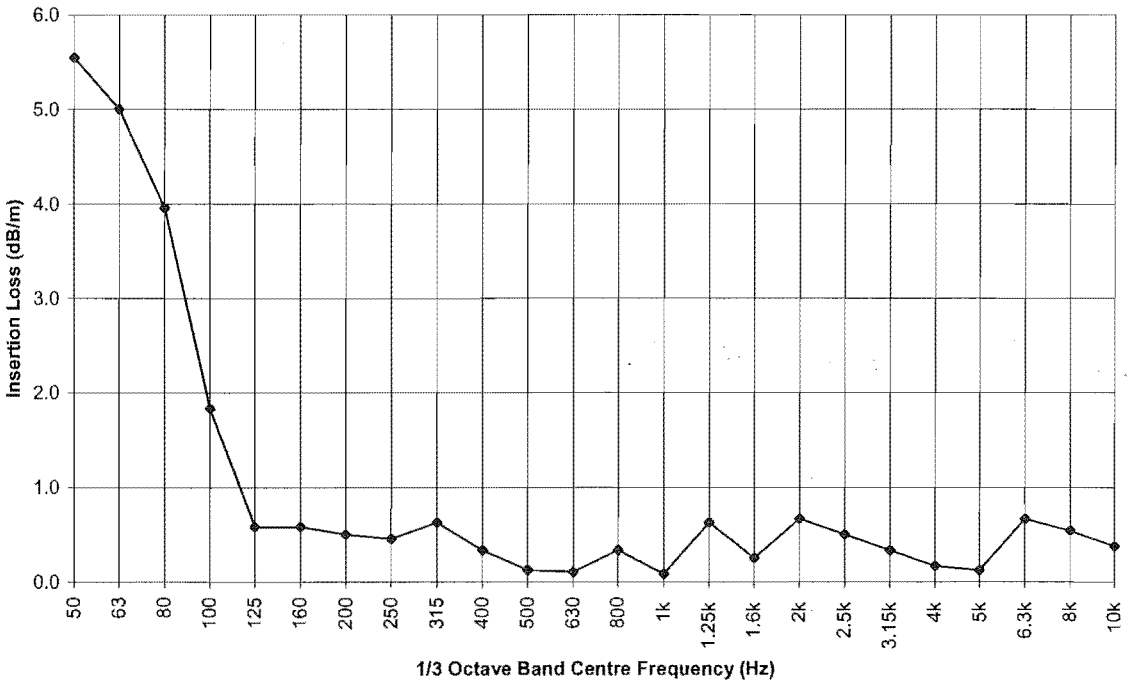

Figure 5: Insertion loss of the substitution test duct.

Therefore, it was verified that the insertion loss of the Substitution Test Duct was similar to that of a typical sheetmetal duct.

3.3 Bibliography

Cummings, A., "Building Services Noise – Acoustics of Air-Moving Ducts", Department of Mechanical Engineering, The University of Canterbury, Christchurch New Zealand.

3.4 References

1. International Standard ISO 7235. 1991 'Acoustics – measurement procedures for ducted silencers – insertion loss, flow noise and total pressure loss'

4

ABSORBER TESTING

Summary

Three rigid framed absorbing materials (polyester, fibreglass and melamine resin foam) and one elastic framed material (polyether polyurethane foam) were tested. In general, the rigid framed materials had superior insertion loss. This was attributed to the impedance at the boundary between the absorber and duct wall being unfavourable for absorption in the frame of the elastic absorber. Increasing absorber thickness from 25mm to 50mm caused the insertion loss peak frequency to decrease. This decrease was greater for the isotropic materials (polyether polyurethane foam and melamine resin foam) than for the non-isotropic materials (polyester and fibreglass).

All facings tested produced one or two insertion loss peaks over narrow frequency bands. Increasing the surface density of a facing caused insertion loss peaks to decrease in frequency. The application of a perforated facing to a fibreglass absorber produced a particularly high insertion loss peak. This was attributed to additional absorption via a Helmholtz resonance created by the perforations.

An absorber pinned to the duct wall had greater overall insertion loss than when adhesively bonded to the duct wall, and had insertion loss peaks at lower frequency. This was attributed to the difference in impedance at the boundary between the rear surface and the duct wall.

The insertion loss of all absorbers tested was measured at airflow velocities between 0 and 21 m/s. At 21 m/s peak insertion loss was significantly reduced, whilst the insertion loss at other frequencies was unaffected. This was attributed to the high

mean flow reducing the insertion loss in the downstream direction. Evidence of this effect was found in a number of previous experimental and theoretical investigations.

Table of Contents

4.1 Introduction

Absorbers were selected for the testing program based on suitability for use in air moving ducts. This selection, shown in Table 1, included isotropic and non-isotropic, rigid and elastic framed materials. A selection of facings representative of those commonly used for absorbers was applied to these materials.

Table 1: Materials selected for the testing program.

Absorbing Material	Frame Type	Absorber Thickness	Facings	Fixing Methods
Resin bonded fibreglass	Non-isotropic Rigid	25 mm 50 mm	Fibreglass tissue Perforated aluminum foil 137 g/m^2 metallic foil	Pinned
Polyester	Non-isotropic Rigid	25 mm 50 mm	Spun-bonded polyester	Pinned
Melamine resin foam	Isotropic Rigid	25 mm 50 mm 75 mm	70 g/m^2 metallic foil	Pinned Bonded Centrally suspended
Polyether polyurethane foam	Isotropic Elastic	25 mm 50 mm 75 mm	70 g/m^2 metallic foil 137 g/m^2 metallic foil	Pinned Bonded

Insertion loss data for all absorbers tested is presented in Appendix 7.

4.2 Aims

The aims of the testing program were to determine the effects of the following parameters on the insertion loss of in-duct absorbers:

1. Absorbing material.
2. Absorber thickness.
3. Absorber facings.
4. Fixing method.
5. The airflow velocity through the test duct, and static pressure inside the test duct.

6. To determine the relationship between insertion loss and absorption coefficient.

4.3 Theory

Calculation of insertion loss:

$$IL(f) = [SPL_1(f) - SPL_2(f)] - [SPL_{1S}(f) - SPL_{2S}(f)] \quad \ldots\{1\}$$

Where IL is insertion loss, SPL is sound pressure level in (dB re 20μPa), and f is frequency in Hz. The subscripts 1 and 2 indicate the upstream and downstream measurement planes, and the subscript s indicates the presence of the substitution test duct.

Because the variation in SPL over the measurement planes was small an arithmetic average of SPL's at four positions (shown in Figure 1) was considered to be a sufficiently accurate representation of the average SPL over the cross section.

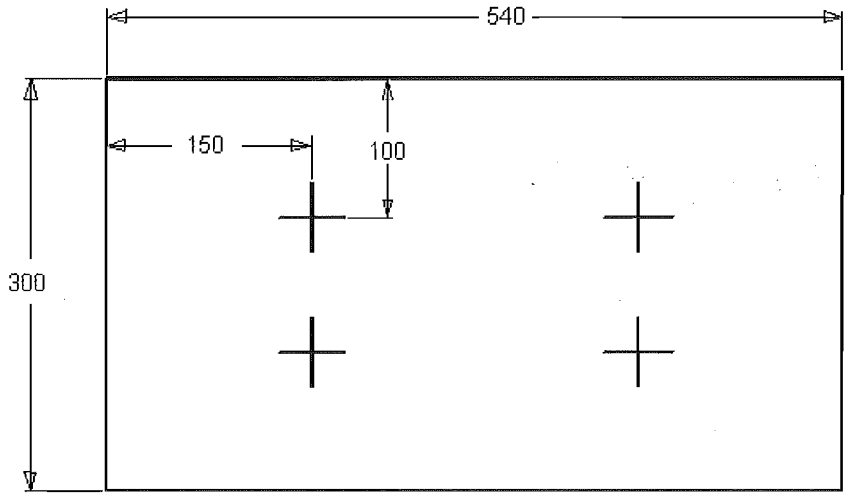

Figure 1: Microphone measurement positions.

The SPL at each measurement plane was therefore:

$$SPL = \frac{(SPL_{11} + SPL_{12} + SPL_{21} + SPL_{22})}{4} \quad \ldots\{2\}$$

The velocity and static pressure of the air flowing through an in-duct absorber influence insertion loss; therefore the insertion loss of the absorbers in-duct absorber was measured at airflow velocities of 0 m/s, 4 m/s, 8 m/s, 14 m/s and 21 m/s. The airflow velocity at the measurement positions in the two 4x5 Pitot tube arrays was calculated from the dynamic pressure:

$$U = \frac{\sqrt{2}}{\sqrt{\rho}} \begin{bmatrix} \sqrt{P_{11}} & \cdots & \sqrt{P_{15}} \\ \vdots & & \vdots \\ \sqrt{P_{41}} & \cdots & \sqrt{P_{45}} \end{bmatrix} \quad \ldots \{3\}$$

Where ρ is the density of air at room temperature and atmospheric pressure, and P is dynamic pressure. The mean airflow velocity at each of the measurement positions was therefore:

$$\overline{u} = \frac{\sqrt{2}}{\sqrt{\rho}} \sum_{i=1}^{4} \sum_{j=1}^{5} \left[P_{ij}\right]^{1/2} \quad \ldots \{4\}$$

The total internal static pressure was the arithmetic average of the static pressure at four positions, one on each of the vertical walls at each of the reference planes:

$$P_S = \frac{P_{S1} + P_{S2} + P_{S3} + P_{S4}}{4} + P_{ATM} \quad \ldots \{5\}$$

Where P_S is internal gauge pressure and P_{ATM} is atmospheric pressure.

4.4 Equipment

The insertion loss test facility is described in chapter three 'Test Facility Design'.

4.5 Procedure

A sound field of the sound pressure spectrum shown in Figure 2 was created at the entrance of the test duct using the sound source equipment; the centrifugal fan was used to provide airflow. With the substitution duct installed, the SPL was measured at four positions (shown in Figure 1) within the upstream and downstream reference planes (shown in Figure 3) at five airflow velocities from 0 to 21 m/s.

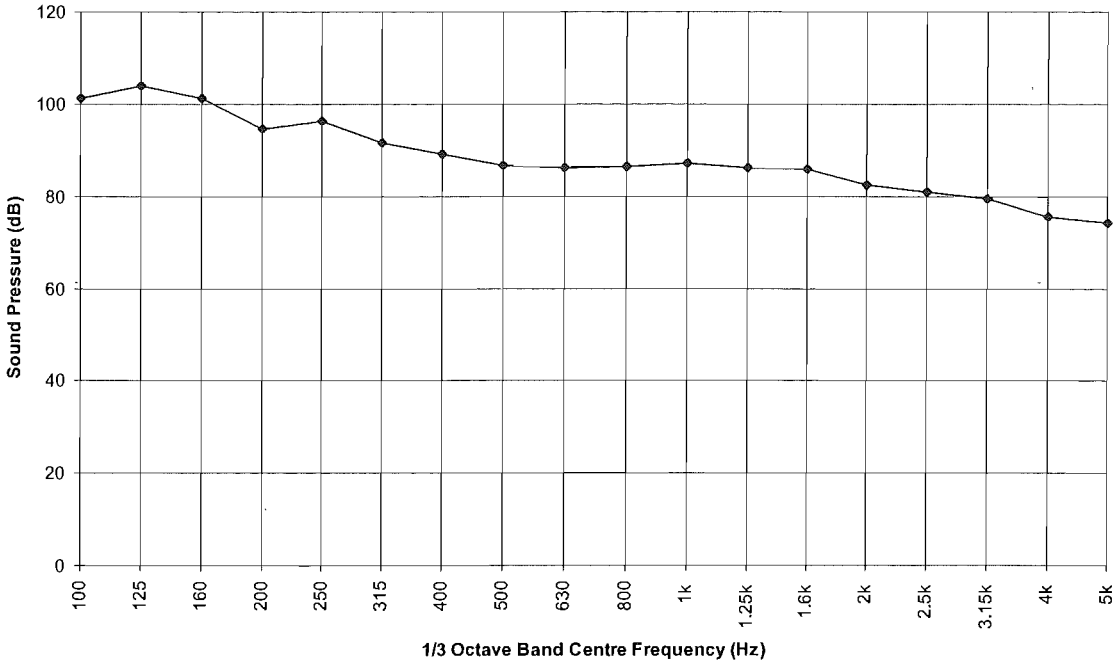

Figure 2: Typical sound pressure at entrance to test section

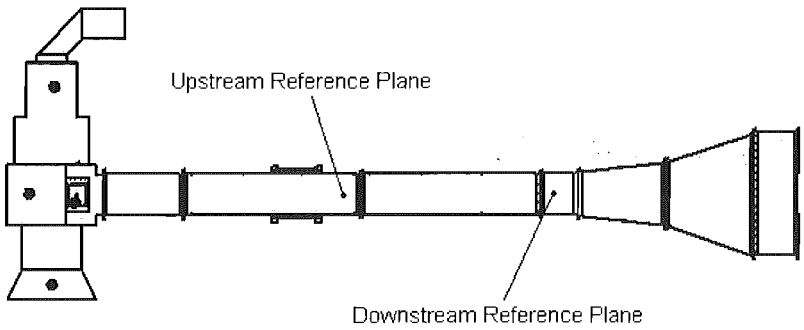

Figure 3: Reference planes.

The substitution duct was replaced with a duct containing the test absorber, and the insertion loss measured at the same airflow velocities. The insertion loss of the absorber was then calculated from equations {1} and {2}.

4.6 Results

4.6.1 Conventions

The performance of an absorbing material is commonly measured in a reverberation room and recorded as an absorption coefficient. The insertion loss of an in-duct

absorber, measured in an appropriate test facility, is the standard measure of the performance of an absorbing material inside a duct. In this thesis, insertion loss refers to the insertion loss of an absorber as measured in an appropriate test facility, and absorption or absorption coefficient refers to the absorption coefficient as measured in a reverberation room.

Abbreviations for absorbing materials and facings are used for chart legends. These abbreviations are shown in Table 2.

Table 2: Abbreviations for material and facing names.

Absorbing Material	Abbreviation	Facing	Abbreviation
Resin bonded fibreglass	FGR	Fibreglass Tissue	FGT
		Perforated Aluminum Foil	PAF
		137 g/m metallic foil	MMF 137
Polyester	POL	Spun-bonded polyester	SBP
Melamine resin foam	MRF	70 g/m^2 metallic foil	MMF 70
Polyether polyurethane foam	PPU	70 g/m^2 metallic foil	MMF 70
		137 g/m^2 metallic foil	MMF 137

4.6.2 Substitution Duct Insertion Loss

The insertion loss of the substitution test duct was measured in accordance with the procedure described in section 4.5 'Procedure'. The relationship between static air pressure and airflow velocity inside the test section is shown in Figure 4 and the insertion loss of the substitution test duct at five airflow velocities is shown in Figure 5, and. The most significant increases in static pressure occur at 15 m/s and 21 m/s. The insertion loss peak of the substitution test duct shifts upward by a third octave at each of these velocities, which indicates that the increase in the frequency at which maximum insertion loss occurred was caused by greater internal pressure load on the walls.

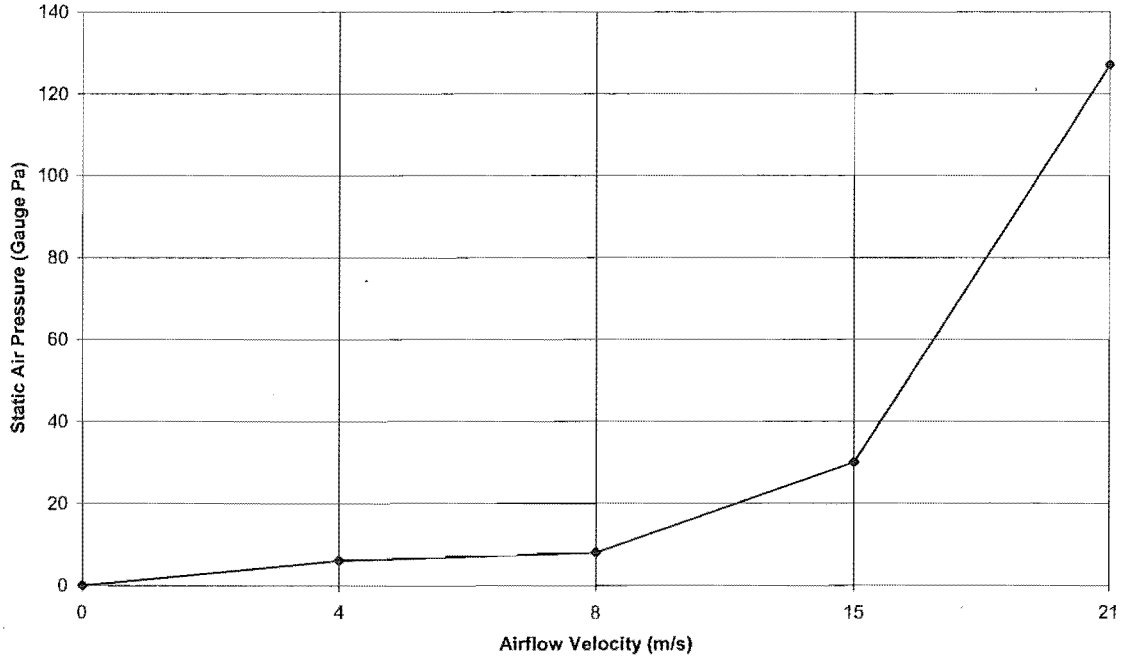

Figure 4: Internal static air pressure at different airflow velocities.

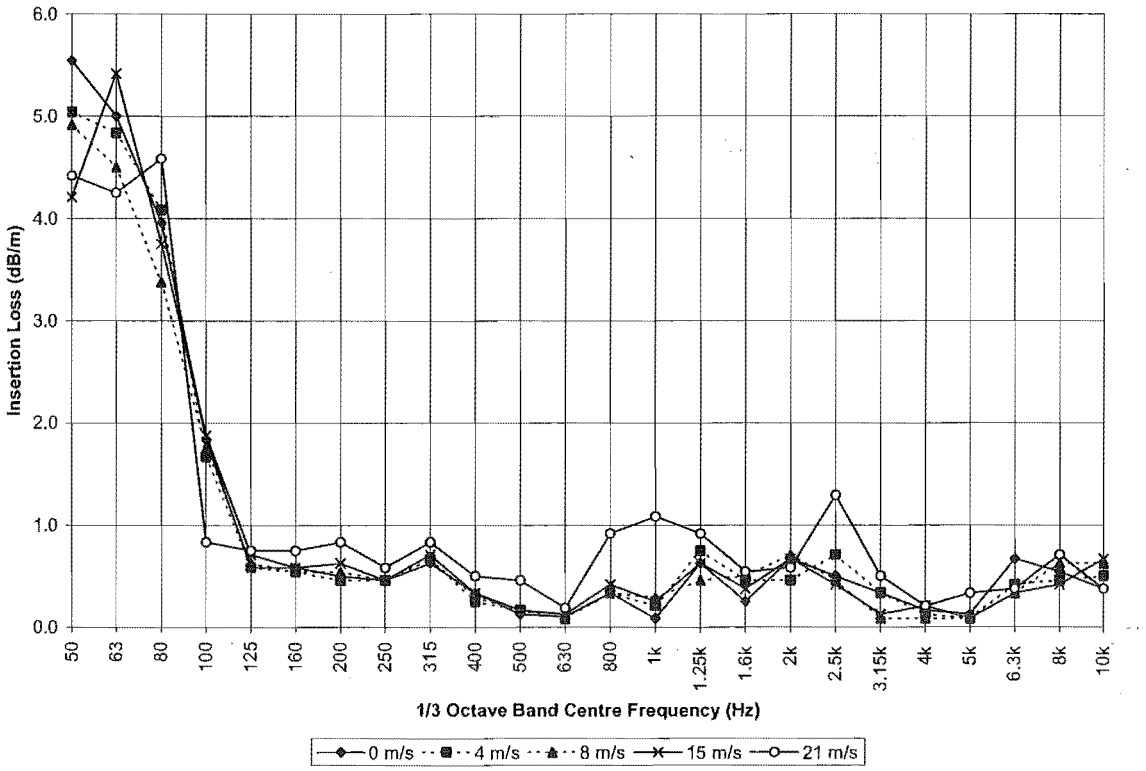

Figure 5: Insertion loss of the substitution test duct at different airflow velocities.

4.6.3 Absorber Material

The insertion losses of a range of the absorbers tested, and measured data for 25 mm thick fibreglass faced with fibreglass tissue from Wassilieff [1] are shown in Figure 6. Wassileiff [1] used a 400 mm square duct lined on four sides; therefore his data is not directly equivalent to the data from this work. The difference between data of this work and that of Wassilief [1] is attributed to the smaller airway and greater absorber area of Wassilieff's [1] duct producing greater insertion loss.

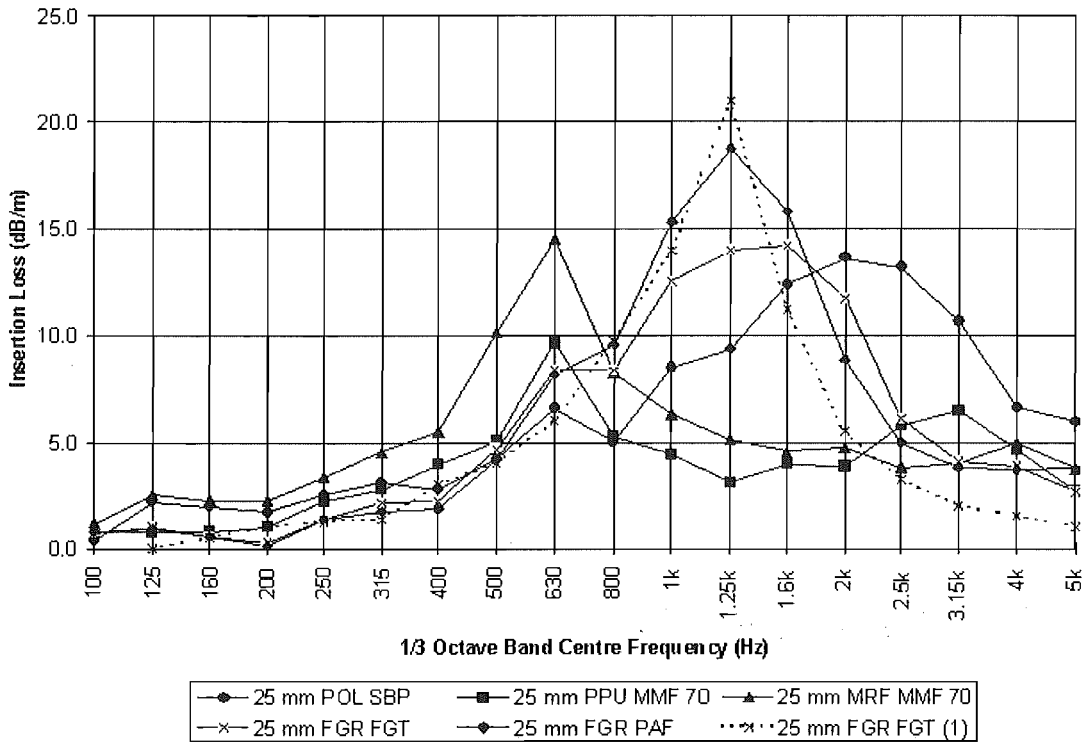

Figure 6: Pinned insertion loss of a representative range of the absorbers tested

The static flow resistance, overall insertion loss and frequency of peak insertion loss of each of the materials tested is shown in Table 3. From Table 3, it can be seen that materials of higher flow resistance tend to have higher peak insertion loss frequency. However, it is well known that the relationship between flow resistance and peak insertion loss is more complex. The relationship between insertion loss and flow resistance was further investigated using a model developed by Ingard.

Table 3: Peak pinned insertion loss and flow resistance of the permeable materials tested.

Material	Normalised Static Flow Resistance	Predicted Peak Pinned Insertion Loss and Frequency [3]	Measured Peak Pinned Insertion Loss and Frequency
Melamine Resin Foam	0.7	-	9.8 dB/m at 630 Hz
Resin bonded fibreglass faced with fibreglass tissue	3.4	12 dB/m at 1143 Hz	15 dB/m at 1125 Hz
Polyester faced with spun bonded polyester	10.5	8 dB/m at 2287 Hz	15 dB/m at 2000 Hz

According to Ingard there is a theoretical normalised static flow resistance (approximately 4) for locally reacting (rigid framed), materials that produces optimum insertion loss. The model of Ingard predicts that the fibreglass absorber faced with fiberglass tissue tested should have peak insertion loss at 1143 Hz of approximately 12 dB/m, which is in good agreement with the results obtained in this work. The model also shows that the normalized flow resistance of fibreglass is close to the theoretical optimum.

Agreement between calculated and measured insertion loss data for polyester faced with spun bonded polyester is poor, probably because the flow resistance of the absorbing material is much lower than that of the facing. Ingard did not provide flow resistance data applicable to melamine resin foam.

When used as architectural absorbers, elastic framed absorbers typically have greater absorption than rigid absorbers at low frequency because additional absorption occurs in the elastic frame. It was expected that this would also be true for absorbers in ducts.

Absorbers used to line ducts are either pinned (as shown in Figure 13) or adhesively bonded to the duct walls over the entire rear surface, whereas architectural absorbers are typically bonded to the rear surface only near the edges. The acoustic impedance at the boundary between an absorber and rear surface must be greater when the absorber is pinned or bonded over the entire surface than when the absorber is loose laid or bonded at the edges. Therefore, the poor low frequency insertion loss of the polyether polyurethane foam absorber is probably caused by low absorption in the frame due to unfavourable impedance conditions at the boundary between the absorber and the duct wall.

4.6.4 Absorber Thickness

For all absorbers tested, increasing the thickness of the bulk absorber from 25 mm to 50 mm decreased the frequency of the peak insertion loss. This effect is shown in Figure 7. For all materials except melamine resin foam, the shape of the insertion loss characteristic was essentially independent of material thickness.

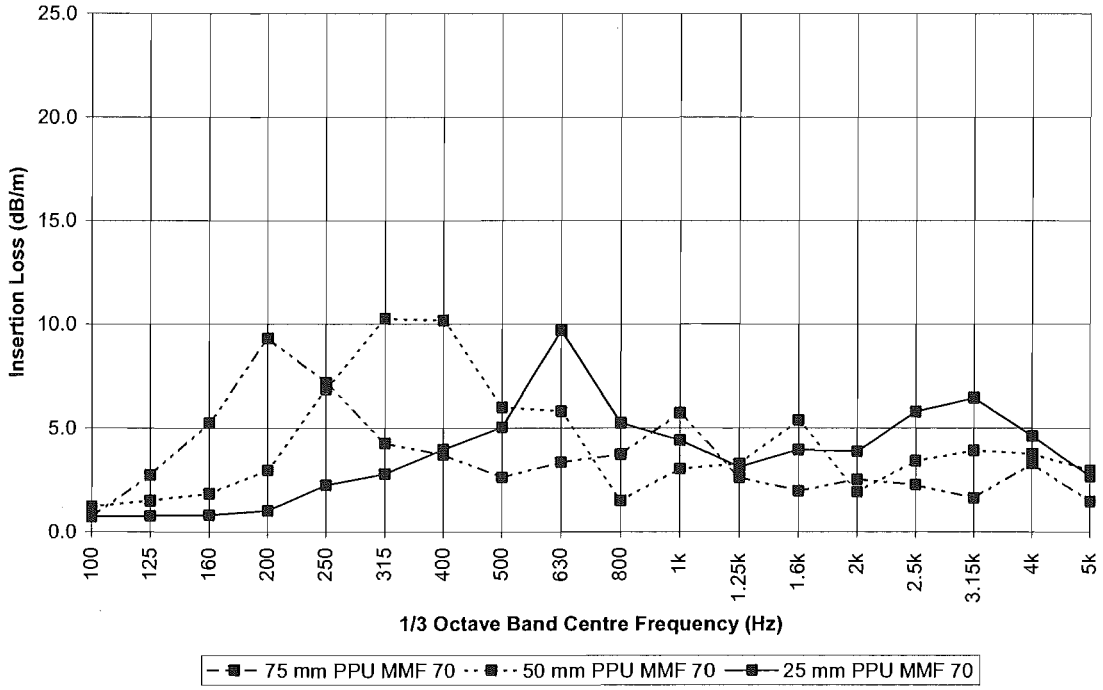

Figure 7: Effect of absorber thickness on the pinned insertion loss of polyether polyurethane foam faced with metallic foil.

The absorption peaks of the isotropic absorbers (melamine resin foam and polyether polyurethane foam) moved further than those of the non-isotropic absorbers (fibreglass and polyester), as shown in Figure 8. The absorption peaks of the non-isotropic absorbers moved one octave to the left, whereas the peaks of the isotropic materials only moved 2/3 of an octave. This difference is attributed to differences in the effect of increases in flow resistance in isotropic and non-isotropic materials.

If the fibreglass absorbers are approximately locally reacting (the transverse flow resistance is close to infinity), the axial velocity component is close to zero. According to Ingard, the attenuation of such an absorber can be expected to change monotonically with flow resistance. For isotropic liners, transverse velocity decreases with frequency due to the stiffness of the air layer over the exposed surface of the

absorber, causing the relative significance of the axial velocity (which is unaffected by the air layer) to increase. This means that the relationship between static flow resistance and peak insertion loss is not monotonic, and thus different to that for non-isotropic absorbers.

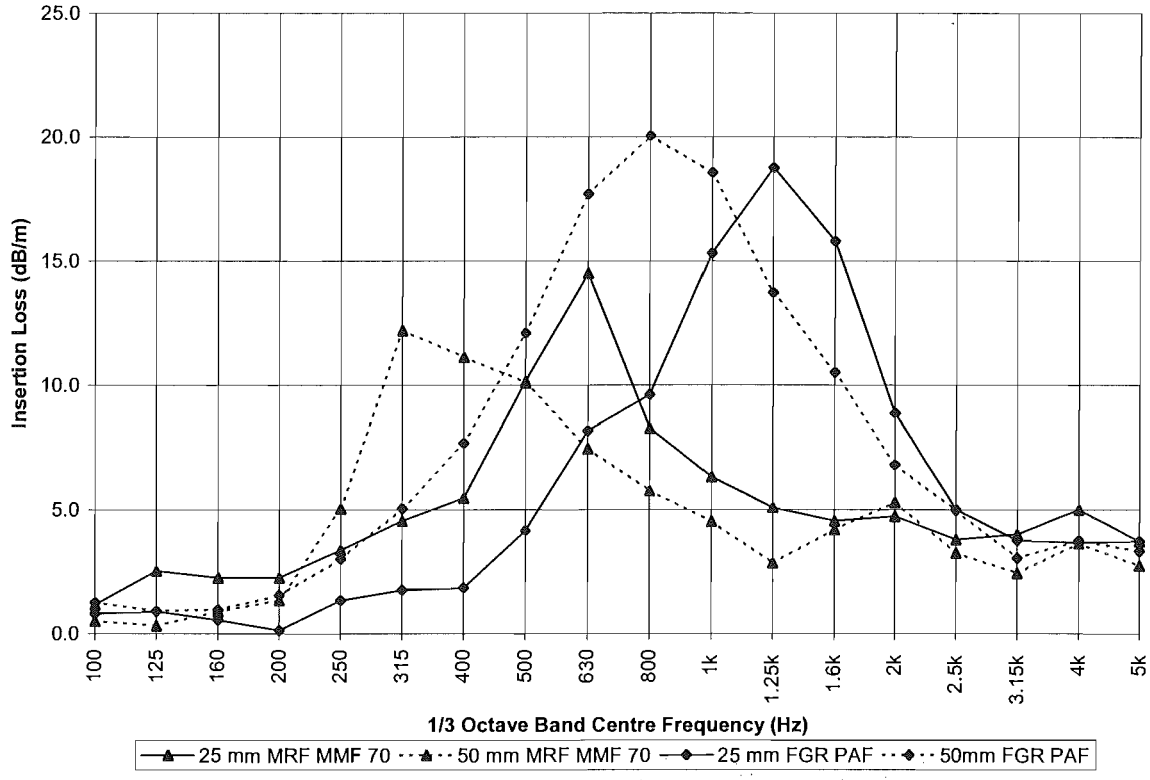

Figure 8: Effect of absorber thickness on the pinned insertion loss of fibreglass faced with perforated aluminium foil (non-isotropic) and melamine resin foam faced with metallic foil (isotropic).

The insertion loss of melamine resin foam faced with metallic foil at different thickness is shown in Figure 9. As expected for an isotropic absorbing material, reductions in the peak insertion loss frequency with increasing thickness (and therefore increasing flow resistance) seem to be non-monotonic.

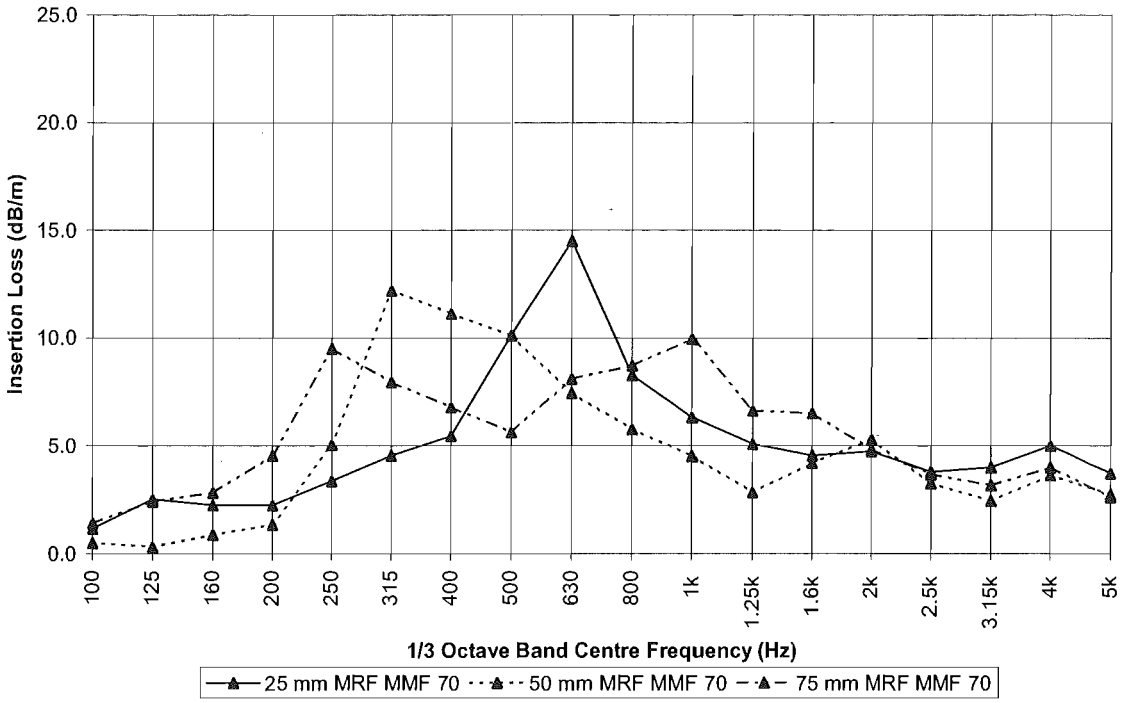

Figure 9: Effect of absorber thickness on the pinned insertion loss of melamine resin foam with metallic foil facing.

4.6.5 Facings

Facings are often used in combination with an absorbing material to produce a 'tuned' absorber. Many of the absorbers selected for the testing program were commercial products; therefore not all of the possible bulk absorber and film facing combinations were tested. However, trends relating facing type to insertion loss were identified from the data.

The insertion loss of the absorbers with non-isotropic absorbing materials is shown in Figure 10. Fibreglass faced with perforated foil was the only absorber tested that that was designed specifically for use in air moving ducts; therefore it was expected that it would have a high insertion loss. Cummings [2] found that perforated facings tune absorbers to give higher absorption peaks at lower frequencies, and that the use of perforated facings tends to reduce performance at high frequencies. Therefore, the greater insertion loss of fibreglass faced with perforated foil is probably due to the perforated facing.

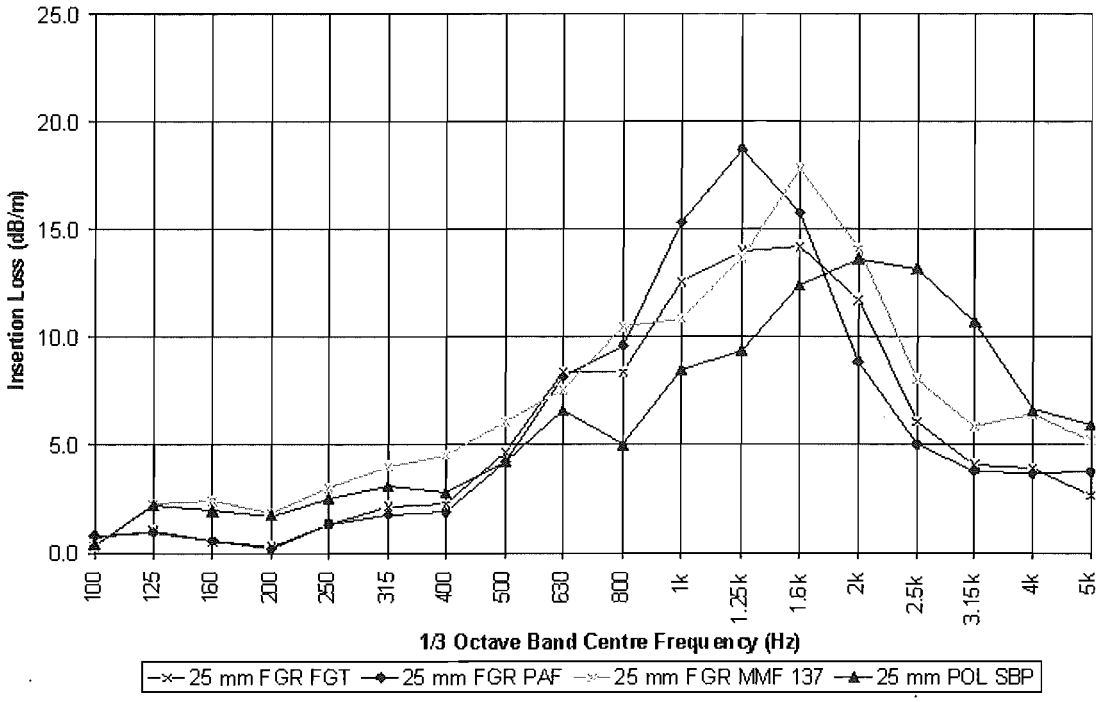

Figure 10: Pinned insertion loss of all absorbers with non-isotropic absorbing materials at 25mm thickness.

The sensitivity of fibreglass absorbers to the film facing was investigated. The insertion loss of 25m fibreglass with glass tissue facing (permeable), and with 137 g/m^2 metallic foil facing (impermeable) is shown in Figure 10. It can be seen that fibreglass is relatively insensitive to differences in film facing. A smaller than expected difference in the insertion loss characteristic was produced, given that the film facings had very different surface densities and permeability characteristics.

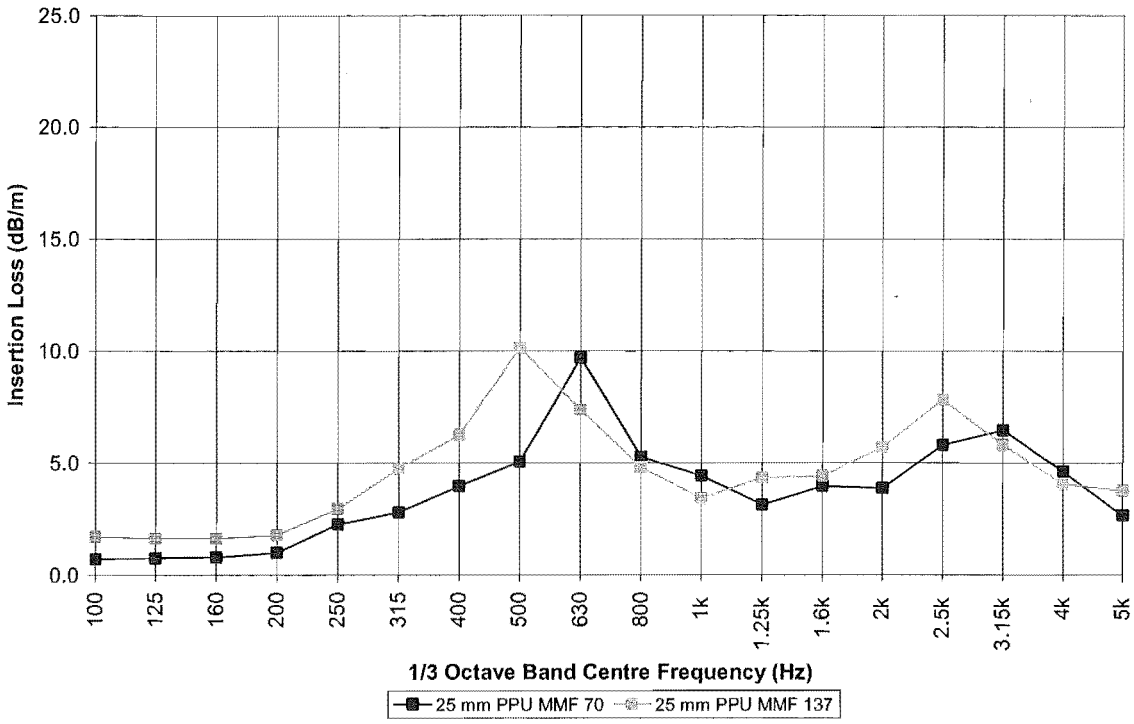

Figure 11: Effect of facing surface density on the pinned insertion loss of polyether polyurethane.

The effect of facing surface density on the insertion loss of polyether polyurethane faced with metallic foil is shown in Figure 11. This result shows that changing the film facing surface density alters the peak insertion loss frequency of elastic foams such as polyether polyurethane. Ingard states that porous materials of low flow resistance, such as polyether polyurethane, tend to act as ¼ wavelength resonators. The data shown in Figure 11 indicates that facing mass affects the resonant frequencies of the polyether polyurethane absorber.

The insertion loss of 25 mm melamine resin foam with and without a metallised Mylar facing is shown in Figure 12. The film facing improved the peak absorption of the bulk absorber, but did not cause the peak to move. The sensitivity of melamine resin foam to film facings at 25 mm thickness is similar to that of fibreglass, and quite different from that of polyether polyurethane foam.

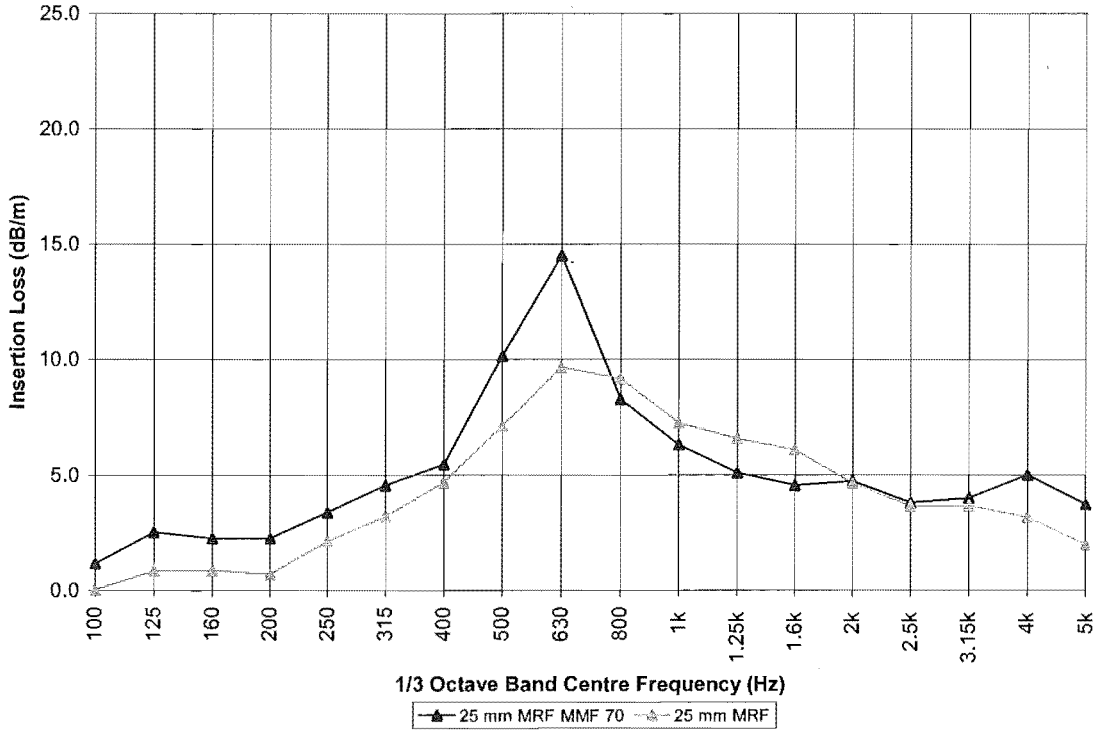

Figure 12: Effect of metallic foil facing on the pinned insertion loss of melamine resin foam at 25mm thickness.

Both fibreglass and melamine resin foam are rigid framed absorbers, whilst polyether polyurethane is an elastic framed absorber. Fibreglass and melamine resin foam do not have similarities in any of the other parameters that are important in determining absorption (flow resistance, mass density or structure factor). Therefore, the mass of a film facing may only interact with the ¼ wavelength resonance of an absorber of low flow resistance if the absorber is elastic.

4.6.6 Fixing Method

The effects on insertion loss of the two commonly used methods for fixing absorbers in ducts, 'pinning' and 'bonding', were investigated. Fibrous materials were excluded from this investigation, as they could not be adhesively bonded to the duct walls. In the 'pinning' method, 4mm diameter steel pins on 40mm square adhesive pads are attached to the duct walls. The absorber is forced on to the pins so that they penetrate it and the absorber is secured on the pins with 35mm square washers. A section of a pinned absorber is shown in Figure 13. In the 'bonding' method an absorber is fixed to the duct wall with a contact adhesive over the entire rear surface.

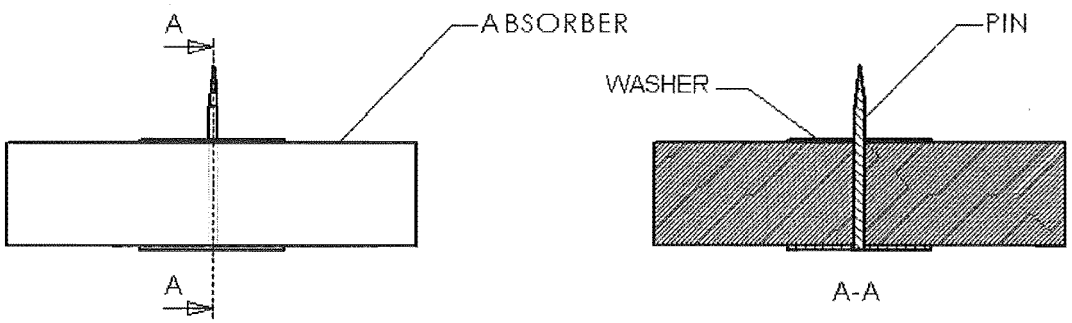

Figure 13: The pinning method. The absorber is held against the duct wall by an interference fit between the pin and the washer.

The effects of fixing method on insertion loss were the same for both absorbing materials tested; these effects are shown in Figure 14. Absorbers adhesively bonded to a duct wall have greater acoustic impedance at the rear surface then absorbers that are pinned. Therefore, it is probable that the effects of different fixing methods on insertion loss are caused by differences in impedance at the rear surface of an absorber.

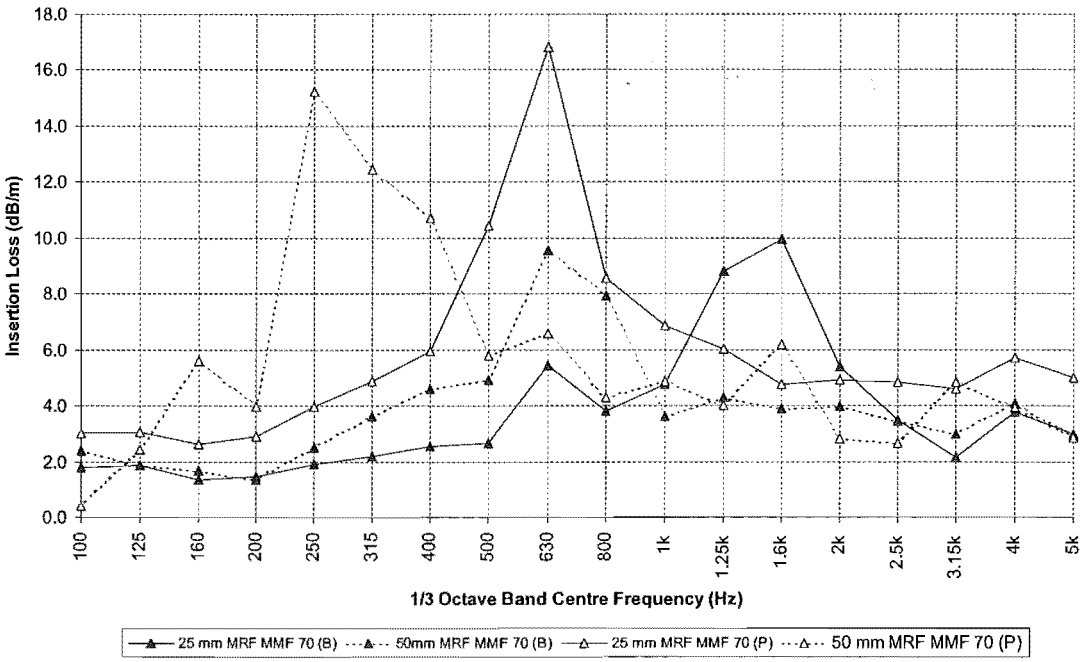

Figure 14: Comparison of the insertion loss of bonded (B) and pinned (P) melamine resin foam with metallic foil facing at 25 mm and 50 mm thickness.

From Figure 14 it can be seen the peak absorption coefficient for the absorbers of greater thickness is particularly sensitive to changes in rear surface boundary conditions. The reason for this is unclear.

4.6.7 Airflow Conditions

Two mechanisms by which airflow conditions can affect the insertion loss of an in-duct absorber are described in the literature. These are change in plane-wave phase velocity, and diffraction by the velocity profile.

The insertion loss of all of the absorbers tested showed similar sensitivity to changes in airflow conditions, as shown in Figure 15 and Figure 16. In general, peak insertion loss was reduced at high flow velocities; there was no sensitivity to airflow conditions below an airflow velocity of 14 m/s.

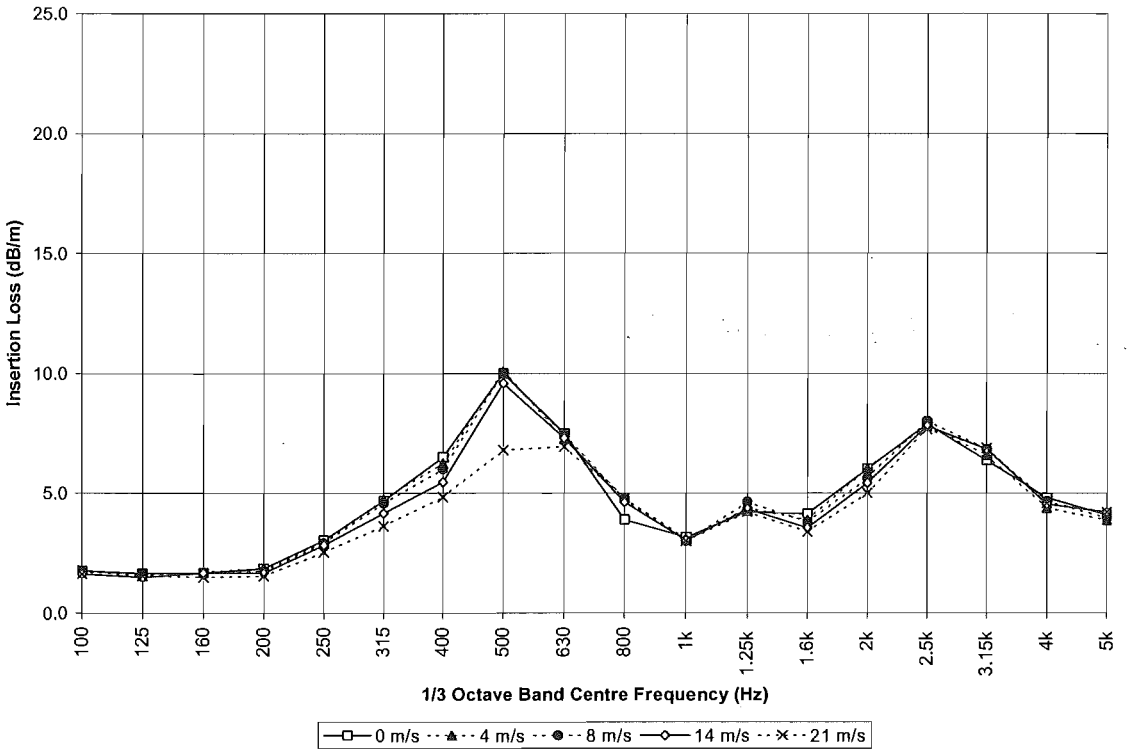

Figure 15: Pinned insertion loss of 25 mm polyether polyurethane faced with 137 g/m^2 metallic foil at different flow velocities.

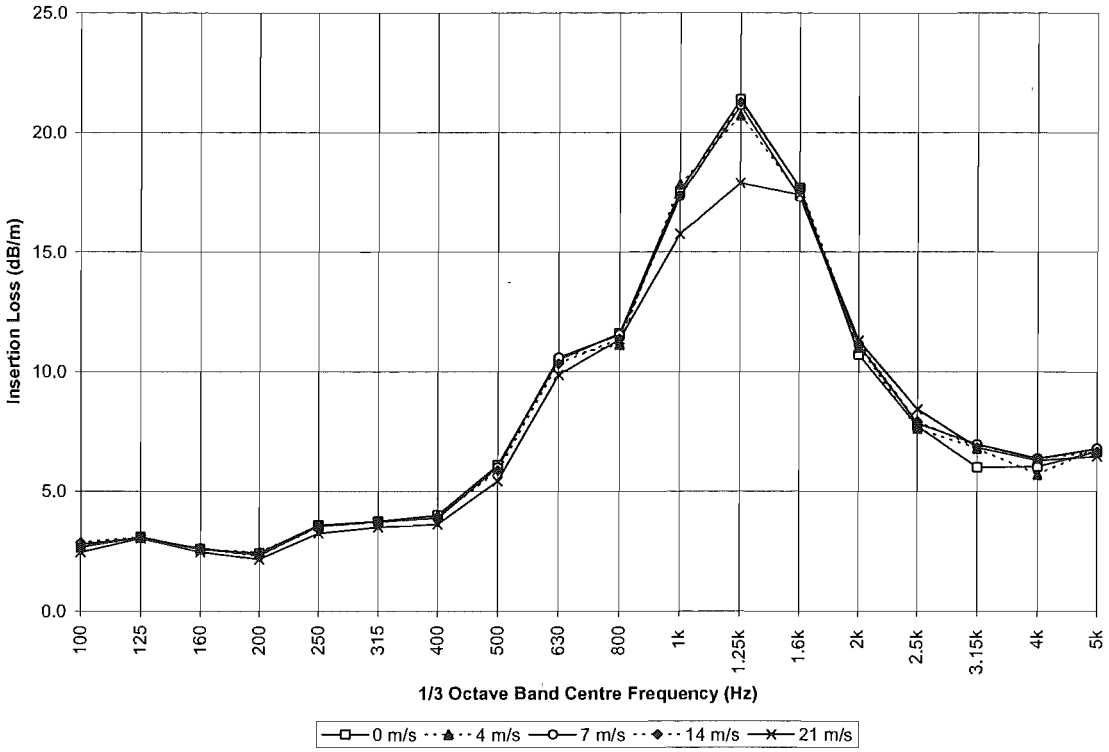

Figure 16: Pinned insertion loss of 25 mm fibreglass faced with perforated aluminium foil at different airflow velocities.

As discussed in the literature survey, a reduction in insertion loss in the downstream direction at high mean airflow was predicted by Pridmore Brown (1958) [3], Mariano (1971) [4], and Cummings and Astley (1981) [5] and 1996 [6]; and found in the experimental work of Bokor (1969) [7] and Cummings and Astley (1981) [5] and 1996 [6].

Based on the results of these previous investigations, it is concluded that the reduction in downstream insertion loss is caused by a combination of an increase in plane wave phase velocity and diffraction by the velocity profile.

4.6.8 Bar Absorbers

The insertion losses of five melamine resin foam 'bar absorbers' with differently shaped cross-sections were measured. A summary of the bar absorbers are presented in Table 4.

Table 4: Summary of the bar absorbers.

Cross-section Shape	Base (mm)	Height (mm)	Diameter (mm)	Facing (mm)	Abbreviation
Circular	-	-	185	-	CIR
Square	164	164	-	-	SQR
Square	164	164	-	MMF 70 on two sides	SQR 2S MMF
Square	164	164	-	MMF 70 on four sides	SQR 4S MMF
Triangle	164	329	-	-	TRI

The volume of the absorbing material in the bar absorbers was the same as that of two 25 mm thick un-faced melamine resin foam absorbers. The insertion losses of the bar absorbers are compared to the insertion loss of two 25 mm thick melamine resin foam absorbers in Figure 17.

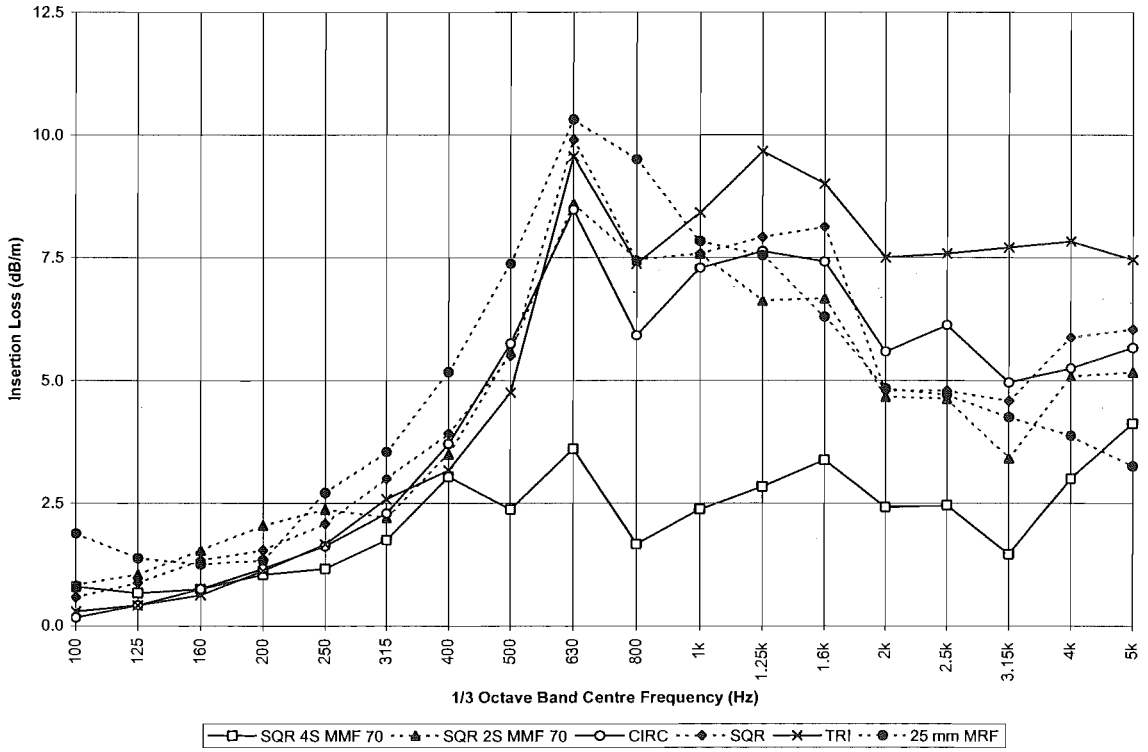

Figure 17: Insertion loss of all bar absorbers and of 25 mm melamine resin foam.

The insertion losses of the un-faced square, square faced on two sides and circular bar absorbers were very similar to that of 25 mm thick melamine resin foam. This similarity shows that the insertion loss of bar absorbers with approximately constant thickness is primarily determined by absorbent volume.

The bar absorber with triangular cross-section had significantly greater insertion loss at frequencies greater than 1.5 kHz. This is attributed to the change in thickness, and therefore flow resistance, of the cross-section of the bar absorber from the base to the apex. The change flow resistance along the cross-section means that different volumes of the bar absorber have flow resistance optimal for the absorption of different frequency bands. Therefore, the triangular bar absorber has high insertion loss over a wider range of frequencies than the other bar absorbers.

It was expected that the insertion loss of the square bar absorber faced on four sides with metallic foil would be similar to that of two 25 mm thick melamine resin foam wall absorbers faced with metallic foil. The insertion loss of these absorbers is shown in Figure 18.

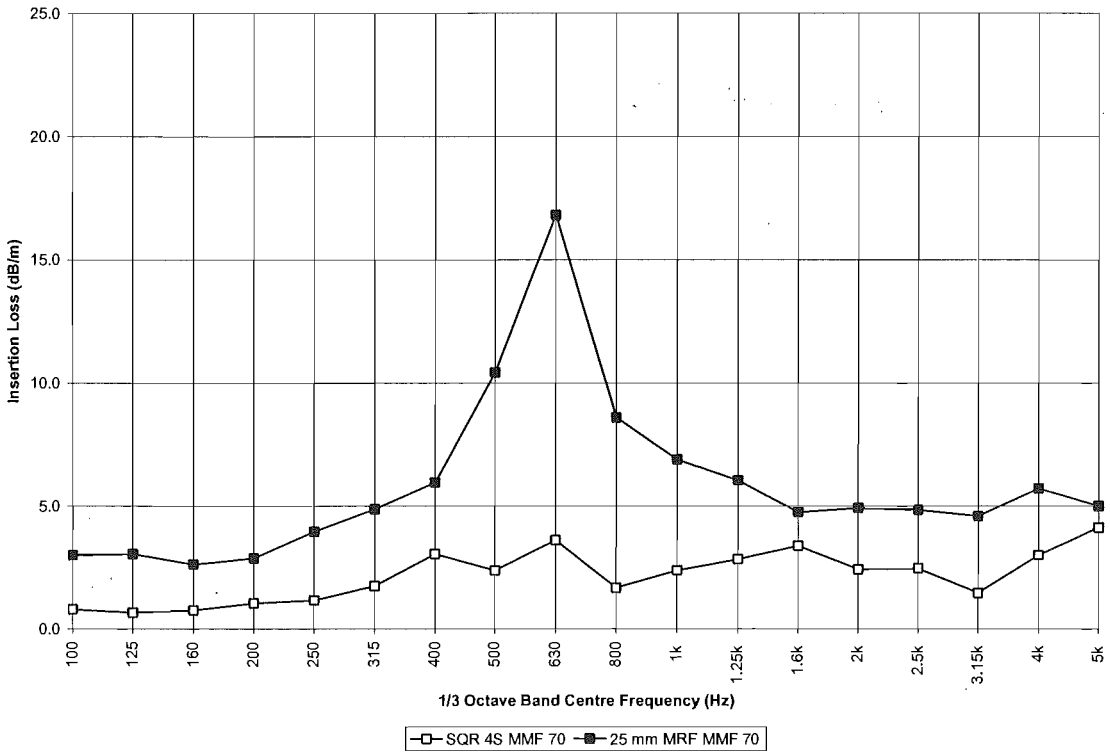

Figure 18: Insertion loss of square bar silencer faced on four sides with metallic foil, and pinned 25 mm melamine resin foam faced with metallic foil.

The difference in the insertion loss of the absorbers shown in Figure 18 is attributed to the difference in impedance at the surfaces of the absorbers. The rear of the wall absorber is supported by an essentially rigid surface, whereas the bar absorber is suspended in air. The essentially zero impedance of the air surrounding the bar absorber may make the transfer of sound energy across the facing to the absorbent very inefficient, thus significantly reducing insertion loss.

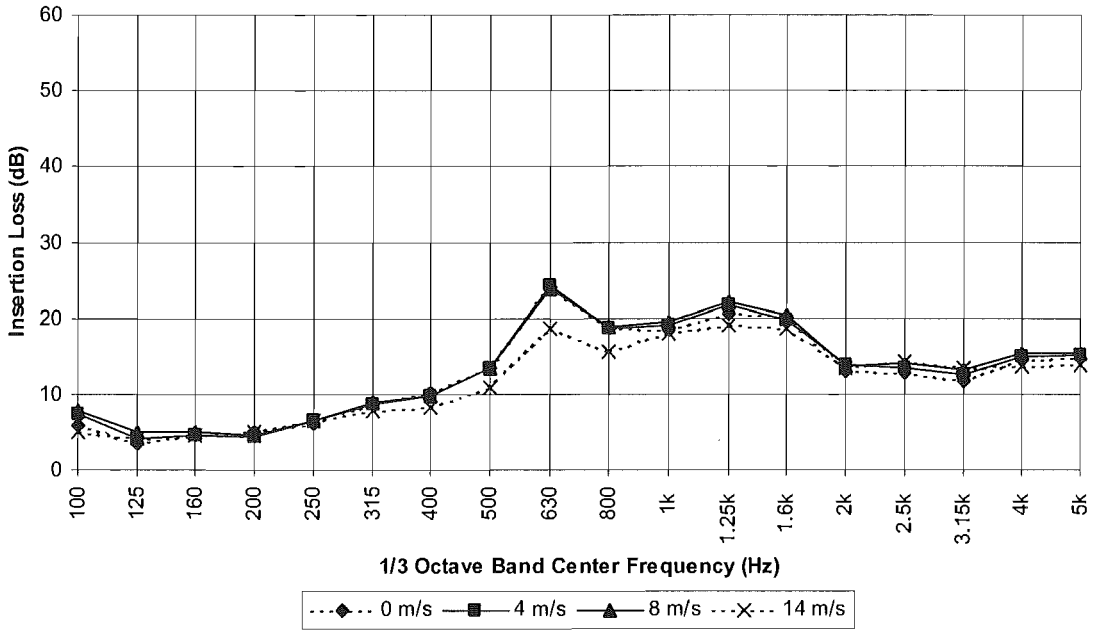

Figure 19: Insertion loss of the square cross-section bar silencer at airflow velocities between 0 and 21 m/s.

The effect of airflow velocity on the insertion loss of the bar silencers was measured. The insertion loss of the square cross-section bar silencer at airflow velocities between 0 m/s and 14 m/s is shown in Figure 19. The effect of airflow velocity on the insertion loss of bar silencers was the same as that of airflow on the insertion loss of wall absorbers. See section 4.6.7 'Airflow Conditions' for a discussion of these effects.

4.6.9 Insertion Loss and Absorption Coefficient

The relationship between the insertion loss and absorption coefficient of an absorber was investigated. Knowledge of this relationship is important because the attenuation performance of commercially available in-duct absorbers is frequently quoted in the form of an absorption coefficient measured in a reverberation room.

The absorption coefficient and absorption coefficient when pinned to 18 gauge steel sheet of 25 mm thick polyether polyurethane faced with 70 g/m^2 metallic foil was measured in the reverberation room in the University of Canterbury Department of Mechanical Engineering. The steel sheets used in these measurements were of the same dimensions and material as the top and bottom walls of the Test Section Duct. The measurements are compared to the insertion loss of the same material in Figure 20.

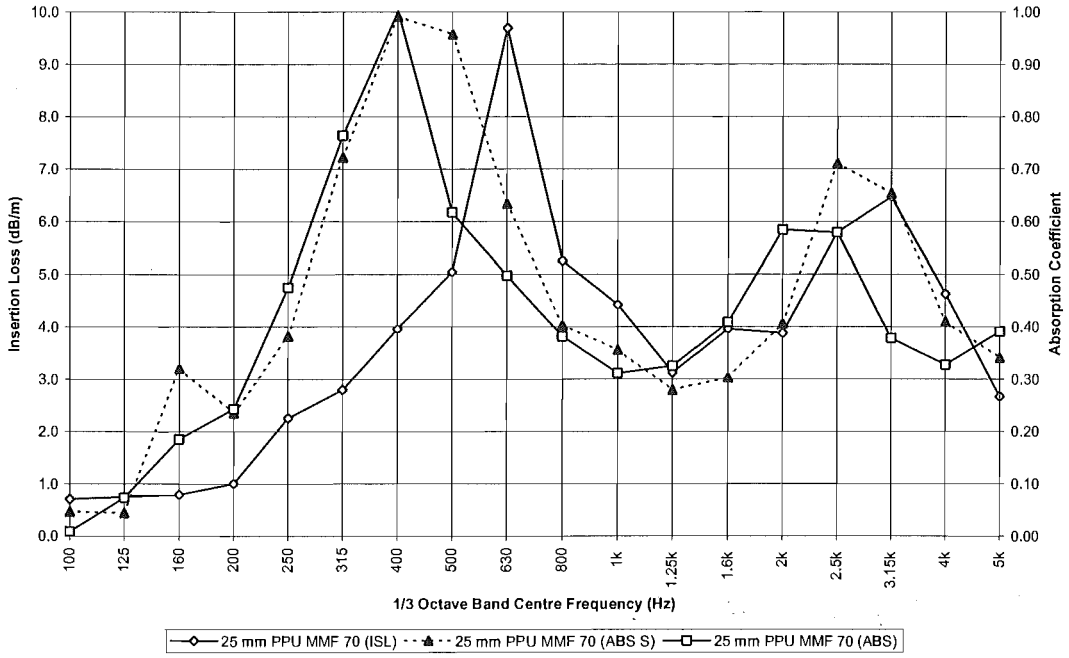

Figure 20: The loose laid absorption coefficient (ABS), absorption coefficient when pinned to 18 gauge steel sheet (ABS S), and pinned insertion loss of 25 mm thick polyether polyurethane (ISL) faced with 70 g/m^2 metallic foil. The peak in the absorption of 25 mm PPU MMF 70 (ABS S) is attributed to a resonance of the steel sheet.

The change in the peak absorption frequencies caused by pinning an absorber to a steel sheet shows that the difference between the insertion loss and absorption peak frequencies is due to differences in the impedance at the rear surface of the absorber. In this respect, the relationship between absorption coefficient and insertion loss is similar to that between pinned and bonded insertion loss.

It was expected that the pinned absorption coefficient of 25 mm thick polyether polyurethane faced with 70 g/m^2 metallic foil would have peaks at the same frequencies as the pinned insertion loss. The absorbers pinned to steel sheets in the

reverberation were laid in a single plane facing the ceiling, whereas the absorbers pinned in the insertion loss test facility were facing the opposite lined wall of the Test Section Duct. Therefore, the difference in the peak frequencies may be due to the difference in relative orientation of the absorbers when in the reverberation room and when in the insertion loss test facility.

4.6.10 Repeatability

A repeatability test was carried out on a 25mm thick polyether polyurethane foam absorber faced with 137 g/m^2 metallic foil. Five insertion loss measurements were made at different times over a period of two days, but with the same absorber and measurement procedures. The data from these measurements is shown in Figure 21. The largest deviation from the mean was 0.9 dB, which was deemed acceptable. The results of the repeatability test give a good indication of the reliability of the equipment and procedures used for insertion loss measurements. Clearly, confidence can be placed in the measured results.

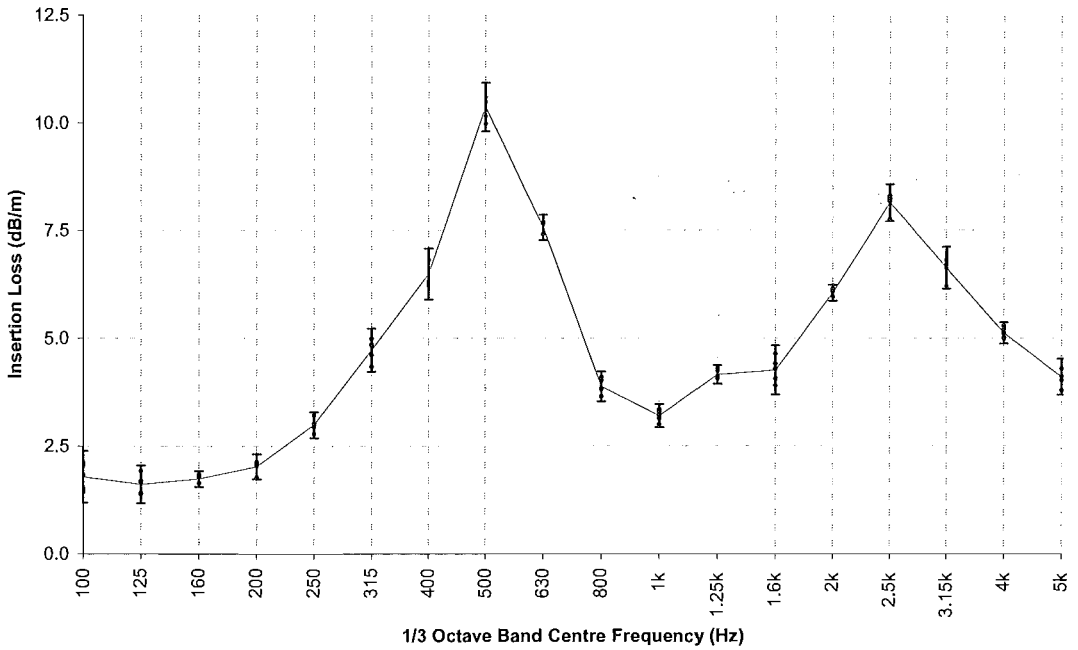

Figure 21: Repeatability of insertion loss measurements. The error bars show the maximum deviations from the mean. The pinned insertion loss of 25 mm polyether polyurethane foam faced with 137 g/m^2 metallic foil is shown.

4.7 Conclusions

The effects of absorber material, absorber thickness, facing material, fixing method and the velocity of airflow through the test duct were determined, facilitating the creation of guidelines for the application of absorbers in air moving ducts.

As expected, greater material thickness produced lower frequency absorption peaks. Thin facings were successfully used to alter the frequency at which peak insertion loss occurred, or to increase the peak insertion loss. Of the bulk absorber materials tested, melamine resin foam was most effective at low frequency, fibreglass at medium frequency, and polyester at high frequency.

It was found that absorber performance was very sensitive to the impedance at the boundary between the rear surface and duct wall. Pinning absorbers to the duct wall produced insertion loss peaks at lower frequency than those produced by adhesive bonding. It was also found that the impedance at the rear surface determined the relationship between insertion loss and absorption coefficient.

The insertion loss of bar absorbers with approximately constant thickness was very similar to the insertion loss of two wall absorbers of equal total volume, which showed that the insertion loss of these bar absorbers was primarily determined by absorbent volume. The bar absorber with triangular cross-section had significantly greater insertion loss at frequencies greater than 1.5 kHz. This was attributed to the change in thickness, and therefore flow resistance, of the cross-section of the bar absorber from the base to the apex providing optimal flow resistance for a wider frequency band.

4.8 Bibliography

Parkinson, J. P. 'Acoustic absorber design', Master of Engineering Thesis, University of Canterbury Department of Mechanical Engineering, Christchurch, New Zealand.

Ingard, K. U. (1994) 'Notes on Sound Absorption Technology' fig 6.5.2 pp 6-25, Noise Control Foundation, Arlington Branch, Poughkeepsie NY, USA.

4.9 References

1. Wassilieff, C. (1985) 'Performance of Duct Acoustic Linings Available in New Zealand', Transactions of the Institute of Professional Engineers New Zealand, vol. 12, 1985.
2. Cummings A. (1976) 'Sound attenuation in ducts lined on two opposite walls with porous material, with some application to splitters', Journal of Sound and Vibration **49**(1), 9-35.
3. Pridmore-Brown, D.C. (1958), "Sound propagation in a fluid flowing through an attenuating duct", Journal of Fluid Mechanics **4**, 393-406.
4. Mariano, S. (1971), "Effect of shear layers on attenuation in acoustically lined rectangular ducts", Journal of Sound and Vibration **19**(3), 261-275.
5. Astley R.J., Cummings A. (1987), "A finite element scheme for attenuation in ducts lined with porous material: comparison with experiment", Journal of Sound and Vibration **116**(2), 239-263.
6. Astley R.J., Cummings A. (1996), "Finite element computation of attenuation in bar-silencers and comparison with measured data", Journal of Sound and Vibration **196**(3), 351-369.
7. Bokor, A. (1969), "Attenuation of sound in lined ducts", Journal of Sound and Vibration **10**(3), 390-430.

5

PROJECT FINDINGS

Summary

Guidelines for the application of acoustic absorbers in air moving ducts were developed from the results of the testing program. None of the absorbers tested had high insertion loss over the entire test frequency range (100 Hz to 5 kHz). Therefore, the absorbers most suitable for low, medium and high frequency applications were identified.

The in-duct insertion loss of commonly used absorbing materials and the effects of thin facings on the insertion loss of these materials were recorded. This data can be used to for product improvement or new product development, or to create customised absorbers for specific applications.

The effects of different methods commonly used to fix absorbers in ducts were determined, and guidelines for the installation of absorbers in ducts were developed from this information.

Table of Contents

5.1. Introduction

The primary aim of this project was to develop guidelines for the use of absorbers in air ducts. The guidelines developed include the insertion losses of the absorbing materials tested at commonly used thicknesses, the effects of thin facings on the insertion loss of these materials, and the effects of commonly used methods for fixing absorbers in ducts. The guidelines can be used to guide the application or improvement of current in-duct absorbers, to aid in the creation of customised absorbers for specific applications, or to guide the development of new absorber products.

In the guidelines developed, the insertion loss cost and fire resistance of each absorber is presented. Cost and fire resistance were outside the scope of the project, however the inclusion of these parameters allows a more complete presentation of the total 'worth' of each absorber.

5.2. Aims

1. To develop guidelines for the use of the tested absorbers in air moving ducts.

5.3. Results

The presentation of the guidelines of for the use of absorbers in air moving ducts is based on absorbing material, as this is the most important parameter in the insertion loss of a ducted absorber. It is most efficient to select an absorber for a particular application by first selecting the absorbing material. Absorber materials most suitable for low, medium and high frequency applications are presented in Table 1.

Table 1: Absorber materials.

Frequency Range (1/3 octave band centre frequency, Hz)	Material with Highest Insertion Loss
100 - 1000	Melamine Resin Foam
1000 - 2000	Fibreglass
2000 - 5000	Polyester
Multiple Ranges	Polyether Polyurethane Foam

Table 2: Fire resistance of the absorbing materials tested.

Material	Smoke Developed Index (0-10)
Melamine Resin Foam	0-1
Fibreglass	0-1
Polyester	2
Polyether Polyurethane Foam	5

5.3.1. Melamine Resin Foam

Table 3: Summary of melamine resin foam absorbers.

Trade Name	Facing	Thickness (mm)	Insertion Loss				Cost ($NZ /m²)
			Pinned		Bonded		
			Peak (dB/m at Hz)	Average (dB/m)	Peak (dB/m at Hz)	Average (dB/m)	
Basotech Bonded Foil	MMF 70	25	16.8 at 630	5.6	10.0 at 1600	4.3	57.24
		50	15.2 at 250	5.3	9.6 at 630	3.6	101.35
		75	10.0 at 1000	6.3	-	-	161.68
Basotech	-	25	10.3 at 630	4.8	-	-	41.6

Melamine resin foam absorbers are most suitable for low frequency (315 Hz to 1 kHz) absorption. The peak insertion loss of the melamine foam wall absorbers tested increased when a metallised Mylar film was bonded to the exposed surface. Therefore, it is likely that the performance of melamine wall absorbers could be improved via a more detailed investigation into the effects of facings on this material. Such an investigation could involve facings of different surface density, or the use of perforated facings.

Melamine foam absorbers that were pinned to the duct walls had insertion loss peaks at much lower frequencies than those that were bonded. In addition, pinned melamine foam absorbers had greater overall insertion loss.

Table 4: Summary of melamine resin foam bar absorbers.

Cross-Section Shape	Facing	Dimensions (mm)		Insertion Loss		Cost ($NZ/m³)
				Peak (dB/m at Hz)	Average (dB/m)	
Square	None	Width	164	9.9 at 630	4.7	60.97
		Height	164			
Square	Two Sides MMF 70	Width	164	8.6 at 630	4.4	85.46
		Height	164			
Square	Four Sides MMF 70	Width	164	3.6 at 630	2.2	87.39
		Height	164			
Triangular	None	Base	164	9.6 at 630	6.4	60.97
		Height	329			
Circular	None	Diameter		8.5 at 630	5.3	60.97

The insertion loss of bar absorbers with approximately constant cross-sectional thickness is primarily determined by absorbent volume. The bar absorber with triangular cross-section has significantly greater insertion loss at frequencies greater than 1.5 kHz, which was attributed to the varying thickness, and therefore flow resistance, along the cross-section. Therefore, the performance of bar absorbers could best be improved by further investigating the effect of varying absorbent thickness on insertion loss.

The very poor insertion loss of the square bar absorber faced on four sides with 70 g/m^2 metallised Mylar film indicates that the insertion loss of bar absorbers cannot be improved by application of film facings.

5.3.2. *Fibreglass*

Table 5: Summary of fibreglass absorbers.

Trade Name	Facing	Thickness (mm)	Insertion Loss		Cost ($NZ/m²)
			Peak (dB/m at Hz)	Average (dB/m)	
Ductliner	PAF	25	18.8 at 1250	6.6	19.50
		50	20 at 800	8.8	28.50
Siliner	FGT	25	14.2 at 1600	6.1	18.99
		50	18.8 at 800	9.1	29.90
-	MMF 137	25	17.8 at 1600	7.6	-

Fibreglass absorbers are most suitable for medium frequency (1 kHz to 2 kHz) absorption. Fibreglass faced with perforated aluminium foil, had the highest peak insertion loss of all absorbers tested. Fibreglass is the only absorbing material of those tested that is not flammable. Increasing the thickness of fibreglass absorbers reduced the peak insertion loss frequency.

The insertion loss performance of fibreglass absorbers could be improved by further investigating the effects of perforated facings. Evidence was found that perforated facings increase the insertion loss of fibrous absorbers by creating a Helmholtz resonator. It is likely that perforated facings could be used to customise, or 'tune', fibreglass absorbers for specific applications.

It was found that the insertion loss of fibreglass is relatively insensitive to facing material parameters other than perforation. Fibreglass is a rigid framed material, therefore insertion loss cannot be improved by increasing frame borne absorption.

5.3.3. *Polyester*

Table 6: Summary of polyester absorbers.

Trade Name	Facing	Thickness (mm)	Insertion Loss		Cost ($NZ/m²)
			Peak (dB/m at Hz)	Average (dB/m)	
Quiet Stuff	SBP	25	13.6 at 2000	6.2	18.35
		50	17.8 at 1600	7.6	26.90

Polyester absorbers are most effective at high frequencies (2 kHz to 5 kHz). Polyester is a rigid framed non-isotropic absorbing material, thus the insertion loss properties of the material are very similar to those of fibreglass.

The effect of increasing thickness from 25 mm to 50 mm was to reduce the peak insertion loss frequency. The sensitivity of polyester to differences in facing material was not investigated. Because the properties of polyester are similar to those of fibreglass it is likely that the insertion loss of the material could be increased or the peak frequency changed by applying a perforated facing.

5.3.4. Polyether Polyurethane Foam

Table 7: Summary of polyether polyurethane foam absorbers.

Trade Name	**Facing**	**Thickness** (mm)	**Insertion Loss**				Cost ($NZ/m²)
			Pinned		**Bonded**		
			Peak (dB/m at Hz)	**Average** (dB/m)	**Peak** (dB/m at Hz)	**Average** (dB/m)	
Acoustop Absorber Bonded Foil (AABF)	MMF 70	25	9.7 at 630	3.8	8.9 at 1250	3.6	37.24
		50	10.3 at 315	4.6	7.6 at 800	4.5	62.19
		75	13.5 at 200	4.1	-	-	87.80
Acoustop Absorber Heavy Foil (940 Foil)	MMF 137	25	10.0 at 500	4.8	-	-	39.77

The insertion loss of the polyether polyurethane absorbers did not exceed the insertion losses of all the other absorbers tested at any frequency in the test range. However, film faced polyether polyurethane was the only absorber tested that had multiple insertion loss peaks at 25mm thickness. Absorbers of greater than 25 mm thickness are not commonly used in ducts because airway obstruction becomes too great; therefore, the material would be the most effective of those tested in absorbing noise with multiple peaks.

The insertion loss of film faced polyether polyurethane foam can be modified by changing the surface density of the film facing or by changing the thickness of the material. Facings of greater density and increases in thickness reduce the peak insertion loss frequencies. Because the insertion loss of polyether polyurethane foam is sensitive to material thickness and to film facing density, absorbers of this material could be easily customised for

applications where the noise field has multiple peaks. More detailed knowledge of the effects of these parameters on the induct insertion loss of the material is required to enable such a customisation to be performed.

5.4. Conclusions

It was found that melamine resin foam absorbers are most effective for low frequency applications, fibreglass absorbers for medium frequency applications and polyester absorbers for high frequency applications. It was also found that film faced polyether polyurethane is most suitable for applications where the noise field has multiple peaks.

The insertion loss of melamine resin foam wall absorbers could be improved by further investigating the effects of a thin facing bonded to the exposed surface of the absorbing material. Melamine resin foam bar absorbers with varying cross-sectional thickness have significantly greater insertion loss, which indicates that the performance of bar absorbers could best be improved by further investigating the effect of varying absorbent thickness on insertion loss.

The insertion loss of fibreglass and polyester absorbers could be increased or the peak frequency altered by further investigating the effects of thin perforated facing. This could also be achieved by altering the flow resistance of the materials, however such an investigation is more technically difficult.

Film faced polyether polyurethane foam could be easily customised for applications where the noise field has multiple peaks, however more detailed knowledge of the effects of film surface density and material thickness are required for such customisation.

PROJECT CONCLUSION

The objectives of the project were to measure the in-duct attenuation performance of a range of acoustic absorbers, and to develop guidelines for the design and application of in-duct absorbers.

A survey of literature relevant to absorption in ducts was carried out. The results of this survey were used in selecting the best insertion loss measurement method, to select absorbing and facing materials for the testing program, and in analysis of the measured data from the testing program.

A test facility for measuring in-duct insertion loss was designed and constructed to meet the requirements of ISO 7235, and used for the testing program. Data from the testing program was analysed, and the effects on insertion loss of absorbing material, absorber thickness, facing type, airflow conditions, and the cross section of bar absorbers were determined.

Further Work

Sound Field in the Test Section Duct

More detailed knowledge of the sound field within the Test Section Duct is required for in-depth analysis of absorber performance in ducts, and before significant improvements to the sound measurement system can be made. Therefore, it is recommended a detailed survey of the sound field in the Substitution Test Duct be carried out.

The number of measurement points used must be sufficient to allow accurate interpolation between the measured data, and thus allow detailed visualization of the sound field, such as could be achieved with contour plots. It is recommended that 20 measurement positions be used initially.

Airflow Through the Test Section Duct

The pressure drop across bar absorbers is an important factor in their overall performance; therefore detailed knowledge of the airflow through the test section duct is required for further design and development of bar absorbers. Future improvement of the airflow measurement

equipment must also be based on detailed knowledge of the airflow through the Test Section Duct. It is recommended that the transverse velocity profile of airflow through the Test Section Duct be accurately determined at several points along the duct, over typical airflow conditions in building services ducts. The survey could be carried out by traversing a hot-wire anemometer inside the Substitution Test Duct.

Acoustic Instrumentation

The time required to make an insertion loss measurement could be greatly reduced if an array of microphones, rather than a single microphone, were used at each reference position. The results of the work in this thesis indicate that an array of four microphones would be required, however the number of microphones used should be based on a detailed survey of the sound field, as discussed above.

Airflow Instrumentation

Future development of bar absorbers requires dedicated instrumentation capable of more accurate measurement of the airflow velocity profile within the test duct than that used in this work. Therefore, it is recommended that Pitot tube arrays with at least double the number of measurement positions (20) as those used in this work be developed.

Bar Absorbers

The insertion loss performance of bar absorbers with significant variation in thickness was better than those with approximately constant thickness. Therefore it is recommended that bar absorbers with varying thickness be investigated further. Because material costs for bar absorbers are relatively high, numerical prediction techniques for bar absorber insertion loss may be attractive, particularly if used in conjunction with experiment.

Perforated Facings

The fibreglass absorber with a perforated facing of 12% open area had a particularly high peak insertion loss, and consequently the effects of perforated facings merit further investigation. The parameters investigated should include percentage of open area, orifice size, and the response of a range of absorbing materials to perforated facings.

Fixing Method

It was found that the method used to fix absorbers to the duct walls was very significant in determining insertion loss. The results of this work indicate that insertion loss performance can be significantly improved by using an appropriately designed fixing method. Fixing systems that could be usefully investigated include different pinning arrangements, and systems that create a cavity between the absorbent and the duct wall.

Duct Aspect Ratio

It is well known that the aspect ratio of a lined duct is an important factor in determining insertion loss. The effects of aspect ratio on insertion loss were not investigated in this work. A wide range of aspect ratios are used in building services ducts, and therefore such knowledge would be very valuable.

Test Facility Drawings

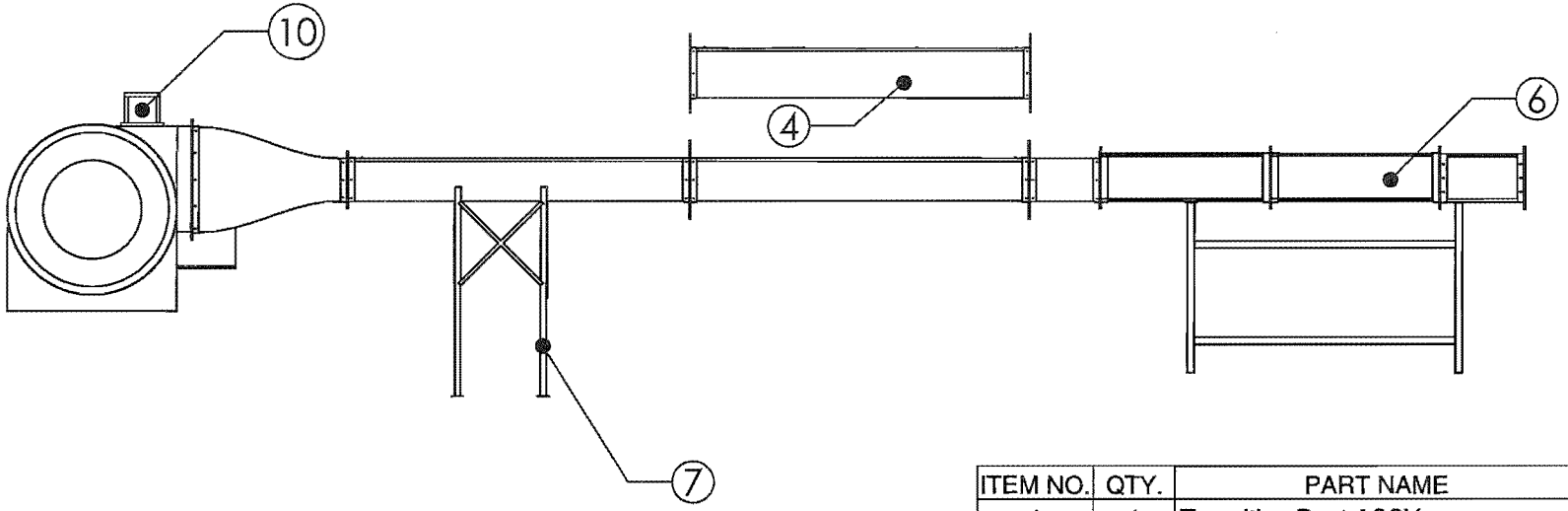

ITEM NO.	QTY.	PART NAME	DRG. NO.
1	1	Transition Duct ASSY	1
2	1	Test Section Inlet Duct ASSY	2
3	1	Substitution Test Duct ASSY	3
4	1	25mm Test Section	5
5	1	Test Section Outlet Duct ASSY	5
6	1	Anechoic Termination	6
7	1	Ducting Stand	7
8	1	Fan ASSY	8
9	1	Motor Enclosure ASSY.	9
10	1	Speaker Box ASSY.	10

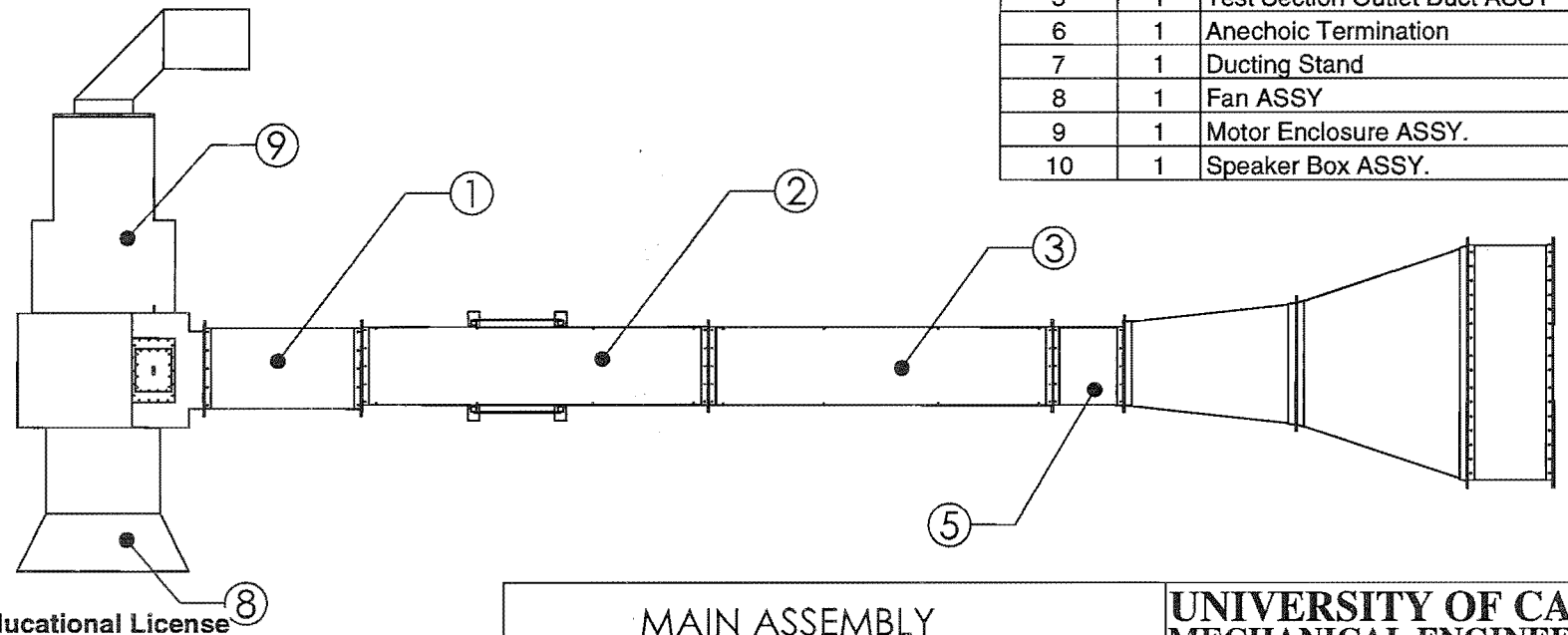

MAIN ASSEMBLY

SCALE : 1:50 ALL DIMENSIONS IN mm

UNIVERSITY OF CANTERBURY
MECHANICAL ENGINEERING DEPT. CH.CH. N.Z.

DRAWN : PETTERSSON | DATE : 12/12/01

CHECKED : SPARKS | DRG. No : ASSY

APPROVED : PEARSE

ITEM NO.	QTY.	PART NAME	DRG. NO.
1	1	Transition Duct	1-1
2	1	Large Transition Duct Flange	1-2
3	1	Small Transition Duct Flange	1-3

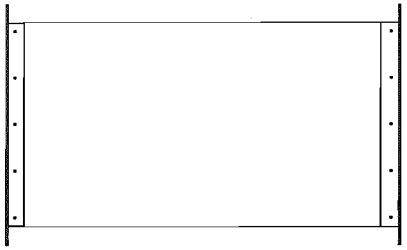

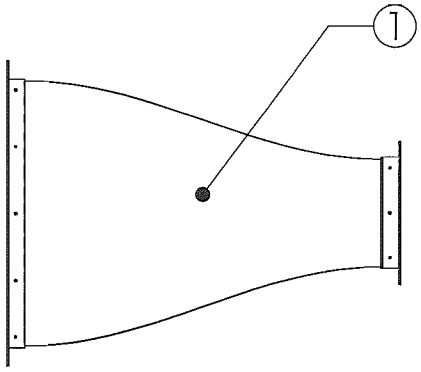

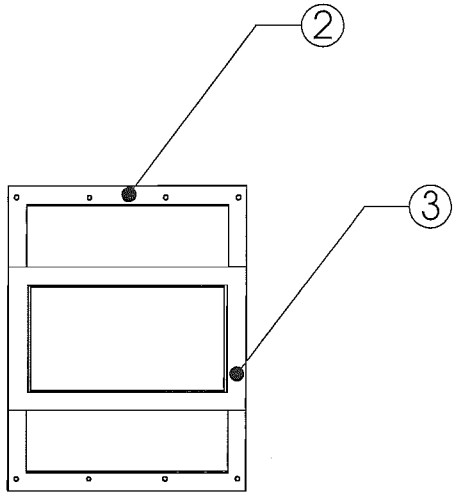

TRANSITION DUCT ASSY

SCALE : 1:20 ALL DIMENSIONS IN mm

UNIVERSITY OF CANTERBURY
MECHANICAL ENGINEERING DEPT. CH.CH. N.Z.

DRAWN : PETTERSSON | DATE : 10/12/01
CHECKED : SPARKS | DRG. No : 1
APPROVED : PEARSE

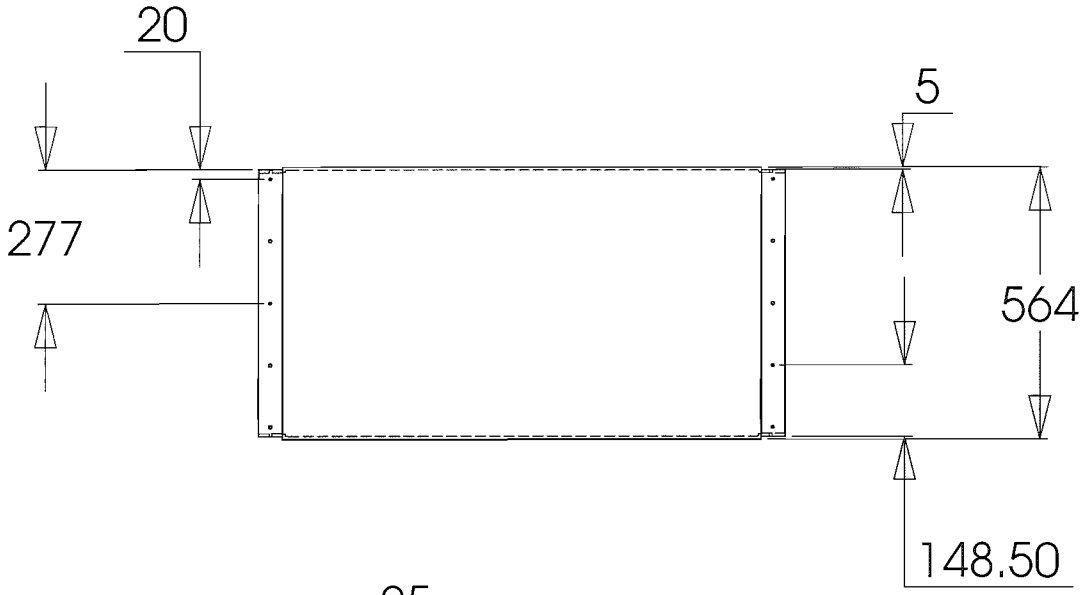

TO BE CONSTRUCTED
FROM 5mm PLYBOARD
HELD TOGETHER WITH
WOOD SCREWS AND
ADHESIVE

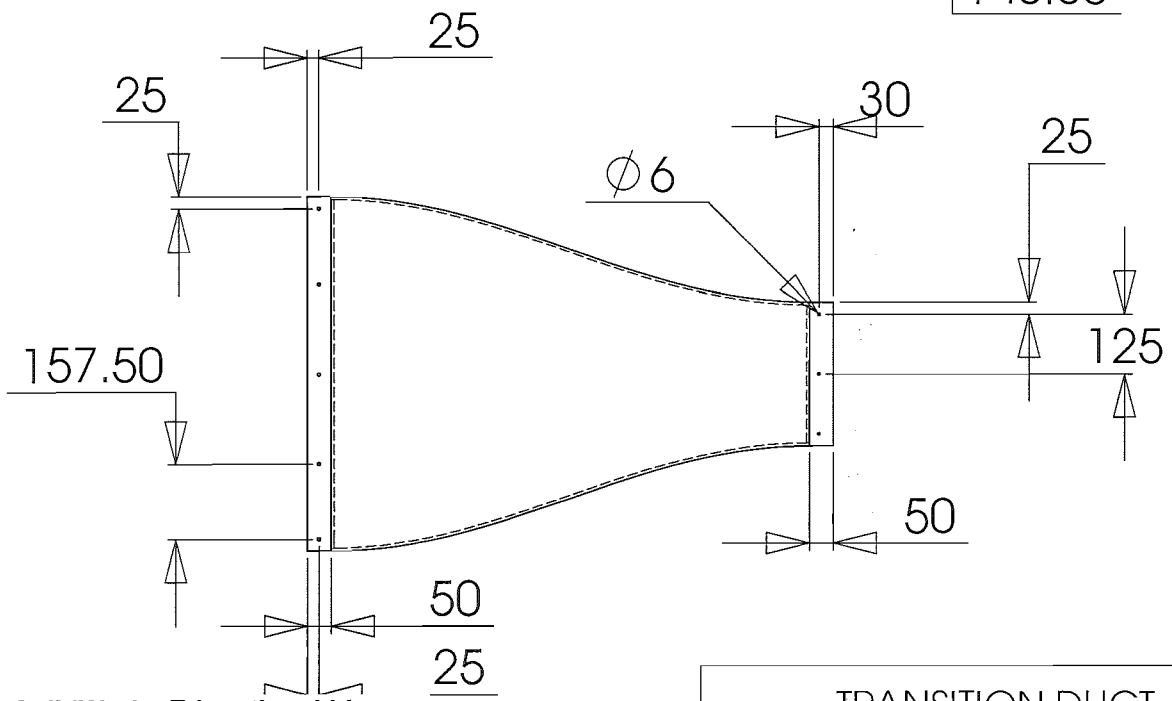

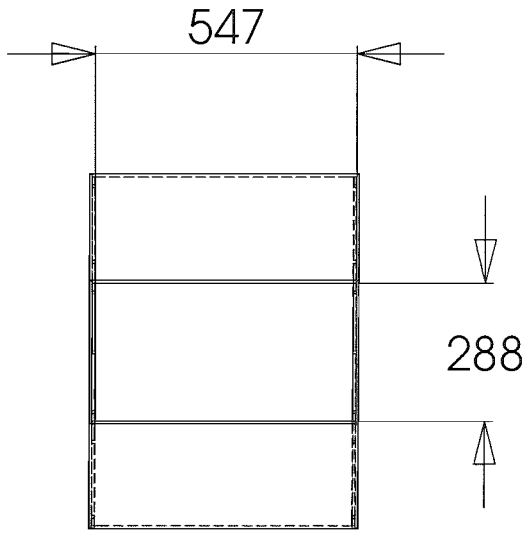

TRANSITION DUCT

SCALE : 1:15

ALL DIMENSIONS IN mm

UNIVERSITY OF CANTERBURY
MECHANICAL ENGINEERING DEPT. CH.CH. N.Z.

DRAWN : PETTERSSON	DATE : 11/12/01
CHECKED : SPARKS	DRG. No : 1-1
APPROVED : PEARSE	

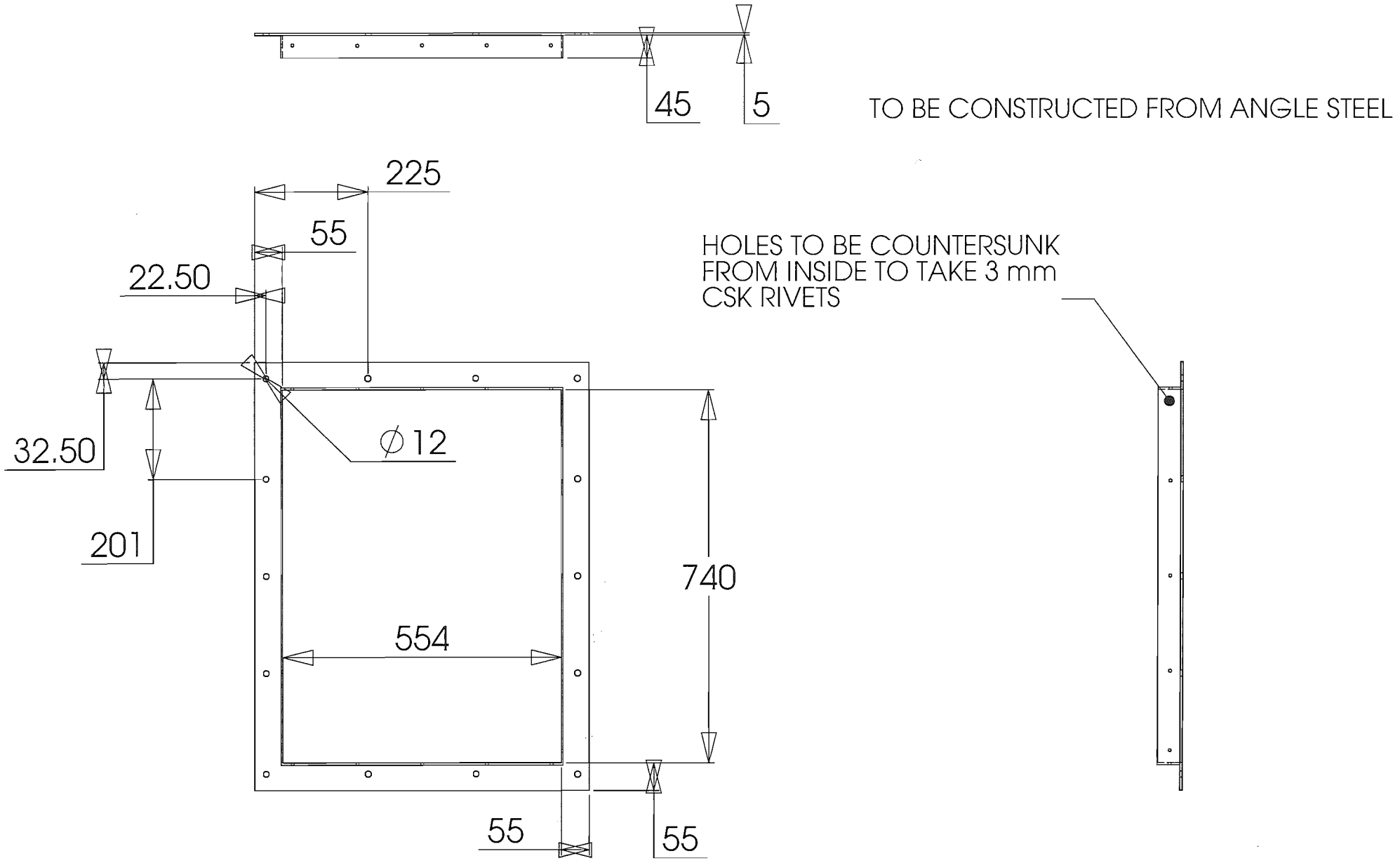

LARGE TRANSITION DUCT FLANGE

SCALE : 1:10 ALL DIMENSIONS IN mm

UNIVERSITY OF CANTERBURY
MECHANICAL ENGINEERING DEPT. CH.CH. N.Z.

DRAWN : PETTERSSON	DATE : 10/12/01
CHECKED : SPARKS	DRG. No : 1-2
APPROVED : PEARSE	

TO BE CONSTRUCTED FROM ANGLE STEEL

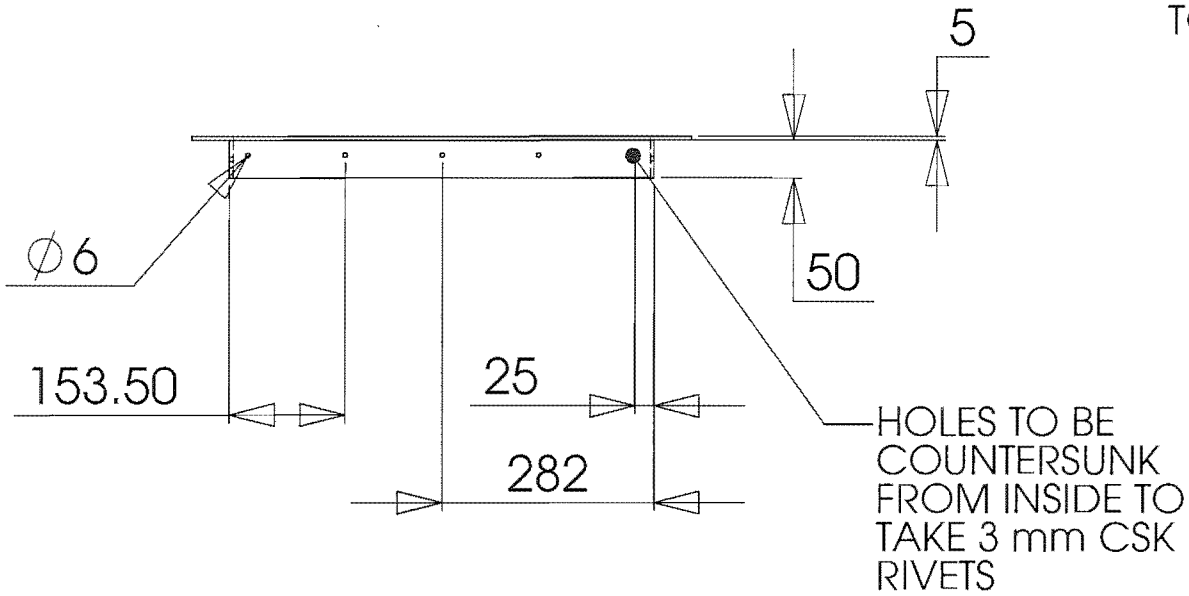

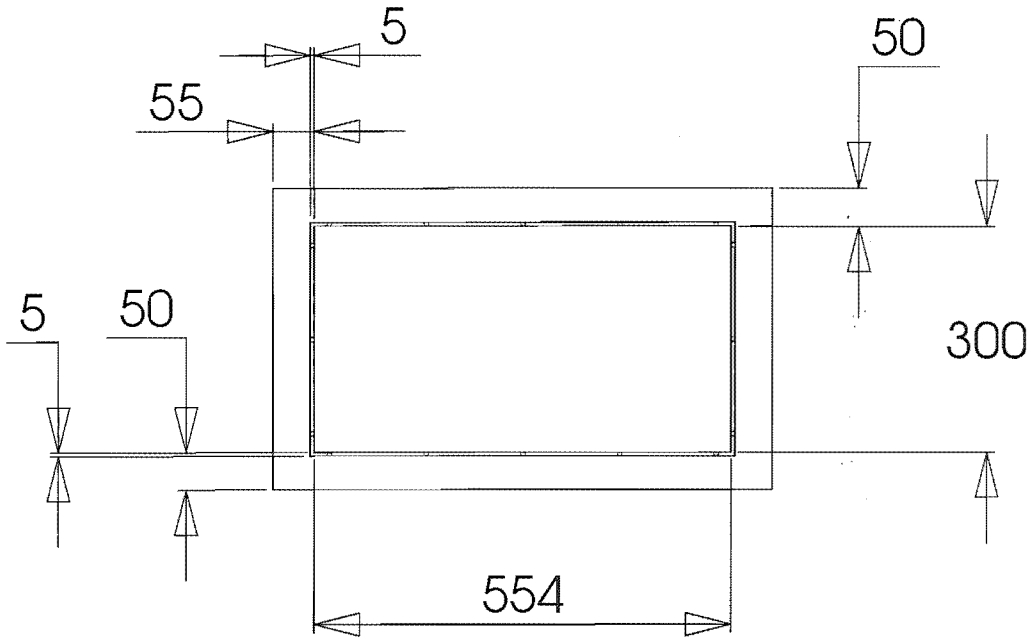

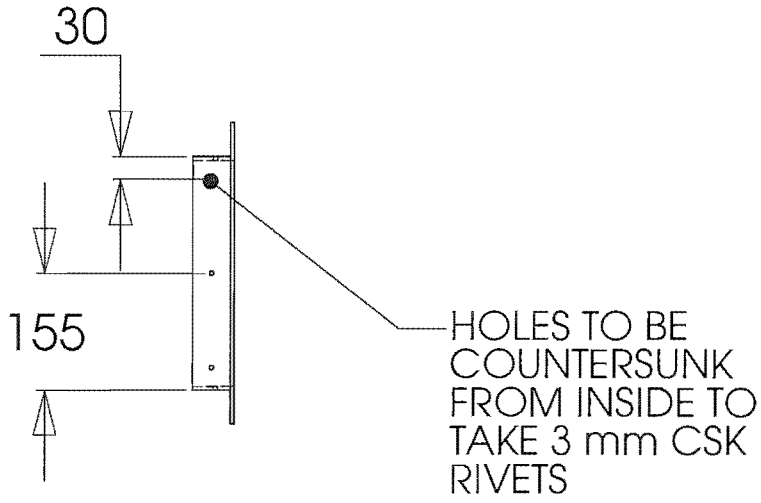

SMALL TRANSITION DUCT FLANGE	UNIVERSITY OF CANTERBURY MECHANICAL ENGINEERING DEPT. CH.CH. N.Z.	
	DRAWN : PETTERSSON	DATE : 10/12/01
	CHECKED : SPARKS	DRG. No : 1-3
SCALE : 1:10 ALL DIMENSIONS IN mm	APPROVED : PEARSE	

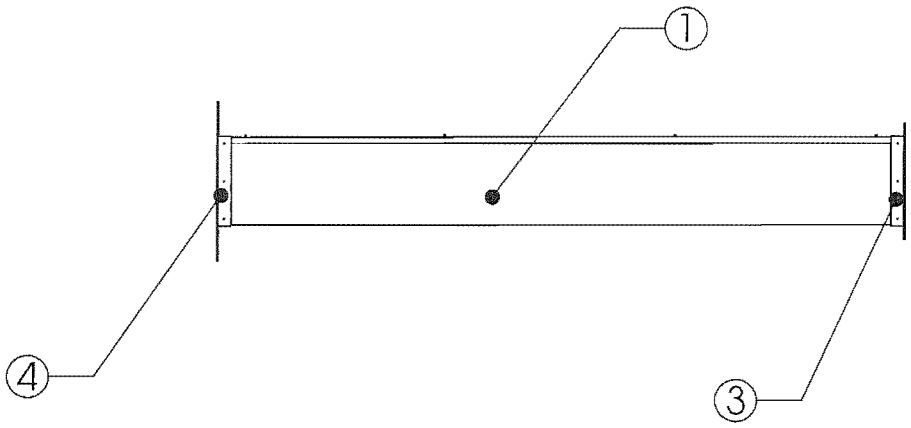

ITEM NO.	QTY.	PART NAME	DRG. NO.
1	1	Test Section Inlet Duct	2-1
2	1	Test Section Inlet Duct Lid	2-2
3	1	Intlet Outlet Duct Flange	2-3
4	1	Test Section Flange	2-4

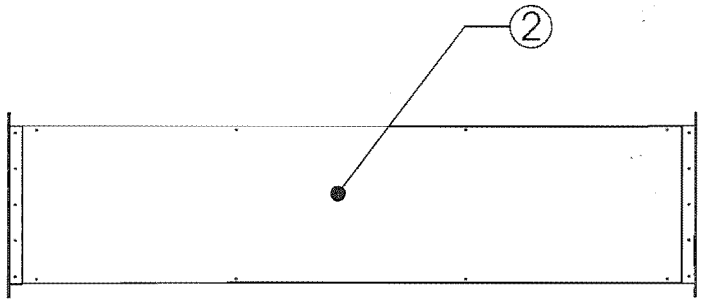

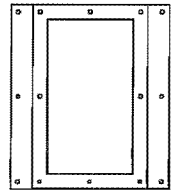

TEST SECTION INLET DUCT ASSY

SCALE : 1:25 ALL DIMENSIONS IN mm

UNIVERSITY OF CANTERBURY
MECHANICAL ENGINEERING DEPT. CH.CH. N.Z.

DRAWN : PETTERSSON DATE : 10/12/01
CHECKED : SPARKS DRG. No : 2
APPROVED : PEARSE

TO BE CONSTRUCTED FROM 18 GAUGE STEEL SHEET

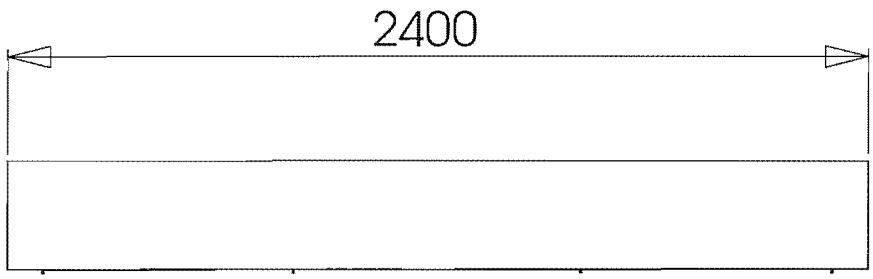

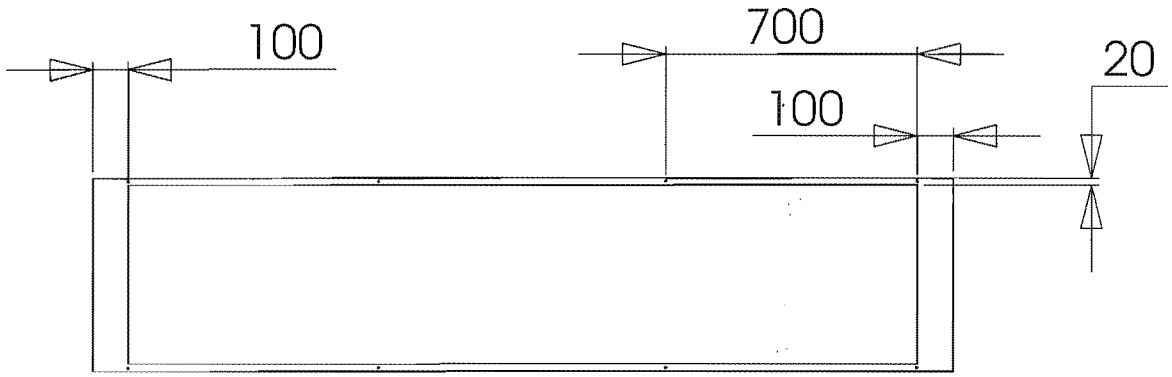

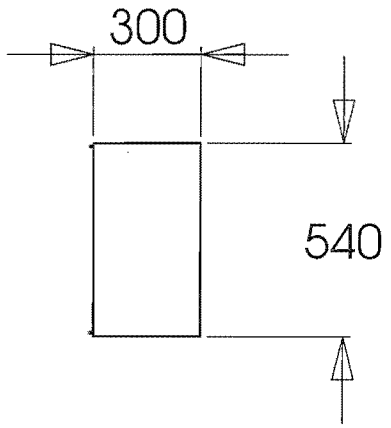

TEST SECTION INLET DUCT	UNIVERSITY OF CANTERBURY MECHANICAL ENGINEERING DEPT. CH.CH. N.Z.	
	DRAWN : PETTERSSON	DATE : 10/12/01
	CHECKED : SPARKS	DRG. No : 2-1
SCALE : 1:25 ALL DIMENSIONS IN mm	APPROVED : PEARSE	

TO BE CONSTRUCTED FROM 18 GAUGE STEEL SHEET

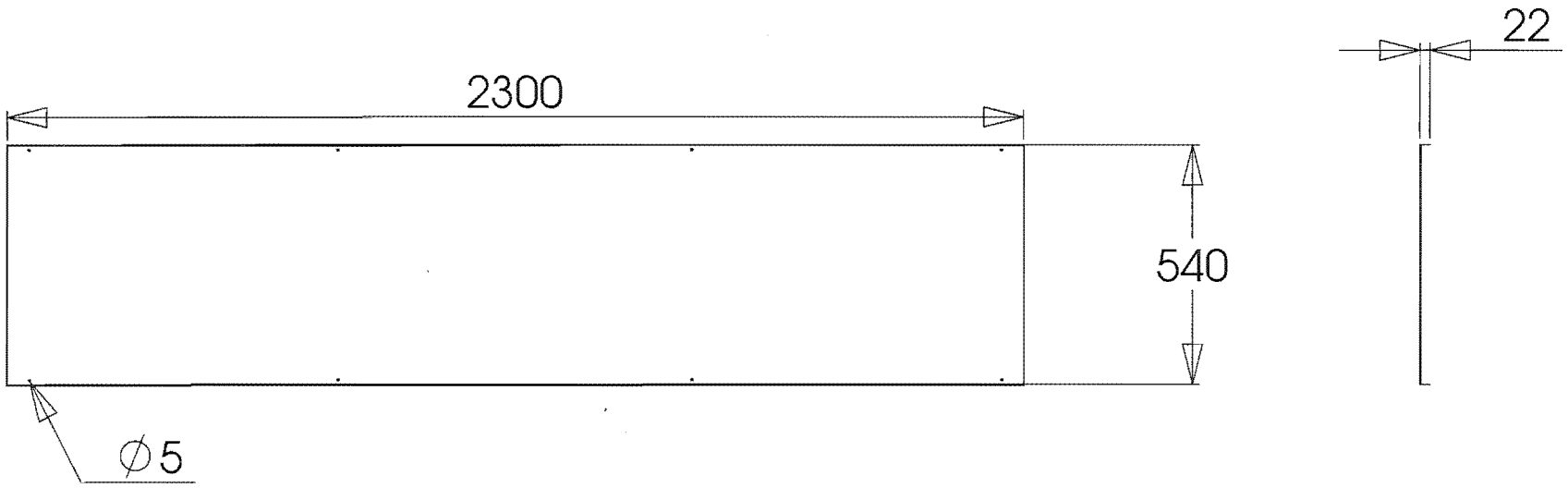

TEST SECTION INLET DUCT LID

SCALE : 1:15 ALL DIMENSIONS IN mm

UNIVERSITY OF CANTERBURY
MECHANICAL ENGINEERING DEPT. CH.CH. N.Z.

DRAWN : PETTERSSON	DATE : 10/12/01
CHECKED : SPARKS	DRG. No : 2-2
APPROVED : PEARSE	

TO BE CONSTRUCTED FROM ANGLE STEEL

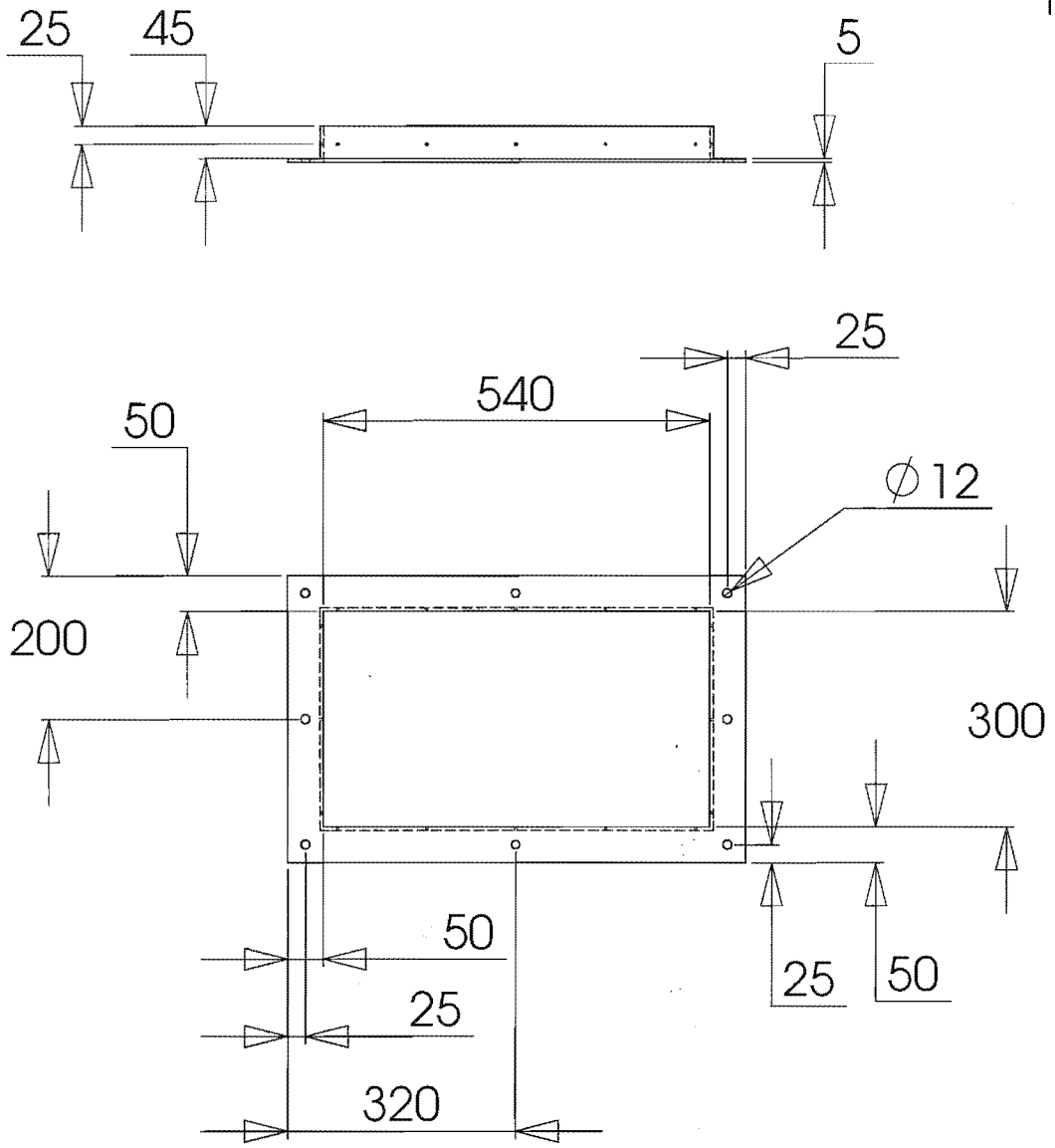

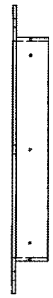

INLET OUTLET DUCT FLANGE

SCALE : 1:10 ALL DIMENSIONS IN mm

UNIVERSITY OF CANTERBURY
MECHANICAL ENGINEERING DEPT. CH.CH. N.Z.

DRAWN : PETTERSSON	DATE : 10/12/11
CHECKED : SPARKS	DRG. No : 2-3
APPROVED : PEARSE	

TO BE CONSTRUCTED FROM ANGLE STEEL

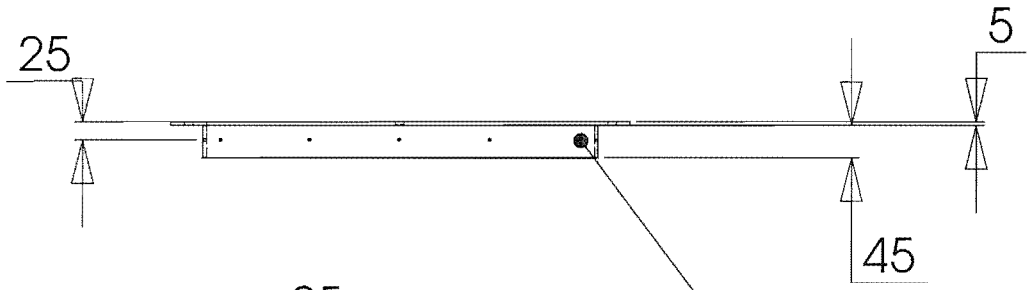

HOLES TO BE COUNTERSUNK TO
TAKE 3 mm CSK RIVETS

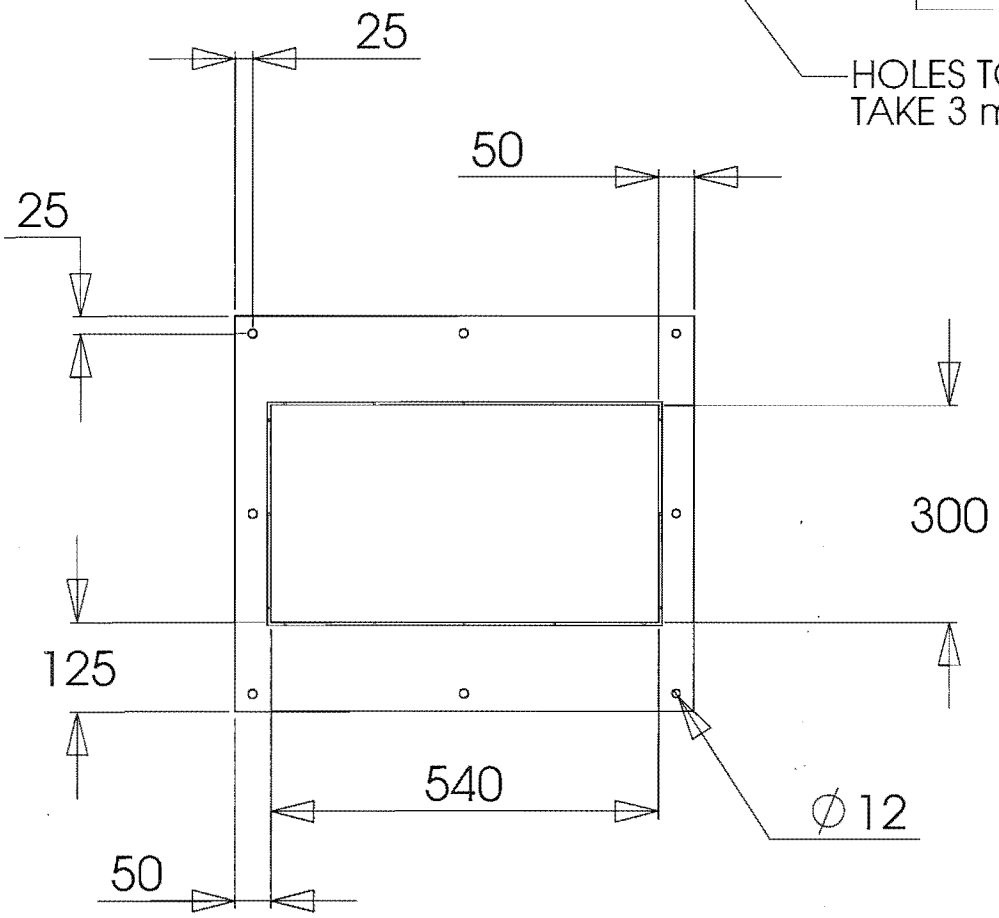

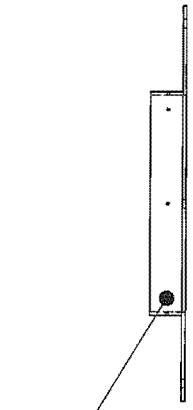

HOLES TO BE COUNTERSUNK TO
TAKE 3 mm CSK RIVETS

TEST SECTION FLANGE	UNIVERSITY OF CANTERBURY MECHANICAL ENGINEERING DEPT. CH.CH. N.Z.	
	DRAWN : PETTERSSON	DATE : 10/12/01
	CHECKED : SPARKS	DRG. No : 2-4
SCALE : ALL DIMENSIONS IN mm	APPROVED : PEARSE	

ITEM NO.	QTY.	PART NAME	DRG. NO.
1	1	Test Section Inlet Duct	2-1
2	1	Test Section Inlet Duct Lid	2-2
3	2	Test Section Flange	2-4

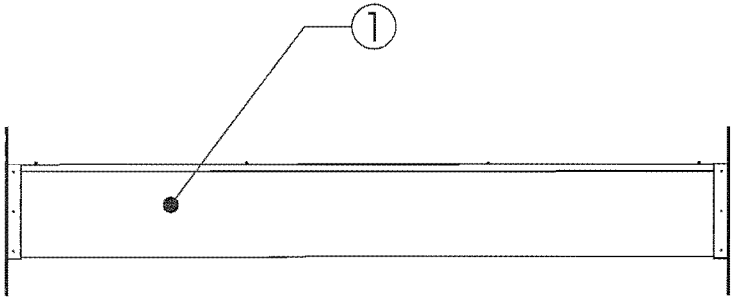

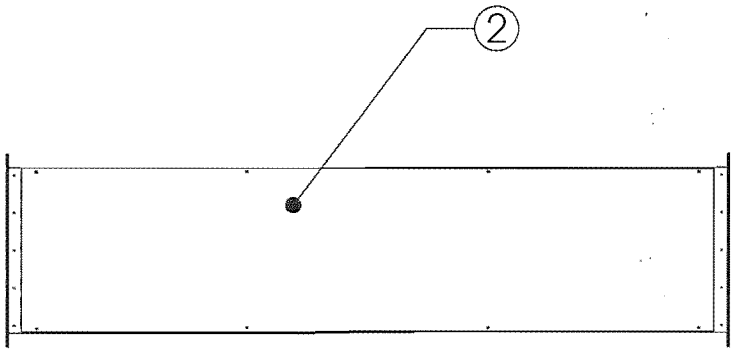

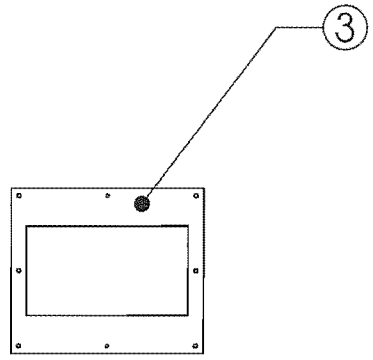

SUBSTITUTION TEST DUCT ASSY

SCALE : 1:25 ALL DIMENSIONS IN mm

UNIVERSITY OF CANTERBURY
MECHANICAL ENGINEERING DEPT. CH.CH. N.Z.

DRAWN : PETTERSSON DATE : 10/12/01
CHECKED : SPARKS DRG. No : 3
APPROVED : PEARSE

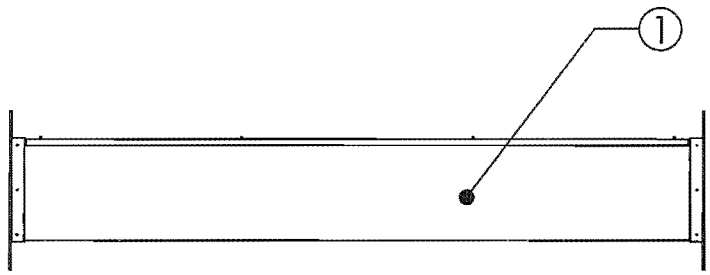

ITEM NO.	QTY.	PART NAME	DRG. NO.
1	1	25mm Test Section Duct	4-1
2	2	25mm Test Section Flange	4-2
3	1	Test Section Inlet Duct Lid	2-2

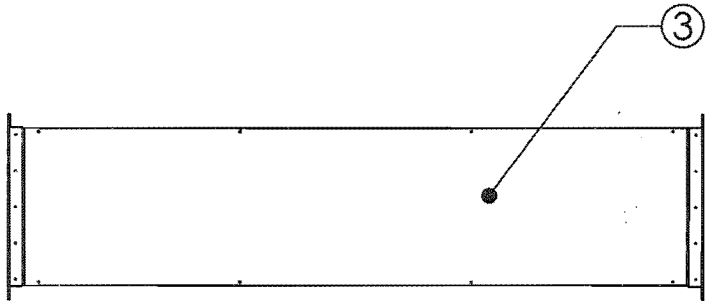

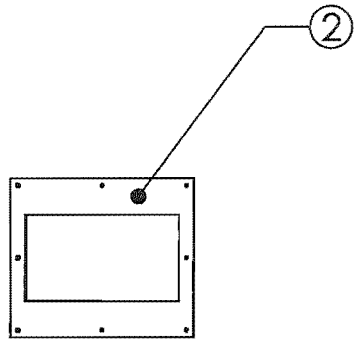

25mm TEST SECTION ASSY.

SCALE : 1:25 ALL DIMENSIONS IN mm

UNIVERSITY OF CANTERBURY
MECHANICAL ENGINEERING DEPT. CH.CH. N.Z.

DRAWN : PETTERSSON | DATE : 10/12/01
CHECKED : SPARKS | DRG. No : 4
APPROVED : PEARSE

TO BE MANUFACTURED FROM 18 GAUGE STEEL SHEET

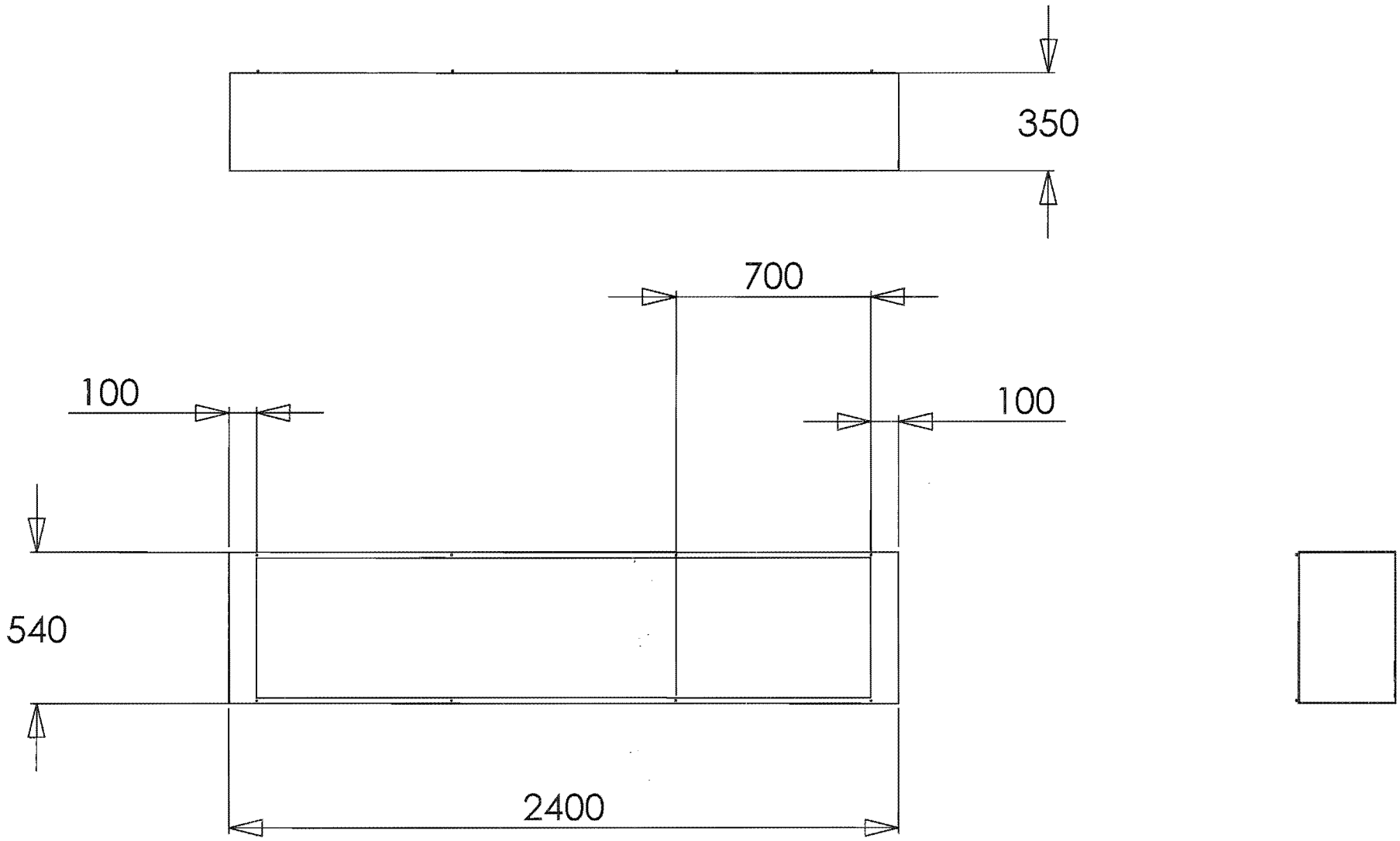

25mm TEST SECTION DUCT

SCALE : 1:20 ALL DIMENSIONS IN mm

UNIVERSITY OF CANTERBURY
MECHANICAL ENGINEERING DEPT. CH.CH. N.Z.

DRAWN : PETTERSSON	DATE : 10/12/01
CHECKED : SPARKS	DRG. No : 4-1
APPROVED : PEARSE	

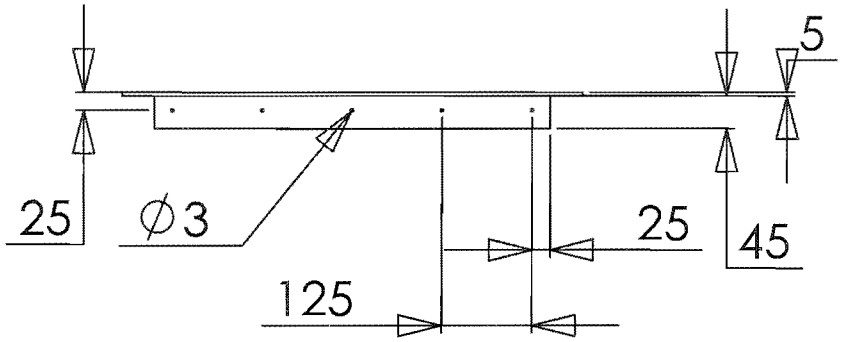

TO BE CONSTRUCTED FROM 5mm THICK
ANGLE STEEL AND 5mm STEEL PLATE

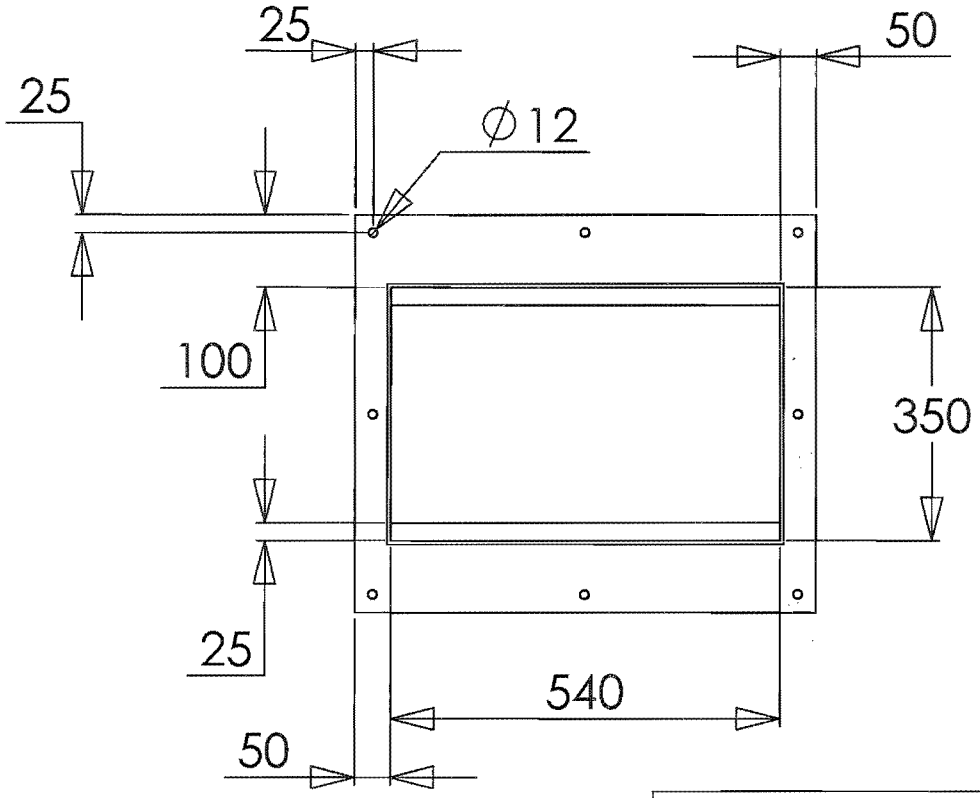

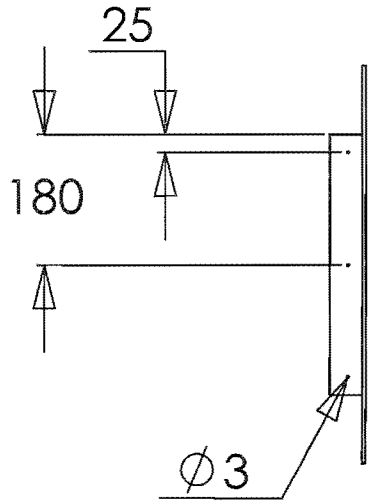

25mm TEST SECTION FLANGE

SCALE : 1:10 ALL DIMENSIONS IN mm

UNIVERSITY OF CANTERBURY
MECHANICAL ENGINEERING DEPT. CH.CH. N.Z.

DRAWN : PETTERSSON	DATE : 10/12/01
CHECKED : SPARKS	DRG. No : 4-2
APPROVED : PEARSE	

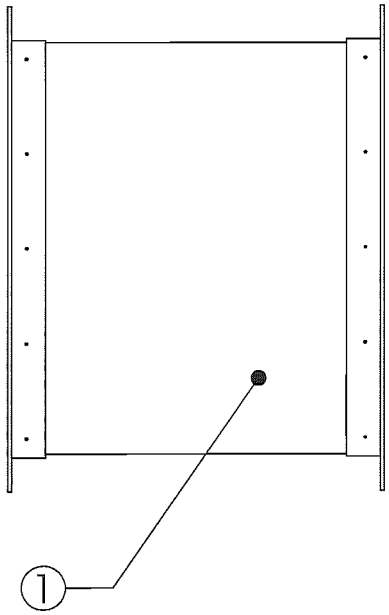

ITEM NO.	QTY.	PART NAME	DRG. NO.
1	1	Test Section Outlet Duct	5-1
2	1	Intlet Outlet Duct Flange	2-3
3	1	Test Section Flange	2-4

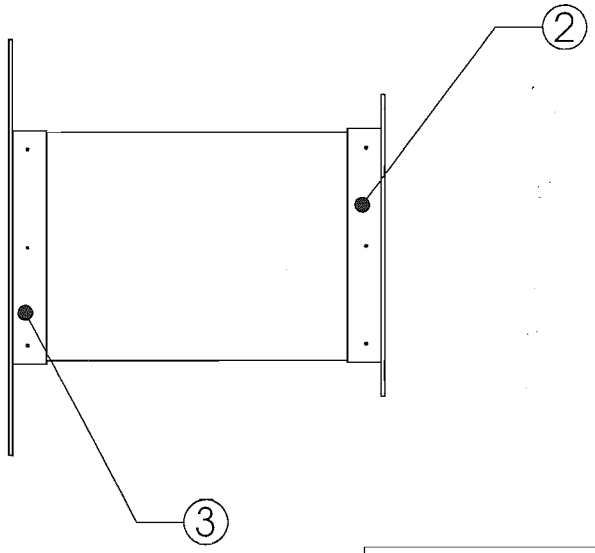

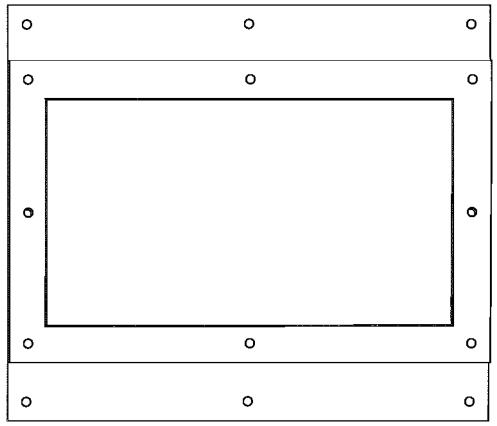

TEST SECTION OUTLET DUCT

SCALE : 1:10 ALL DIMENSIONS IN mm

UNIVERSITY OF CANTERBURY
MECHANICAL ENGINEERING DEPT. CH.CH. N.Z.

DRAWN : PETTERSSON DATE : 10/12/01
CHECKED : SPARKS DRG. No : 5
APPROVED : PEARSE

TO BE CONSTRUCTED FROM 18 GAUGE STEEL SHEET

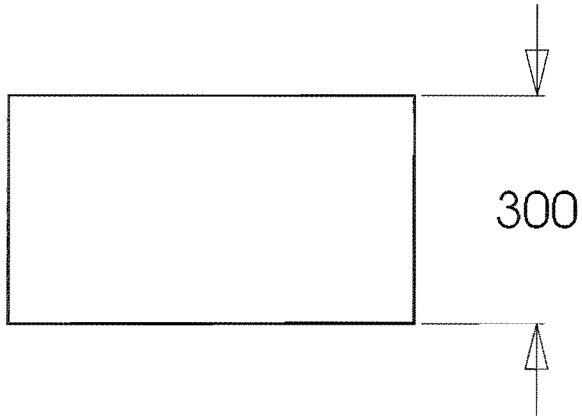

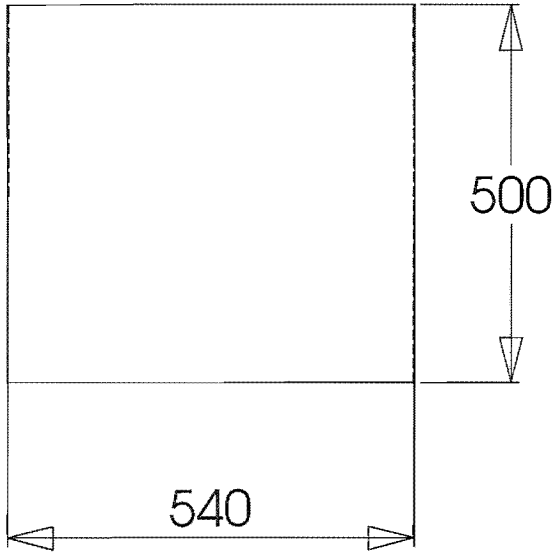

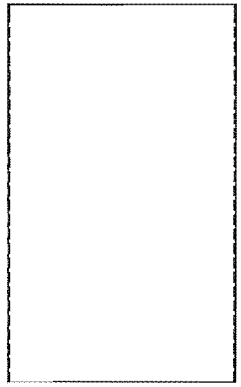

TEST SECTION OUTLET DUCT

SCALE : 1:10 ALL DIMENSIONS IN mm

UNIVERSITY OF CANTERBURY
MECHANICAL ENGINEERING DEPT. CH.CH. N.Z.

DRAWN : PETTERSSON	DATE : 10/12/01
CHECKED : SPARKS	DRG. No : 5-1
APPROVED : PEARSE	

ITEM NO.	QTY.	PART NAME	DRG. NO.
1	1	Anechoic Termination Section One	6-1
2	1	Anechoic Termination Section Two	6-2
3	1	Anechoic Termination Section Three	6-3
4	1	Termination Stand	6-4

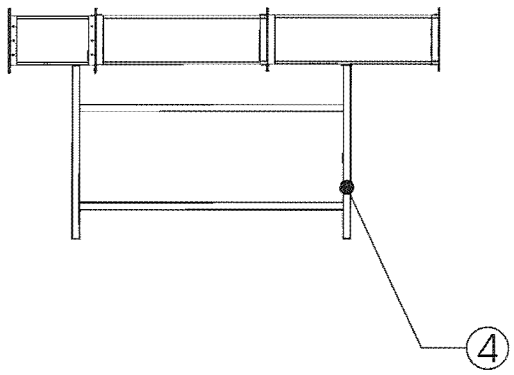

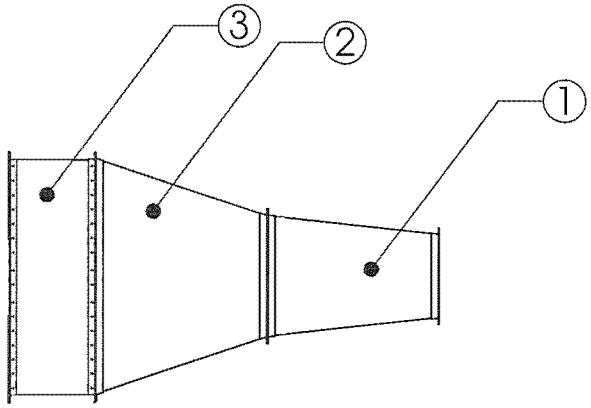

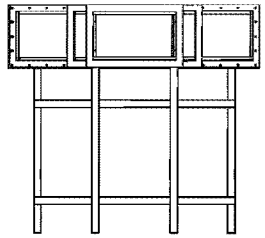

ANECHOIC TERMINATION ASSY

SCALE : 1:50 ALL DIMENSIONS IN mm

UNIVERSITY OF CANTERBURY
MECHANICAL ENGINEERING DEPT. CH.CH. N.Z.

DRAWN : PETTERSSON | DATE : 10/12/01
CHECKED : SPARKS | DRG. No : 6
APPROVED : PEARSE

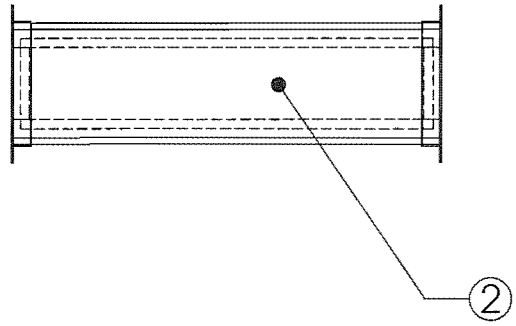

ITEM NO.	QTY.	PART NAME	DRG. NO.
1	2	Section One Top Wall	6-1-1
2	2	Section One Side Wall	6-1-2
3	1	Section One Large Flange	6-1-3
4	1	Section One Small Flange	6-1-4
5	2	Long Internal Wall ASSY	6-1-5

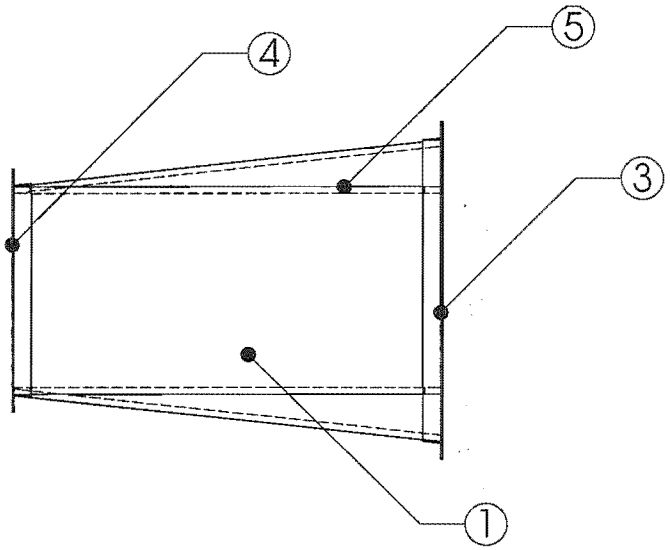

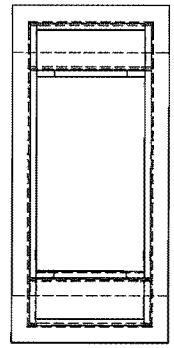

SECTION ONE OF THE ANECHOIC TERMINATION

SCALE : 1:20 ALL DIMENSIONS IN mm

UNIVERSITY OF CANTERBURY
MECHANICAL ENGINEERING DEPT. CH.CH. N.Z.

DRAWN : PETTERSSON | DATE : 10/12/01
CHECKED : SPARKS | DRG. No : **6-1**
APPROVED : PEARSE

TO BE CONSTRUCTED FROM 18mm MDF

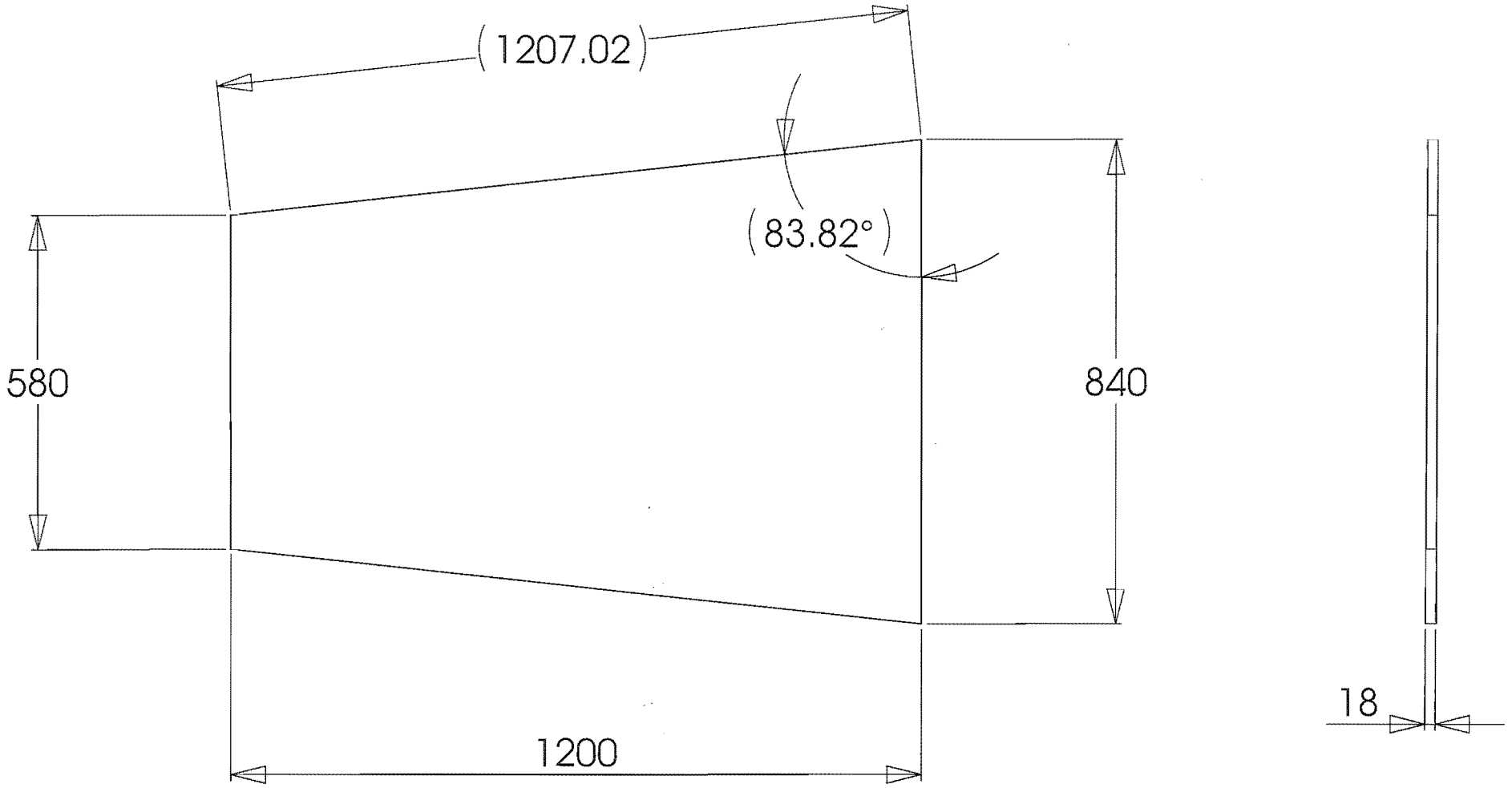

SECTION ONE TOP WALL

SCALE : 1:10 ALL DIMENSIONS IN mm

UNIVERSITY OF CANTERBURY
MECHANICAL ENGINEERING DEPT. CH.CH. N.Z.

DRAWN : PETTERSSON	DATE : 10/12/01
CHECKED : SPARKS	DRG. No : 6-1-1
APPROVED : PEARSE	

TO BE CONSTRUCTED FROM 18mm MDF

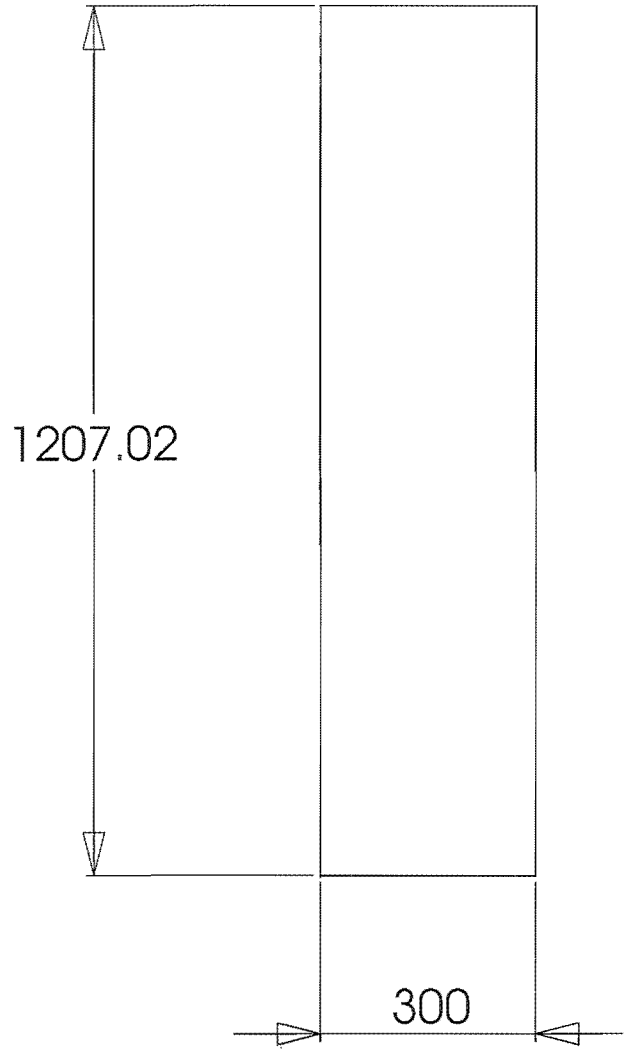

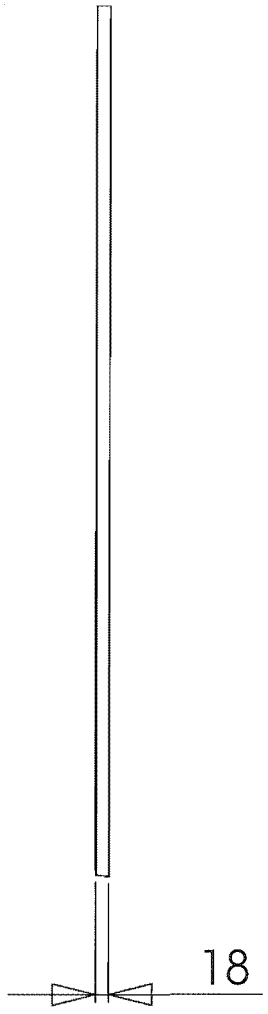

SECTION ONE SIDE WALL

SCALE : 1:10 ALL DIMENSIONS IN mm

UNIVERSITY OF CANTERBURY
MECHANICAL ENGINEERING DEPT. CH.CH. N.Z.

DRAWN : PETTERSSON	DATE : 10/12/01
CHECKED : SPARKS	DRG. No : 6-1-2
APPROVED : PEARSE	

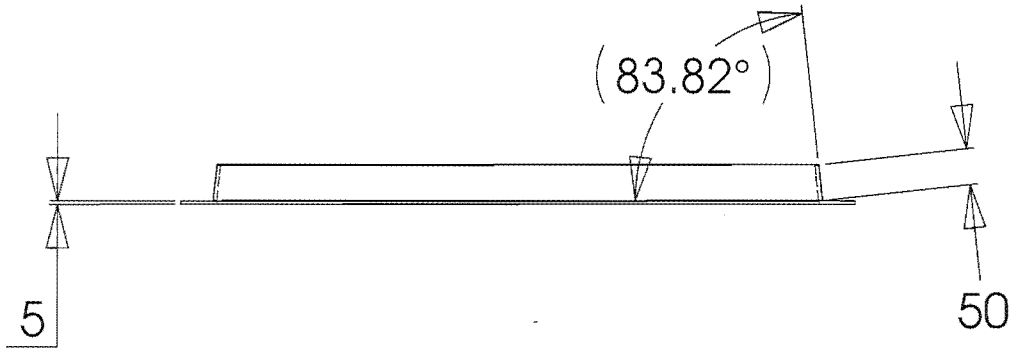

TO BE CONSTRUCTED FROM ANGLE STEEL

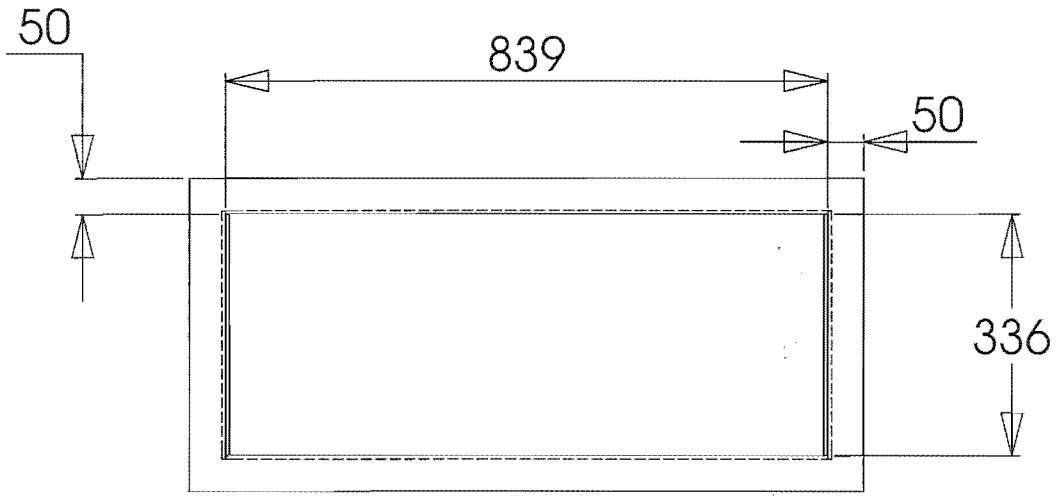

SECTION ONE LARGE FLANGE	UNIVERSITY OF CANTERBURY MECHANICAL ENGINEERING DEPT. CH.CH. N.Z.	
	DRAWN : PETTERSSON	DATE : 10/12/01
	CHECKED : SPARKS	DRG. No : 6-1-3
SCALE : 1:10 ALL DIMENSIONS IN mm	APPROVED : PEARSE	

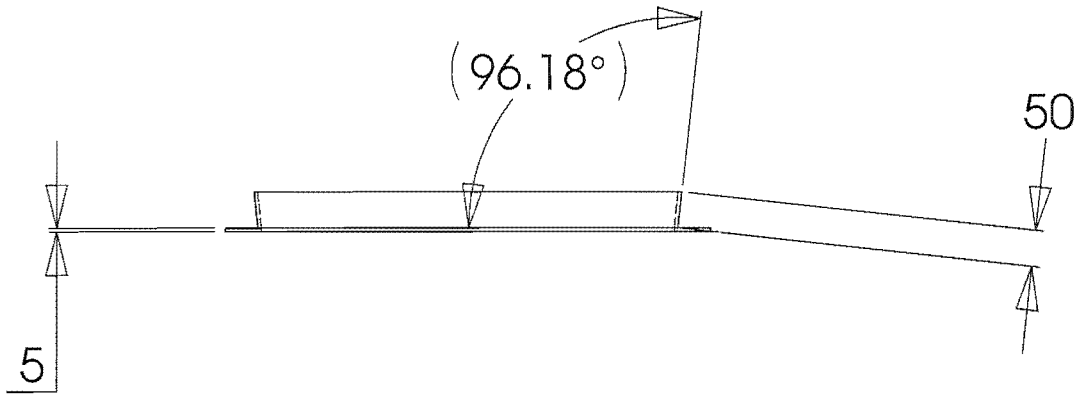

TO BE CONSTRUCTED FROM ANGLE STEEL

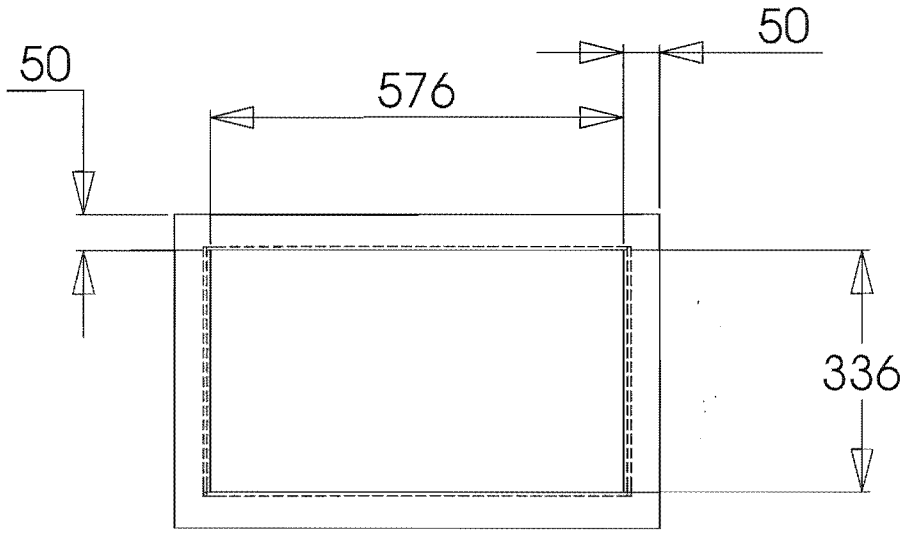

SECTION ONE SMALL FLANGE

SCALE : 1:10 ALL DIMENSIONS IN mm

UNIVERSITY OF CANTERBURY
MECHANICAL ENGINEERING DEPT. CH.CH. N.Z.

DRAWN : PETTERSSON | DATE : 10/12/01
CHECKED : SPARKS | DRG. No : 6-1-4
APPROVED : PEARSE

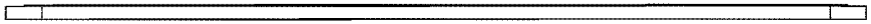

ITEM NO.	QTY.	PART NAME	DRG. NO.
1	1	Long Screen	6-1-5-1
2	2	Internal Wall Long Cross Beam	6-1-5-1
3	2	Internal Wall Column	6-1-5-1

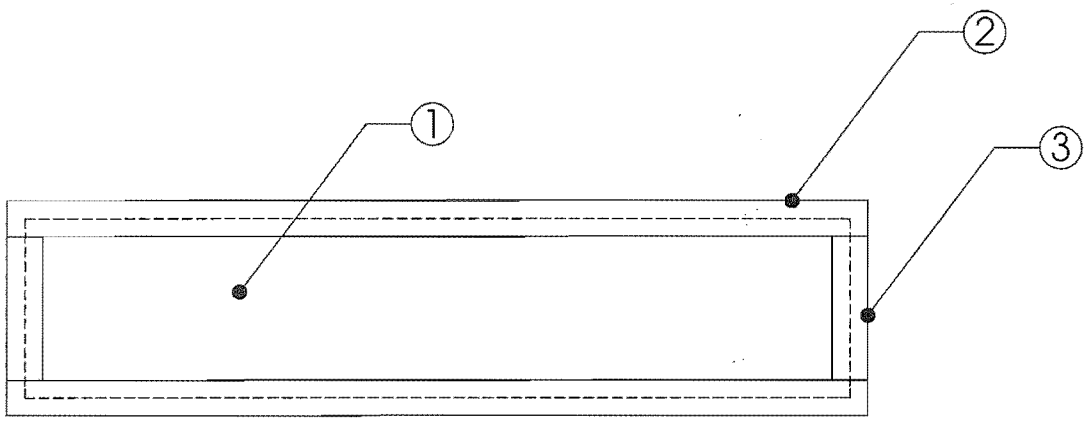

LONG INTERNAL WALL ASSY.

SCALE : 1:10 ALL DIMENSIONS IN mm

UNIVERSITY OF CANTERBURY
MECHANICAL ENGINEERING DEPT. CH.CH. N.Z.

DRAWN : PETTERSSON | DATE : 10/12/01
CHECKED : SPARKS | DRG. No : 6-1-5
APPROVED : PEARSE

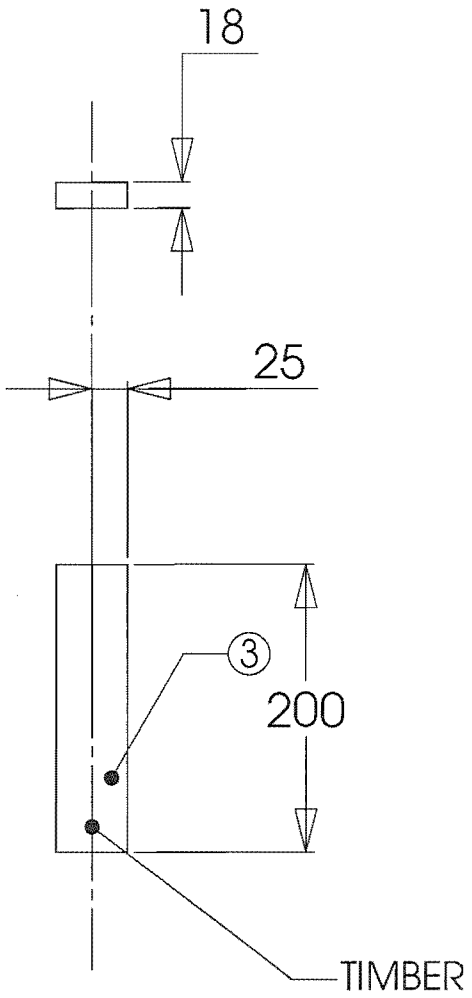

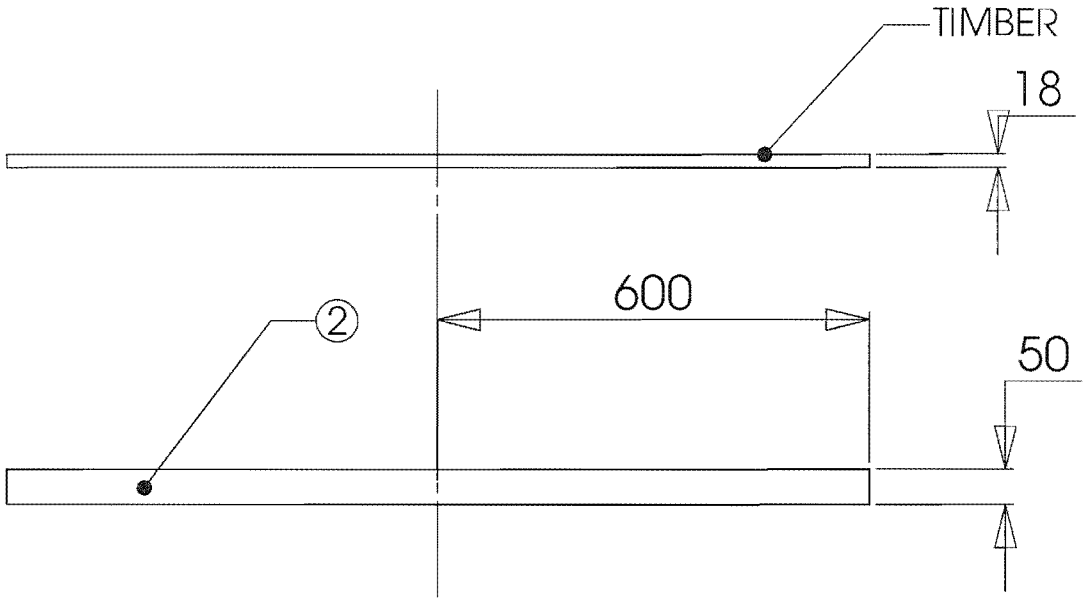

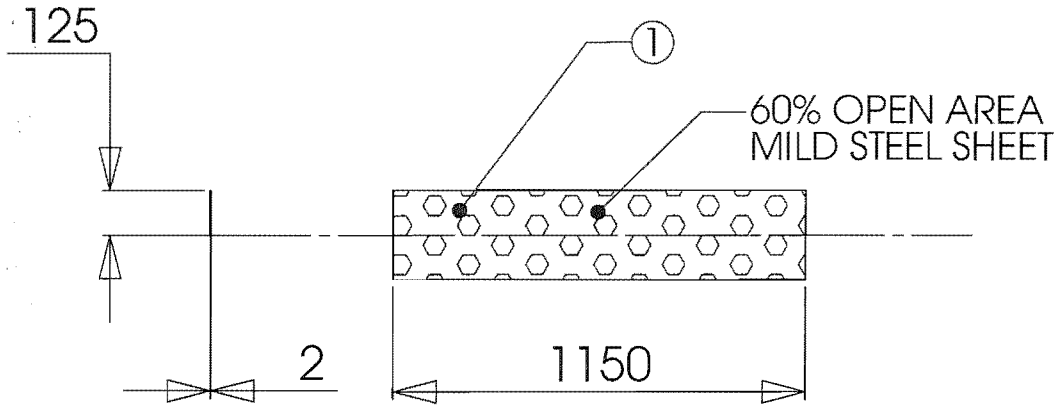

LONG INTERNAL WALL PARTS

SCALE : 1:5

ALL DIMENSIONS IN mm

UNIVERSITY OF CANTERBURY
MECHANICAL ENGINEERING DEPT. CH.CH. N.Z.

DRAWN : PETTERSSON

CHECKED : SPARKS

APPROVED : PEARSE

DATE : 10/12/01

DRG. No : **6-1-5-1**

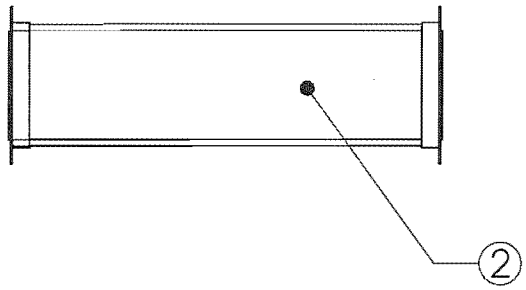

ITEM NO.	QTY.	PART NAME	DRG. NO.
1	2	Section Two Top Wall	6-2-1
2	2	Section Two Side Wall	6-2-2
3	1	Section Two Large Flange	6-2-3
4	1	Section Two Small Flange	6-2-4
5	2	Long Internal Wall ASSY	6-1-5

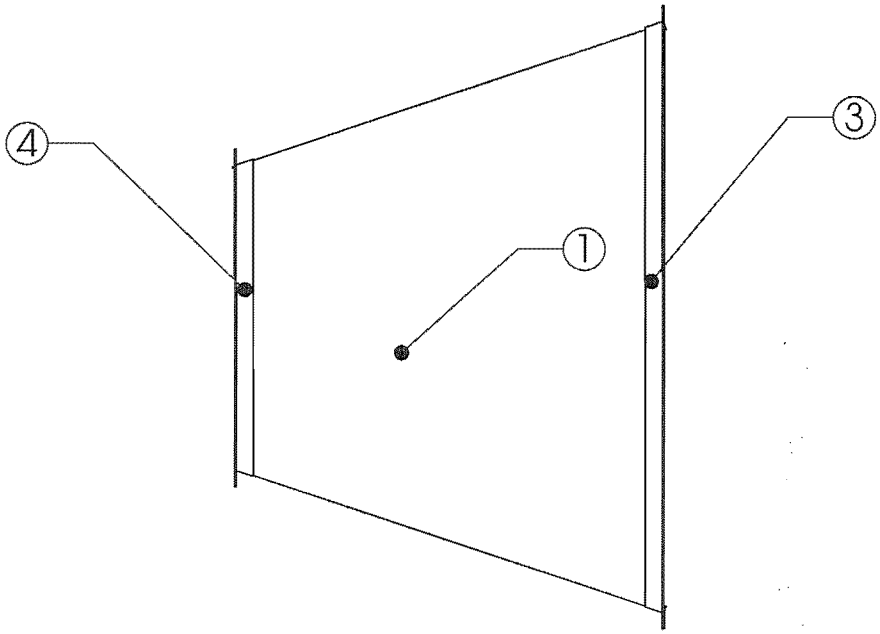

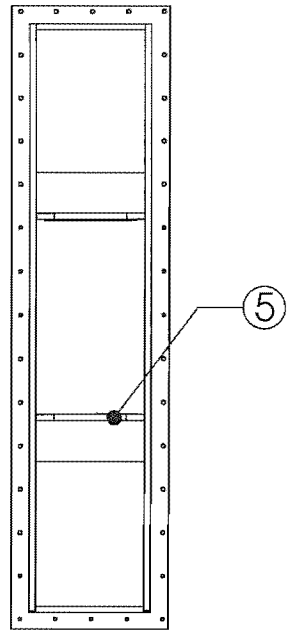

SECTION TWO OF THE ANECHOIC TERMINATION

SCALE : 1:20 ALL DIMENSIONS IN mm

UNIVERSITY OF CANTERBURY
MECHANICAL ENGINEERING DEPT. CH.CH. N.Z.

DRAWN : PETTERSSON DATE : 10/12/01
CHECKED : SPARKS DRG. No : 6-2
APPROVED : PEARSE

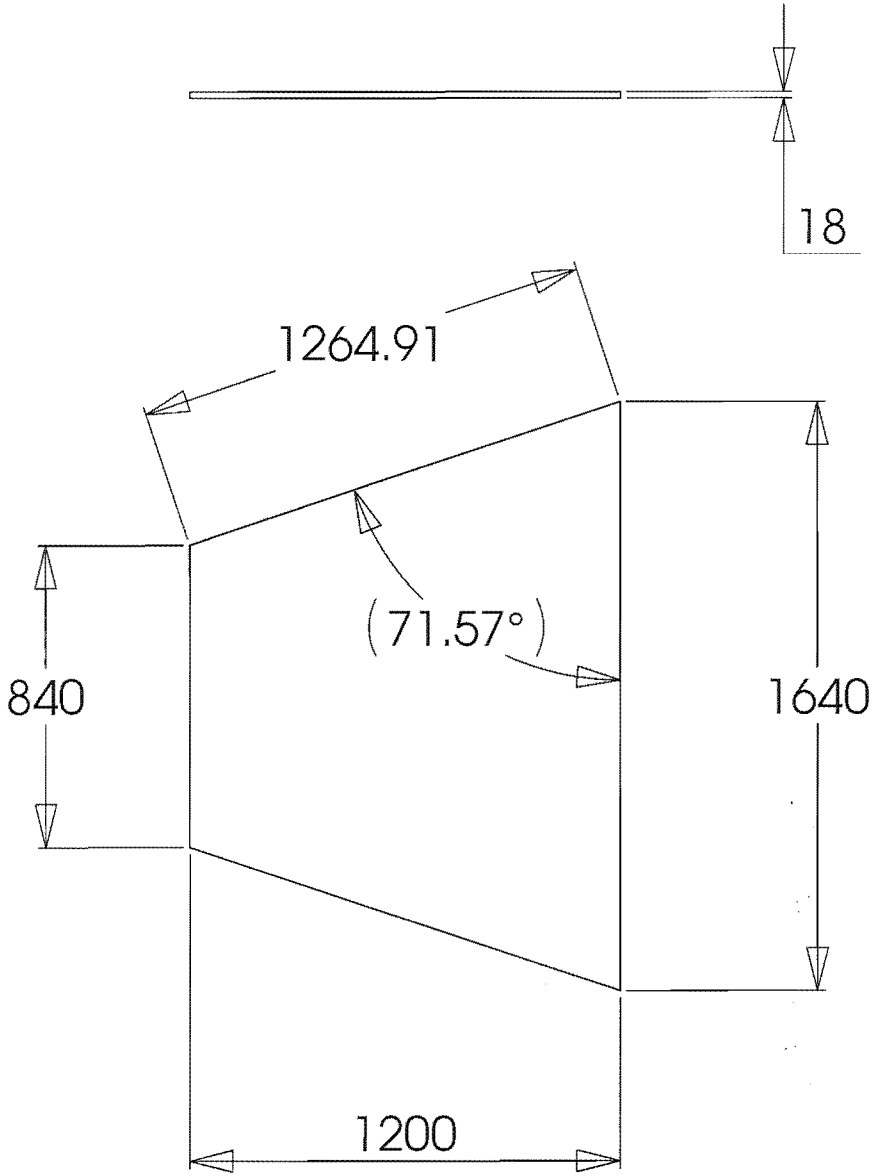

TO BE CONSTRUCTED FROM 18mm MDF

SECTION TWO TOP WALL

SCALE : 1:20 ALL DIMENSIONS IN mm

UNIVERSITY OF CANTERBURY
MECHANICAL ENGINEERING DEPT. CH.CH. N.Z.

DRAWN : PETTERSSON	DATE : 12/10/01
CHECKED : SPARKS	DRG. No : 6-2-1
APPROVED : PEARSE	

TO BE CONSTRUCTED FROM 18mm MDF

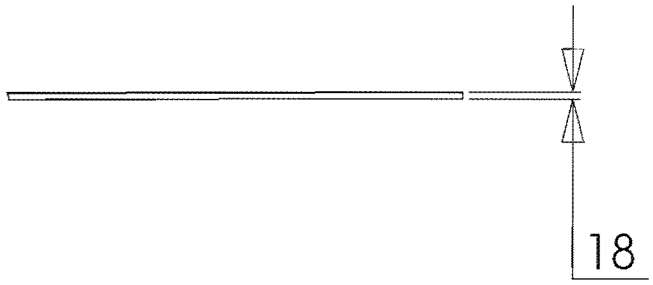

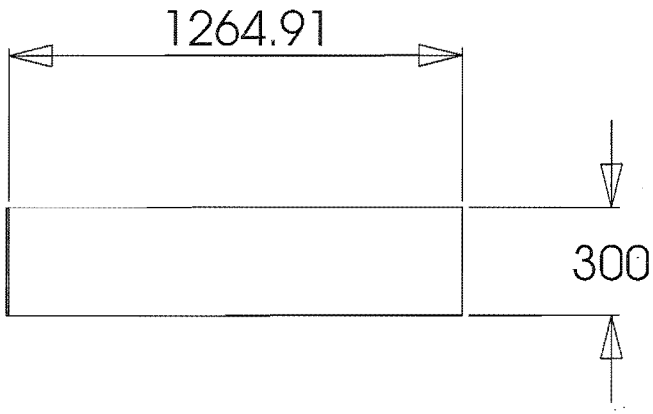

SECTION TWO SIDE WALL

SCALE : 1:20 ALL DIMENSIONS IN mm

UNIVERSITY OF CANTERBURY
MECHANICAL ENGINEERING DEPT. CH.CH. N.Z.

DRAWN : PETTERSSON | DATE : 10/12/01
CHECKED : SPARKS | DRG. No : 6-2-2
APPROVED : PEARSE

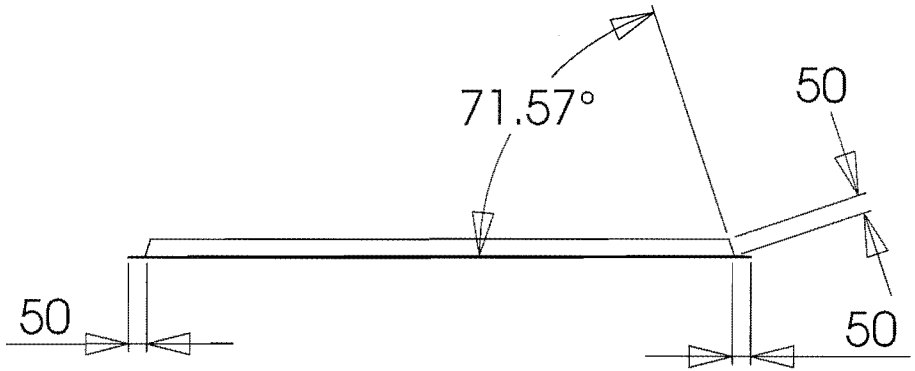

TO BE CONSTRUCTED FROM 5mm STEEL PLATE

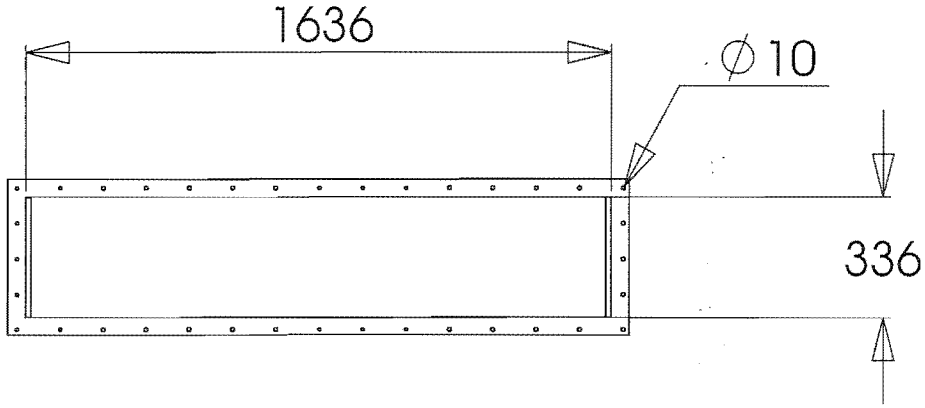

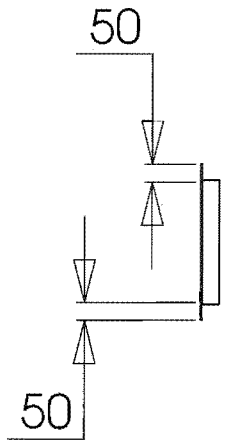

SECTION TWO LARGE FLANGE

SCALE : 1:20 ALL DIMENSIONS IN mm

UNIVERSITY OF CANTERBURY
MECHANICAL ENGINEERING DEPT. CH.CH. N.Z.

DRAWN : PETTERSSON | DATE : 10/12/01
CHECKED : SPARKS | DRG. No : 6-2-3
APPROVED : PEARSE

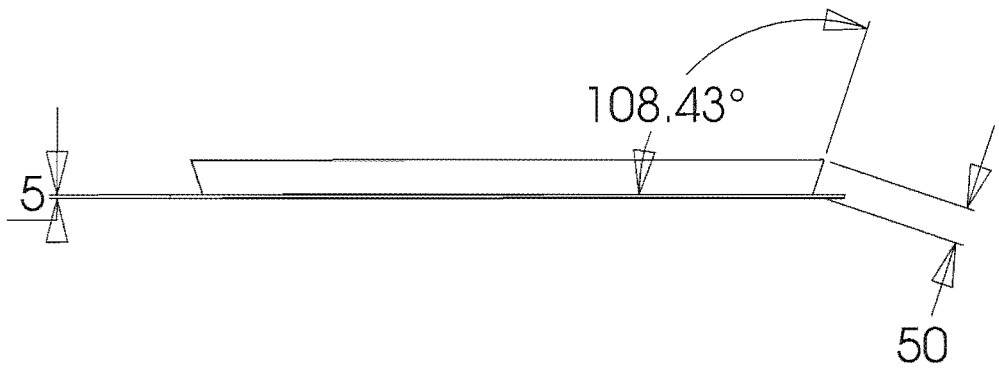

TO BE CONSTRUCTED FROM 5mm STEEL PLATE

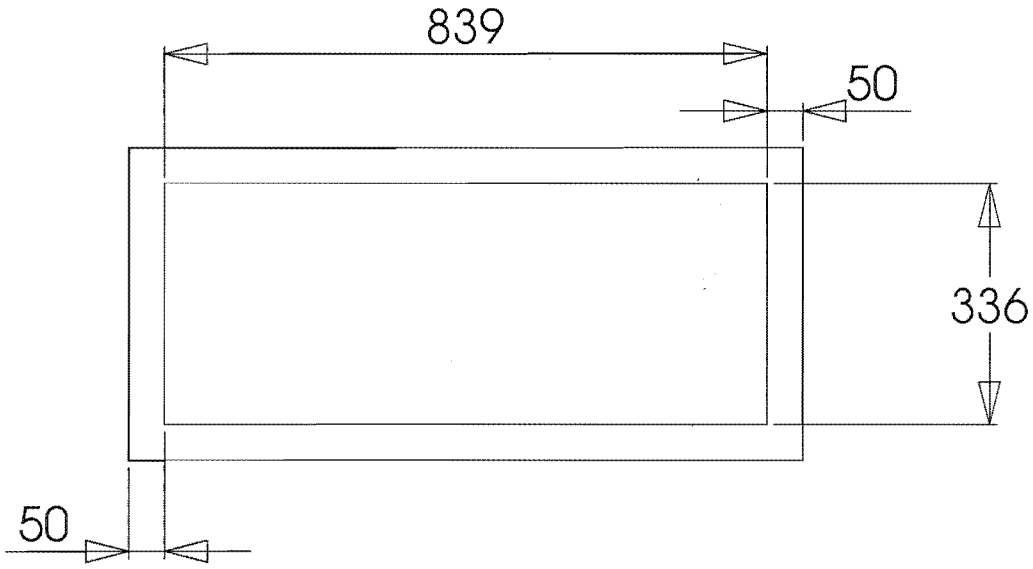

SECTION TWO SMALL FLANGE

SCALE : 1:10 ALL DIMENSIONS IN mm

UNIVERSITY OF CANTERBURY
MECHANICAL ENGINEERING DEPT. CH.CH. N.Z.

DRAWN : PETTERSSON | DATE : 10/12/01

CHECKED : SPARKS | DRG. No : 6-2-4

APPROVED : PEARSE

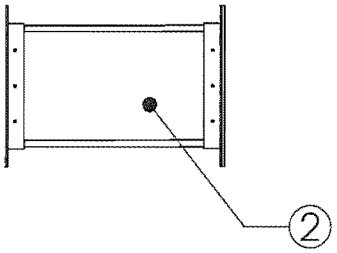

ITEM NO.	QTY.	PART NAME	DRG. NO.
1	2	Section Three Top Wall	6-3-1
2	2	Section Three Side Wall	6-3-2
3	2	Section Three Flange	6-3-3
4	2	Short Internal Wall ASSY	6-3-4
5	2	Termination End Wall	6-3-5

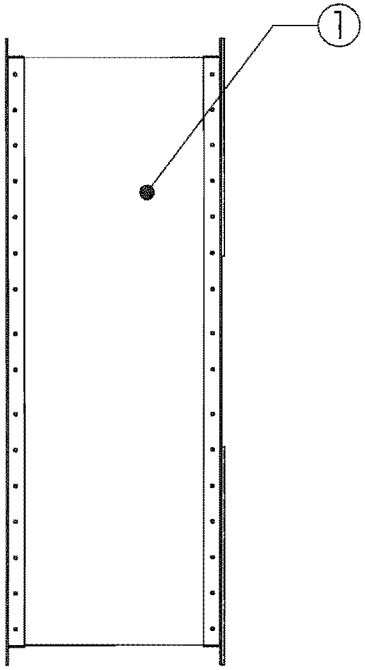

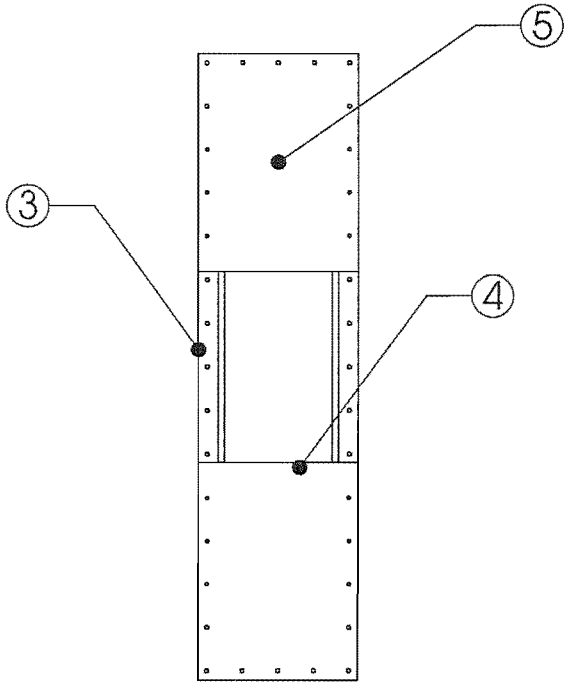

SECTION THREE OF THE ANECHOIC TERMINATION

SCALE : 1:20 ALL DIMENSIONS IN mm

UNIVERSITY OF CANTERBURY
MECHANICAL ENGINEERING DEPT. CH.CH. N.Z.

DRAWN : PETTERSSON DATE : 10/12/01

CHECKED : SPARKS DRG. No : 6-3

APPROVED : PEARSE

TO BE CONSTRUCTED FROM 18mm MDF

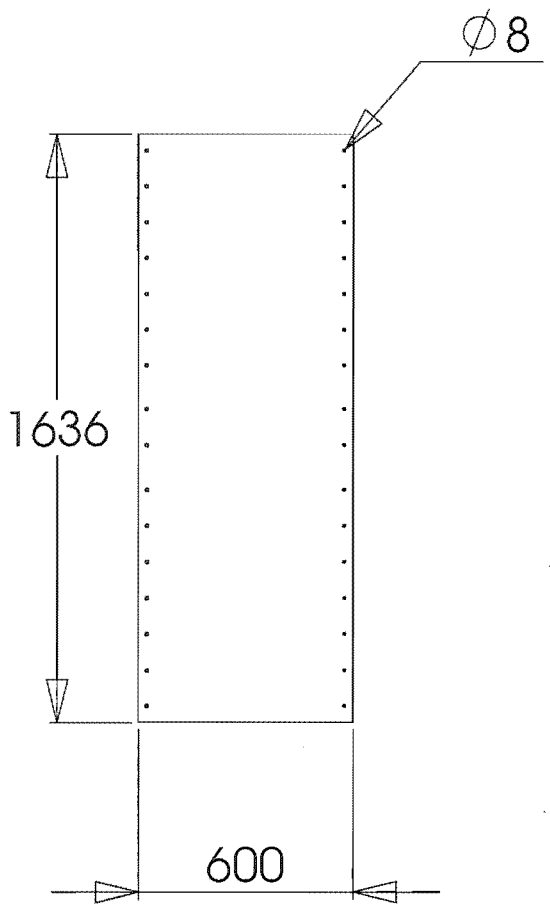

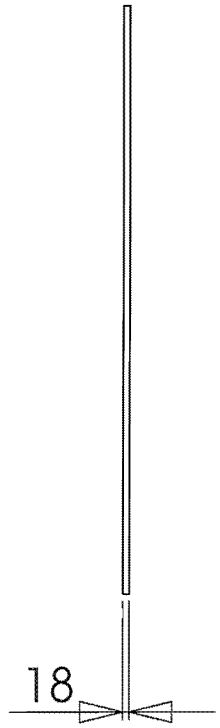

SECTION THREE TOP WALL

SCALE : 1:20 ALL DIMENSIONS IN mm

UNIVERSITY OF CANTERBURY
MECHANICAL ENGINEERING DEPT. CH.CH. N.Z.

DRAWN : PETTERSSON DATE : 10/12/01

CHECKED : SPARKS DRG. No : 6-3-1

APPROVED : PEARSE

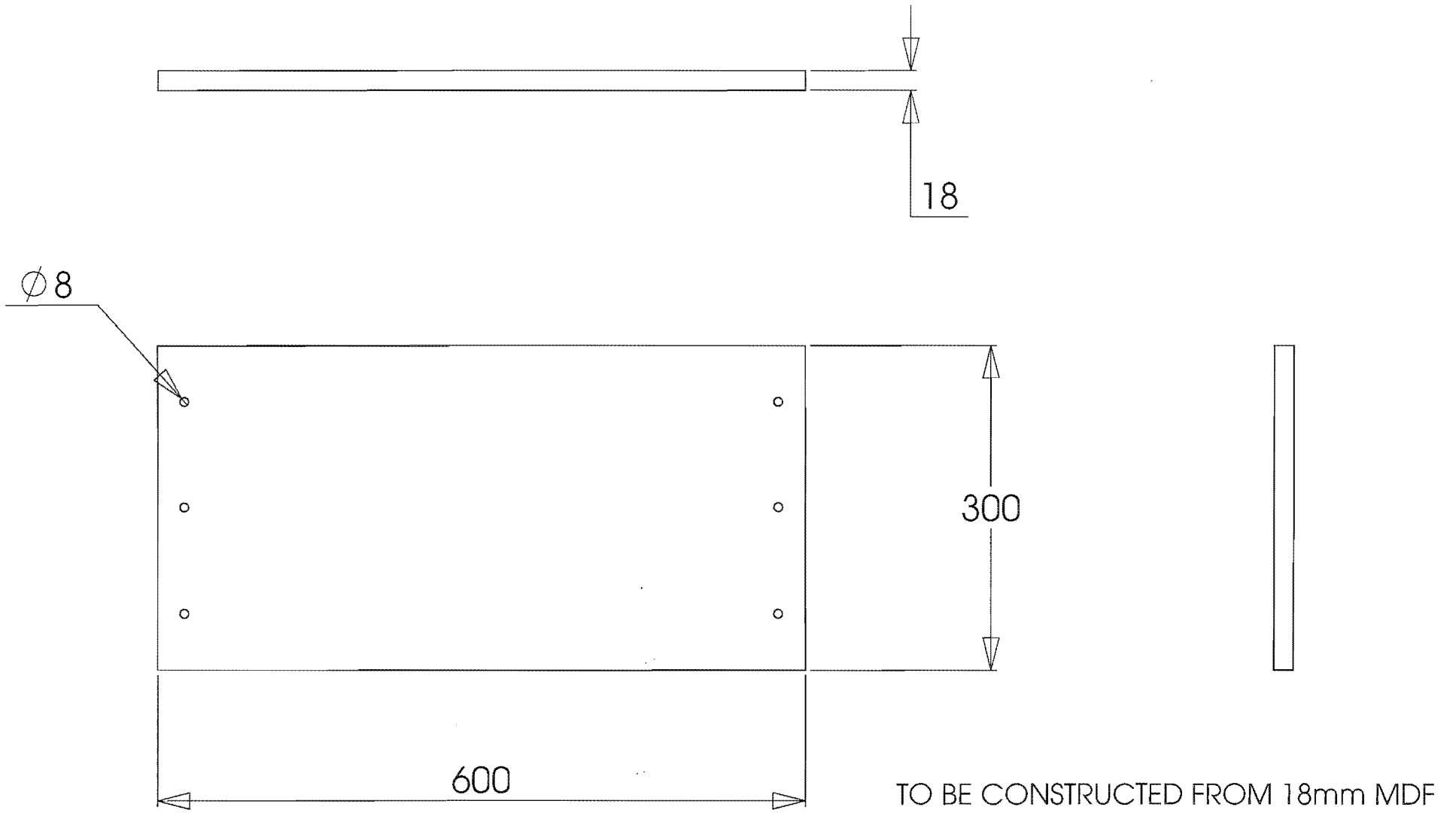

TO BE CONSTRUCTED FROM 18mm MDF

SECTION THREE SIDE WALL

SCALE : 1:5 ALL DIMENSIONS IN mm

UNIVERSITY OF CANTERBURY
MECHANICAL ENGINEERING DEPT. CH.CH. N.Z.

DRAWN : PETTERSSON | DATE : 10/12/01
CHECKED : SPARKS | DRG. No : 6-3-2
APPROVED : PEARSE

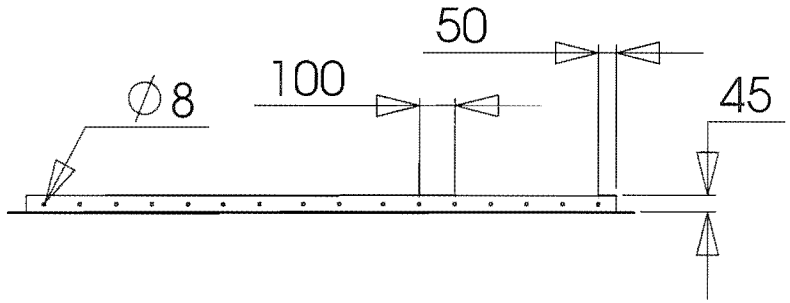

TO BE CONSTRUCTED FROM 5mm THICK ANGLE STEEL

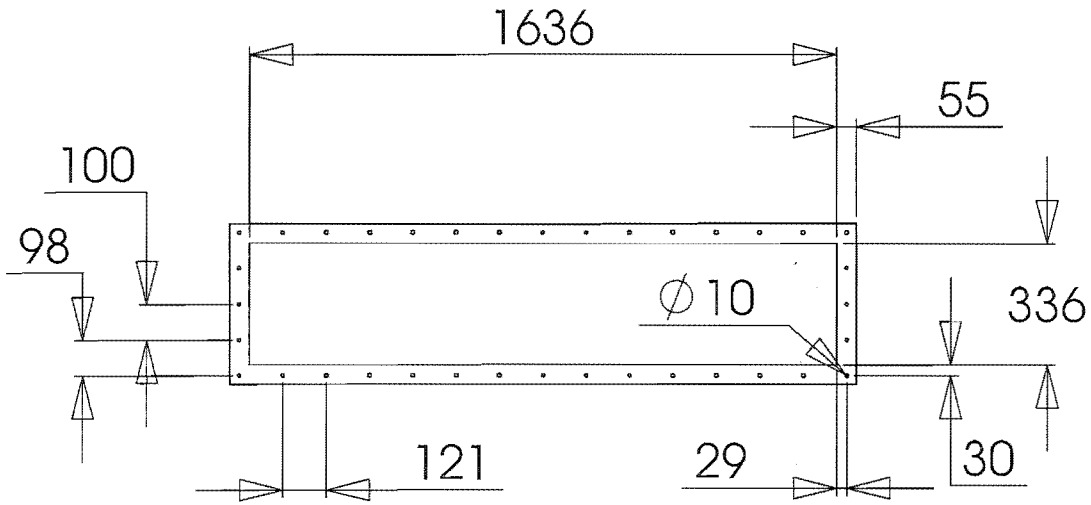

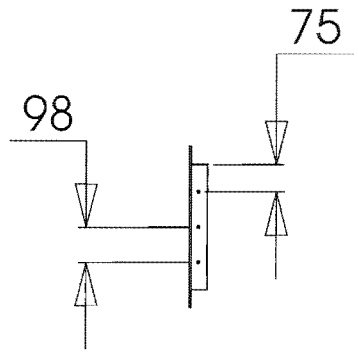

SECTION THREE FLANGE	UNIVERSITY OF CANTERBURY MECHANICAL ENGINEERING DEPT. CH.CH. N.Z.	
	DRAWN : PETTERSSON	DATE : 10/12/01
	CHECKED : SPARKS	DRG. No : 6-3-3
SCALE : 1:20 ALL DIMENSIONS IN mm	APPROVED : PEARSE	

ITEM NO.	QTY.	PART NAME	DRG. NO.
1	1	Short Screen	6-3-4-1
2	2	Internal Wall Short Cross Beam	6-3-4-2
3	2	Internal Wall Column	6-1-5-1

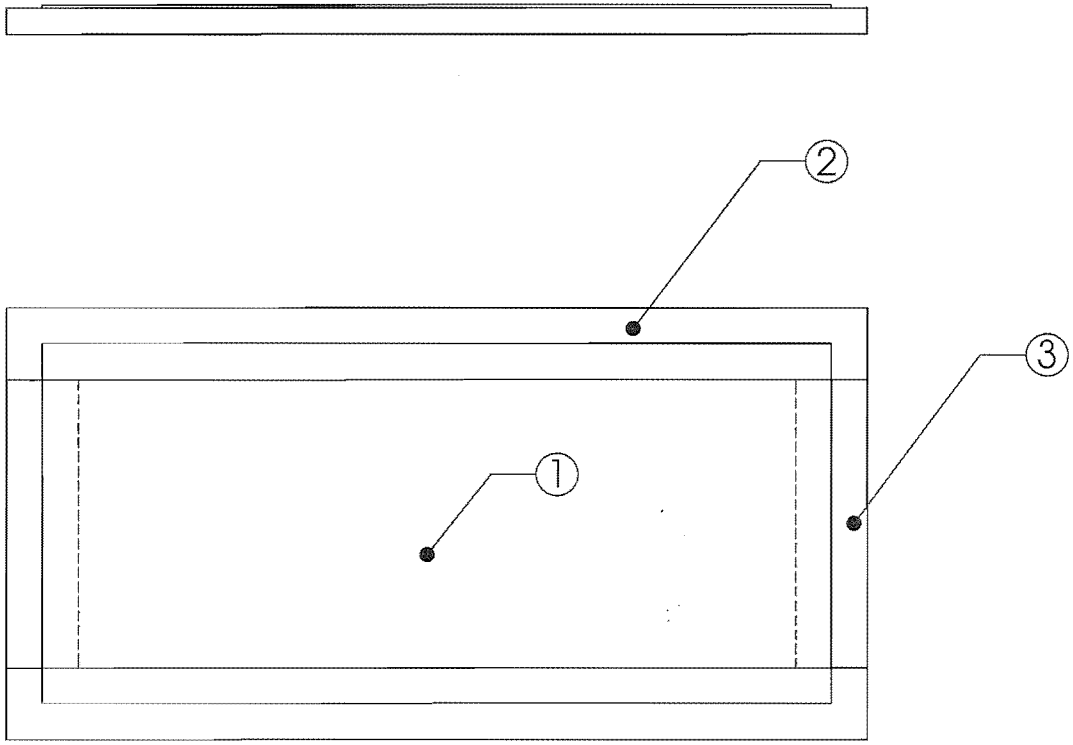

SHORT INTERNAL WALL ASSY.

SCALE : 1:5 ALL DIMENSIONS IN mm

UNIVERSITY OF CANTERBURY
MECHANICAL ENGINEERING DEPT. CH.CH. N.Z.

DRAWN : PETTERSSON
CHECKED : PETTERSSON
APPROVED : PEARSE

DATE : 10/12/01

DRG. No : 6-3-4

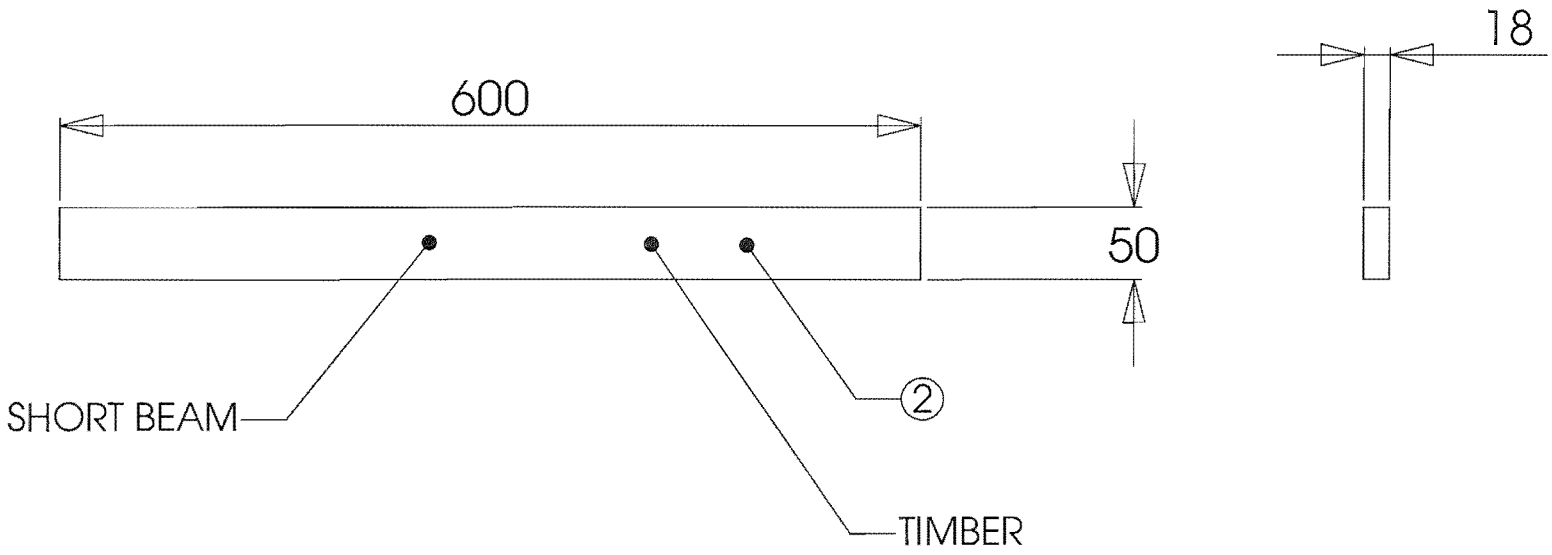

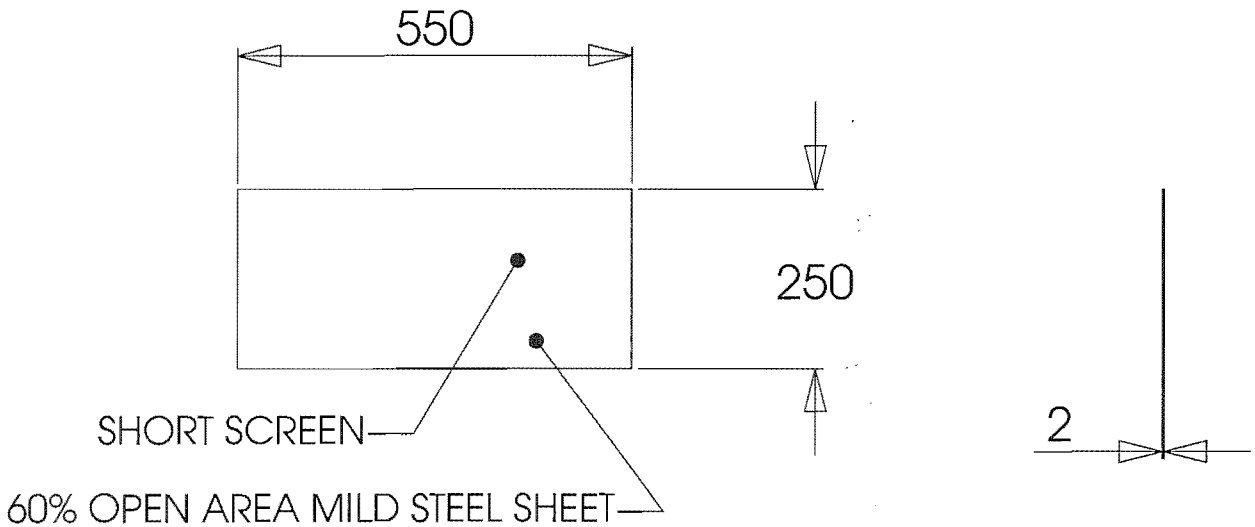

SHORT INTERNAL WALL PARTS

SCALE : 1:10 ALL DIMENSIONS IN mm

UNIVERSITY OF CANTERBURY
MECHANICAL ENGINEERING DEPT. CH.CH. N.Z.

DRAWN : PETTERSSON | DATE : 10/12/01

CHECKED : SPARKS | DRG. No : 6-3-4-1

APPROVED : PEARSE

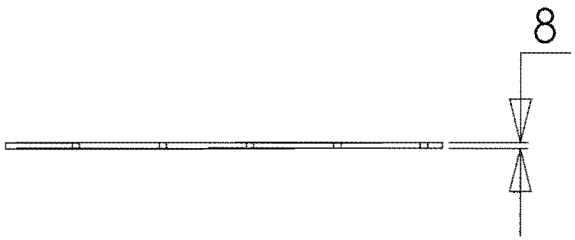

TO BE CONSTRUCTED FROM 8mm MDF

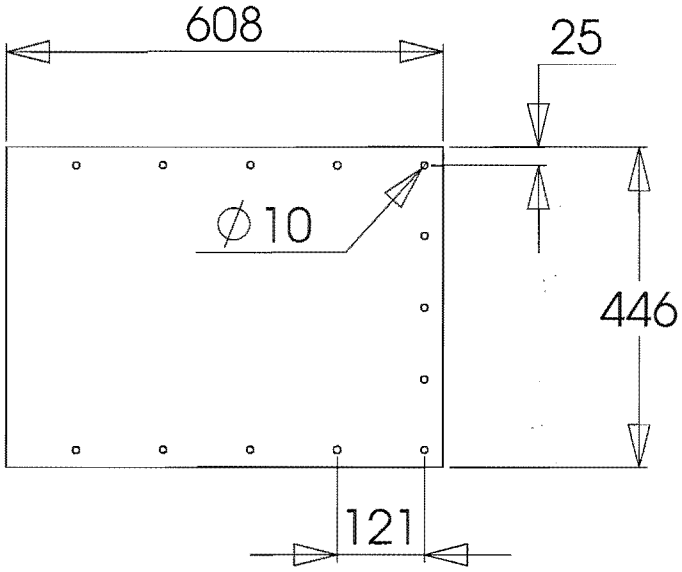

TERMINATION END WALL

SCALE : 1:10 ALL DIMENSIONS IN mm

UNIVERSITY OF CANTERBURY
MECHANICAL ENGINEERING DEPT. CH.CH. N.Z.

DRAWN : PETTETRSSON | DATE : 10/12/01

CHECKED : SPARKS | DRG. No : 6-3-5

APPROVED : PEARSE

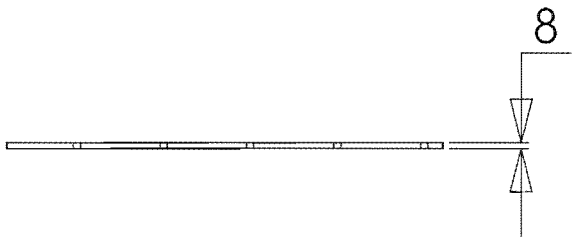

TO BE CONSTRUCTED FROM 8mm MDF

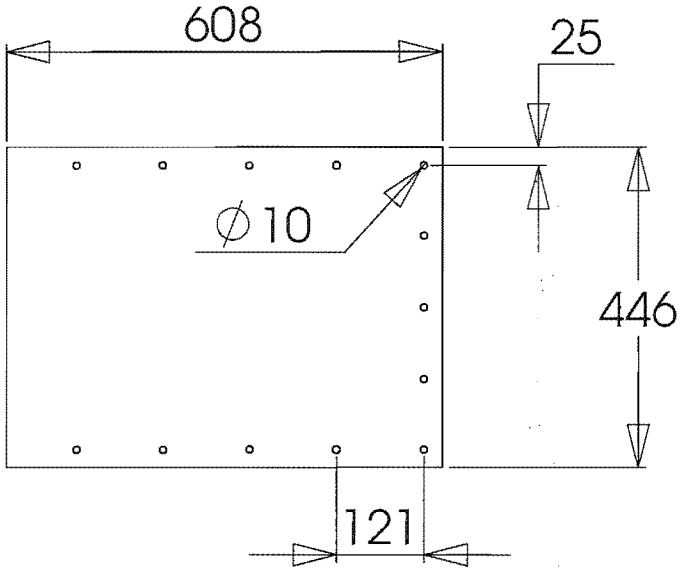

TERMINATION END WALL	UNIVERSITY OF CANTERBURY MECHANICAL ENGINEERING DEPT. CH.CH. N.Z.	
	DRAWN : PETTETRSSON	DATE : 10/12/01
	CHECKED : SPARKS	DRG. No : 6-3-5
SCALE : ALL DIMENSIONS IN mm	APPROVED : PEARSE	

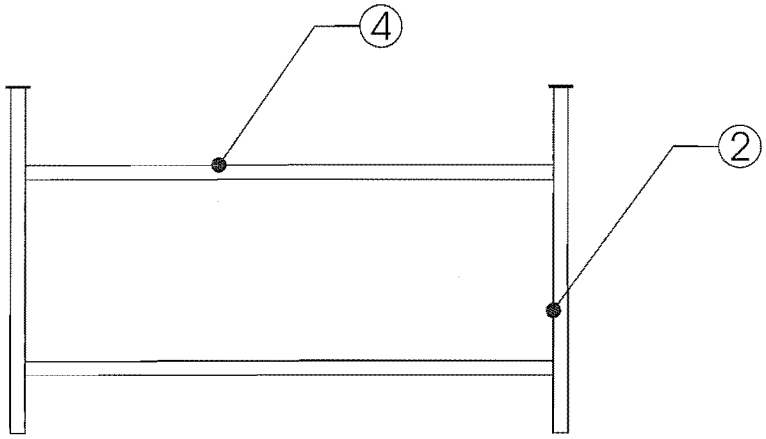

ITEM NO.	QTY.	PART NAME	DRG. NO.
1	2	Long Cross Beam	6-4-1
2	4	Column	6-4-1
3	2	Short Cross Beam	6-4-1
4	4	Main Beam	6-4-1
5	4	Mounting Plate	6-4-1

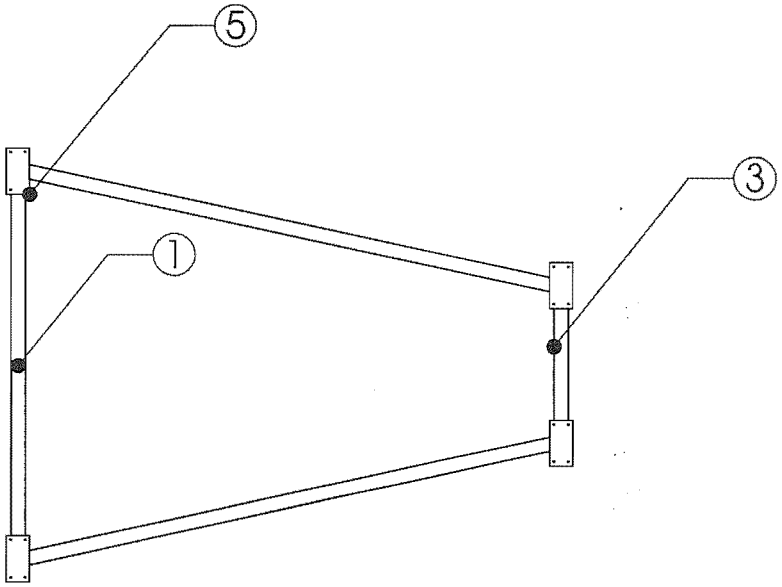

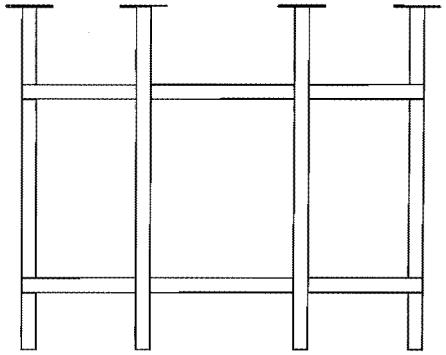

ANECHOIC TERMINATION STAND

SCALE : 1:25 ALL DIMENSIONS IN mm

UNIVERSITY OF CANTERBURY
MECHANICAL ENGINEERING DEPT. CH.CH. N.Z.

DRAWN : PETTERSSON DATE : 10/12/01

CHECKED : SPARKS DRG. No : **6-4**

APPROVED : PEARSE

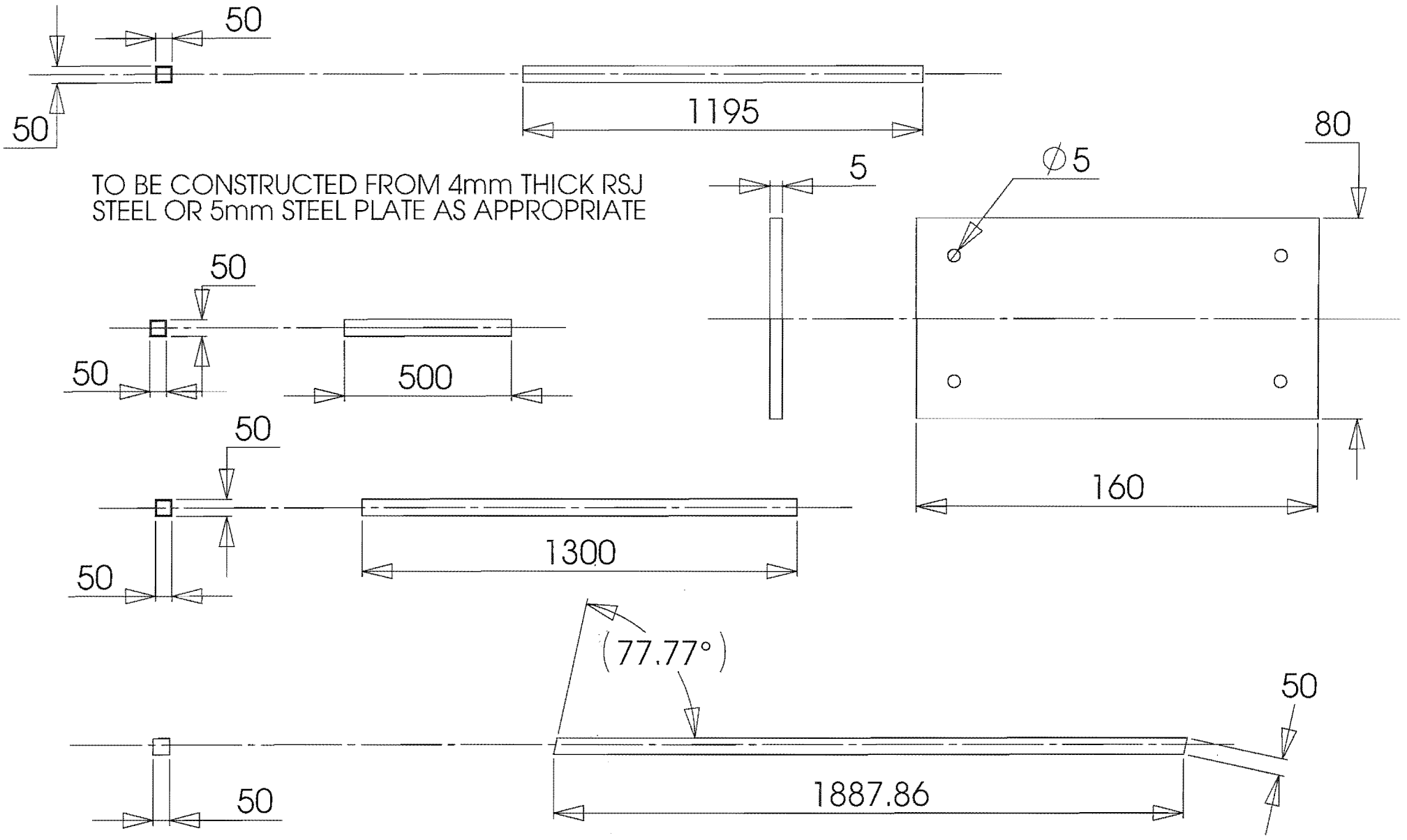

ANECHOIC TERMINATION
STAND PARTS

SCALE : 1:15 ALL DIMENSIONS IN mm

UNIVERSITY OF CANTERBURY
MECHANICAL ENGINEERING DEPT. CH.CH. N.Z.

DRAWN : PETTERSSON	DATE : 10/12/01
CHECKED : SPARKS	DRG. No : **6-4-1**
APPROVED : PEARSE	

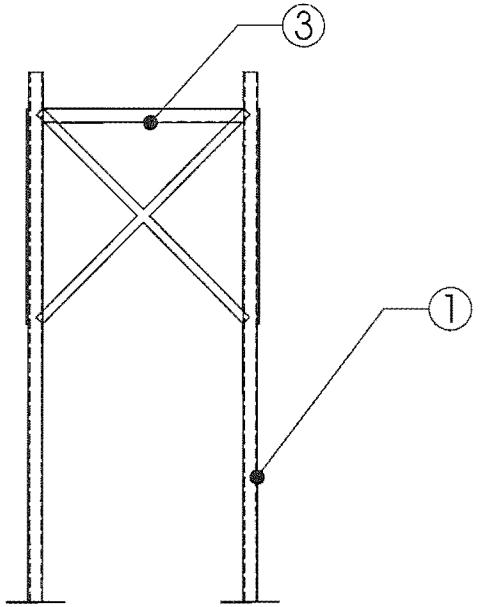

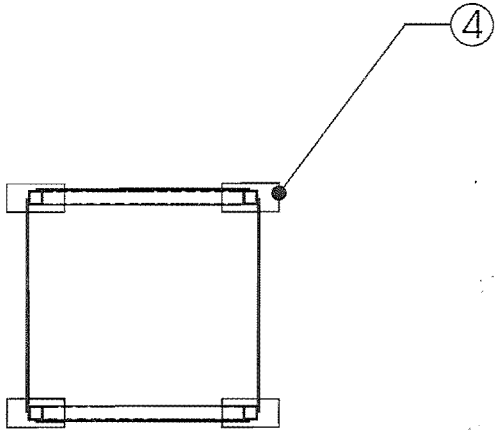

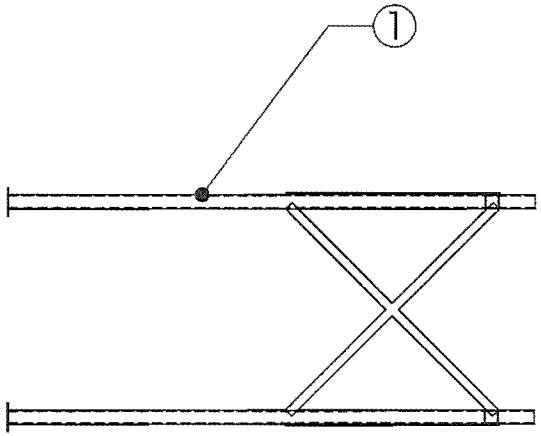

ITEM NO.	QTY.	PART NAME	DRG. NO.
1	4	Ducting Stand Column	7-1
2	4	Cross Tie	7-1
3	2	Ducting Stand Beam	7-1
4	4	Foot	7-1

DUCTING STAND SUB ASSY.

SCALE : 1:20 ALL DIMENSIONS IN mm

UNIVERSITY OF CANTERBURY
MECHANICAL ENGINEERING DEPT. CH.CH. N.Z.

DRAWN : PETTERSSON DATE : 10/12/01
CHECKED : SPARKS DRG. No : 7
APPROVED : PEARSE

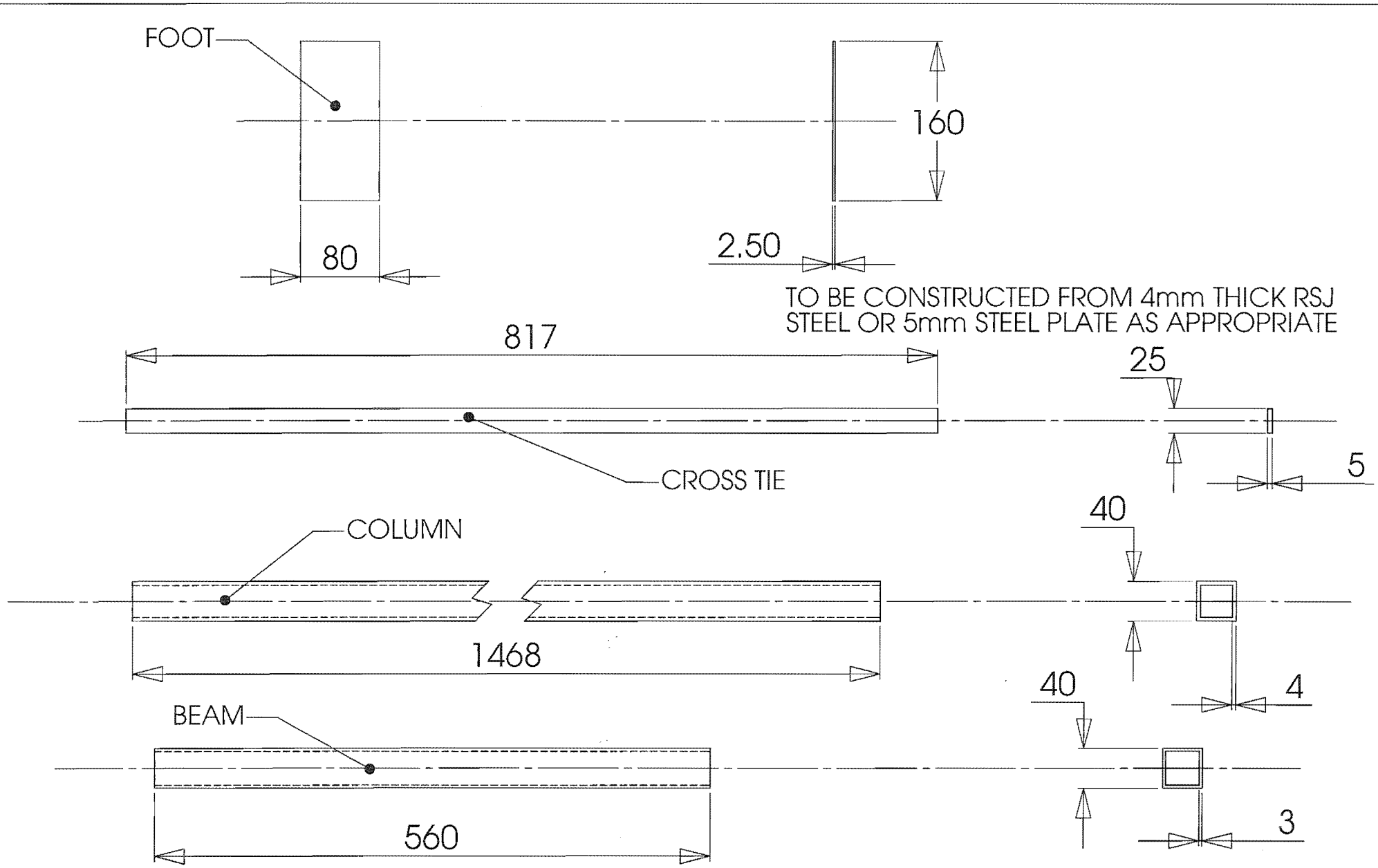

DUCTING STAND PARTS

SCALE : 1:5

ALL DIMENSIONS IN mm

UNIVERSITY OF CANTERBURY
MECHANICAL ENGINEERING DEPT. CH.CH. N.Z.

DRAWN : PETTERSSON

DATE : 10/12/01

CHECKED : SPARKS

DRG. No : 7-1

APPROVED : PEARSE

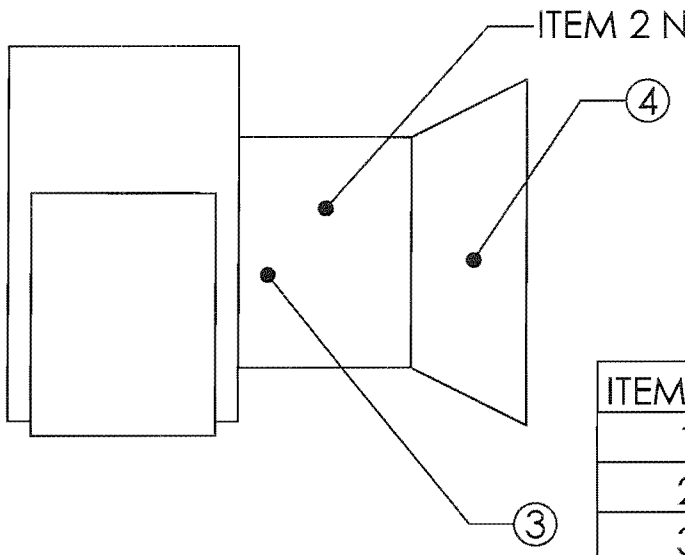

ITEM NO.	QTY.	PART NAME	DRG. NO.
1	1	Fan	N/A
2	1	Fan Inlet Duct	8-1
3	1	Cylindrical Fan Inlet Absorber	8-1
4	1	Conical Fan Inlet Absorber	8-1

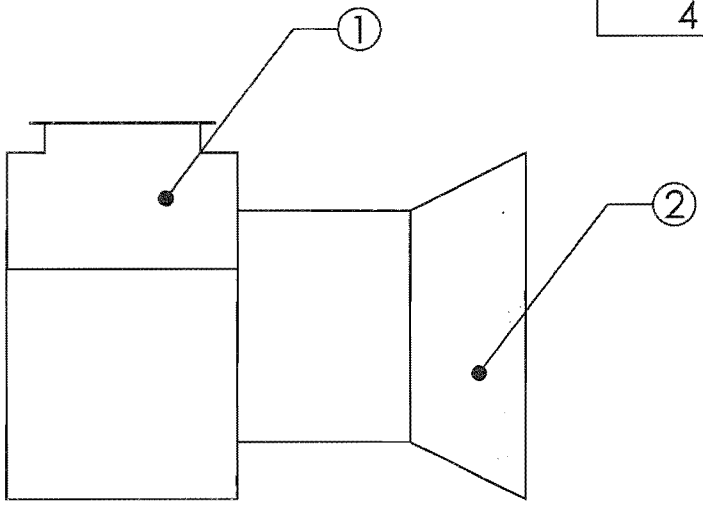

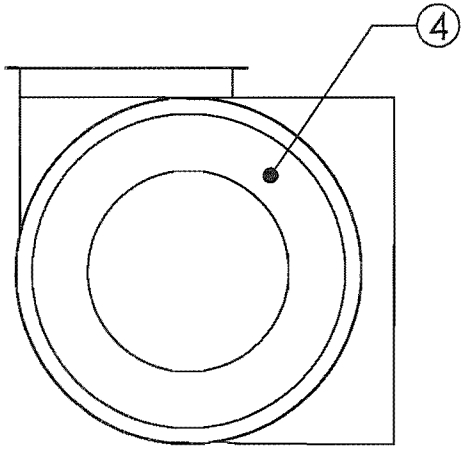

FAN ASSY.

SCALE : ALL DIMENSIONS IN mm

UNIVERSITY OF CANTERBURY
MECHANICAL ENGINEERING DEPT. CH.CH. N.Z.

DRAWN : PETTERSSON | DATE : 10/12/01

CHECKED : SPARKS | DRG. No : 8

APPROVED : PEARSE

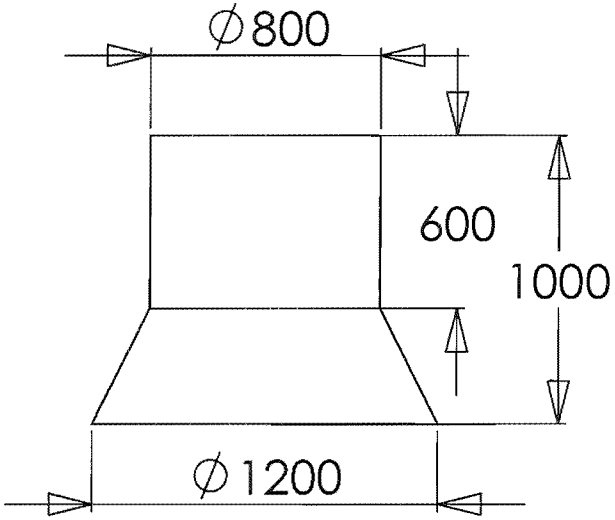

TO BE CONSTRUCTED FROM 50mm
ACOUSTOP ACOUSTIC FOAM

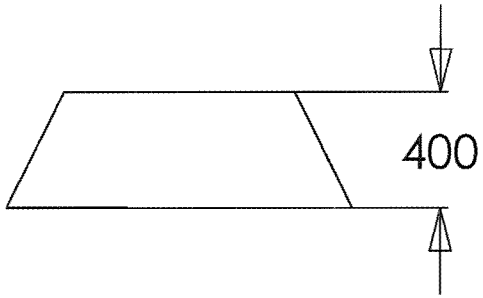

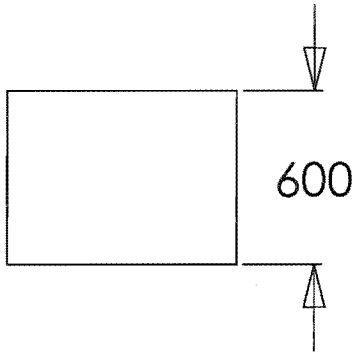

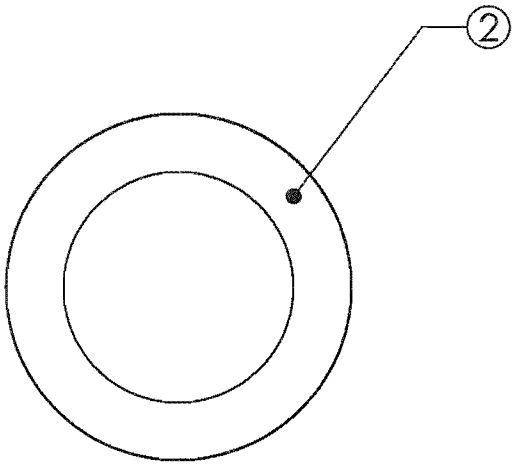

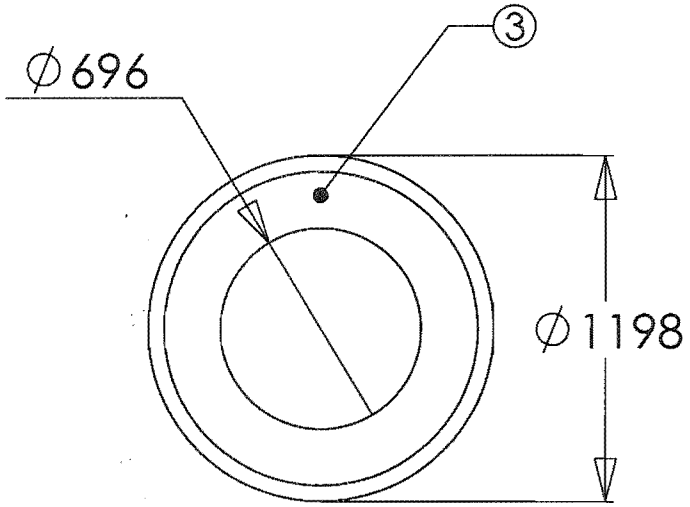

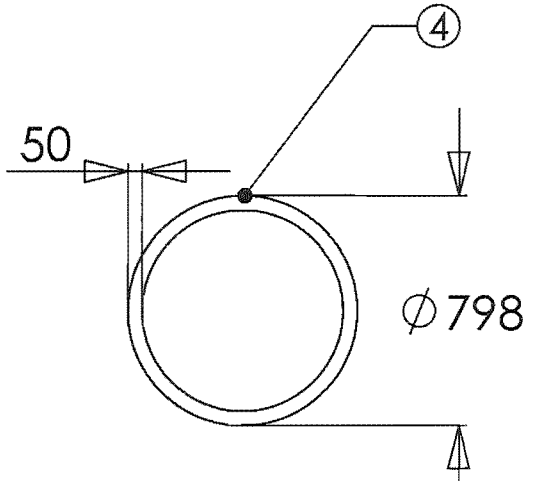

TO BE CONSTRUCTED FROM
18 GAUGE STEEL SHEET

TO BE CONSTRUCTED FROM 50mm
ACOUSTOP ACOUSTIC FOAM

FAN ASSY. PARTS

UNIVERSITY OF CANTERBURY
MECHANICAL ENGINEERING DEPT. CH.CH. N.Z.

DRAWN : PETTERSSON | DATE : 10/12/01
CHECKED : SPARKS | DRG. No : **8-1**
SCALE : 1:25 | ALL DIMENSIONS IN mm | APPROVED : PEARSE

ITEM NO.	QTY.	PART NAME	DRG. NO.
1	1	Base Wall	9-1
2	1	Top	9-2
3	2	Inner Wall	9-3
4	2	Outer Wall	9-3
5	1	End Wall	9-3
6	1	Base Absorber	9-4
7	1	Top Absorber	9-5
8	2	Outer Wall Absorber	9-6
9	2	Inner Wall Absorber	9-6
10	1	End Wall Absorber	9-6
11	1	Inlet Muffler ASSY.	9-7

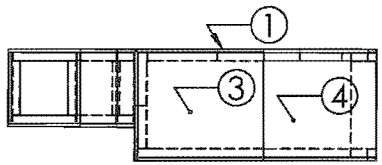

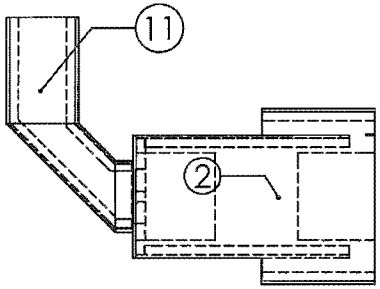

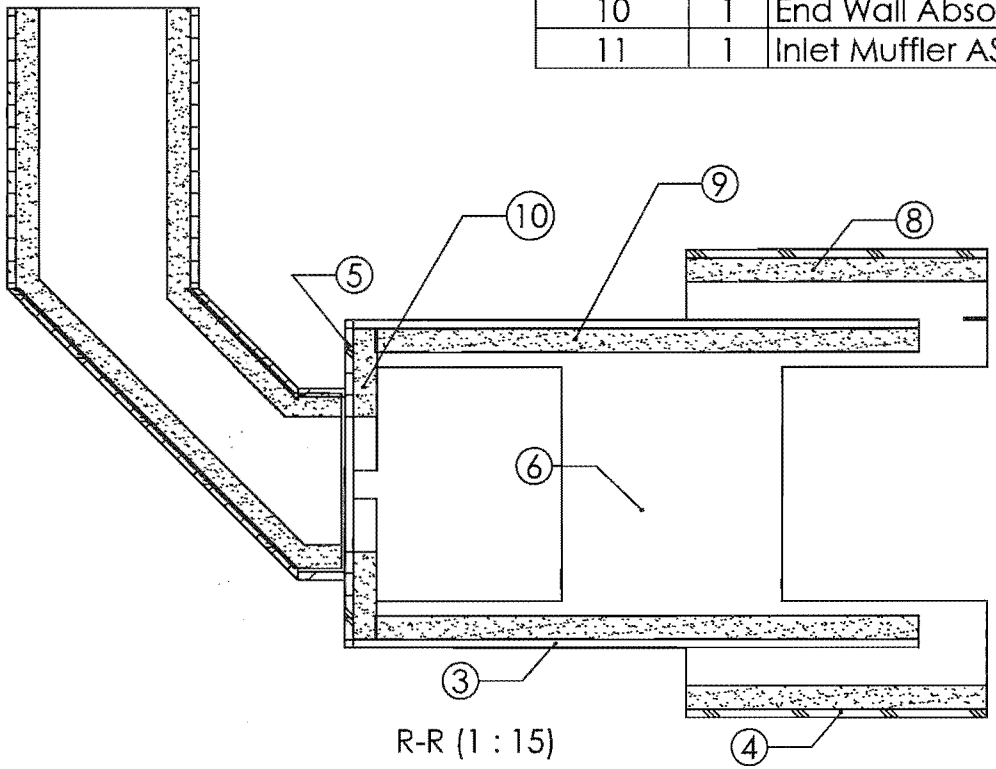

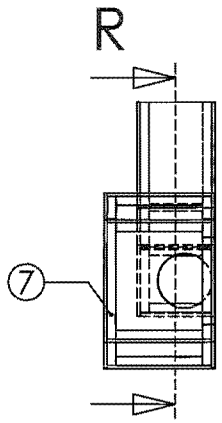

R-R (1 : 15)

SolidWorks Educational License
Instructional Use Only

MOTOR ENCLOSURE ASSY.

SCALE : 1:40 ALL DIMENSIONS IN mm

UNIVERSITY OF CANTERBURY
MECHANICAL ENGINEERING DEPT CH.CH. N. Z.

DRAWN : PETTERSSON	DATE :	25/01/01
CHECKED : SPARKS	DRG. No :	9
APPROVED : PEARSE		

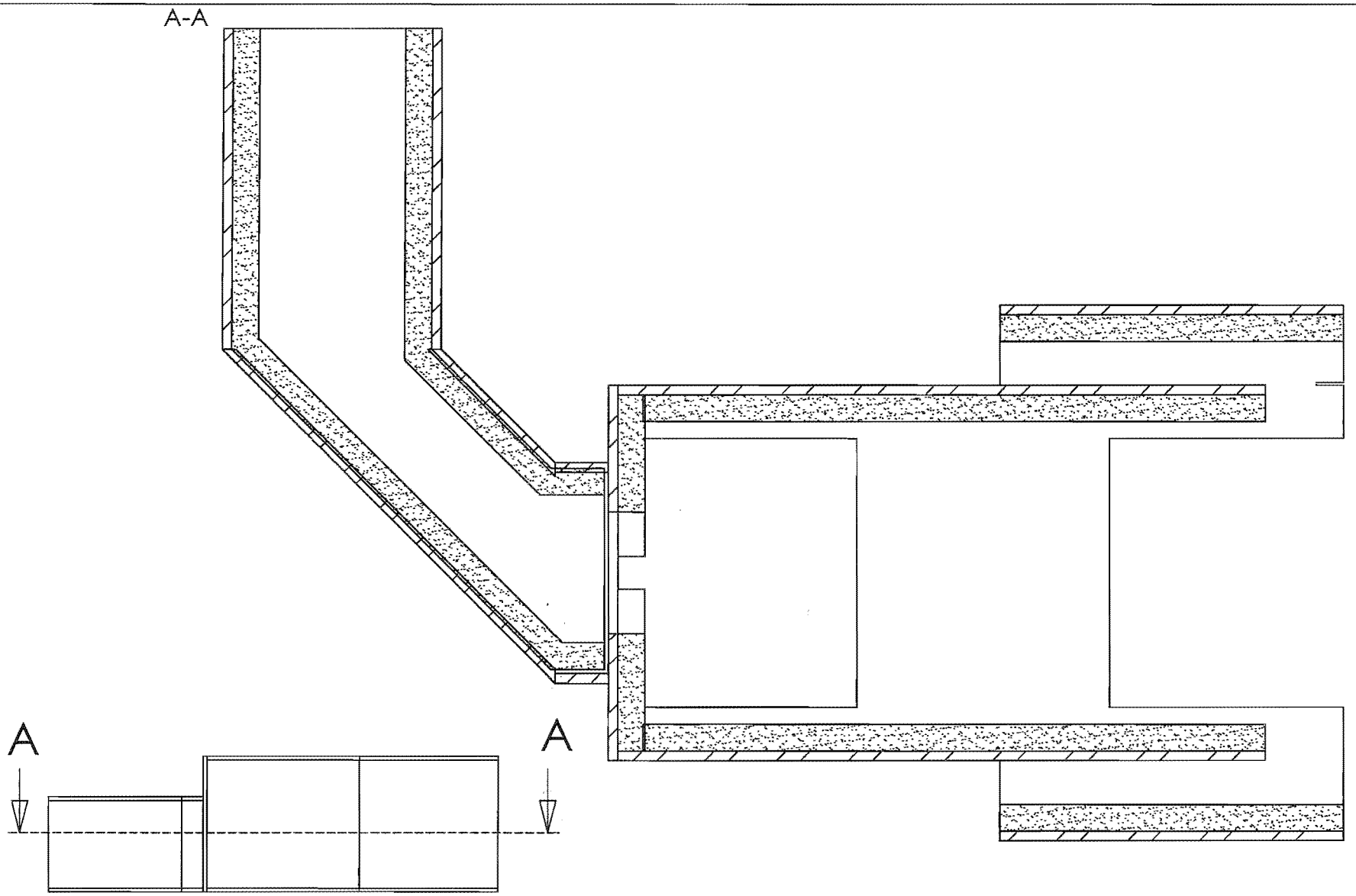

HORIZONTAL SECTION

SCALE : 1:10 ALL DIMENSIONS IN mm

UNIVERSITY OF CANTERBURY
MECHANICAL ENGINEERING DEPT CH.CH. N.Z.

DRAWN : PETTERSSON	DATE :	
CHECKED : SPARKS	DRG. No :	9A
APPROVED : PEARSE		

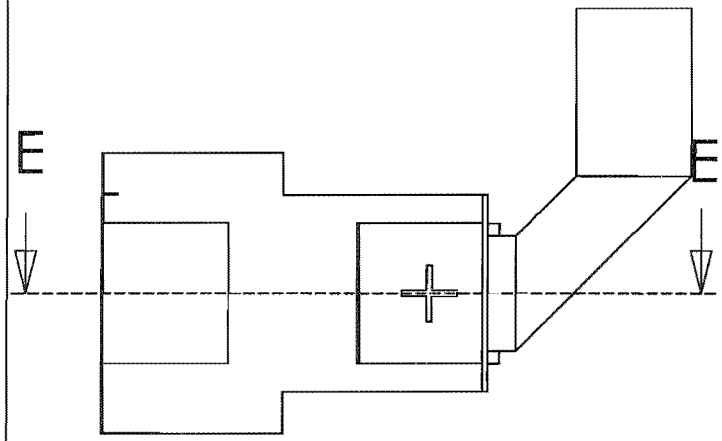

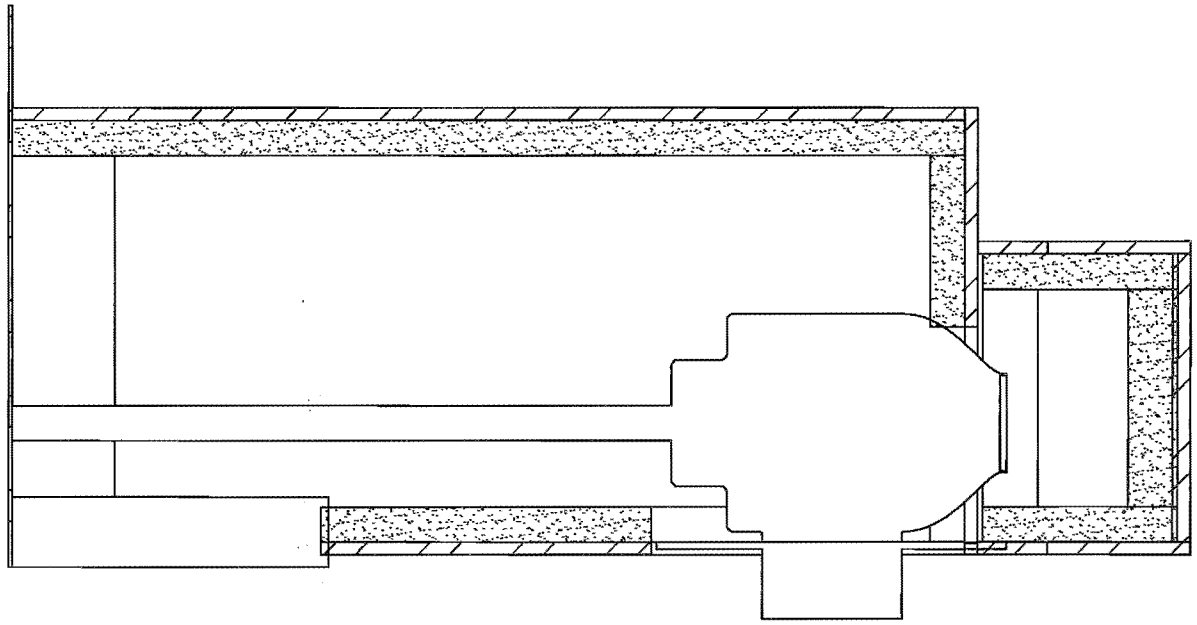

BOTTOM VIEW

E-E (1 : 10)

VERITICAL SECTION WITH ARRANGEMENT OF PLANT

SCALE : 1:20 ALL DIMENSIONS IN mm

UNIVERSITY OF CANTERBURY
MECHANICAL ENGINEERING DEPT CH.CH. N. Z.

DRAWN : PETTERSSON	DATE :	25/01/01
CHECKED : SPARKS	DRG. No :	9B
APPROVED : PEARSE		

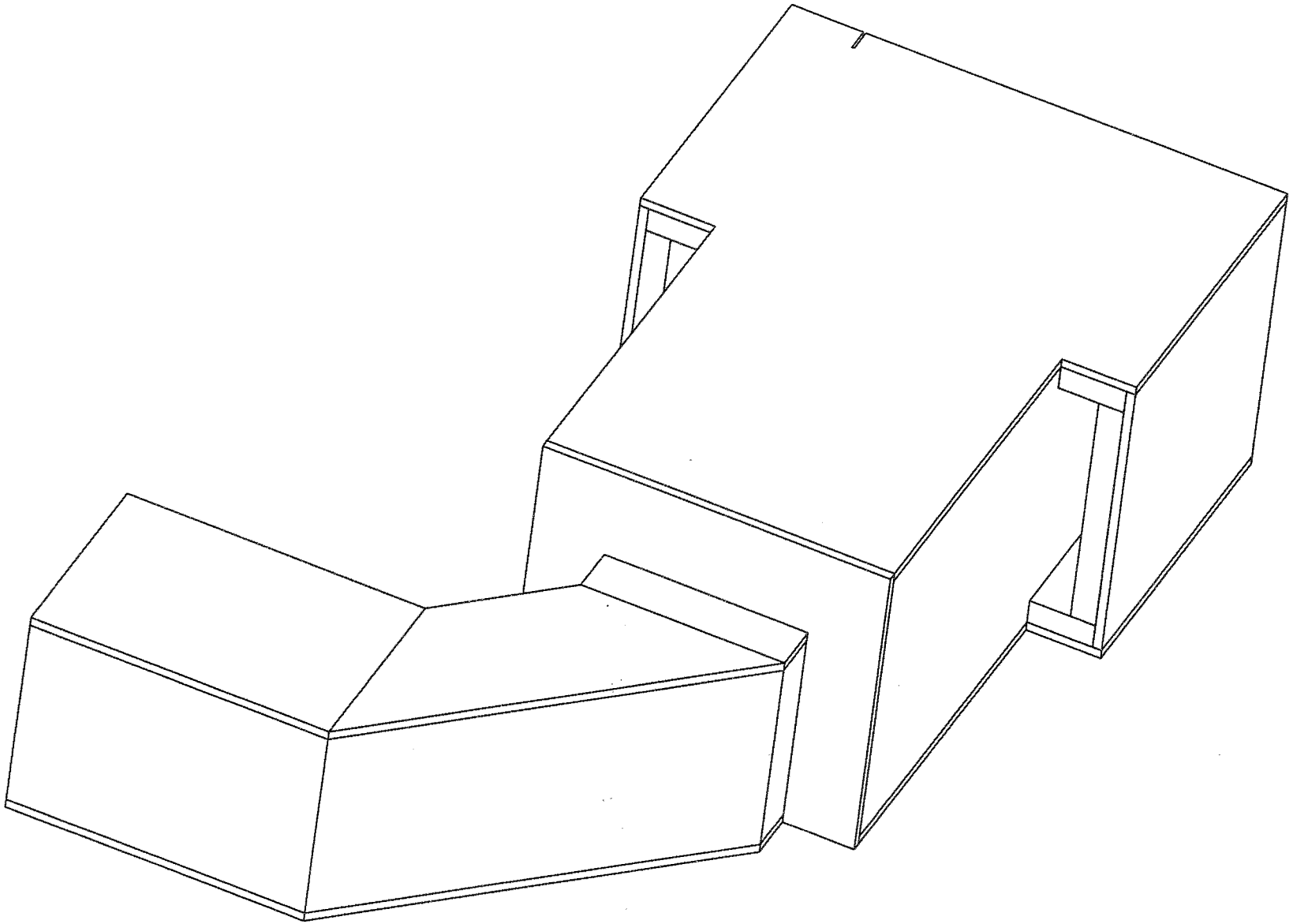

MOTOR ENCLOSURE
- TOP ISOMETRIC

SCALE : 1:10 ALL DIMENSIONS IN mm

UNIVERSITY OF CANTERBURY
MECHANICAL ENGINEERING DEPT CH.CH. N. Z.

DRAWN : PETTERSSON	DATE :	25/01/01
CHECKED : SPARKS	DRG. No :	9C
APPROVED : PEARSE		

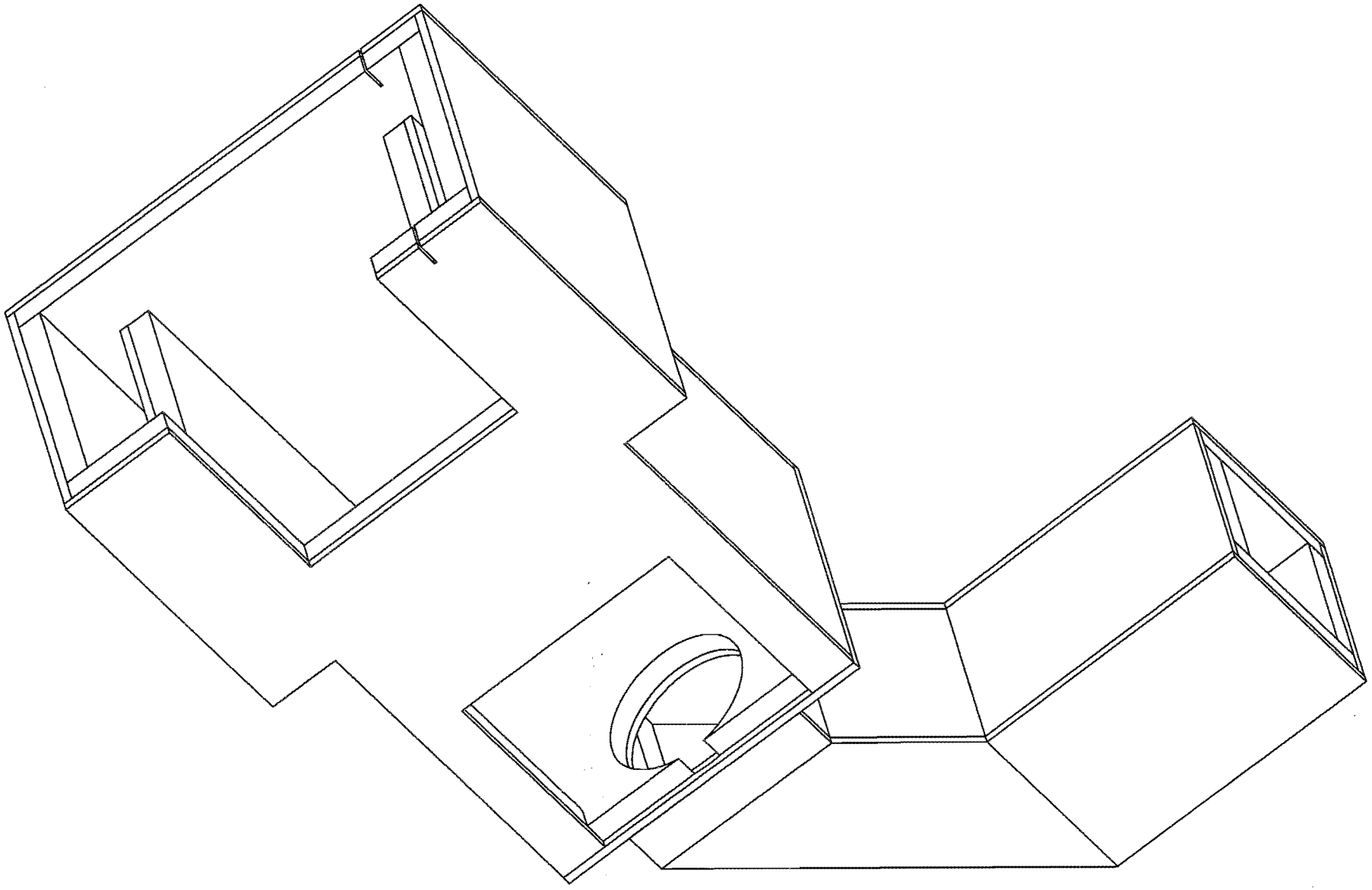

MOTOR ENCLOSURE
-BOTTOM ISOMETRIC

SCALE : 1:10 ALL DIMENSIONS IN mm

UNIVERSITY OF CANTERBURY
MECHANICAL ENGINEERING DEPT CH.CH. N. Z.

DRAWN : PETTERSSON	DATE :	25/01/01
CHECKED : SPARKS	DRG. No :	9D
APPROVED : PEARSE		

TO BE CONSTRUCTED
FROM 18mm MDF

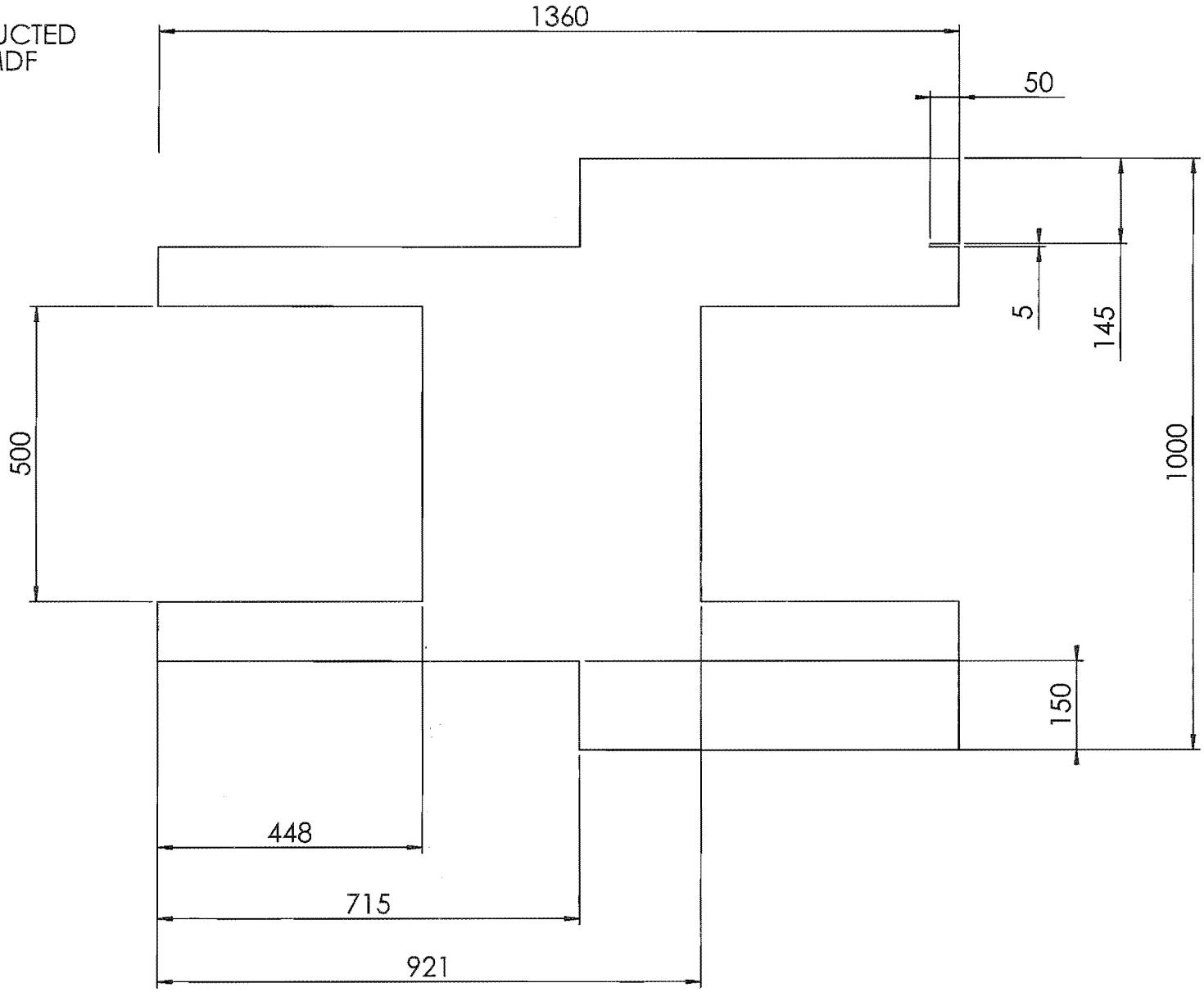

BASE WALL

SCALE : 1:20

ALL DIMENSIONS IN mm

UNIVERSITY OF CANTERBURY
MECHANICAL ENGINEERING DEPT. CH.CH. N.Z.

DRAWN : PETTERSSON	DATE : 25/01/01
CHECKED : SPARKS	DRG. No : **9-1**
APPROVED : PEARSE	

TO BE CONSTRUCTED
FROM 18mm MDF

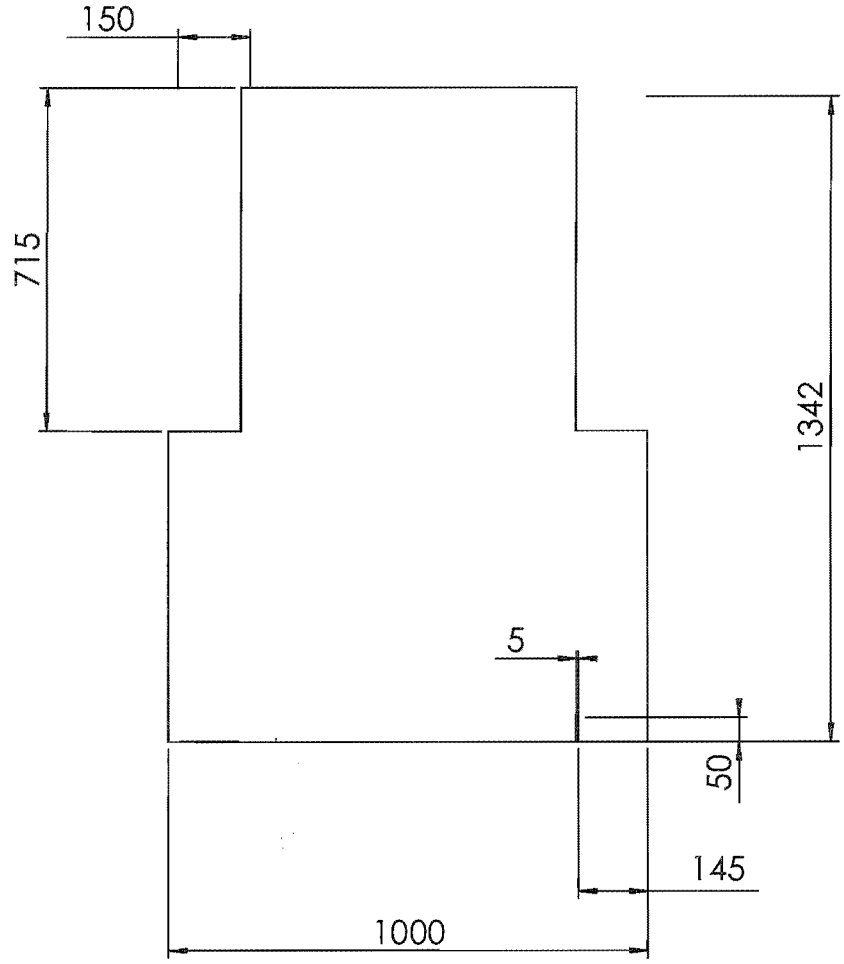

TOP WALL	UNIVERSITY OF CANTERBURY MECHANICAL ENGINEERING DEPT. CH.CH. N.Z.	
	DRAWN : PETTERSSON	DATE : 25/01/01
	CHECKED : SPARKS	DRG. No : 9-2
SCALE : 1:15 ALL DIMENSIONS IN mm	APPROVED : PEARSE	

INNER WALL

TO BE CONSTRUCTED
FROM 18mm MDF

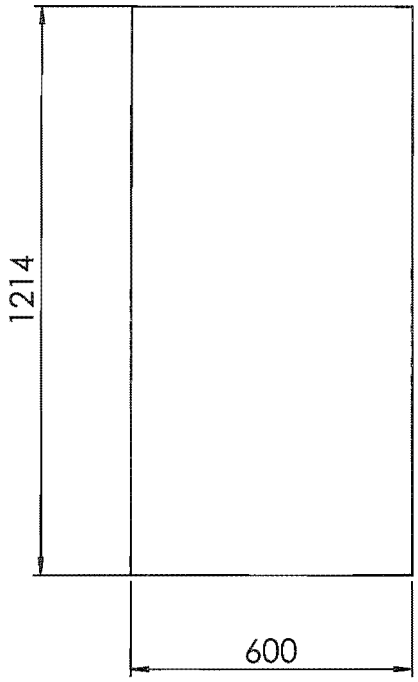

END WALL

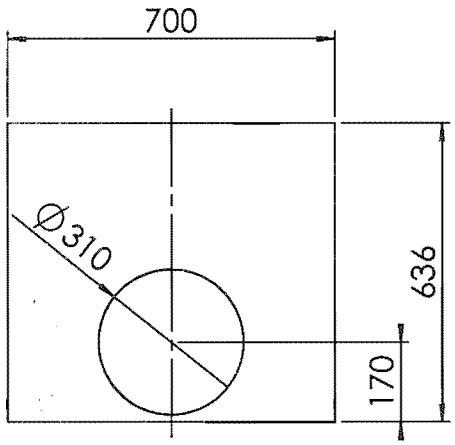

OUTER WALL

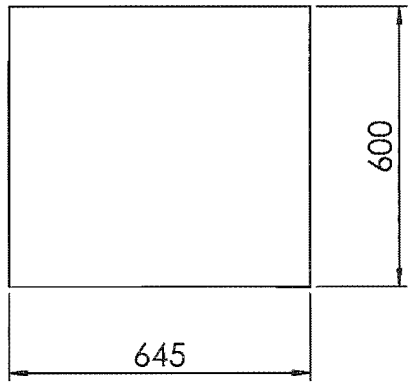

WALLS

SCALE : 1:15 ALL DIMENSIONS IN mm

UNIVERSITY OF CANTERBURY
MECHANICAL ENGINEERING DEPT CH.CH. N.Z.

DRAWN : PETTERSSON	DATE :	25/01/01
CHECKED : SPARKS	DRG. No :	9-3
APPROVED : PEARSE		

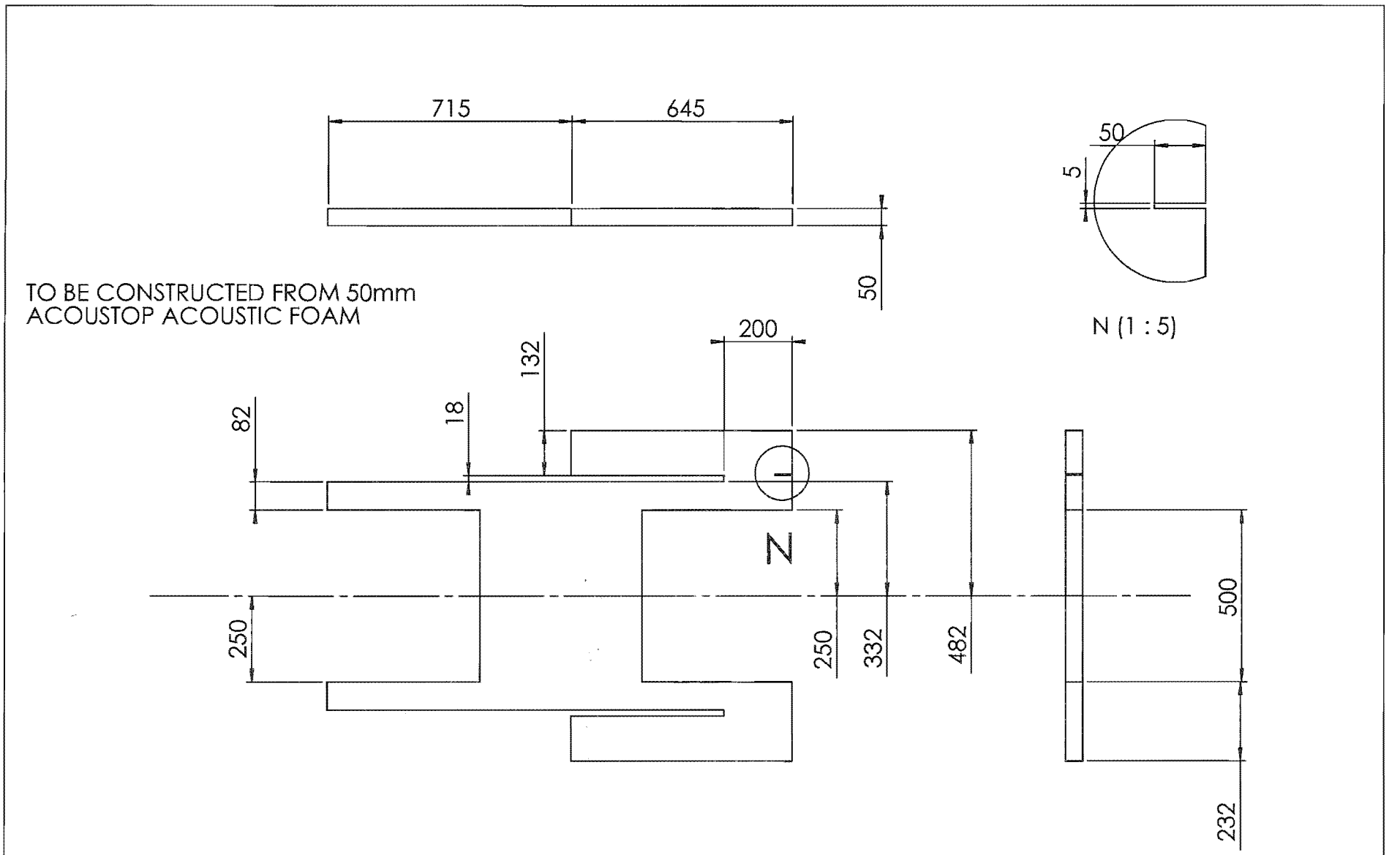

BASE ABSORBER

SCALE : 1:15 ALL DIMENSIONS IN mm

UNIVERSITY OF CANTERBURY
MECHANICAL ENGINEERING DEPT CH.CH. N.Z.

DRAWN : PETTERSSON	DATE :	25/01/01
CHECKED : SPARKS	DRG. No :	9-4
APPROVED : PEARSE		

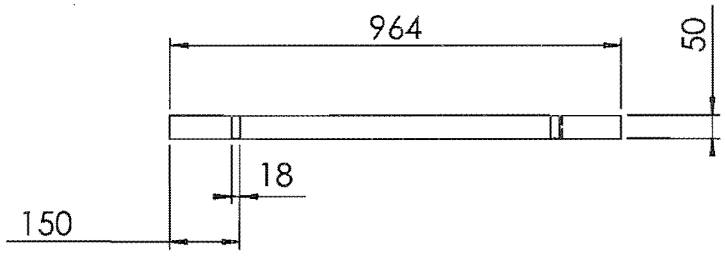

TO BE CONSTRUCTED FROM 50mm
ACOUSTOP ACOUSTIC FOAM

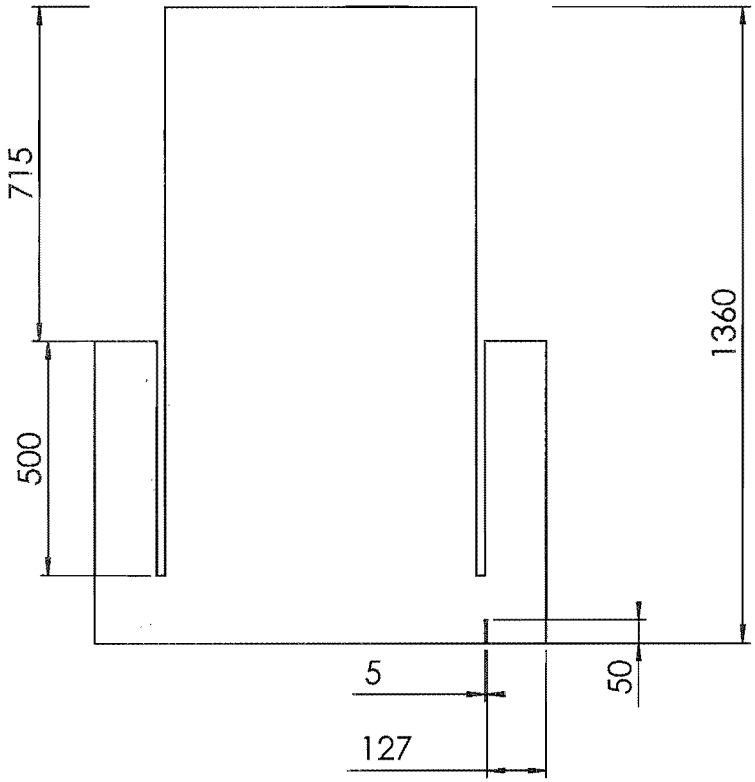

TOP ABSORBER

SCALE : 1:20 ALL DIMENSIONS IN mm

UNIVERSITY OF CANTERBURY
MECHANICAL ENGINEERING DEPT CH.CH. N.Z.

DRAWN : PETTERSSON	DATE :	25/01/01
CHECKED : SPARKS	DRG. No :	9-5
APPROVED : PEARSE		

INNER WALL ABSORBER

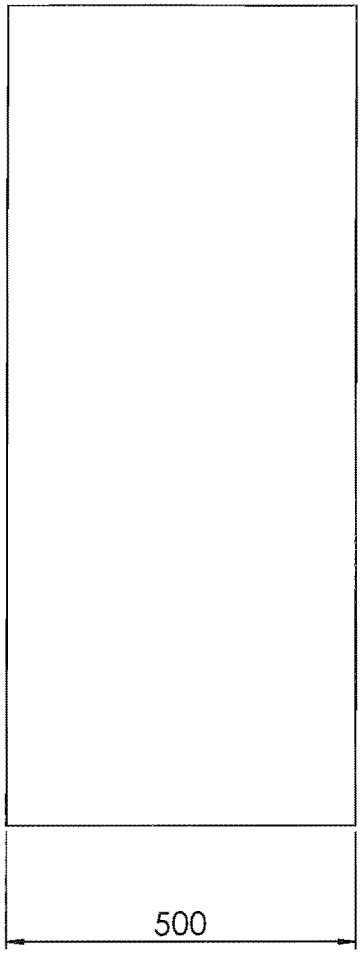

TO BE CONSTRUCTED FROM 50mm
ACOUSTOP ACOUSTIC FOAM

OUTER WALL ABSORBER

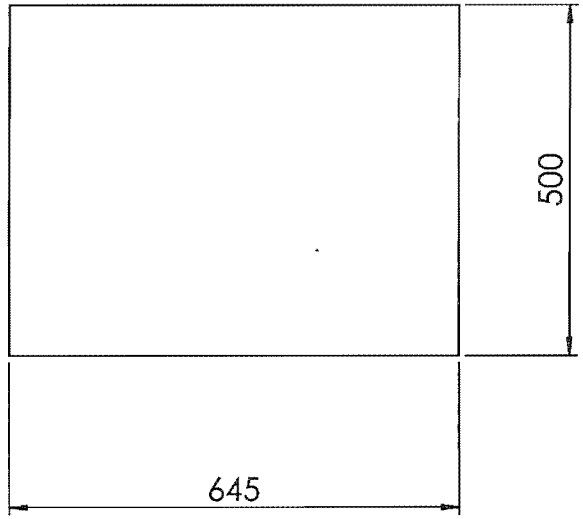

END WALL ABSORBER

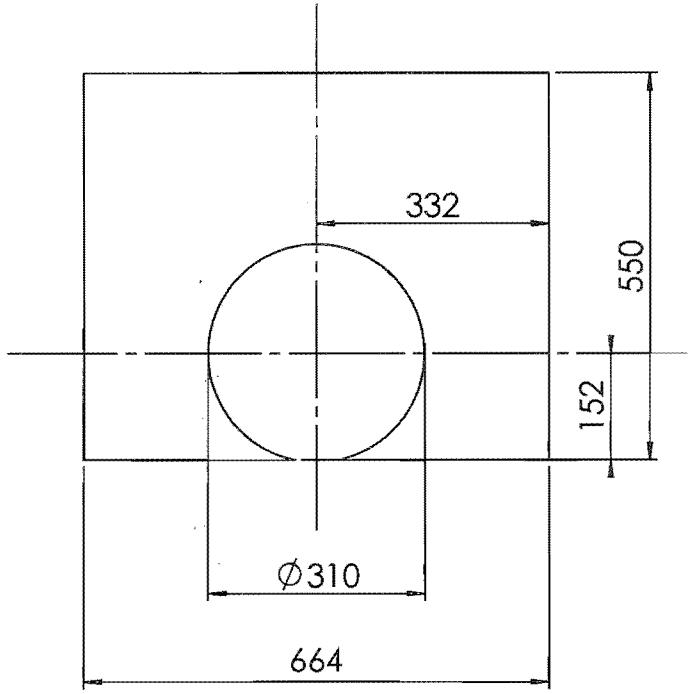

WALL ABSORBERS

SCALE : 1:10 ALL DIMENSIONS IN mm

UNIVERSITY OF CANTERBURY
MECHANICAL ENGINEERING DEPT CH.CH. N.Z.

DRAWN : PETTERSSON	DATE :	25/01/01
CHECKED : SPARKS	DRG. No :	9-6
APPROVED : PEARSE		

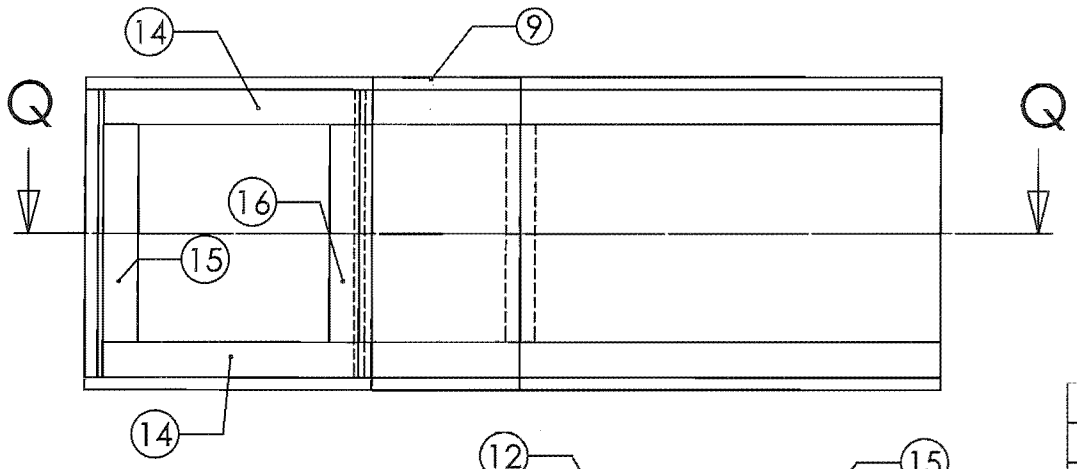

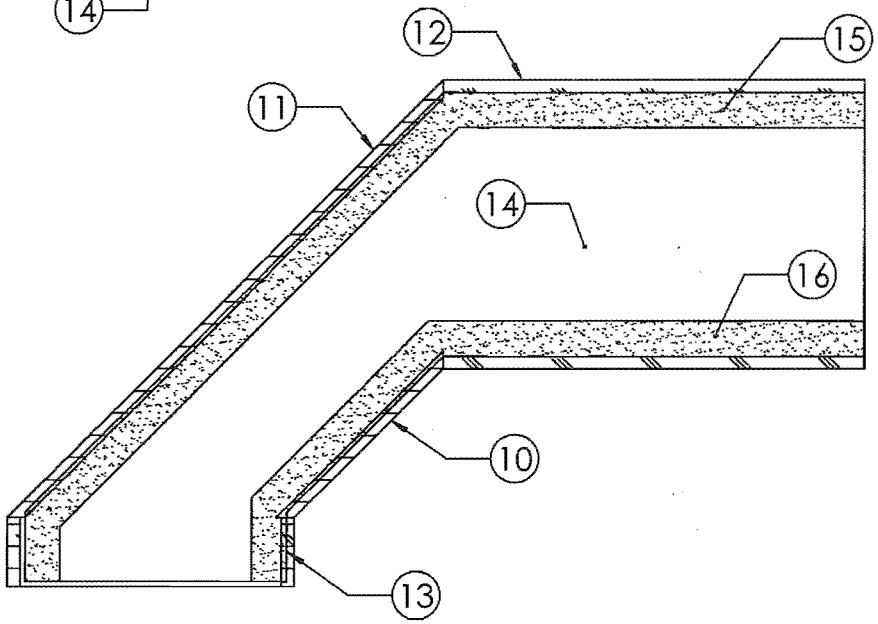

Q-Q

ITEM NO.	QTY.	PART NAME	DRG. NO.
9	2	Muffler Top Wall	9-7-1
10	1	Muffler Side Wall	9-7-1
11	1	Muffler Long Side Wall	'2-1
12	4	Muffler Plenum Wall	9-7-1
13	4	Muffler Plenum Short Wall	9-7-1
14	2	Muffler Base Absorber	9-7-2
15	1	Muffler Wall Absorber	9-7-2
16	1	Muffler Inside Wall Absorber	9-7-2

INLET MUFFLER
SUB ASSEMBLY

SCALE : 1:10 ALL DIMENSIONS IN mm

UNIVERSITY OF CANTERBURY
MECHANICAL ENGINEERING DEPT CH.CH. N.Z.

DRAWN : PETTERSSON DATE : 25/01/01
CHECKED : SPARKS DRG. No : 9-7
APPROVED : PEARSE

OUTSIDE ANGLED WALL

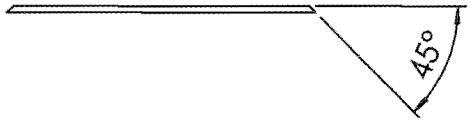

TO BE CONSTRUCTED
FROM 18mm MDF

ANGLED BASE

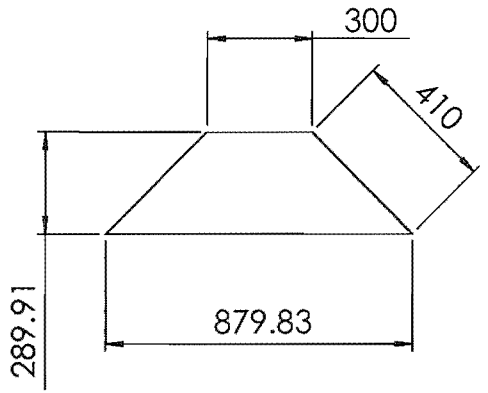

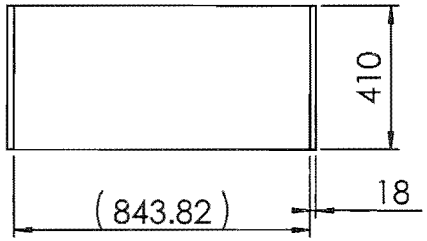

SHORT WALL

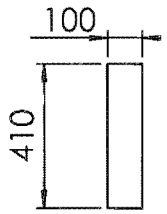

INSIDE ANGLED WALL

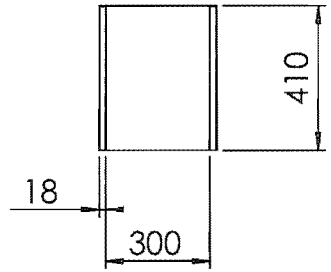

LONG WALL

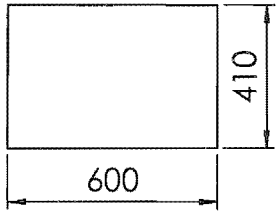

INLET MUFFLER PARTS

SCALE : 1:20 ALL DIMENSIONS IN mm

UNIVERSITY OF CANTERBURY
MECHANICAL ENGINEERING DEPT CH.CH. N.Z.

DRAWN : PETTERSSON	DATE :	25/01/01
CHECKED : SPARKS	DRG. No :	9-7-1
APPROVED : PEARSE		

INSIDE WALL ABSORBER

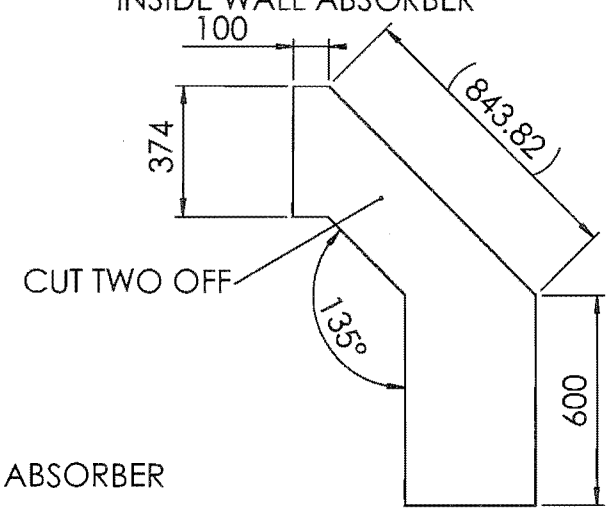

OUTSIDE WALL ABSORBER

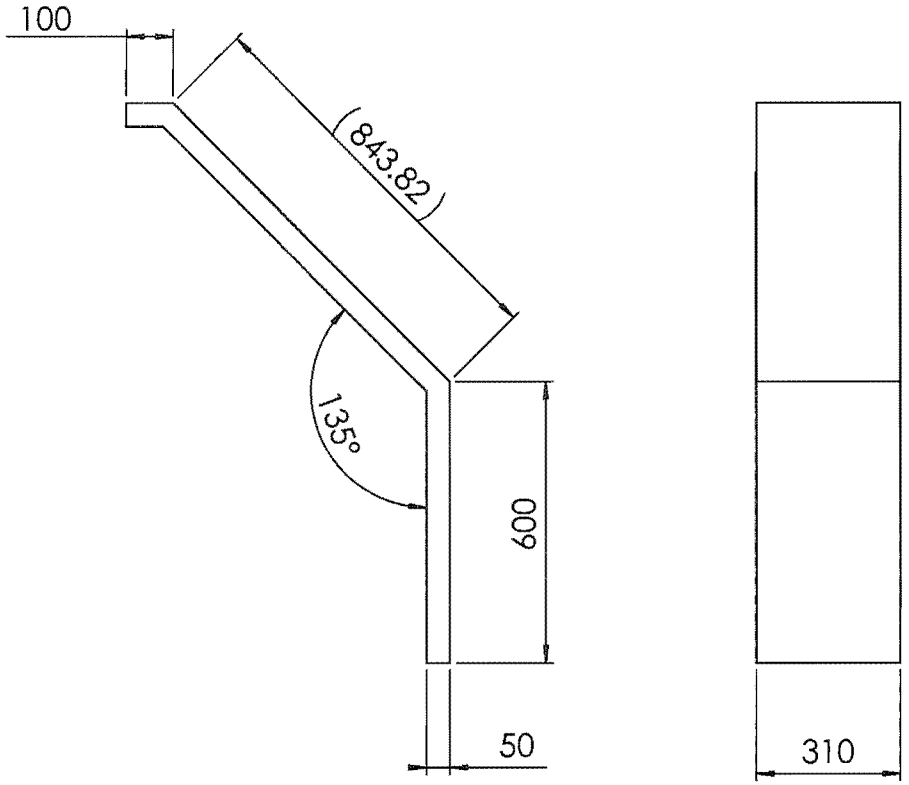

BASE ABSORBER

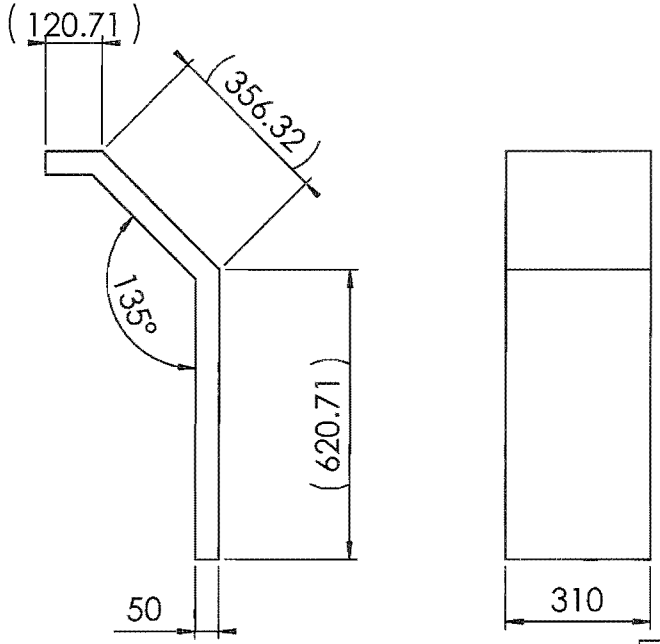

TO BE CUT FROM 50 mm ACOUSTOP ACOUSTIC FOAM

INLET MUFFLER ABSORBERS	UNIVERSITY OF CANTERBURY MECHANICAL ENGINEERING DEPT CH.CH. N.Z.
	DRAWN : PETTERSSON DATE : 25/01/01
	CHECKED : SPARKS DRG. No : 9-7-2
SCALE : 1:15 ALL DIMENSIONS IN mm	APPROVED : PEARSE

ITEM NO.	QTY.	PART NAME	DRG. NO.
1	1	Speaker Box Top Wall	10-1
2	2	Speaker Box Long Wall	10-2
3	2	Speaker Box Short Wall	10-3
4	1	Speaker Box Baffle Plate	10-4

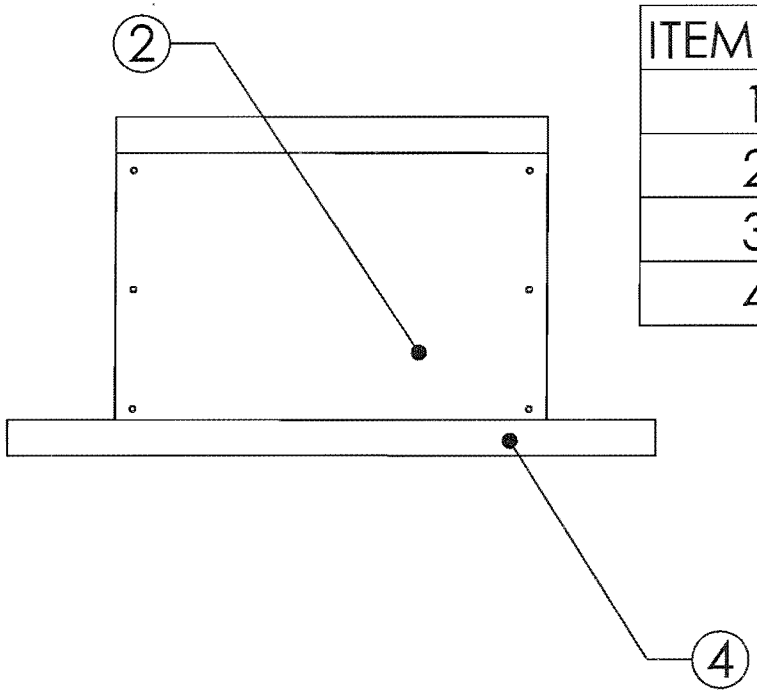

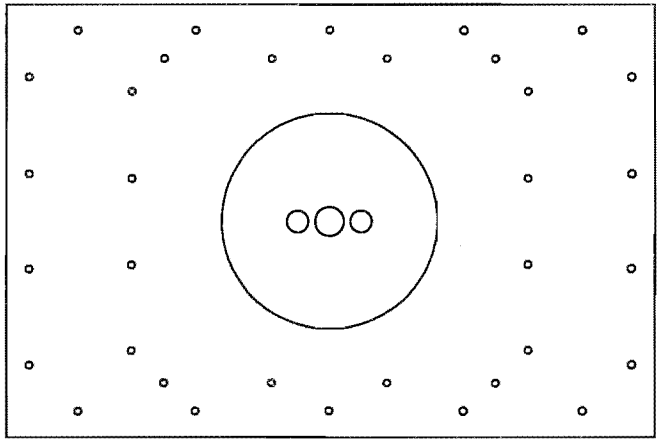

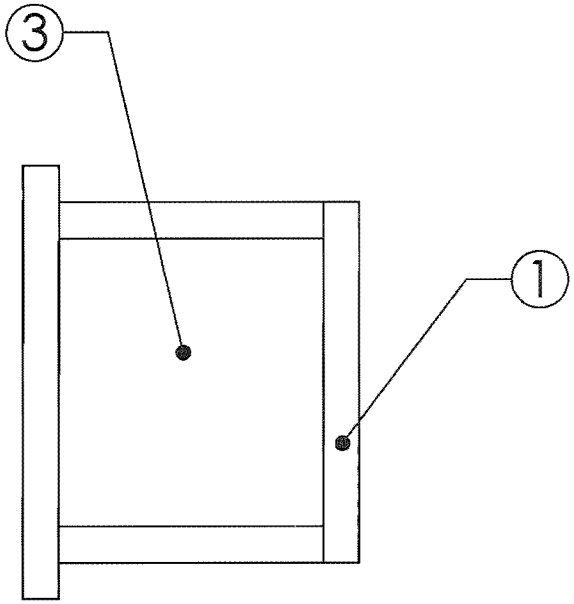

SPEAKER BOX ASSY.

SCALE : 1:5 ALL DIMENSIONS IN mm

UNIVERSITY OF CANTERBURY
MECHANICAL ENGINEERING DEPT. CH.CH. N.Z.

DRAWN : MATTHEW PETTERSSON | DATE : 15/10/01

CHECKED :

APPROVED :

DRG. No : **10**

TO BE CONSTRUCTED FROM 25mm MDF

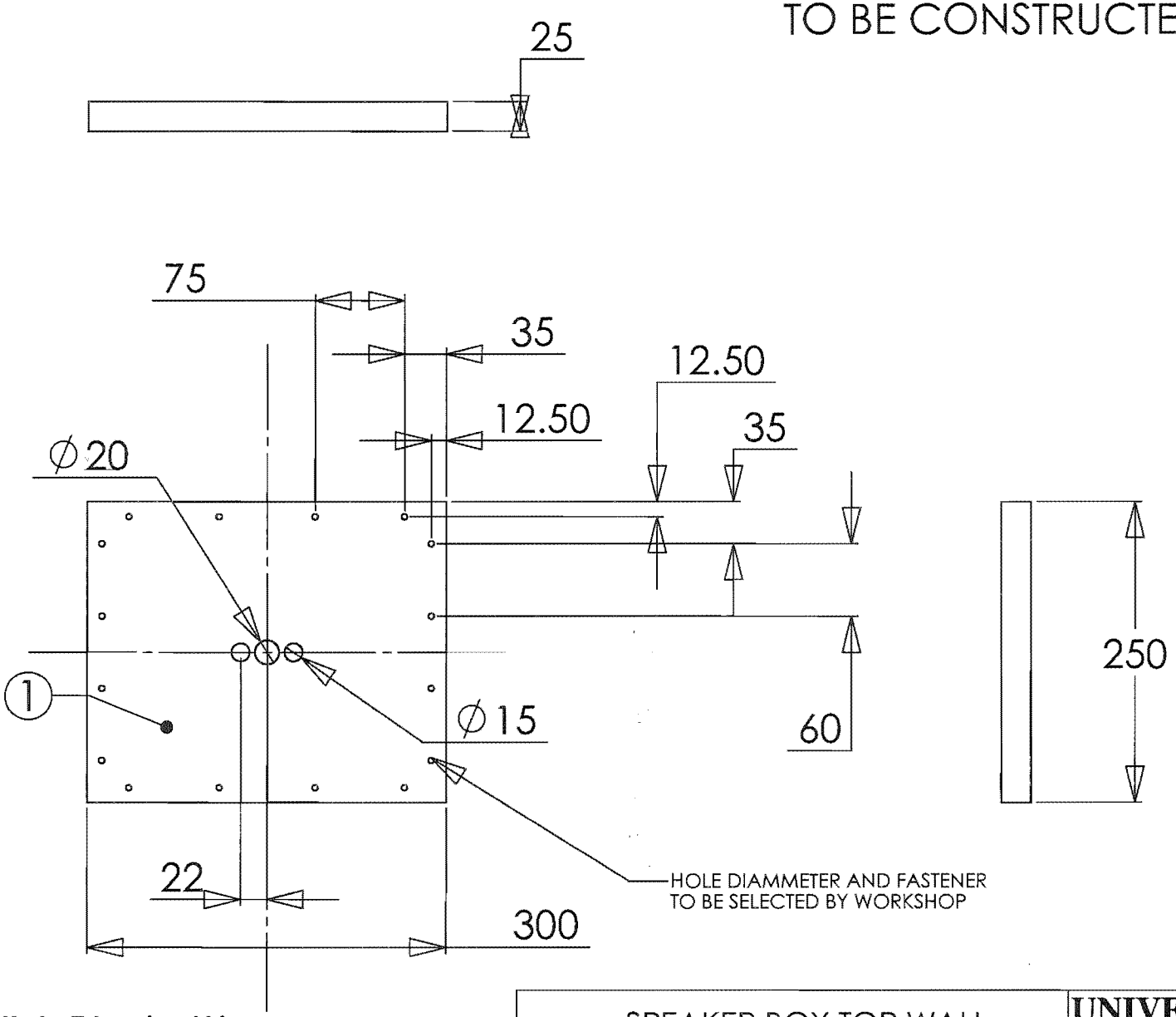

SPEAKER BOX TOP WALL

SCALE : 1:5 ALL DIMENSIONS IN mm

UNIVERSITY OF CANTERBURY
MECHANICAL ENGINEERING DEPT. CH.CH. N.Z.

DRAWN: PETTERSSON DATE : 15/10/01

CHECKED : SPARKS DRG. No : 10-1

APPROVED : PEARSE

TO BE CONSTRUCTED FROM 25mm MDF

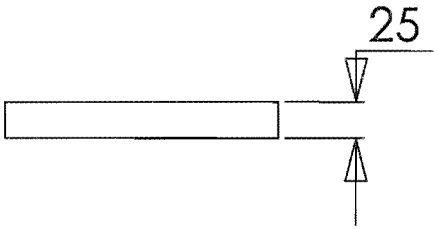

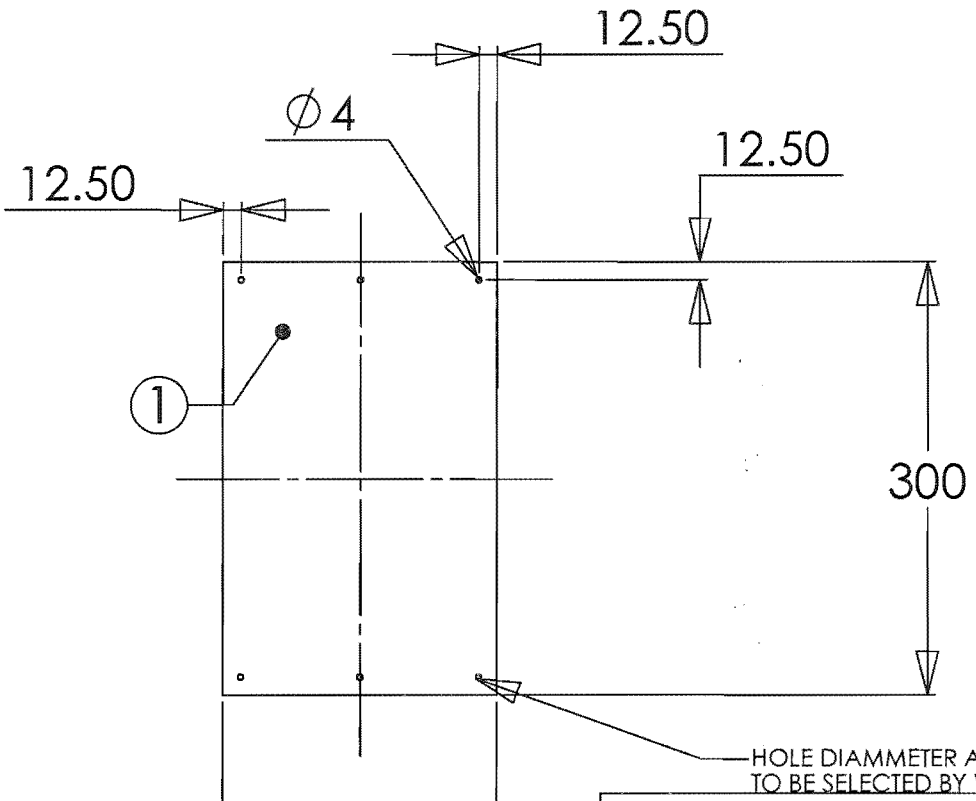

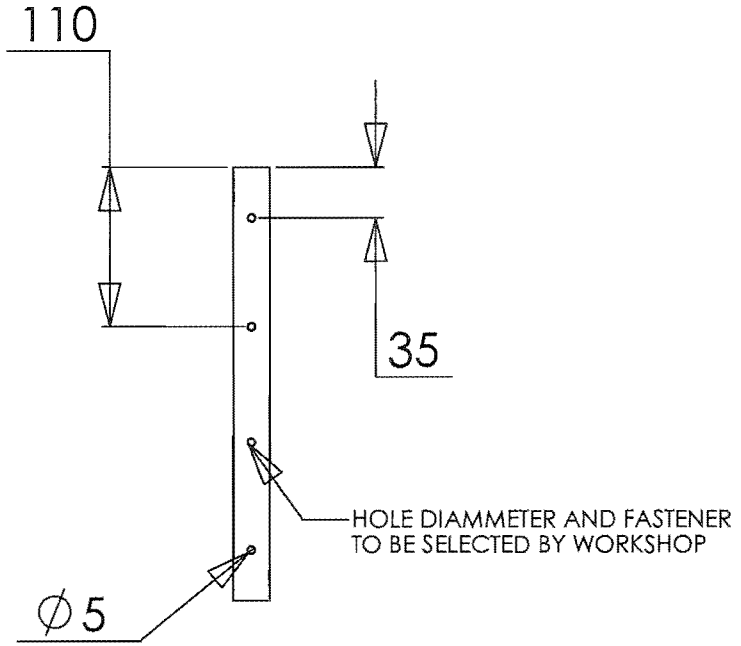

SPEAKER BOX LONG WALL

SCALE : 1:5 ALL DIMENSIONS IN mm

UNIVERSITY OF CANTERBURY
MECHANICAL ENGINEERING DEPT. CH.CH. N.Z.

DRAWN: PETTERSSON	DATE : 15/10/01
CHECKED : SPARKS	DRG. No : **10-2**
APPROVED : PEARSE	

ITEM NO.	PART NAME	MATRIAL
3	ShortWall	25mm MDF

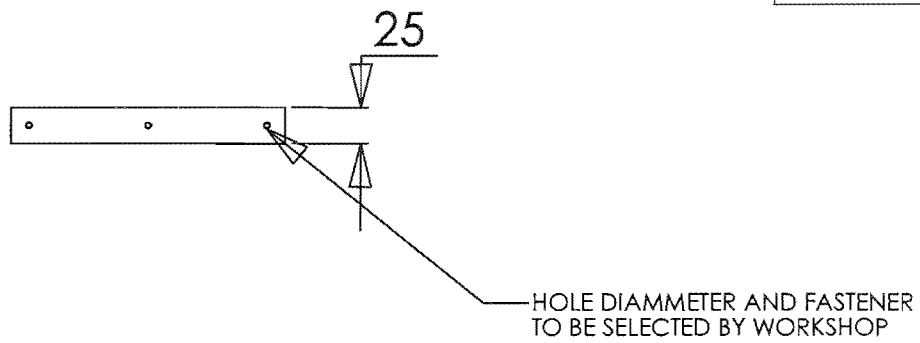

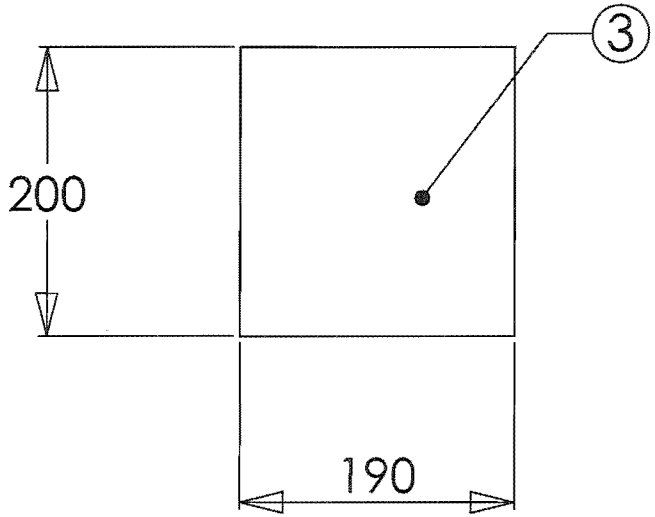

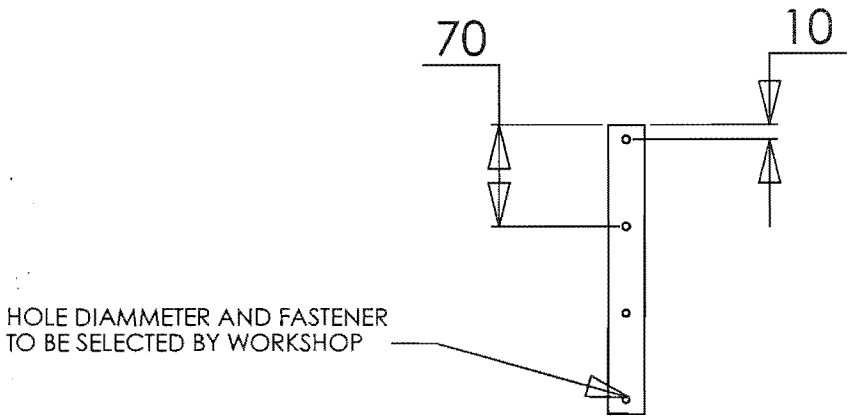

SPEAKER BOX SHORT WALL

SCALE : 1:5 ALL DIMENSIONS IN mm

UNIVERSITY OF CANTERBURY
MECHANICAL ENGINEERING DEPT. CH.CH. N.Z.

DRAWN: PETTERSSON	DATE : 15/10/01
CHECKED : SPARKS	DRG. No : **10-3**
APPROVED : PEARSE	

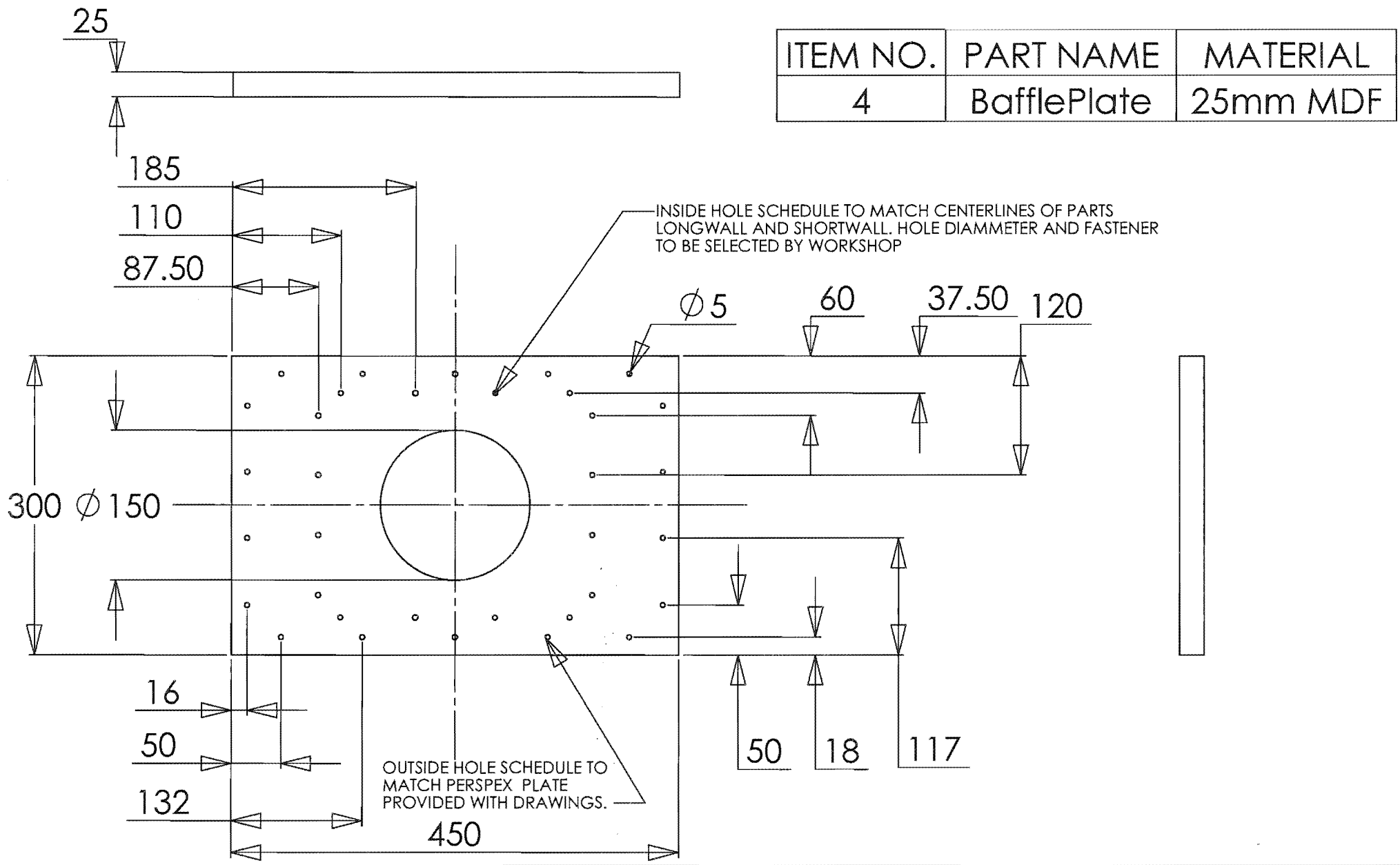

ITEM NO.	PART NAME	MATERIAL
4	BafflePlate	25mm MDF

SPEAKER BOX BAFFLE PLATE

SCALE : 1:5 ALL DIMENSIONS IN mm

UNIVERSITY OF CANTERBURY
MECHANICAL ENGINEERING DEPT. CH.CH. N.Z.

DRAWN: PETTERSSON DATE : 15/10/01

CHECKED : SPARKS DRG. No : **10-4**

APPROVED : PEARSE

SPL Along the Substitution Test Duct

1/3 Octave Band Centre Frequency (Hz)	Maximum Permissible PRC in ISO 7235	PRC of Anechoic Termination
50	0.4	0.15
63	0.35	0.15
80	0.3	0.09
100	0.25	0.09
125	0.15	0.10
160	0.15	0.10
200	0.15	0.07
250	0.15	0.07
315	0.15	0.03
400	0.15	0.07
500	0.15	0.04

Pressure Wave Reflection Coefficient: $PRC = \frac{10^{\Delta l/20} - 1}{10^{\Delta l/20} + 1}$

PRC calculated to the first modal cut-on frequency of the substitution test duct (f_o= 473 Hz): $f_o = 0.586\frac{c}{d}$

where c is the speed of sound in air, and d is the hydraulic equivalent diameter of the duct.

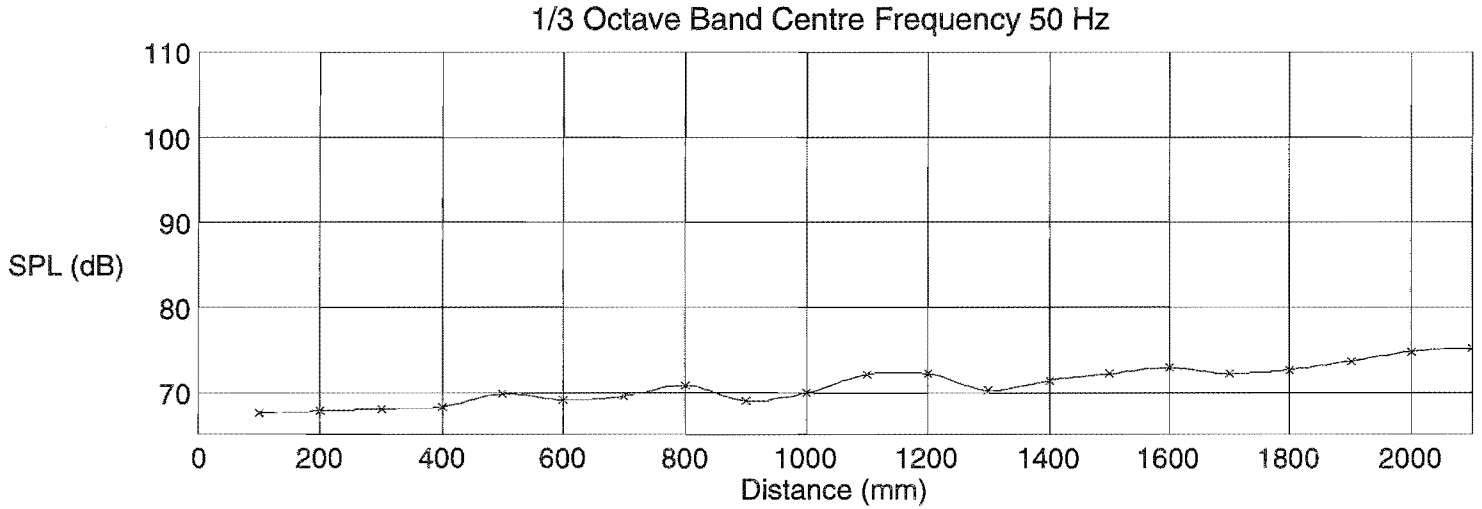
1/3 Octave Band Centre Frequency 50 Hz
SPL (dB)
110
100
90
80
70
0
200
400
600
800
1000
1200
1400
1600
1800
2000
Distance (mm)

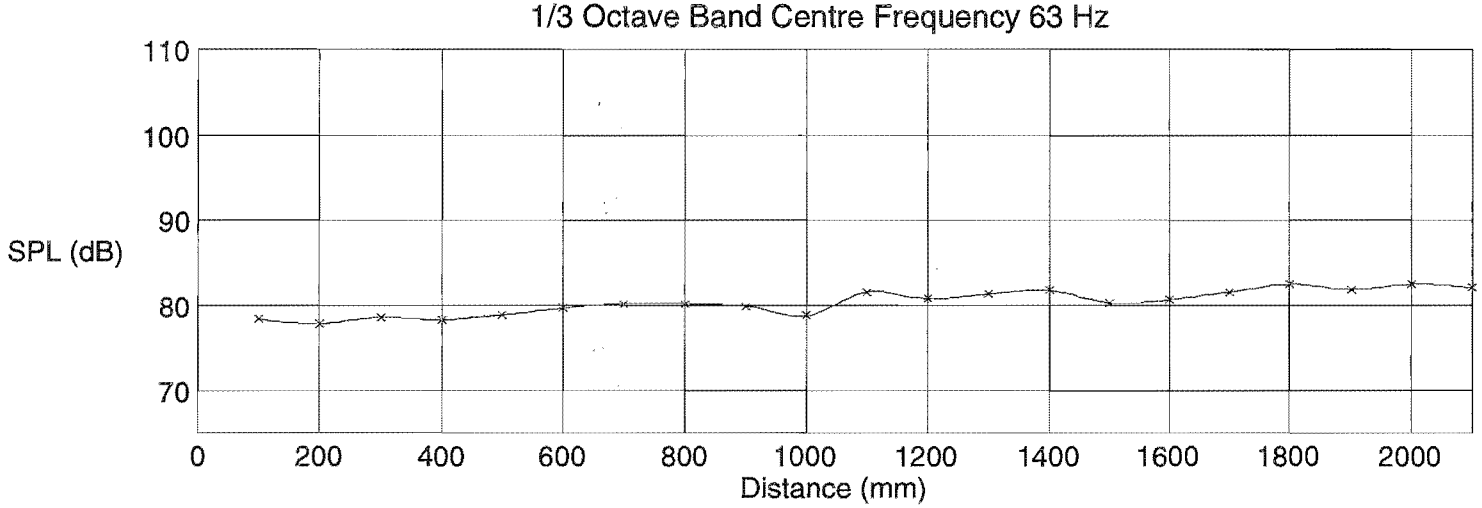
1/3 Octave Band Centre Frequency 63 Hz
SPL (dB)
110
100
90
80
70
0
200
400
600
800
1000
1200
1400
1600
1800
2000
Distance (mm)

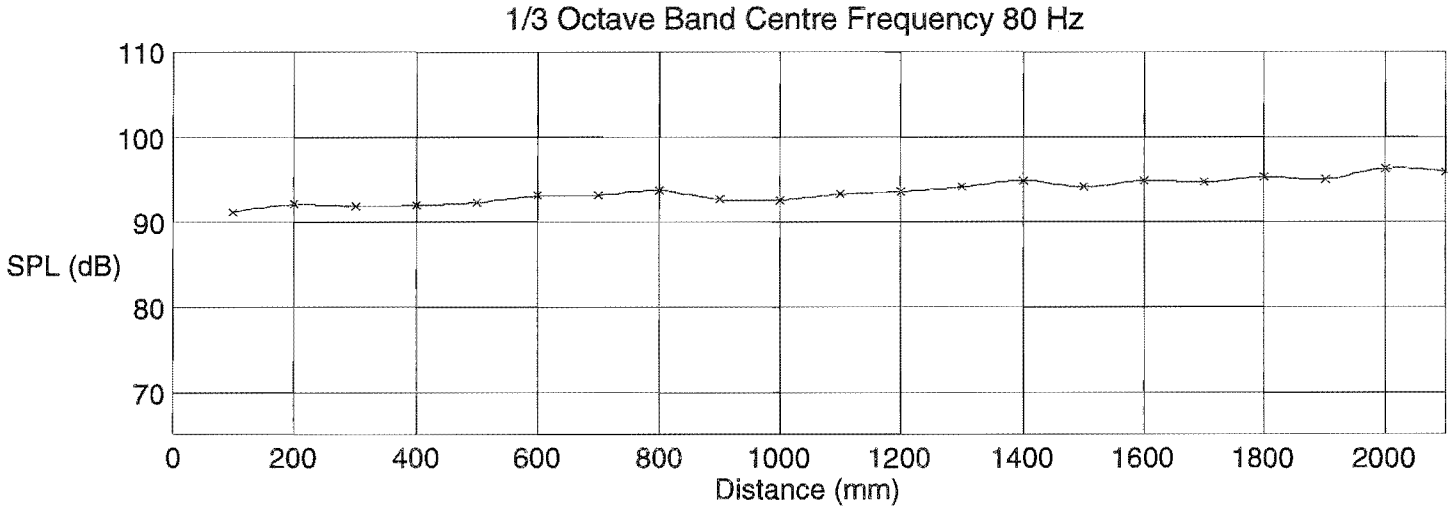
1/3 Octave Band Centre Frequency 80 Hz
110
100
90
80
70
SPL (dB)
0
200
400
600
800
1000
1200
1400
1600
1800
2000
Distance (mm)

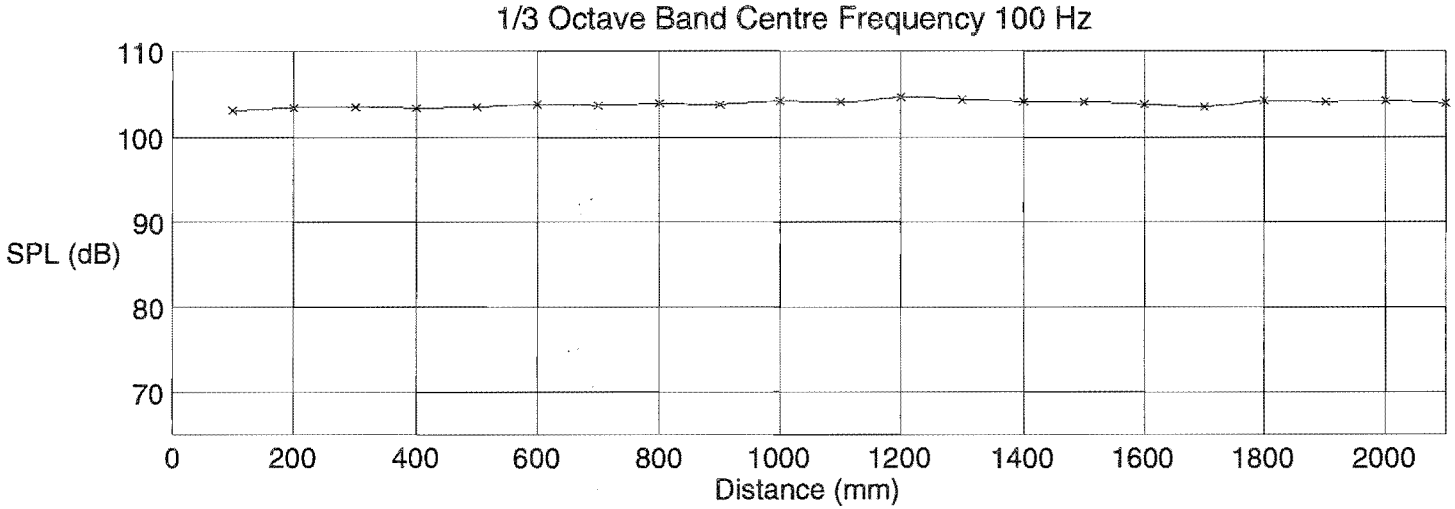
1/3 Octave Band Centre Frequency 100 Hz
110
100
90
80
70
SPL (dB)
0
200
400
600
800
1000
1200
1400
1600
1800
2000
Distance (mm)

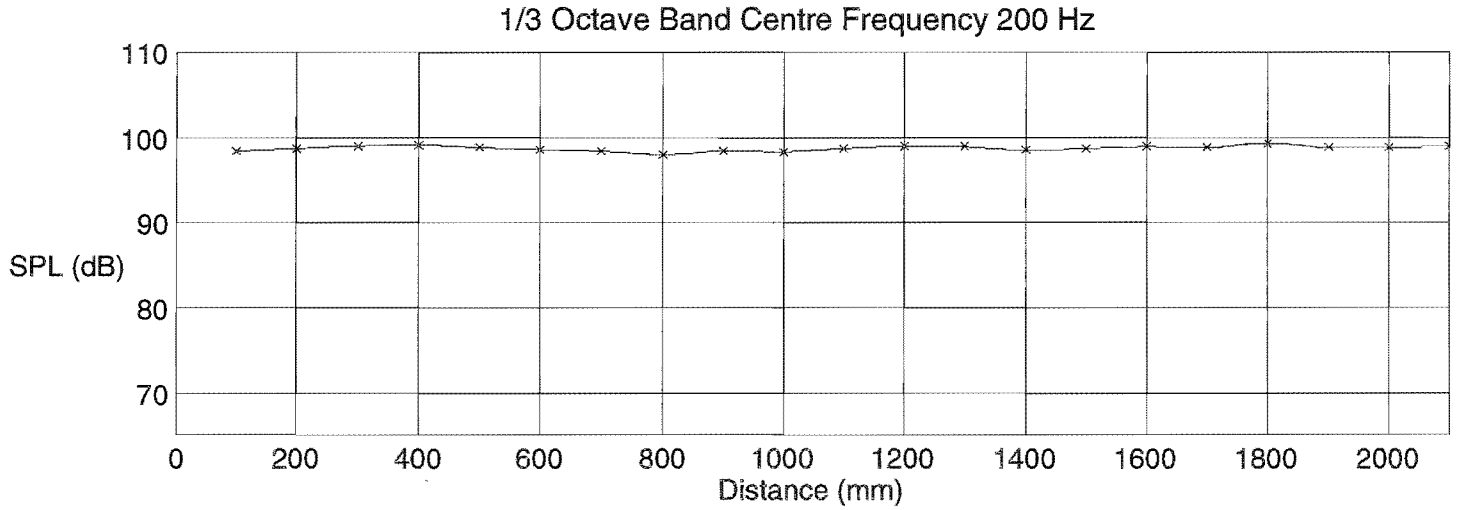
1/3 Octave Band Centre Frequency 200 Hz
110
100
90
80
70
SPL (dB)
0
200
400
600
800
1000
1200
1400
1600
1800
2000
Distance (mm)

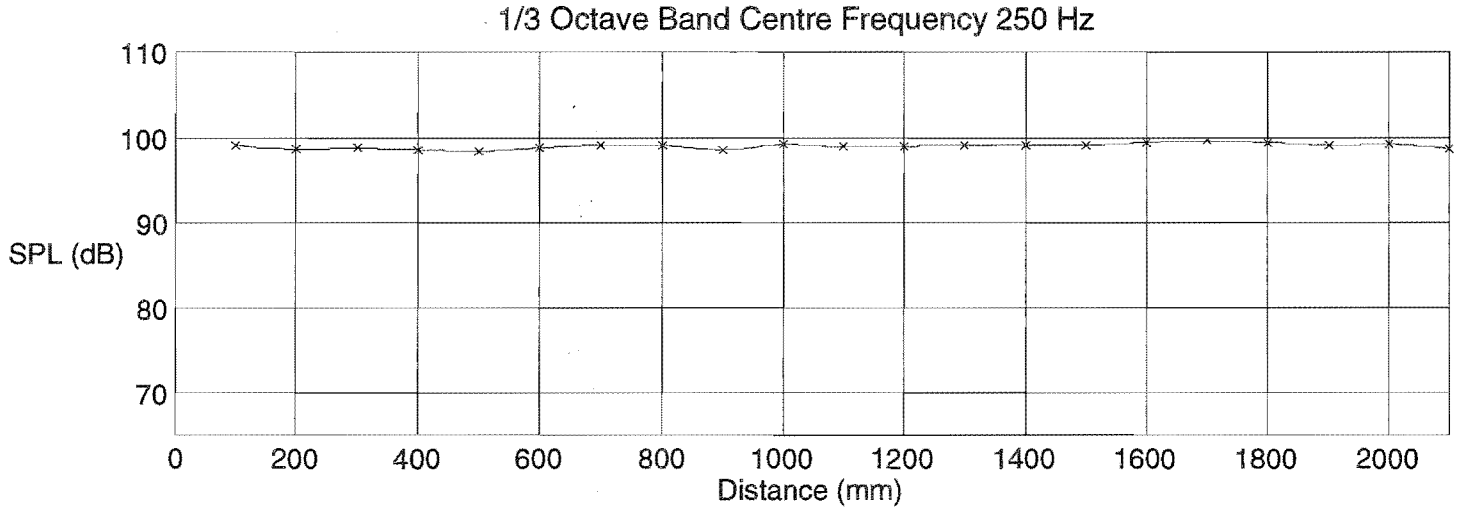
1/3 Octave Band Centre Frequency 250 Hz
110
100
90
80
70
SPL (dB)
0
200
400
600
800
1000
1200
1400
1600
1800
2000
Distance (mm)

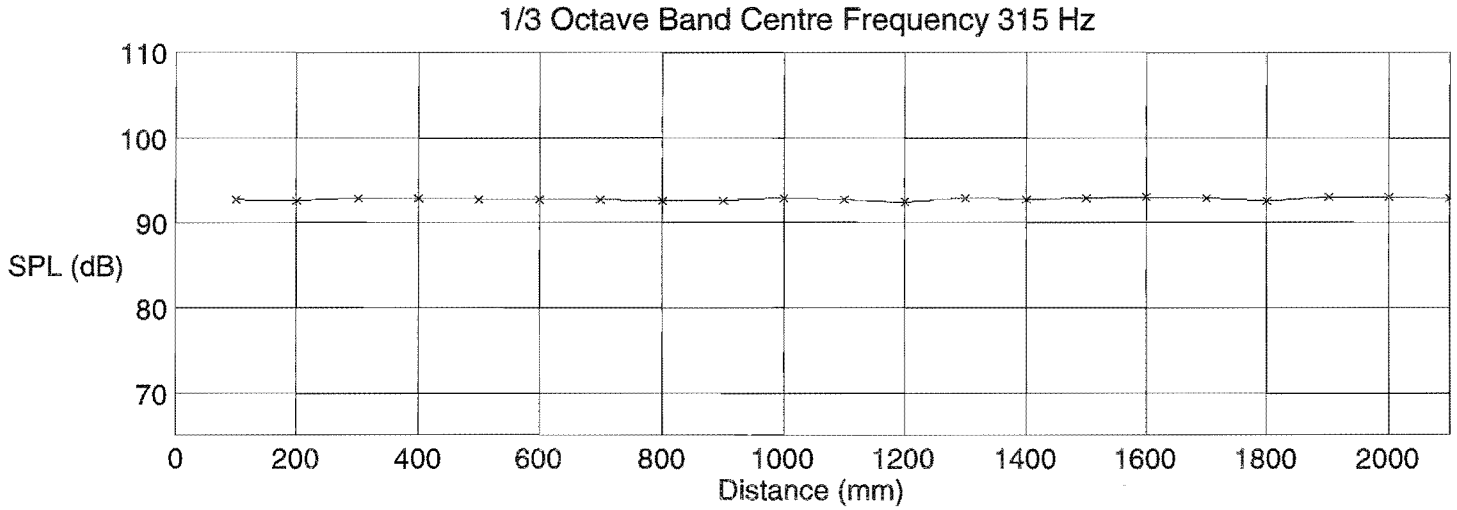
1/3 Octave Band Centre Frequency 315 Hz
110
100
90
80
70
SPL (dB)
0
200
400
600
800
1000
1200
1400
1600
1800
2000
Distance (mm)

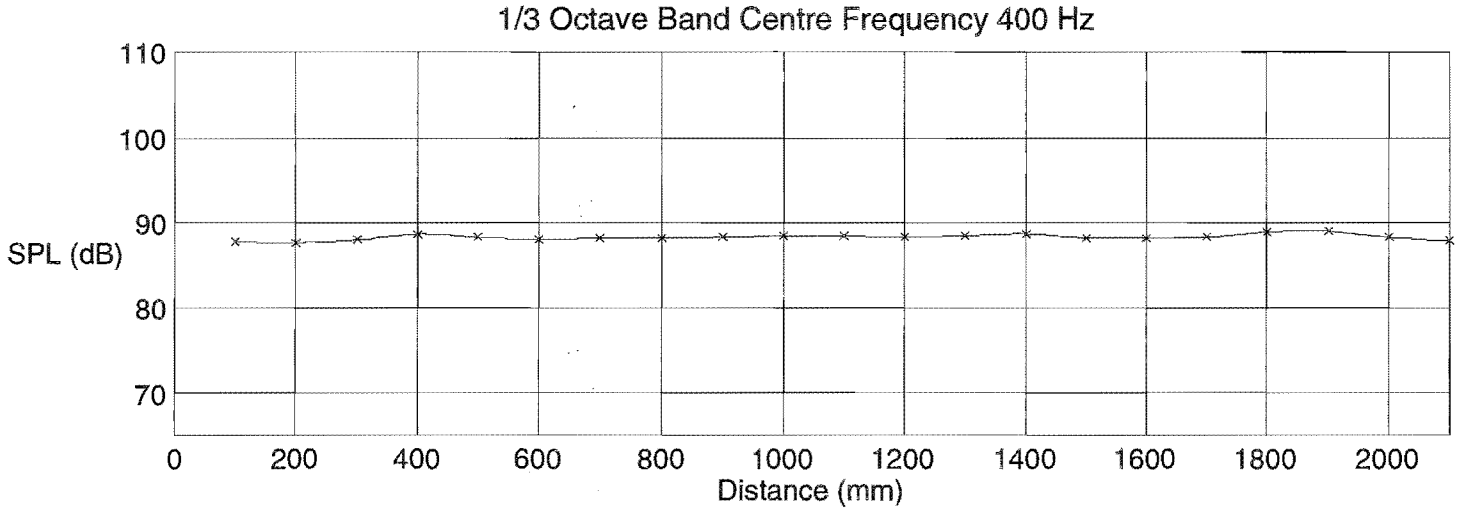
1/3 Octave Band Centre Frequency 400 Hz
110
100
90
80
70
SPL (dB)
0
200
400
600
800
1000
1200
1400
1600
1800
2000
Distance (mm)

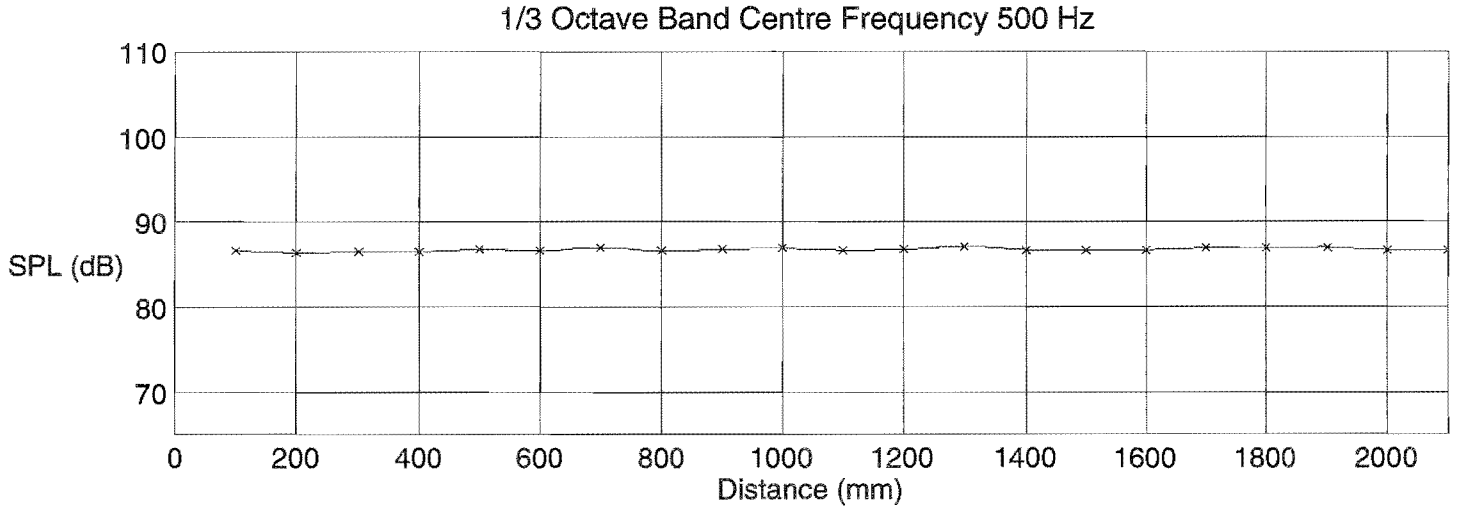
1/3 Octave Band Centre Frequency 500 Hz
110
100
90
80
70
SPL (dB)
0
200
400
600
800
1000
1200
1400
1600
1800
2000
Distance (mm)

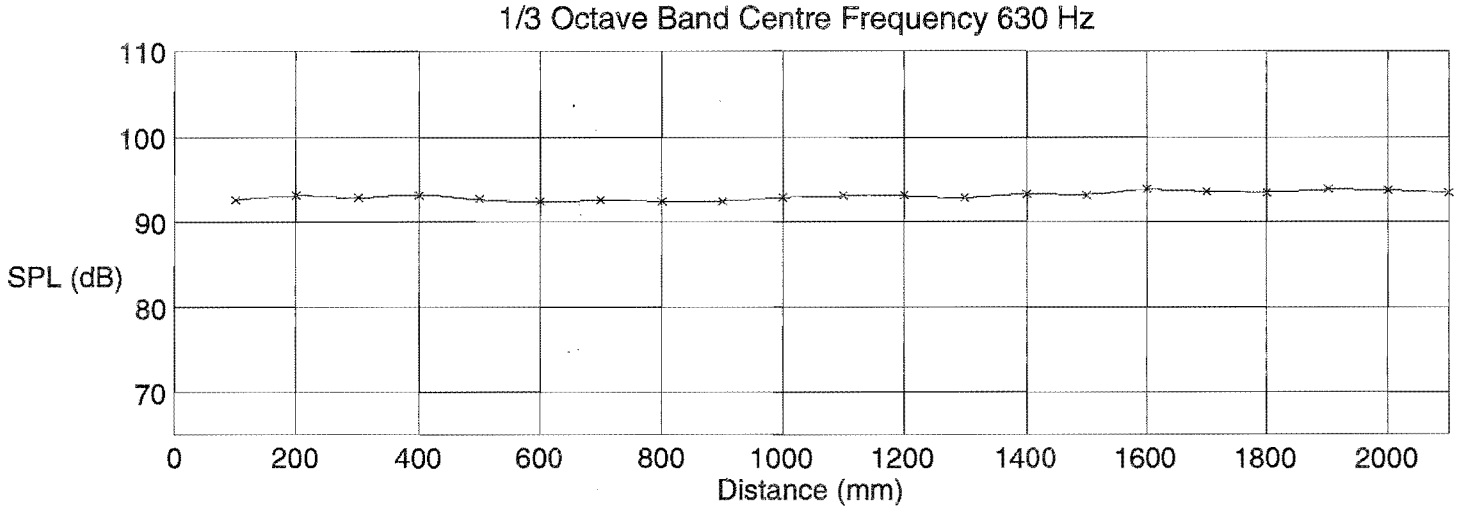
1/3 Octave Band Centre Frequency 630 Hz
110
100
90
80
70
SPL (dB)
0
200
400
600
800
1000
1200
1400
1600
1800
2000
Distance (mm)

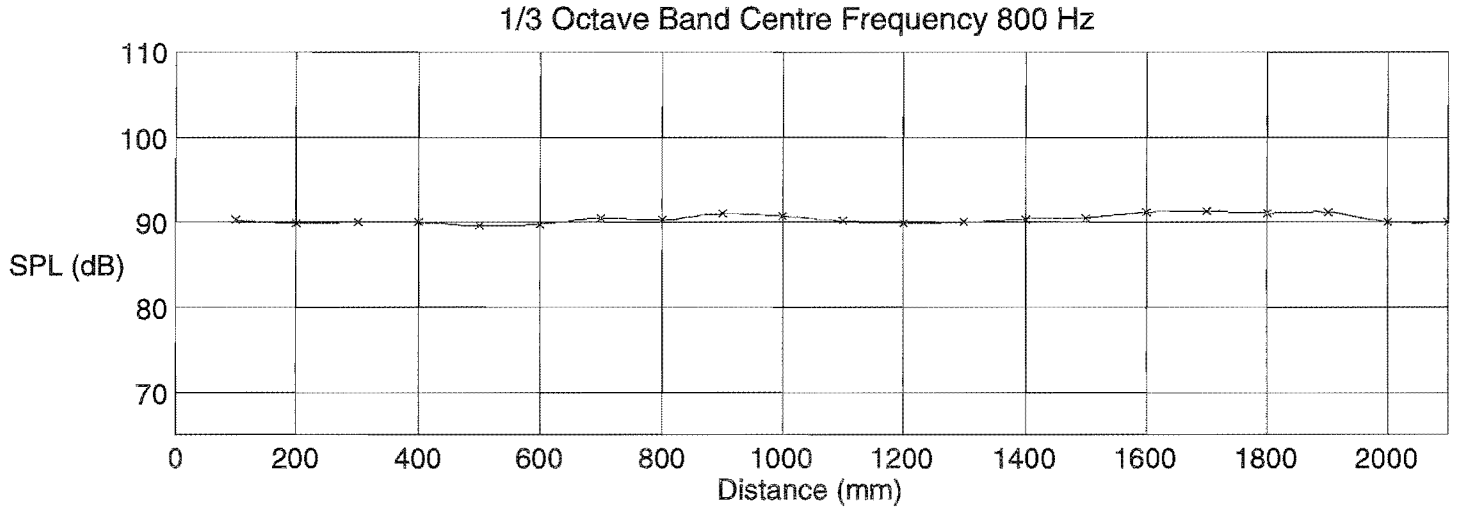
1/3 Octave Band Centre Frequency 800 Hz
110
100
90
80
70
SPL (dB)
0
200
400
600
800
1000
1200
1400
1600
1800
2000
Distance (mm)

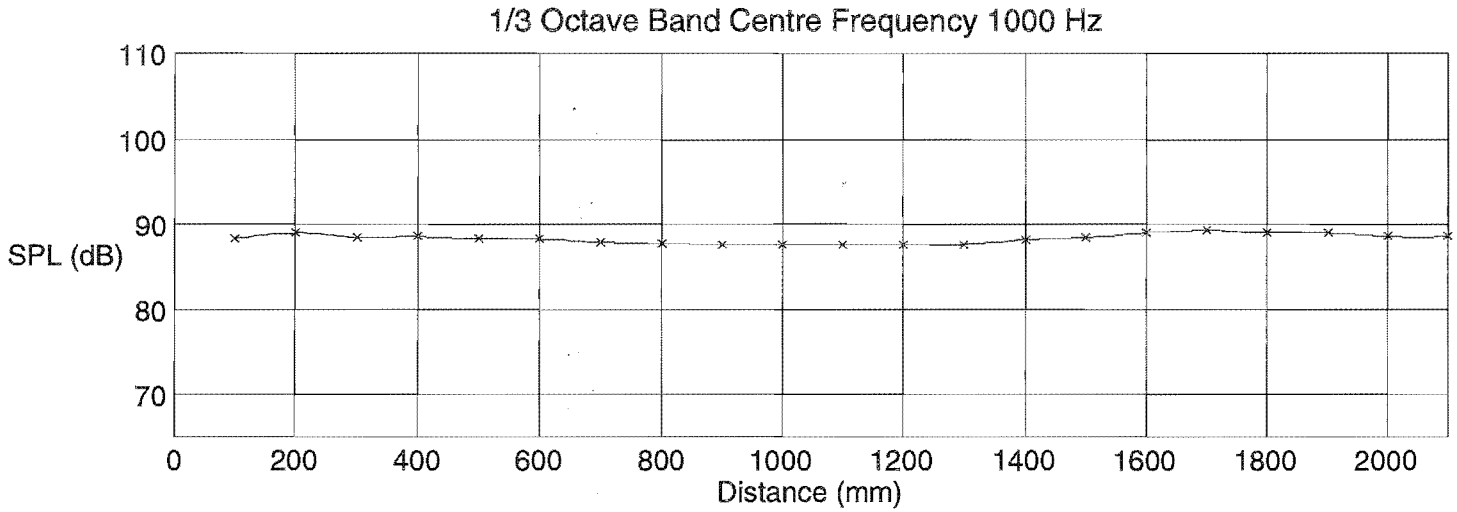
1/3 Octave Band Centre Frequency 1000 Hz
110
100
90
80
70
SPL (dB)
0
200
400
600
800
1000
1200
1400
1600
1800
2000
Distance (mm)

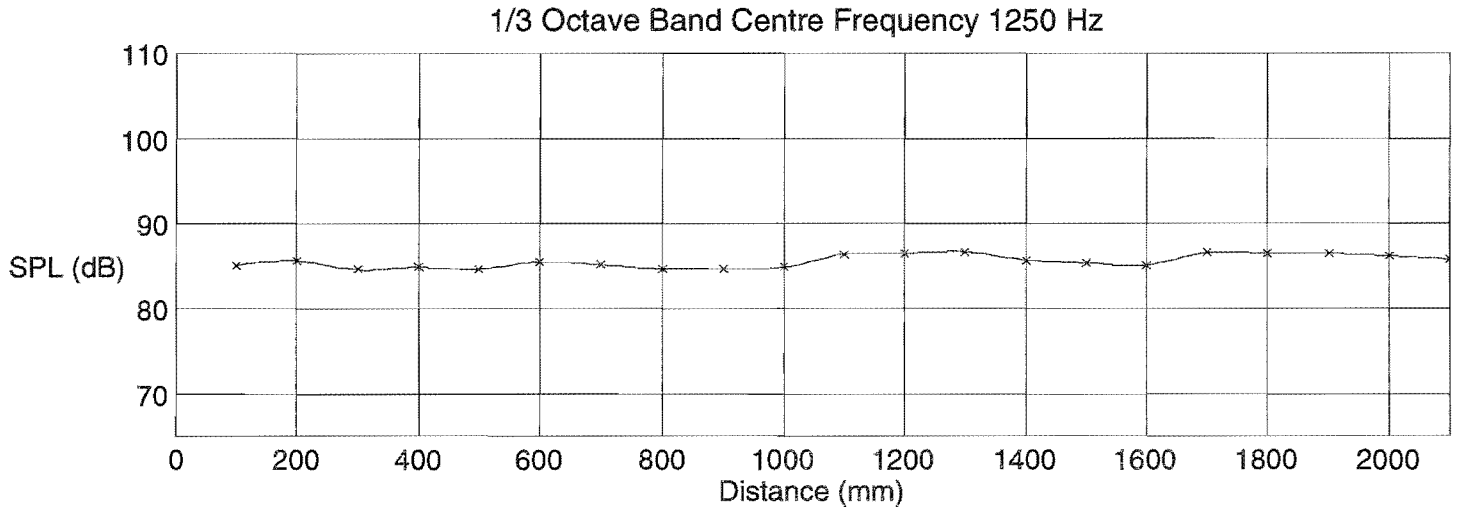
1/3 Octave Band Centre Frequency 1250 Hz
110
100
90
80
70
SPL (dB)
0
200
400
600
800
1000
1200
1400
1600
1800
2000
Distance (mm)

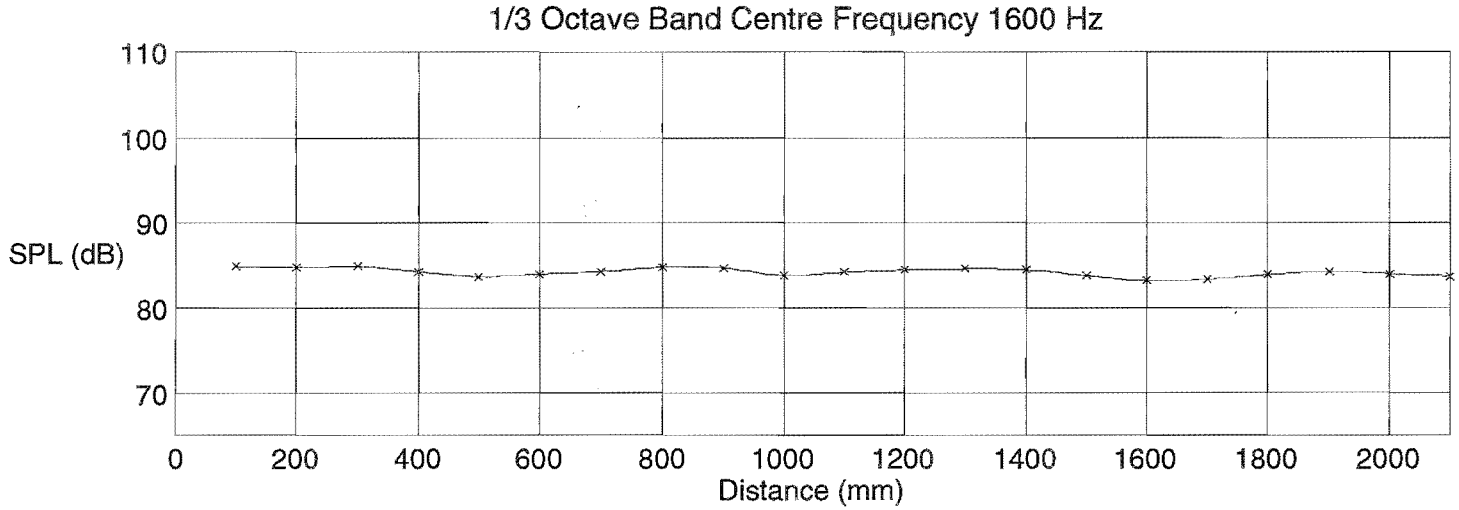
1/3 Octave Band Centre Frequency 1600 Hz
110
100
90
80
70
SPL (dB)
0
200
400
600
800
1000
1200
1400
1600
1800
2000
Distance (mm)

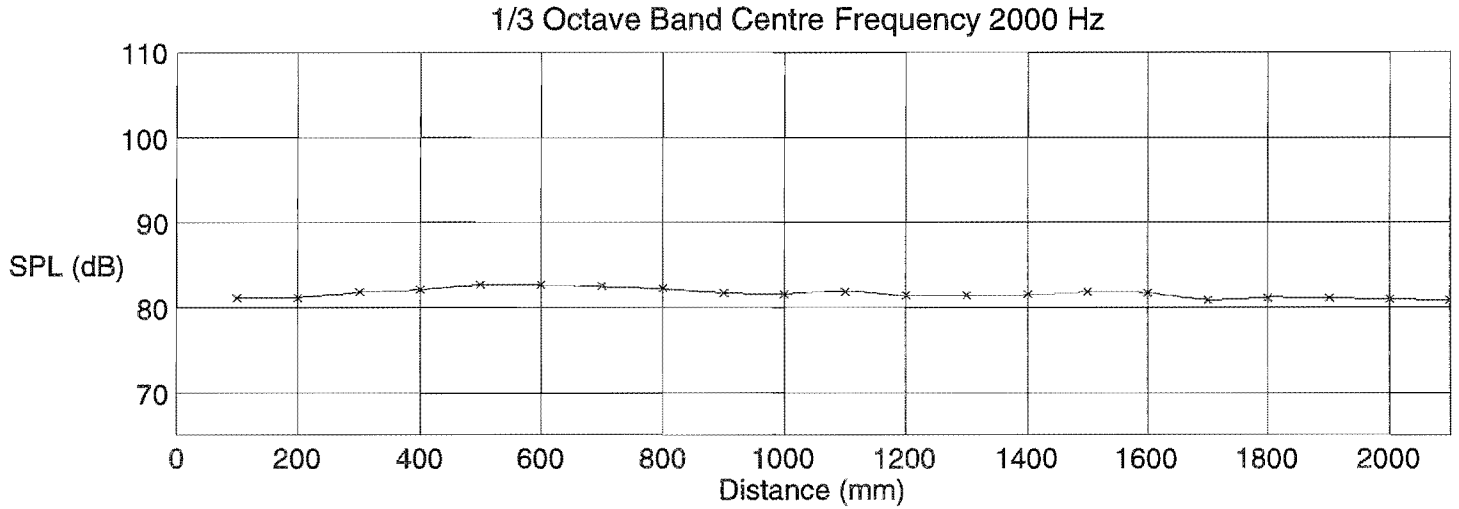
1/3 Octave Band Centre Frequency 2000 Hz
110
100
90
80
70
SPL (dB)
0
200
400
600
800
1000
1200
1400
1600
1800
2000
Distance (mm)

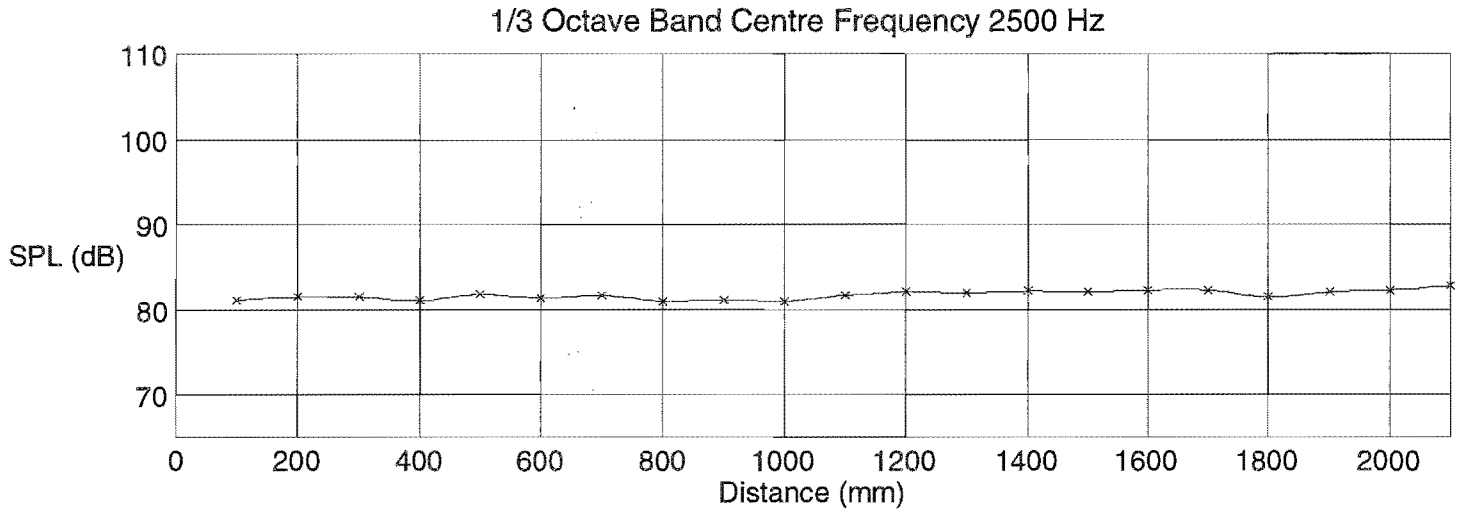
1/3 Octave Band Centre Frequency 2500 Hz
110
100
90
80
70
SPL (dB)
0
200
400
600
800
1000
1200
1400
1600
1800
2000
Distance (mm)

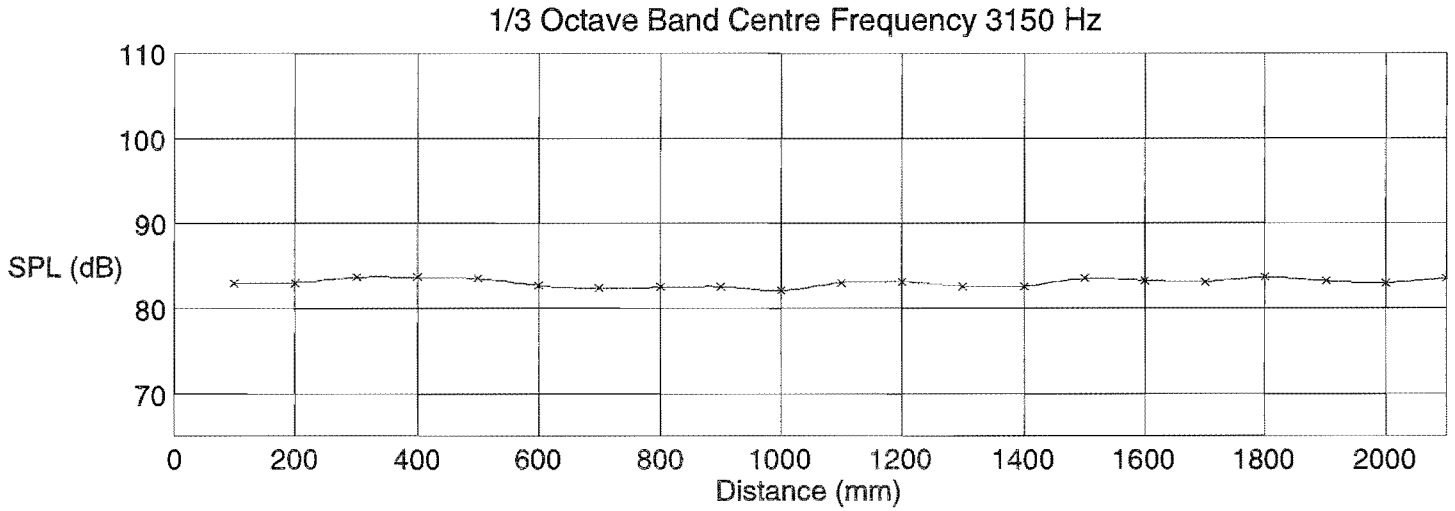
1/3 Octave Band Centre Frequency 3150 Hz
SPL (dB)
110
100
90
80
70
0
200
400
600
800
1000
1200
1400
1600
1800
2000
Distance (mm)

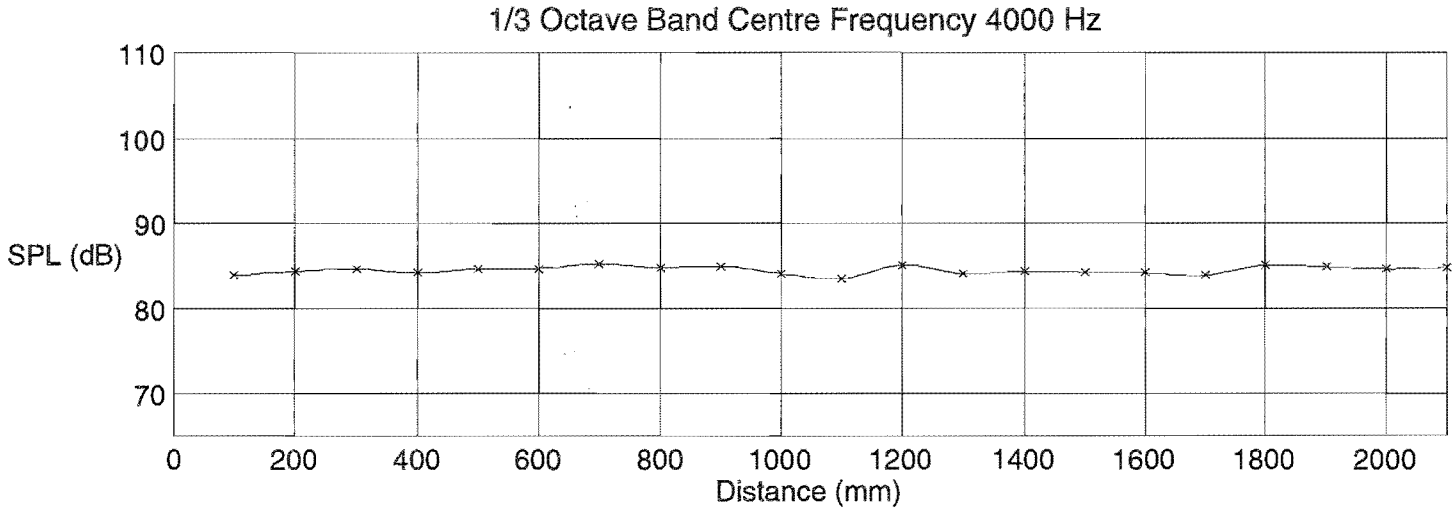
1/3 Octave Band Centre Frequency 4000 Hz
SPL (dB)
110
100
90
80
70
0
200
400
600
800
1000
1200
1400
1600
1800
2000
Distance (mm)

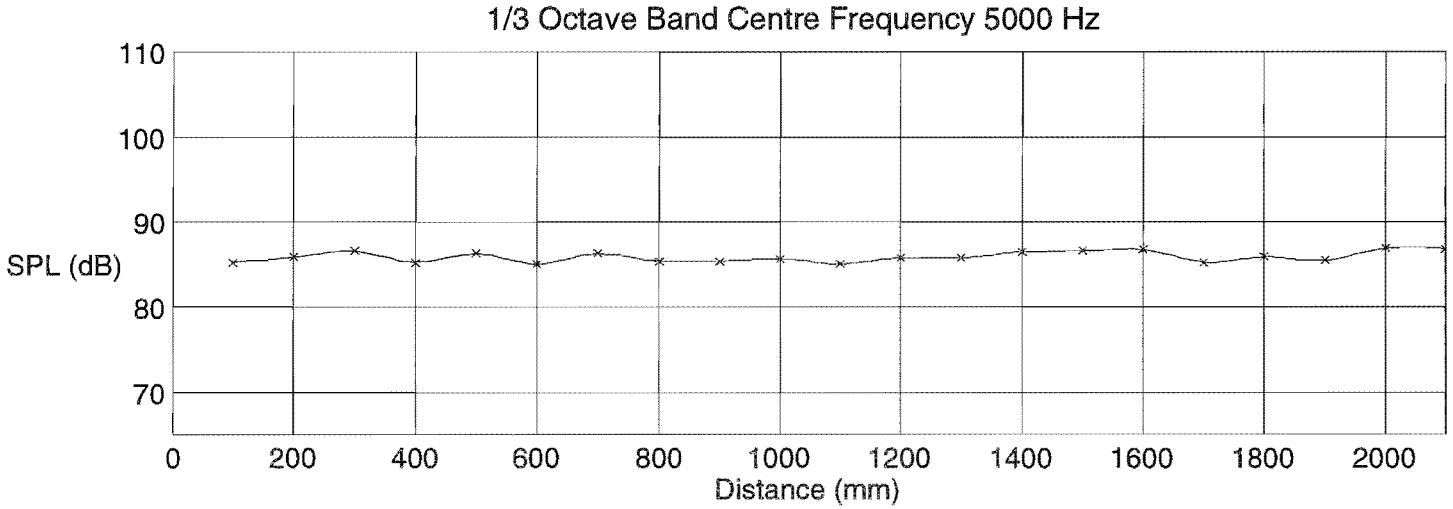
1/3 Octave Band Centre Frequency 5000 Hz
110
100
90
80
70
SPL (dB)
0
200
400
600
800
1000
1200
1400
1600
1800
2000
Distance (mm)

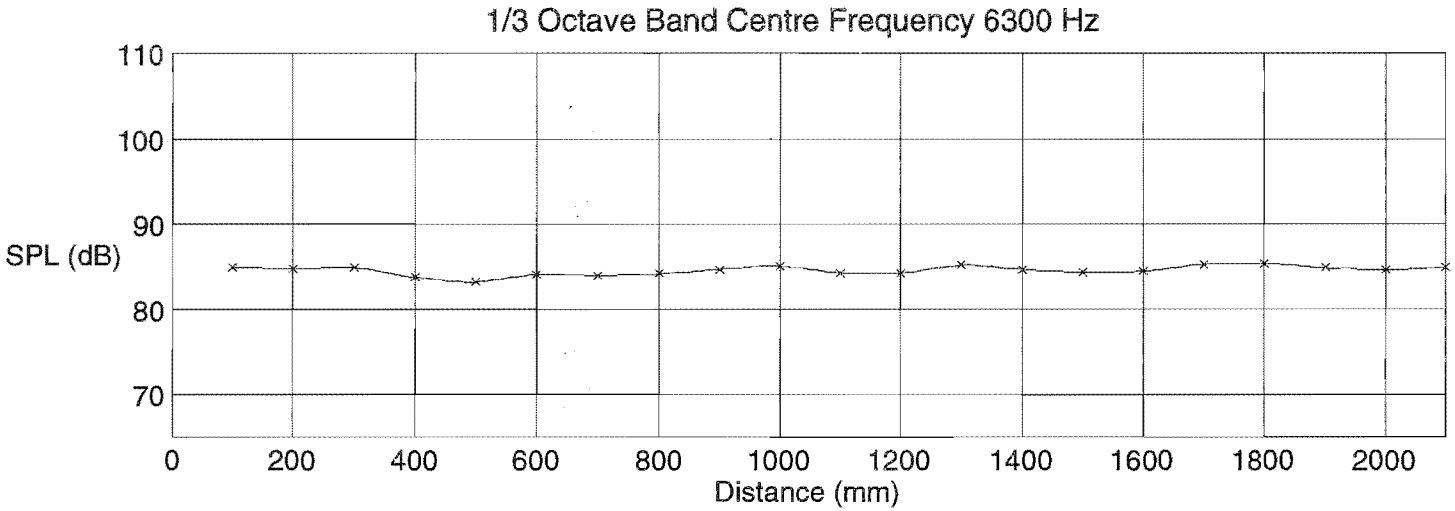
1/3 Octave Band Centre Frequency 6300 Hz
110
100
90
80
70
SPL (dB)
0
200
400
600
800
1000
1200
1400
1600
1800
2000
Distance (mm)

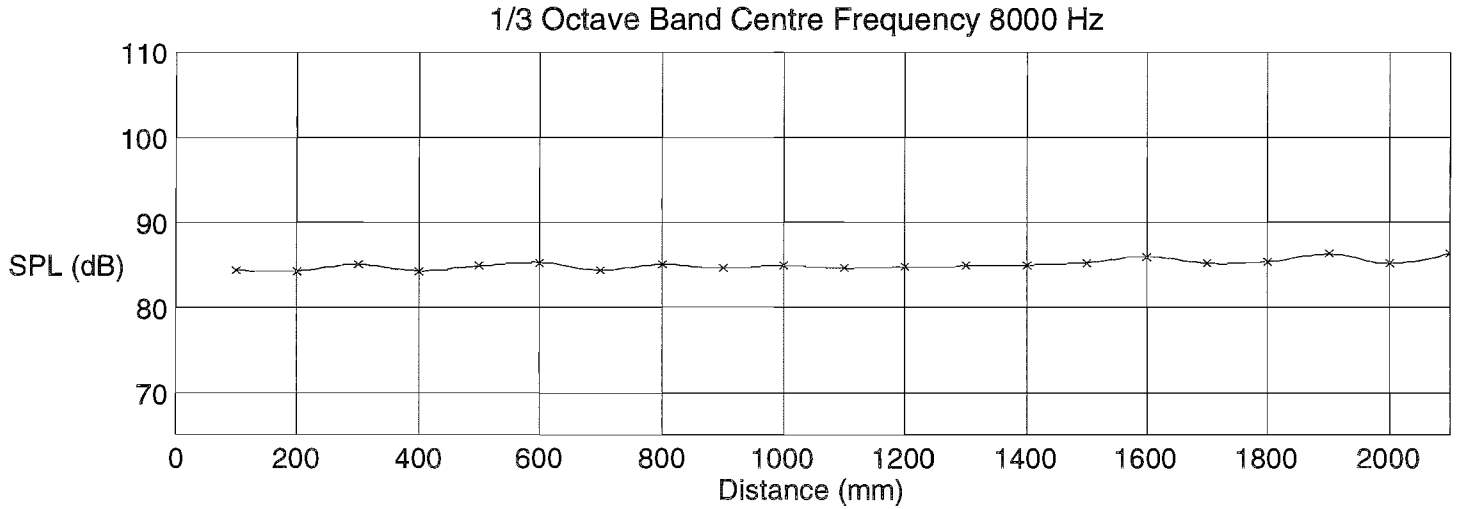
1/3 Octave Band Centre Frequency 8000 Hz
110
100
90
80
70
SPL (dB)
0
200
400
600
800
1000
1200
1400
1600
1800
2000
Distance (mm)

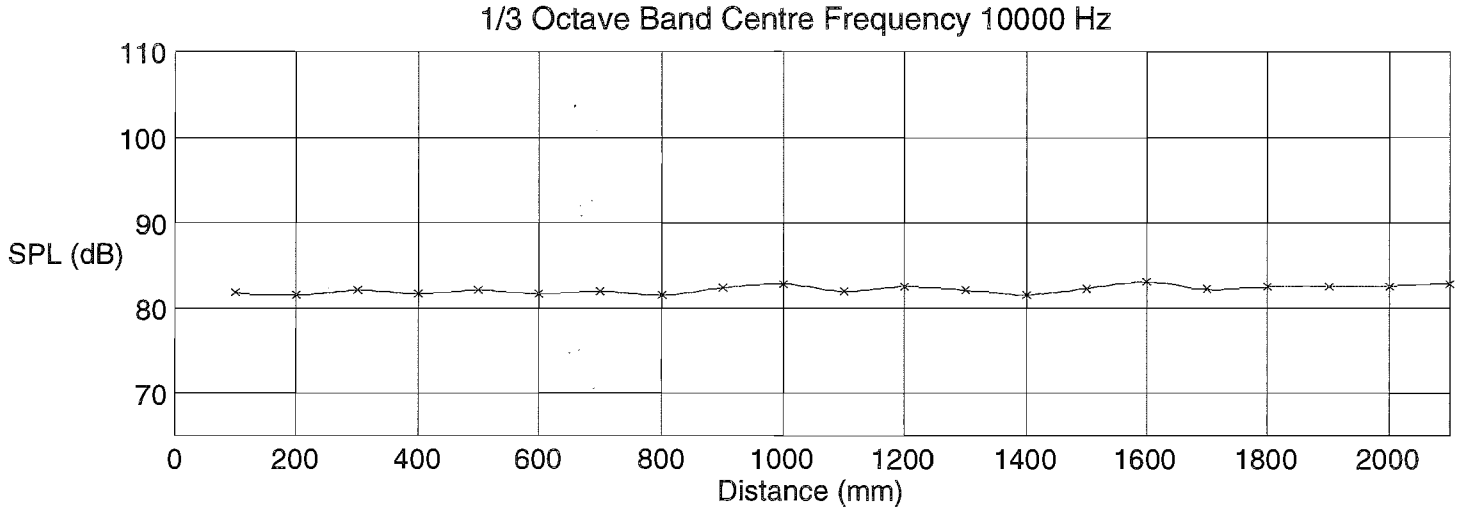
1/3 Octave Band Centre Frequency 10000 Hz
110
100
90
80
70
SPL (dB)
0
200
400
600
800
1000
1200
1400
1600
1800
2000
Distance (mm)

SPL Over the Test Duct Cross Section

The Sound Pressure Level (SPL) was measured at 5 points (arrangement shown in Figure 1) in a transverse section of the test section inlet duct 50 mm inside the duct. The duct was completely closed during the measurements. The results are tabulated below in dB.

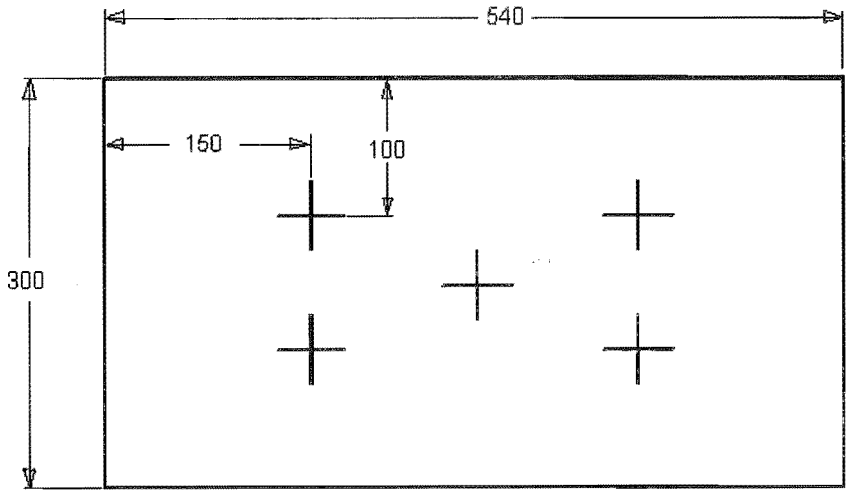

Figure 1: Measurement Positions

50 Hz

80		80.1
	79.8	
80.2		79.9

63 Hz

86.1		87
	85.6	
87.9		87.2

80 Hz

92		91.7
	92.5	
91.7		91.7

100 Hz

102.8		102.3
	102.8	
102.5		102.5

125 Hz

109.2		109.1
	109.3	
109.3		109.2

160 Hz

107		106.8
	107.2	
107.1		106.9

200 Hz

102.1		101.8
	101.9	
102		101.8

250 Hz

102.9		102.5
	102.4	
102.8		102.7

315 Hz

97.4		98.2
	97.9	
97.7		98.1

400 Hz

96.9		95.8
	95.6	
96.7		95.4

500 Hz

93.4		93.7
	93.9	
93.5		93.9

630 Hz

103.1		102.3
	104	
102.3		102.8

800 Hz

98.4		98.9
	100.3	
98.7		99.8

1000 Hz

100.1		101.1
	100.4	
99.9		101

1250 Hz

97.4		97.6
	98.9	
99		98.9

1600 Hz

95.9		95.8
	97.4	
96.3		96.9

2000 Hz

96.2		95.2
	96	
95.8		95.4

2500 Hz

93.6		93.5
	94.4	
93.9		93.8

3150 Hz

91.9		90.9
	90.4	
91.9		91.3

4000 Hz

86.6		86
	86.4	
85.4		86.8

5000 Hz

84.7		85.4
	84.5	
85.4		85.5

6300 Hz

79.3		81.2
	79.9	
81.5		80.2

Flow Induced Noise of Microphone Holders

1/3 Octave Band Centre Frequency (Hz)	Sound Pressure Level (dB)					Maximum Deviation From Mean (dB)
	0 m/s	4 m/s	8 m/s	15 m/s	21 m/s	
100	100.2	99.8	99.9	101.1	101.5	0.85
125	104	103.7	103.6	103.7	104.5	0.45
160	101.5	101.5	101.1	100.5	101.8	0.65
200	95	94.9	94.6	93.8	94.7	0.60
250	96.7	96.5	96.4	96.1	95.7	0.50
315	92.1	91.9	91.6	91	90.9	0.60
400	88.9	88.9	89.1	88.9	89.1	0.10
500	86.6	86.5	86.5	86.3	86.5	0.15
630	86.65	86.4	86.35	86.05	85.2	0.73
800	87.3	87.1	87	86.6	86.3	0.50
1k	88.2	87.9	87.6	86.7	86.9	0.75
1.25k	86.9	86.8	85.7	86.2	85.7	0.60
1.6k	86.2	86.3	86.1	86.1	86.1	0.10
2k	83	81.8	82.4	82.9	81.9	0.60
2.5k	81.6	82.2	81.2	81	81.1	0.60
3.15k	80.7	80.7	79.7	78.5	78.4	1.15
4k	75.5	75.8	75.6	75.7	74.5	0.65
5k	75.1	75	74.8	74	72.3	1.40

Calibration Data for Static Pressure Pitot Tubes

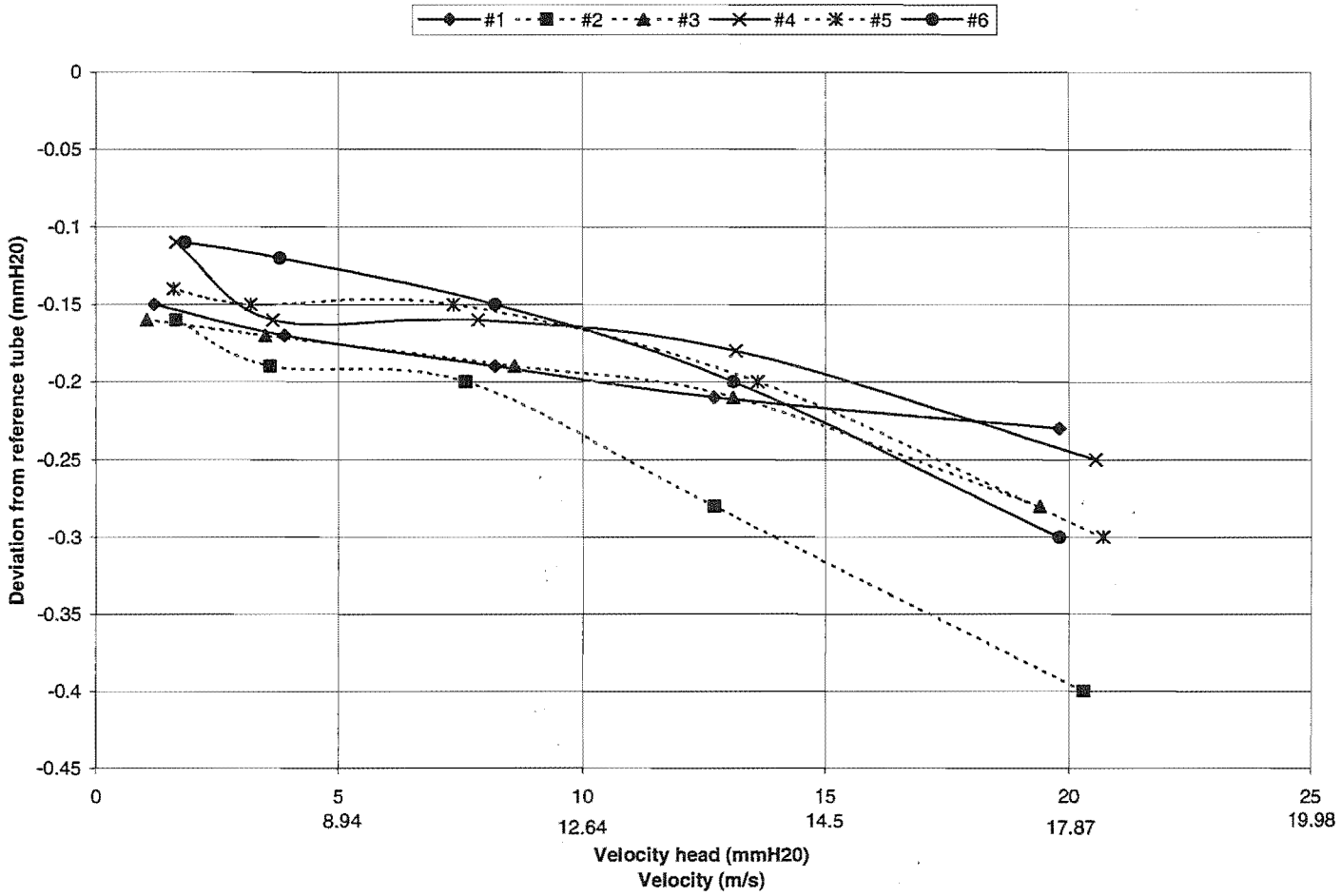

Velocity Profile of Airflow within the Test Duct

Line plots showing velocity data measured at both measurement positions with the airflow instrumentation (described in 2.3.4 'Airflow Instrumentation') are presented in this appendix. The arrangement of the Pitot arrays is shown in Figure 1, and the measurement positions in Figure 2.

Each plot shows velocity measurements along a single rake of five Pitot tubes from left to right relative to the direction of airflow. Rake 1 is the top rake in the array, and rake 4 is the bottom. The points and line at higher velocity are data from the upstream Pitot array.

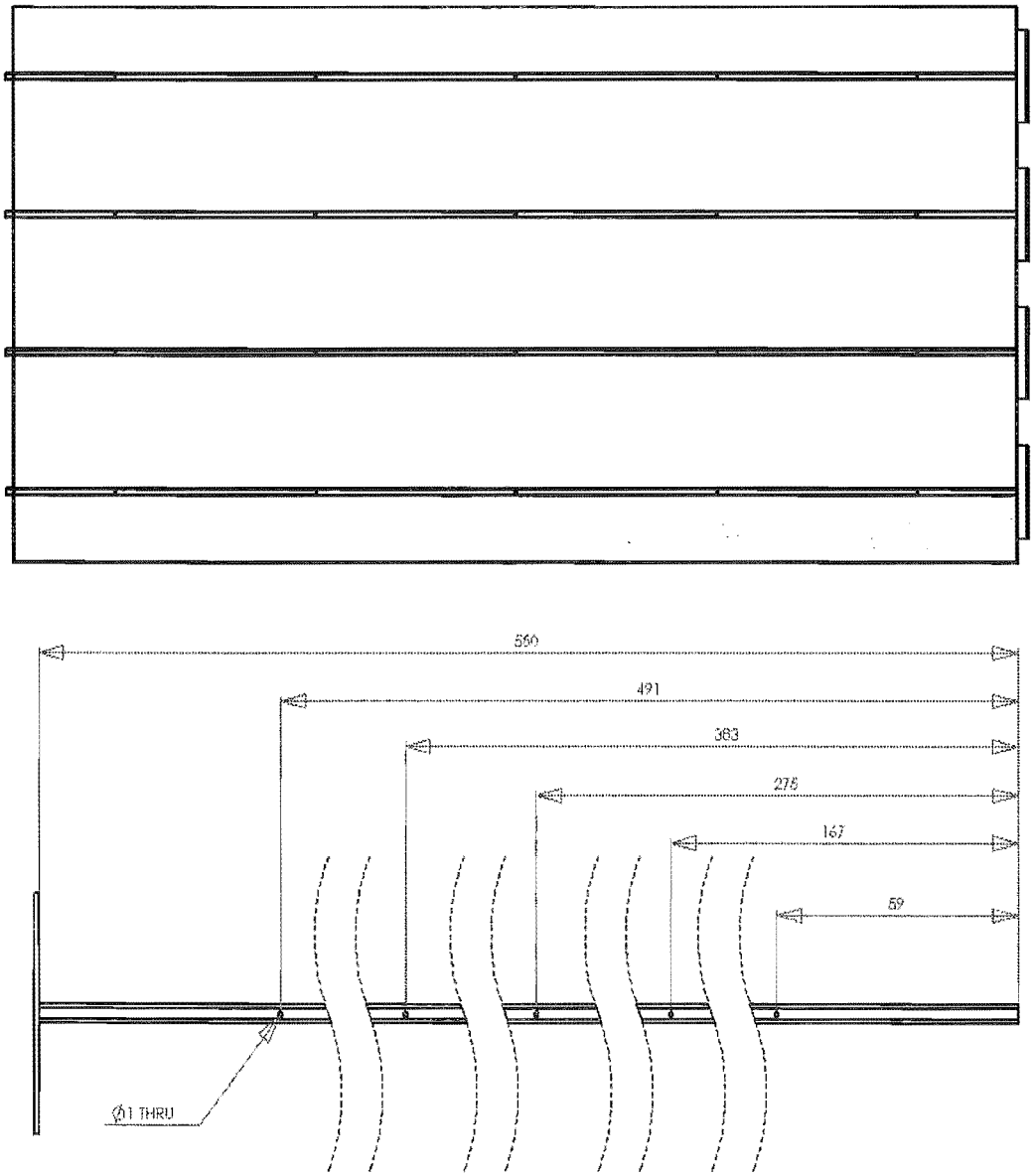

Figure 1: Arrangement of Pitot array.

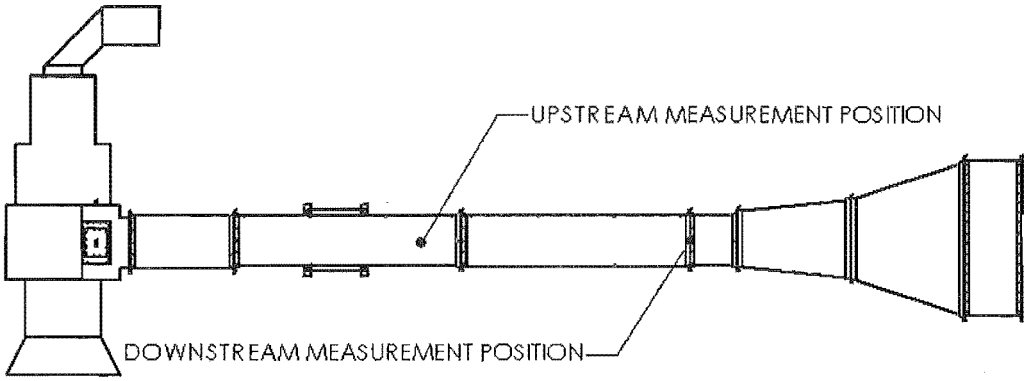

Figure 2: Measurement Positions.

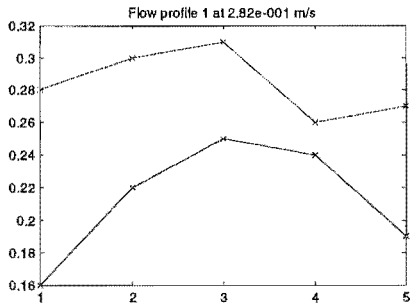
Flow profile 1 at 2.82e-001 m/s
0.32
0.3
0.28
0.26
0.24
0.22
0.2
0.18
0.16
1
2
3
4
5

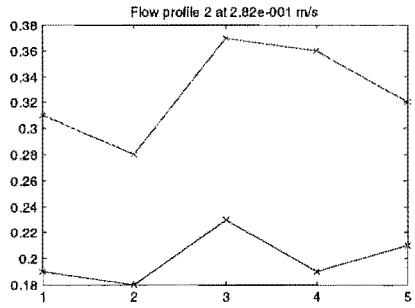
Flow profile 2 at 2.82e-001 m/s
0.38
0.36
0.34
0.32
0.3
0.28
0.26
0.24
0.22
0.2
0.18
1
2
3
4
5

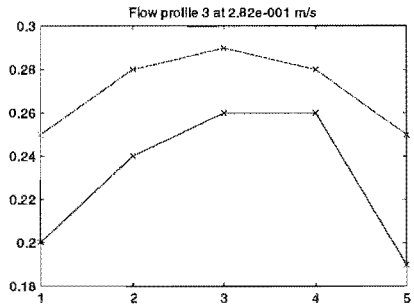
Flow profile 3 at 2.82e-001 m/s
0.3
0.28
0.26
0.24
0.22
0.2
0.18
1
2
3
4
5

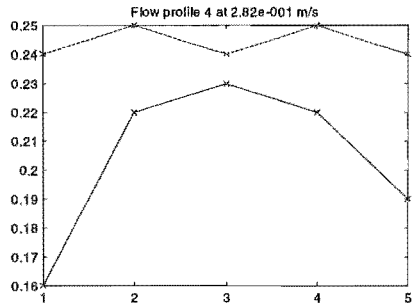
Flow profile 4 at 2.82e-001 m/s
0.25
0.24
0.23
0.22
0.21
0.2
0.19
0.18
0.17
0.16
1
2
3
4
5

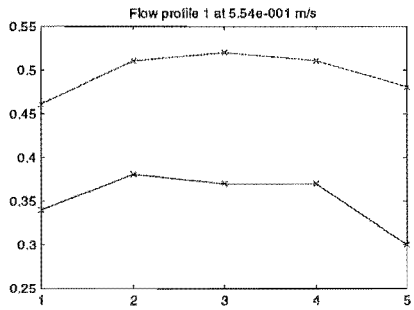
Flow profile 1 at 5.54e-001 m/s
0.55
0.5
0.45
0.4
0.35
0.3
0.25
1
2
3
4
5

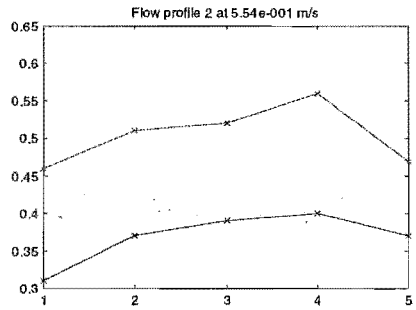
Flow profile 2 at 5.54e-001 m/s
0.65
0.6
0.55
0.5
0.45
0.4
0.35
0.3
1
2
3
4
5

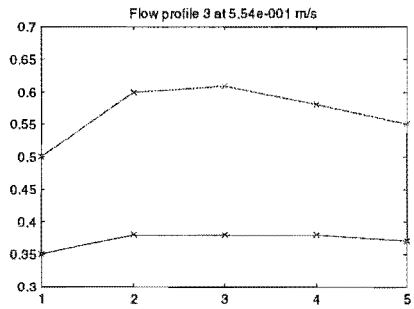
Flow profile 3 at 5.54e-001 m/s
0.7
0.65
0.6
0.55
0.5
0.45
0.4
0.35
0.3
1
2
3
4
5

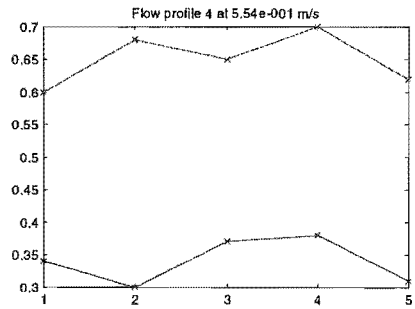
Flow profile 4 at 5.54e-001 m/s
0.7
0.65
0.6
0.55
0.5
0.45
0.4
0.35
0.3
1
2
3
4
5

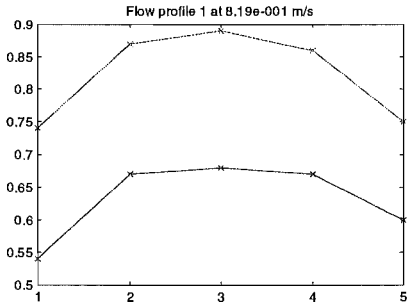
Flow profile 1 at 8.19e-001 m/s
0.9
0.85
0.8
0.75
0.7
0.65
0.6
0.55
0.5
1
2
3
4
5

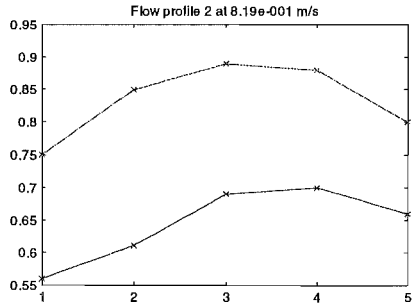
Flow profile 2 at 8.19e-001 m/s
0.95
0.9
0.85
0.8
0.75
0.7
0.65
0.6
0.55
1
2
3
4
5

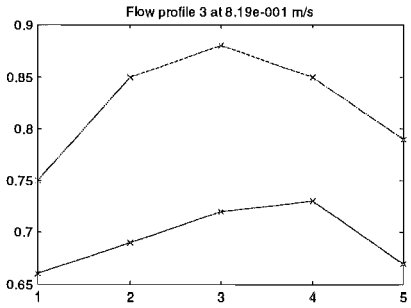
Flow profile 3 at 8.19e-001 m/s
0.9
0.85
0.8
0.75
0.7
0.65
1
2
3
4
5

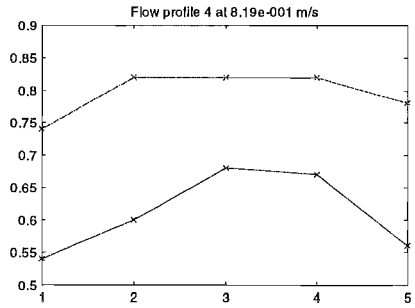
Flow profile 4 at 8.19e-001 m/s
0.9
0.85
0.8
0.75
0.7
0.65
0.6
0.55
0.5
1
2
3
4
5

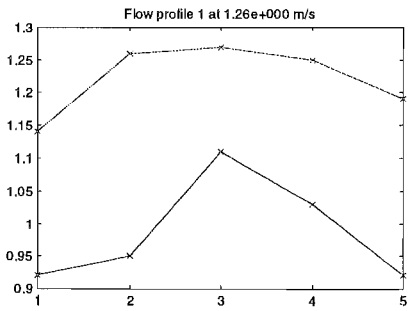
Flow profile 1 at 1.26e+000 m/s
1.3
1.25
1.2
1.15
1.1
1.05
1
0.95
0.9
1
2
3
4
5

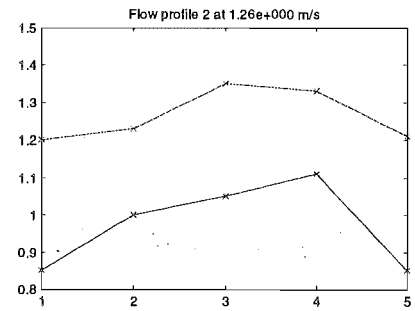
Flow profile 2 at 1.26e+000 m/s
1.5
1.4
1.3
1.2
1.1
1
0.9
0.8
1
2
3
4
5

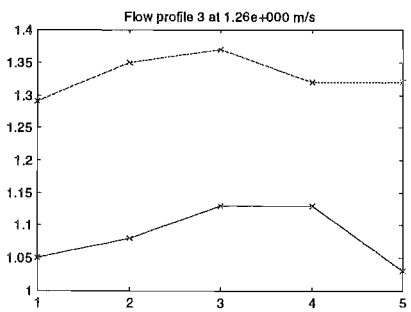
Flow profile 3 at 1.26e+000 m/s
1.4
1.35
1.3
1.25
1.2
1.15
1.1
1.05
1
1
2
3
4
5

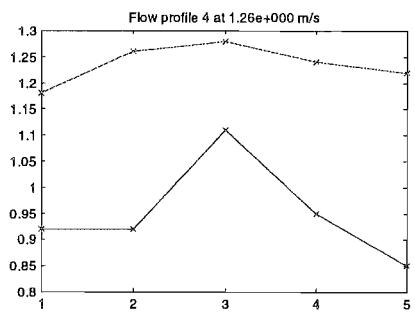
Flow profile 4 at 1.26e+000 m/s
1.3
1.25
1.2
1.15
1.1
1.05
1
0.95
0.9
0.85
0.8
1
2
3
4
5

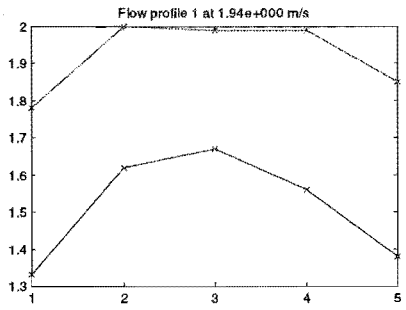
Flow profile 1 at 1.94e+000 m/s
2
1.9
1.8
1.7
1.6
1.5
1.4
1.3
1
2
3
4
5

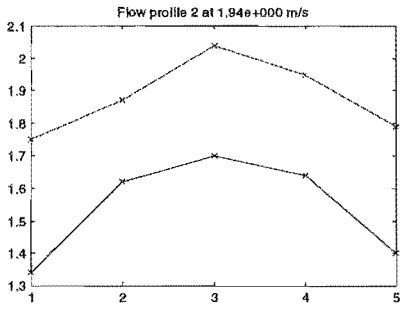
Flow profile 2 at 1.94e+000 m/s
2.1
2
1.9
1.8
1.7
1.6
1.5
1.4
1.3
1
2
3
4
5

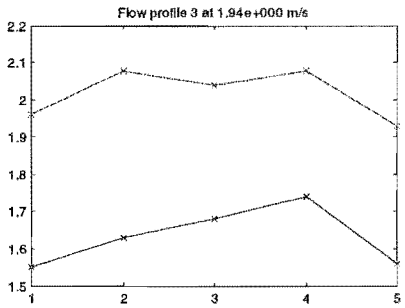
Flow profile 3 at 1.94e+000 m/s
2.2
2.1
2
1.9
1.8
1.7
1.6
1.5
1
2
3
4
5

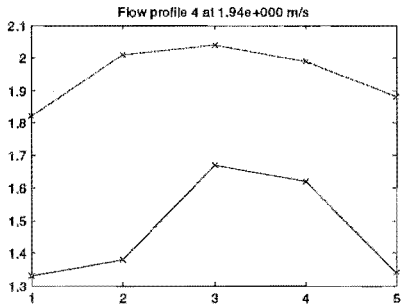
Flow profile 4 at 1.94e+000 m/s
2.1
2
1.9
1.8
1.7
1.6
1.5
1.4
1.3
1
2
3
4
5

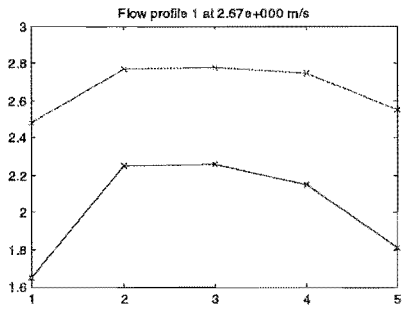
Flow profile 1 at 2.67e+000 m/s
3
2.8
2.6
2.4
2.2
2
1.8
1.6
1
2
3
4
5

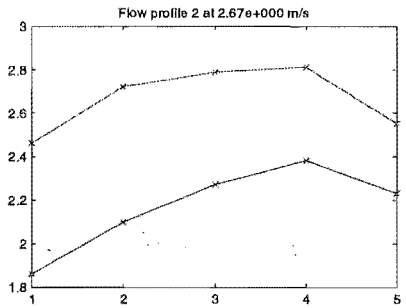
Flow profile 2 at 2.67e+000 m/s
3
2.8
2.6
2.4
2.2
2
1.8
1
2
3
4
5

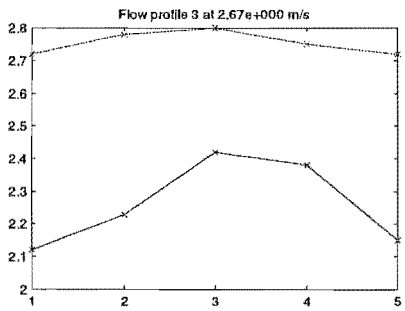
Flow profile 3 at 2.67e+000 m/s
2.8
2.7
2.6
2.5
2.4
2.3
2.2
2.1
2
1
2
3
4
5

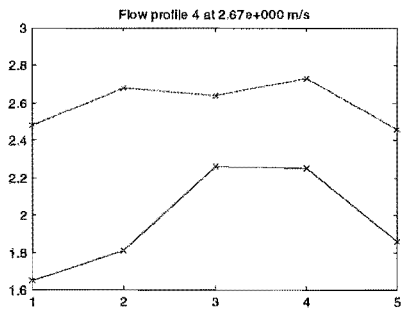
Flow profile 4 at 2.67e+000 m/s
3
2.8
2.6
2.4
2.2
2
1.8
1.6
1
2
3
4
5

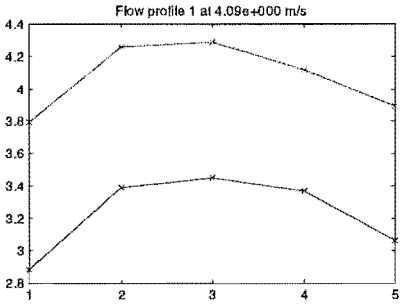
Flow profile 1 at 4.09e+000 m/s

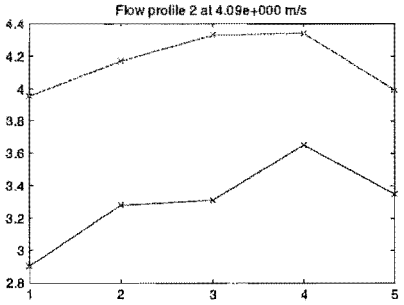
Flow profile 2 at 4.09e+000 m/s

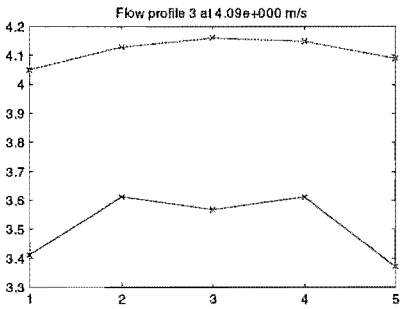
Flow profile 3 at 4.09e+000 m/s

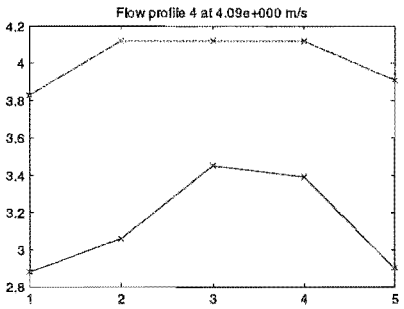
Flow profile 4 at 4.09e+000 m/s

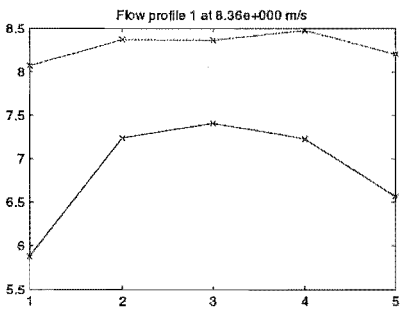
Flow profile 1 at 8.36e+000 m/s

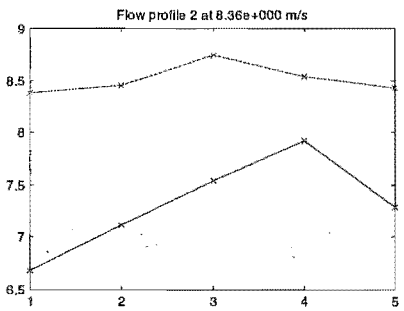
Flow profile 2 at 8.36e+000 m/s

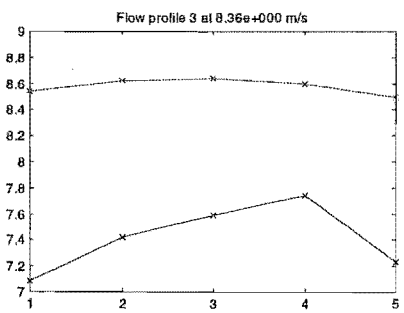
Flow profile 3 at 8.36e+000 m/s

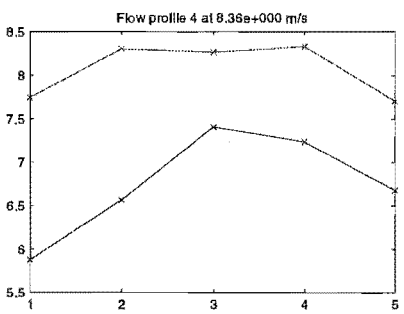
Flow profile 4 at 8.36e+000 m/s

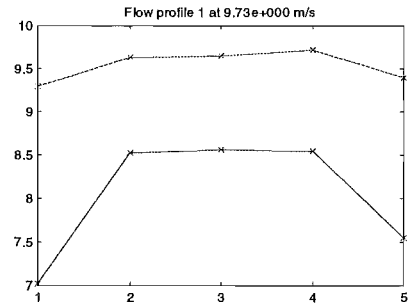
Flow profile 1 at 9.73e+000 m/s
10
9.5
9
8.5
8
7.5
7
1
2
3
4
5

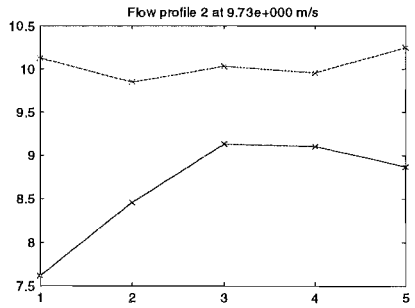
Flow profile 2 at 9.73e+000 m/s
10.5
10
9.5
9
8.5
8
7.5
1
2
3
4
5

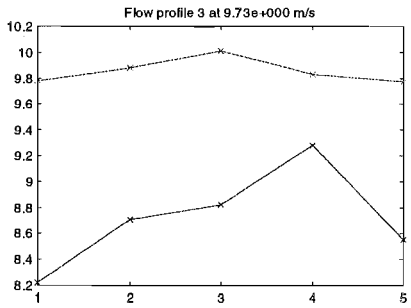
Flow profile 3 at 9.73e+000 m/s
10.2
10
9.8
9.6
9.4
9.2
9
8.8
8.6
8.4
8.2
1
2
3
4
5

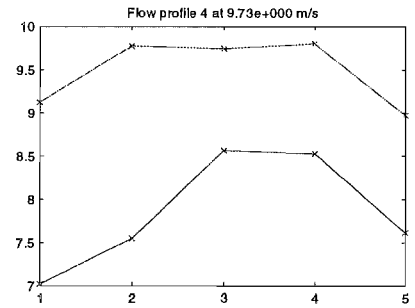
Flow profile 4 at 9.73e+000 m/s
10
9.5
9
8.5
8
7.5
7
1
2
3
4
5

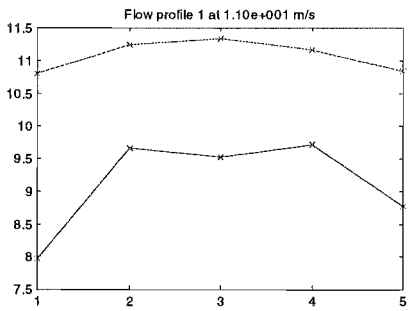
Flow profile 1 at 1.10e+001 m/s
11.5
11
10.5
10
9.5
9
8.5
8
7.5
1
2
3
4
5

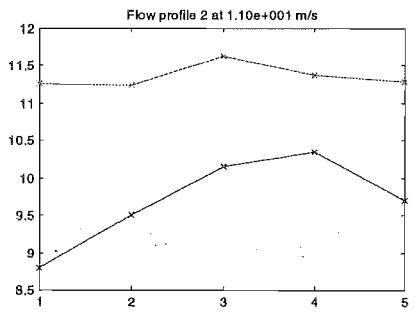
Flow profile 2 at 1.10e+001 m/s
12
11.5
11
10.5
10
9.5
9
8.5
1
2
3
4
5

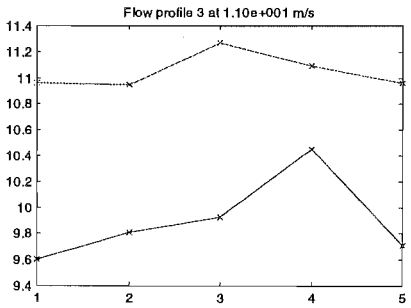
Flow profile 3 at 1.10e+001 m/s
11.4
11.2
11
10.8
10.6
10.4
10.2
10
9.8
9.6
9.4
1
2
3
4
5

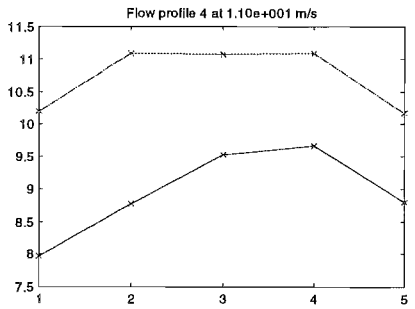
Flow profile 4 at 1.10e+001 m/s
11.5
11
10.5
10
9.5
9
8.5
8
7.5
1
2
3
4
5

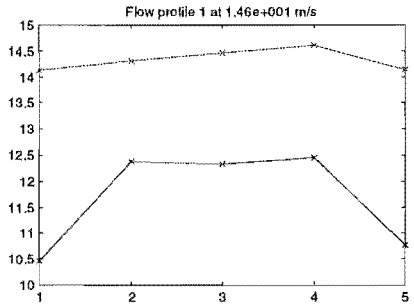
Flow profile 1 at 1.46e+001 m/s
15
14.5
14
13.5
13
12.5
12
11.5
11
10.5
10
1
2
3
4
5

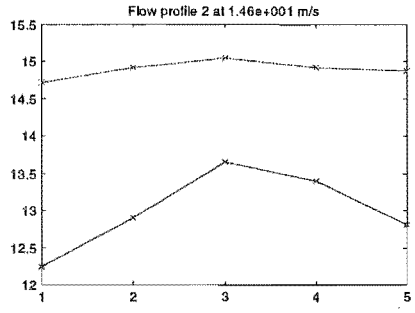
Flow profile 2 at 1.46e+001 m/s
15.5
15
14.5
14
13.5
13
12.5
12
1
2
3
4
5

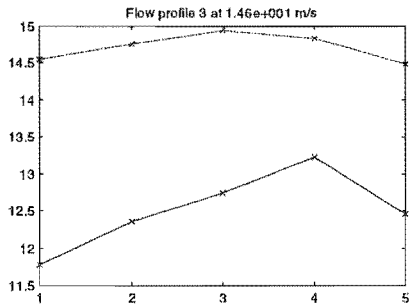
Flow profile 3 at 1.46e+001 m/s
15
14.5
14
13.5
13
12.5
12
11.5
1
2
3
4
5

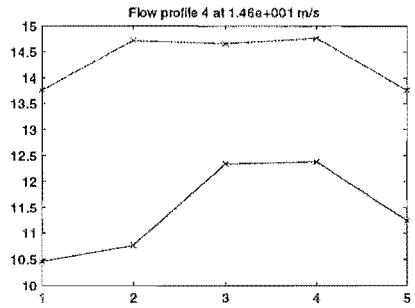
Flow profile 4 at 1.46e+001 m/s
15
14.5
14
13.5
13
12.5
12
11.5
11
10.5
10
1
2
3
4
5

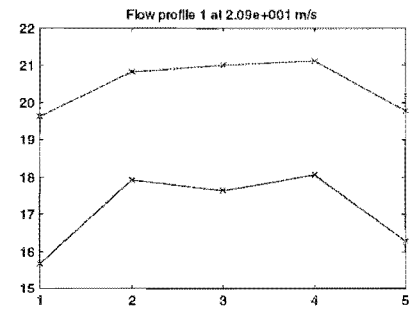
Flow profile 1 at 2.09e+001 m/s
22
21
20
19
18
17
16
15
1
2
3
4
5

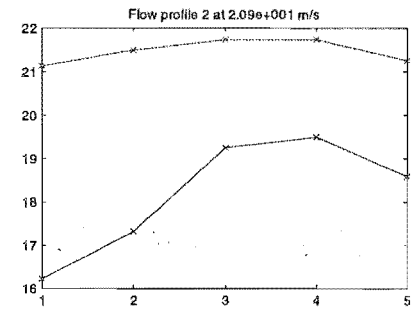
Flow profile 2 at 2.09e+001 m/s
22
21
20
19
18
17
16
1
2
3
4
5

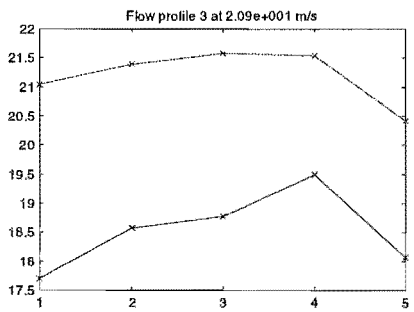
Flow profile 3 at 2.09e+001 m/s
22
21.5
21
20.5
20
19.5
19
18.5
18
17.5
1
2
3
4
5

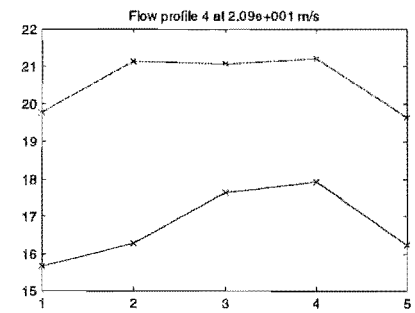
Flow profile 4 at 2.09e+001 m/s
22
21
20
19
18
17
16
15
1
2
3
4
5

Wall Absorbers

Material	Thickness	Facing	Fixing Method
Melamine Resin Foam	25 mm	None	Pinned

Frequency (Hz)	Velocity (m/s)				
	0	**4**	**8**	**15**	**21**
100	1.9	2.1	2.0	1.7	1.4
125	1.4	1.5	1.5	1.4	1.5
160	1.3	1.3	1.3	1.3	1.1
200	1.3	1.4	1.3	1.2	1.1
250	2.7	2.7	2.6	2.5	2.4
315	3.5	3.5	3.5	3.2	2.9
400	5.2	5.2	5.0	4.7	4.0
500	7.4	7.2	7.1	6.8	5.8
630	10.3	10.4	10.5	10.2	8.6
800	9.5	9.4	9.3	9.0	8.7
1k	7.8	8.1	8.2	8.1	7.8
1.25k	7.5	7.5	7.8	7.5	7.3
1.6k	6.3	6.2	6.0	6.2	6.2
2k	4.8	5.5	5.3	5.3	4.8
2.5k	4.7	4.3	4.8	4.9	4.8
3.15k	4.3	3.7	4.1	4.2	4.2
4k	3.9	4.0	4.2	4.1	4.1
5k	3.3	3.3	3.4	3.5	3.4
	Insertion Loss (dB/m)				

Material	Thickness	Facing	Fixing Method
Melamine Resin Foam	25 mm	70 g/m^2 Metallic Foil	Pinned

Frequency (Hz)	Velocity (m/s)				
	0	**4**	**8**	**15**	**21**
100	3.0	3.1	3.1	2.9	2.9
125	3.0	3.1	3.2	3.1	3.3
160	2.6	2.7	2.7	2.7	2.6
200	2.9	2.9	2.9	2.7	2.7
250	4.0	3.9	4.0	3.9	3.7
315	4.9	4.8	4.7	4.5	4.3
400	6.0	6.0	5.9	5.6	5.3
500	10.4	10.3	10.1	9.8	8.0
630	16.8	16.7	16.7	15.7	11.4
800	8.6	8.5	8.5	8.3	8.0
1k	6.9	6.7	6.7	6.6	6.5
1.25k	6.0	5.9	6.3	6.2	6.1
1.6k	4.8	4.6	4.8	5.0	5.2
2k	4.9	5.4	5.3	5.2	4.8
2.5k	4.8	5.2	5.7	5.8	5.4
3.15k	4.6	5.5	5.8	5.9	6.5
4k	5.7	6.0	6.0	5.7	5.8
5k	5.0	4.9	4.8	4.8	4.8
	Insertion Loss (dB/m)				

Wall Absorbers

Material	Thickness	Facing	Fixing Method
Melamine Resin Foam	50 mm	70 g/m^2 Metallic Foil	Pinned

Frequency (Hz)	Velocity (m/s)				
	0	**4**	**8**	**15**	**21**
100	0.4	0.6	0.2	0.8	0.8
125	2.4	2.4	2.5	2.3	2.3
160	5.6	5.6	5.7	5.9	6.1
200	4.0	4.0	4.1	3.6	2.5
250	15.2	15.2	14.9	12.9	8.9
315	12.5	12.5	12.2	11.9	9.7
400	10.7	10.8	10.7	10.4	8.7
500	5.8	5.8	5.7	5.8	5.8
630	6.6	6.6	6.9	6.8	6.7
800	4.3	4.3	4.3	4.1	4.6
1k	4.9	4.7	4.4	4.3	4.4
1.25k	4.0	3.9	4.2	3.9	3.9
1.6k	6.2	6.0	6.0	5.9	6.2
2k	2.8	3.0	2.9	2.9	2.9
2.5k	2.6	2.4	2.7	3.0	2.7
3.15k	4.8	4.9	5.1	5.1	5.1
4k	3.9	3.9	3.9	3.7	3.5
5k	2.8	2.9	3.0	3.3	3.1
	Insertion Loss (dB/m)				

Material	Thickness	Facing	Fixing Method
Melamine Resin Foam	75 mm	70 g/m^2 Metallic Foil	Pinned

Frequency (Hz)	Velocity (m/s)				
	0	**4**	**8**	**15**	**21**
100	1.4	1.6	1.7	1.5	1.4
125	2.4	2.5	2.6	2.6	2.6
160	2.8	2.9	3.0	3.1	3.1
200	4.5	4.7	4.7	4.7	4.6
250	9.5	9.6	9.6	8.1	6.4
315	8.0	8.0	8.1	7.8	6.5
400	6.8	7.0	7.1	7.2	6.3
500	5.6	5.6	5.7	5.7	5.5
630	8.1	8.3	8.4	8.5	8.5
800	8.7	8.9	9.0	8.9	9.3
1k	10.0	9.9	10.0	10.1	10.2
1.25k	6.6	6.5	6.9	6.8	7.1
1.6k	6.5	6.3	6.3	6.5	6.8
2k	4.8	5.2	5.0	5.1	5.3
2.5k	3.7	3.6	3.9	4.1	4.2
3.15k	3.2	3.3	3.7	3.7	3.9
4k	4.0	4.2	4.2	4.2	4.4
5k	2.6	2.7	2.9	3.0	2.9
	Insertion Loss (dB/m)				

Wall Absorbers

Material	Thickness	Facing	Fixing Method
Melamine Resin Foam	25 mm	70 g/m^2 Metallic Foil	Bonded

Frequency (Hz)	Velocity (m/s)				
	0	4	8	15	21
100	1.8	1.4	2.3	1.4	1.8
125	1.9	1.3	1.8	1.7	1.4
160	1.3	1.6	1.3	1.8	1.3
200	1.5	1.5	1.4	1.3	1.3
250	1.9	2.3	1.4	2.1	2.0
315	2.2	1.4	2.4	1.8	2.3
400	2.5	2.2	2.5	2.4	2.9
500	2.7	2.8	2.6	2.7	2.7
630	5.4	4.8	5.5	5.4	5.0
800	3.8	3.7	3.8	3.4	3.9
1k	4.8	4.4	5.3	4.5	4.2
1.25k	8.8	8.7	9.0	7.6	6.7
1.6k	10.0	9.8	9.5	8.3	7.4
2k	5.4	5.7	5.8	5.2	5.7
2.5k	3.5	3.5	4.0	3.3	4.2
3.15k	2.1	2.5	1.8	2.4	2.4
4k	3.7	3.9	4.0	3.4	4.2
5k	3.0	2.4	3.6	2.2	2.7
	Insertion Loss (dB/m)				

Material	Thickness	Facing	Fixing Method
Melamine Resin Foam	50 mm	70 g/m^2 Metallic Foil	Bonded

Frequency (Hz)	Velocity (m/s)				
	0	4	8	15	21
100	2.4	2.4	2.3	1.9	2.0
125	1.9	1.9	1.8	1.6	1.8
160	1.7	1.8	1.7	1.6	1.5
200	1.3	1.3	1.2	1.2	1.1
250	2.5	2.5	2.5	2.4	2.3
315	3.6	3.4	3.4	3.2	2.6
400	4.6	4.3	4.2	3.8	3.3
500	4.9	4.9	4.8	4.7	3.9
630	9.6	10.2	10.1	9.3	7.1
800	7.9	7.3	7.2	6.8	6.0
1k	3.6	3.8	3.8	3.9	3.8
1.25k	4.3	3.9	4.3	4.2	4.1
1.6k	3.9	3.6	3.6	4.2	4.5
2k	4.0	4.7	4.3	4.1	3.9
2.5k	3.4	3.3	3.8	4.0	3.8
3.15k	3.0	2.5	2.8	3.1	3.2
4k	4.1	3.6	3.8	3.6	3.8
5k	2.9	3.0	3.0	3.1	3.0
	Insertion Loss (dB/m)				

Wall Absorbers

Material	Thickness	Facing	Fixing Method
Polyether Polyurethane Foam	25 mm	70 g/m^2 Metallic Foil	Pinned

Frequency (Hz)	Velocity (m/s)				
	0	**4**	**8**	**15**	**21**
100	0.7	0.8	1.0	1.0	0.8
125	0.7	0.7	0.9	1.0	1.0
160	0.8	0.8	0.8	0.9	0.9
200	1.0	1.0	1.1	1.1	1.2
250	2.3	2.2	2.0	2.0	2.0
315	2.8	2.8	2.6	2.5	2.5
400	4.0	4.0	3.8	3.7	3.4
500	5.0	5.0	4.9	4.6	4.1
630	9.7	9.6	9.7	9.6	9.3
800	5.3	5.3	5.3	5.4	5.3
1k	4.4	4.3	4.2	4.2	4.1
1.25k	3.1	3.2	3.2	3.2	3.3
1.6k	4.0	3.8	3.8	3.7	3.8
2k	3.9	4.0	4.1	3.8	3.8
2.5k	5.8	5.8	6.0	6.1	6.1
3.15k	6.5	6.5	6.8	6.8	6.5
4k	4.6	5.0	5.1	5.3	5.2
5k	2.7	3.4	3.6	3.8	3.8
	Insertion Loss (dB/m)				

Material	Thickness	Facing	Fixing Method
Polyether Polyurethane Foam	50 mm	70 g/m^2 Metallic Foil	Pinned

Frequency (Hz)	Velocity (m/s)				
	0	**4**	**8**	**15**	**21**
100	1.2	1.5	1.3	1.1	1.1
125	1.5	1.5	1.5	1.4	1.3
160	1.8	1.8	1.8	1.8	1.7
200	3.0	3.0	2.8	2.6	2.3
250	6.9	6.8	6.8	6.5	5.5
315	10.3	10.2	9.9	8.5	5.3
400	10.2	10.1	10.0	8.9	5.3
500	6.0	6.0	6.1	5.9	4.7
630	5.8	5.8	5.8	5.7	5.1
800	1.5	1.6	1.7	1.5	1.8
1k	3.0	2.6	2.5	2.6	2.4
1.25k	3.3	3.5	3.7	3.8	3.5
1.6k	5.4	5.1	5.2	5.6	5.8
2k	1.9	2.5	2.3	2.0	1.8
2.5k	3.4	2.6	3.2	3.3	2.7
3.15k	3.9	2.9	3.3	3.3	3.1
4k	3.8	3.9	4.0	3.7	3.9
5k	3.0	3.1	3.1	3.0	2.5
	Insertion Loss (dB/m)				

Wall Absorbers

Material	Thickness	Facing	Fixing Method
Polyether Polyurethane Foam	75 mm	70 g/m^2 Metallic Foil	Pinned

Frequency (Hz)	Velocity (m/s)				
	0	**4**	**8**	**15**	**21**
100	4.9	5.4	5.5	5.1	5.4
125	6.9	7.1	7.1	6.7	6.3
160	9.4	9.3	9.6	9.3	9.3
200	13.5	13.0	12.7	13.0	12.3
250	11.3	11.3	11.7	12.0	12.2
315	8.4	7.8	7.6	7.9	8.1
400	7.9	7.9	7.6	7.2	6.7
500	6.8	6.8	7.5	7.6	6.9
630	7.5	7.2	7.0	6.7	6.2
800	7.9	7.6	7.3	7.3	7.6
1k	9.9	10.1	9.9	10.1	10.3
1.25k	6.8	6.3	6.7	6.1	6.2
1.6k	6.1	6.1	5.7	5.9	5.9
2k	6.7	6.3	6.0	5.6	5.1
2.5k	6.4	6.2	5.8	5.5	5.3
3.15k	5.8	5.3	4.9	4.9	5.1
4k	7.5	7.7	7.8	7.7	7.5
5k	5.6	5.1	5.0	5.3	5.1
	Insertion Loss (dB/m)				

Material	Thickness	Facing	Fixing Method
Polyether Polyurethane Foam	25 mm	137 g/m^2 Metallic Foil	Pinned

Frequency (Hz)	Velocity (m/s)				
	0	**4**	**8**	**15**	**21**
100	1.8	1.8	1.7	1.6	1.6
125	1.6	1.5	1.6	1.5	1.5
160	1.7	1.7	1.7	1.7	1.5
200	1.9	1.9	1.8	1.7	1.5
250	3.0	3.0	2.9	2.8	2.5
315	4.7	4.8	4.6	4.2	3.6
400	6.5	6.3	6.0	5.5	4.8
500	10.0	10.1	10.0	9.6	6.8
630	7.5	7.3	7.4	7.3	6.9
800	3.9	4.8	4.8	4.6	4.8
1k	3.2	3.1	3.0	3.0	3.0
1.25k	4.2	4.4	4.6	4.3	4.2
1.6k	4.1	3.9	3.8	3.5	3.4
2k	6.0	6.0	5.6	5.4	5.0
2.5k	7.9	7.8	8.0	7.8	7.7
3.15k	6.4	6.6	6.8	6.8	6.9
4k	4.8	4.4	4.7	4.5	4.6
5k	4.1	3.9	4.0	4.2	4.2
	Insertion Loss (dB/m)				

Wall Absorbers

Material	Thickness	Facing	Fixing Method
Polyether Polyurethane Foam	25 mm	70 g/m^2 Metallic Foil	Bonded

Frequency (Hz)	Velocity (m/s)				
	0	**4**	**8**	**15**	**21**
100	1.0	1.2	1.1	0.8	0.9
125	1.0	1.1	1.0	0.9	1.0
160	0.5	0.7	0.6	0.6	0.5
200	0.7	0.7	0.6	0.5	0.6
250	1.1	1.2	1.1	1.1	1.0
315	1.5	1.5	1.6	1.4	1.2
400	2.0	2.1	2.0	1.8	1.5
500	2.7	2.6	2.6	2.5	2.2
630	5.0	5.0	5.0	4.7	4.4
800	3.5	3.3	3.2	3.0	3.3
1k	5.2	5.4	5.2	5.3	4.8
1.25k	8.9	8.8	9.1	8.8	7.7
1.6k	7.5	7.8	7.9	8.3	7.7
2k	5.8	6.3	5.9	5.7	5.0
2.5k	5.1	4.9	5.3	5.3	5.0
3.15k	3.5	3.9	4.3	4.6	4.7
4k	5.0	5.0	5.2	5.1	5.1
5k	5.0	4.9	5.0	5.1	5.0
	Insertion Loss (dB/m)				

Material	Thickness	Facing	Fixing Method
Polyether Polyurethane Foam	50 mm	70 g/m^2 Metallic Foil	Bonded

Frequency (Hz)	Velocity (m/s)				
	0	**4**	**8**	**15**	**21**
100	2.0	1.9	2.4	2.2	1.8
125	1.8	1.8	1.8	1.9	1.5
160	1.4	1.9	2.0	1.0	1.3
200	1.6	1.4	1.5	1.3	1.8
250	2.3	2.0	2.3	2.3	2.5
315	2.8	3.3	2.6	2.6	2.2
400	3.5	3.5	3.6	4.0	2.5
500	4.1	4.3	4.2	4.4	4.0
630	7.4	7.3	7.7	7.4	7.1
800	7.6	7.6	8.0	7.8	8.1
1k	7.4	7.0	7.3	7.4	7.6
1.25k	5.0	4.4	4.7	5.2	5.2
1.6k	4.2	4.2	4.3	3.9	4.7
2k	6.3	6.2	6.2	6.8	6.3
2.5k	7.3	6.4	7.1	7.0	7.9
3.15k	4.7	5.0	4.8	4.4	5.1
4k	5.3	5.0	5.7	5.1	5.5
5k	5.2	5.1	5.6	5.2	5.5
	Insertion Loss (dB/m)				

Wall Absorbers

Material	Thickness	Facing	Fixing Method
Resin bonded fibreglass	25 mm	10% Open area perforated metallic foil	Pinned

Frequency (Hz)	Velocity (m/s)				
	0	4	8	15	21
100	2.7	2.9	2.8	2.7	2.5
125	3.1	3.1	3.0	3.0	3.0
160	2.6	2.6	2.6	2.6	2.5
200	2.4	2.5	2.3	2.3	2.2
250	3.6	3.5	3.5	3.5	3.3
315	3.8	3.7	3.8	3.7	3.5
400	4.0	4.0	3.9	3.9	3.6
500	6.1	6.0	6.0	5.9	5.4
630	10.5	10.6	10.6	10.3	9.9
800	11.6	11.1	11.5	11.4	11.3
1k	17.5	17.8	17.3	17.3	15.8
1.25k	21.4	20.7	21.1	21.3	17.9
1.6k	17.7	17.3	17.3	17.7	17.4
2k	10.7	11.0	11.1	11.2	11.3
2.5k	7.7	7.6	7.8	7.9	8.4
3.15k	6.0	6.8	7.0	6.8	6.8
4k	6.0	5.7	6.4	6.4	6.3
5k	6.7	6.8	6.8	6.7	6.5
	Insertion Loss (dB/m)				

Material	Thickness	Facing	Fixing Method
Resin bonded fibreglass	25 mm	Fibreglass tissue	Pinned

Frequency (Hz)	Velocity (m/s)				
	0	4	8	15	21
100	2.8	3.0	3.0	2.9	2.7
125	3.2	3.3	3.4	3.2	3.5
160	2.5	2.6	2.7	2.7	2.6
200	2.5	2.6	2.5	2.5	2.3
250	3.6	3.6	3.6	3.5	3.2
315	4.1	4.0	4.0	3.8	3.3
400	4.4	4.3	4.3	4.0	3.5
500	6.6	6.5	6.4	6.0	4.7
630	10.7	10.7	10.4	9.5	7.5
800	10.3	10.1	9.9	9.6	7.1
1k	14.8	14.6	14.3	13.8	9.6
1.25k	14.1	14.1	14.0	14.2	11.1
1.6k	16.1	15.8	15.5	16.2	12.5
2k	13.6	14.0	13.5	13.6	11.2
2.5k	8.8	9.0	9.6	10.1	9.9
3.15k	6.3	7.4	7.6	7.6	7.8
4k	6.3	6.8	6.8	6.5	6.8
5k	5.6	6.4	6.5	6.3	6.0
	Insertion Loss (dB/m)				

Wall Absorbers

Material	Thickness	Facing	Fixing Method
Resin bonded fibreglass	25 mm	137 g/m^2 Metallic Foil	Pinned

Frequency (Hz)	Velocity (m/s)				
	0	**4**	**8**	**15**	**21**
100	2.1	2.4	2.4	2.7	2.9
125	2.8	2.9	3.0	3.4	4.0
160	2.8	2.9	3.1	3.5	3.8
200	2.4	2.5	2.5	2.8	3.0
250	3.5	3.6	3.7	4.2	4.7
315	4.3	4.3	4.4	5.1	5.4
400	5.0	5.2	5.2	5.8	6.2
500	6.3	6.2	6.4	6.8	7.1
630	8.2	8.3	8.4	9.1	9.9
800	10.8	10.7	10.8	10.9	11.5
1k	11.4	11.3	11.4	11.8	12.4
1.25k	14.6	14.6	14.9	15.0	14.9
1.6k	18.0	17.7	17.5	17.6	18.5
2k	14.3	13.9	13.8	14.8	15.3
2.5k	9.1	9.2	9.9	10.0	10.4
3.15k	6.4	7.2	7.6	8.2	9.5
4k	7.1	6.7	7.3	7.3	7.2
5k	6.5	6.6	6.8	6.3	6.4
	Insertion Loss (dB/m)				

Material	Thickness	Facing	Fixing Method
Resin bonded fibreglass	50 mm	10% Open area perforated metallic foil	Pinned

Frequency (Hz)	Velocity (m/s)				
	0	**4**	**8**	**15**	**21**
100	1.2	1.4	1.4	1.2	1.0
125	0.9	1.0	0.9	0.8	0.9
160	1.0	1.0	1.0	0.9	0.7
200	1.5	1.5	1.4	1.2	1.0
250	3.0	3.0	2.9	2.8	2.5
315	5.0	4.9	4.8	4.5	3.8
400	7.7	7.6	7.2	6.5	4.6
500	12.1	11.9	11.8	10.4	6.2
630	17.7	17.8	17.6	14.1	8.4
800	20.0	20.0	19.4	14.9	9.7
1k	18.5	18.6	18.3	14.5	9.8
1.25k	13.7	14.0	14.4	13.2	9.4
1.6k	10.5	10.9	11.0	10.9	9.3
2k	6.8	7.3	7.3	7.2	6.5
2.5k	5.0	5.1	5.5	5.8	6.0
3.15k	3.0	3.8	4.2	4.4	4.8
4k	3.8	3.9	4.2	4.3	4.5
5k	3.3	3.5	3.5	3.5	3.7
	Insertion Loss (dB/m)				

Wall Absorbers

Material	Thickness	Facing	Fixing Method
Resin bonded fibreglass	50 mm	Fibreglass tissue	Pinned

Frequency (Hz)	Velocity (m/s)				
	0	**4**	**8**	**15**	**21**
100	0.9	1.1	1.1	0.9	0.7
125	1.0	1.0	1.0	0.8	0.8
160	0.9	0.9	0.9	0.8	0.7
200	1.5	1.5	1.3	1.2	1.0
250	2.7	2.6	2.6	2.5	2.2
315	4.3	4.2	4.1	3.8	3.3
400	6.4	6.2	6.2	5.6	4.3
500	11.1	10.9	10.7	9.8	6.0
630	17.2	17.3	16.9	14.8	9.1
800	18.8	19.1	18.8	13.9	8.6
1k	20.1	20.3	19.8	14.9	9.8
1.25k	17.7	18.3	18.6	15.0	10.0
1.6k	13.2	13.5	13.8	13.5	10.2
2k	7.8	8.5	8.5	8.4	7.4
2.5k	5.0	5.5	6.2	6.6	6.4
3.15k	4.1	4.8	5.1	5.3	5.6
4k	4.6	4.4	4.5	4.6	5.0
5k	4.0	4.2	4.3	4.1	3.8
	Insertion Loss (dB/m)				

Material	Thickness	Facing	Fixing Method
Polyester	25 mm	Spun Bonded Polyester	Pinned

Frequency (Hz)	Velocity (m/s)				
	0	**4**	**8**	**15**	**21**
100	3.0	3.2	3.2	3.0	3.0
125	3.5	3.5	3.5	3.5	3.5
160	3.2	3.3	3.3	3.2	3.2
200	3.2	3.2	3.1	3.0	3.0
250	3.9	4.0	3.9	3.9	3.8
315	4.3	4.2	4.2	4.0	3.8
400	4.1	4.1	4.1	3.8	3.8
500	5.3	5.2	5.2	5.2	4.8
630	8.1	8.2	8.0	7.8	7.4
800	6.2	6.5	6.5	6.4	6.7
1k	9.9	9.4	9.3	9.4	9.1
1.25k	11.2	11.4	11.8	11.6	11.3
1.6k	13.5	13.0	13.3	13.8	13.4
2k	14.7	14.9	14.9	15.0	13.1
2.5k	15.1	14.6	14.3	13.6	12.6
3.15k	12.1	11.7	11.3	10.3	9.8
4k	8.2	8.4	8.2	7.6	7.5
5k	8.0	7.6	7.3	7.0	6.8
	Insertion Loss (dB/m)				

Wall Absorbers

Material	Thickness	Facing	Fixing Method
Polyester	50 mm	Spun Bonded Polyester	Pinned

Frequency (Hz)	Velocity (m/s)				
	0	**4**	**8**	**15**	**21**
100	2.1	2.4	2.4	2.7	2.9
125	2.8	2.9	3.0	3.4	4.0
160	2.8	2.9	3.1	3.5	3.8
200	2.4	2.5	2.5	2.8	3.0
250	3.5	3.6	3.7	4.2	4.7
315	4.3	4.3	4.4	5.1	5.4
400	5.0	5.2	5.2	5.8	6.2
500	6.3	6.2	6.4	6.8	7.1
630	8.2	8.3	8.4	9.1	9.9
800	10.8	10.7	10.8	10.9	11.5
1k	11.4	11.3	11.4	11.8	12.4
1.25k	14.6	14.6	14.9	15.0	14.9
1.6k	18.0	17.7	17.5	17.6	18.5
2k	14.3	13.9	13.8	14.8	15.3
2.5k	9.1	9.2	9.9	10.0	10.4
3.15k	6.4	7.2	7.6	8.2	9.5
4k	7.1	6.7	7.3	7.3	7.2
5k	6.5	6.6	6.8	6.3	6.4
	Insertion Loss (dB/m)				

Bar Absorbers

Cross-Section Shape	Dimensions			Facing
	Height	Width	Diameter	
Square	164 mm	164 mm	-	-

Frequency (Hz)	Velocity (m/s)				
	0	**4**	**8**	**15**	**21**
100	0.6	1.4	1.5	0.2	-
125	0.9	1.2	1.5	1.0	-
160	1.3	1.3	1.5	1.3	-
200	1.5	1.4	1.4	1.5	-
250	2.1	2.3	2.3	2.2	-
315	3.0	3.0	3.0	2.5	-
400	3.9	3.8	3.8	3.1	-
500	5.5	5.4	5.5	4.3	-
630	9.9	10.0	9.9	7.7	-
800	7.5	7.5	7.5	6.0	-
1k	7.6	7.7	7.9	7.2	-
1.25k	7.9	8.3	8.7	7.3	-
1.6k	8.1	7.8	8.0	7.4	-
2k	4.8	5.3	5.0	5.0	-
2.5k	4.8	4.9	5.4	5.5	-
3.15k	4.6	4.9	5.5	5.5	-
4k	5.9	6.1	6.3	5.5	-
5k	6.0	6.3	6.3	5.7	-
	Insertion Loss (dB/m)				

Bar Absorbers

Cross-Section Shape	Dimensions (mm)			Facing
	Height	Width	Diameter	
Square	164 mm	164 mm	-	Two sides MMF 70

Frequency (Hz)	Velocity (m/s)				
	0	**4**	**8**	**15**	**21**
100	0.8	1.0	1.0	0.8	-
125	1.0	1.0	1.0	1.0	-
160	1.5	1.5	1.5	1.4	-
200	2.0	2.0	2.0	1.8	-
250	2.4	2.3	2.3	2.2	-
315	2.2	2.0	1.9	1.7	-
400	3.5	3.3	3.0	2.8	-
500	5.6	5.5	5.5	4.6	-
630	8.6	8.6	8.5	7.5	-
800	7.5	7.6	7.5	6.5	-
1k	7.6	7.6	7.8	7.6	-
1.25k	6.6	6.7	7.0	6.5	-
1.6k	6.7	6.4	6.3	6.6	-
2k	4.7	5.6	5.3	5.6	-
2.5k	4.6	5.0	5.2	5.3	-
3.15k	3.4	4.0	4.3	4.3	-
4k	5.1	5.3	5.6	5.8	-
5k	5.2	5.0	5.0	4.9	-
	Insertion Loss (dB/m)				

Bar Absorbers

Cross-Section Shape	Dimensions			Facing
	Height	Width	Diameter	
Square	164 mm	164 mm	-	Four sides MMF 70

Frequency (Hz)	Velocity (m/s)				
	0	**4**	**8**	**15**	**21**
100	0.8	0.9	1.0	1.0	-
125	0.7	0.6	0.5	0.8	-
160	0.7	0.8	0.8	0.9	-
200	1.0	1.1	1.0	1.0	-
250	1.2	1.2	1.2	1.1	-
315	1.8	1.8	1.5	1.4	-
400	3.0	3.2	3.1	3.0	-
500	2.4	2.3	2.3	2.1	-
630	3.6	3.6	3.5	3.3	-
800	1.7	2.0	2.0	1.8	-
1k	2.4	1.9	1.9	2.0	-
1.25k	2.8	3.1	3.5	3.2	-
1.6k	3.4	2.9	3.0	3.0	-
2k	2.4	2.8	2.6	2.4	-
2.5k	2.5	2.2	2.4	2.5	-
3.15k	1.5	1.8	2.3	2.7	-
4k	3.0	3.2	3.3	3.6	-
5k	4.1	4.0	3.9	3.9	-
	Insertion Loss (dB/m)				

Bar Absorbers

Cross-Section Shape	Dimensions			Facing
	Height	Width	Diameter	
Circular	-	-	185 mm	-
Frequency (Hz)	Velocity (m/s)			
	0	**4**	**8**	**15**	**21**
100	0.2	0.4	0.3	0.4	-
125	0.4	0.5	0.5	0.7	-
160	0.7	0.8	0.8	0.9	-
200	1.2	1.2	1.1	0.7	-
250	1.6	1.6	1.6	1.3	-
315	2.3	2.3	2.0	0.8	-
400	3.7	3.7	3.3	1.7	-
500	5.8	5.6	4.7	1.6	-
630	8.5	8.5	7.4	3.6	-
800	5.9	5.9	5.4	2.4	-
1k	7.3	7.4	7.1	4.2	-
1.25k	7.6	7.7	7.7	4.8	-
1.6k	7.4	7.3	7.5	5.8	-
2k	5.6	5.9	5.6	4.6	-
2.5k	6.1	6.0	6.3	5.1	-
3.15k	5.0	5.1	5.9	5.4	-
4k	5.3	5.4	6.0	5.5	-
5k	5.7	5.8	6.4	6.0	-
	Insertion Loss (dB/m)				

Bar Absorbers

Cross-Section Shape	Dimensions			Facing
Triangular	Height 329 mm	Width 164 mm	Diameter -	-

Frequency (Hz)	Velocity (m/s)				
	0	**4**	**8**	**15**	**21**
100	0.3	0.5	0.6	0.5	-
125	0.4	0.4	0.4	0.6	-
160	0.6	0.7	0.8	0.7	-
200	1.1	1.1	1.0	0.6	-
250	1.7	1.6	1.7	1.5	-
315	2.6	2.5	2.3	1.1	-
400	3.2	3.3	3.0	1.3	-
500	4.8	4.6	4.5	1.5	-
630	9.6	9.6	9.2	4.5	-
800	7.4	7.7	7.8	3.6	-
1k	8.4	8.3	8.4	5.8	-
1.25k	9.7	9.5	10.0	6.7	-
1.6k	9.0	9.0	9.0	7.9	-
2k	7.5	7.7	7.3	6.9	-
2.5k	7.6	7.6	7.8	7.3	-
3.15k	7.7	7.4	7.8	7.5	-
4k	7.8	7.5	7.8	7.4	-
5k	7.5	7.2	7.3	7.1	-
	Insertion Loss (dB/m)				